uOttawa

L'Université canadienne
Canada's university

FACULTÉ DES ÉTUDES SUPÉRIEURES ET POSTOCTORALES

uOttawa

L'Université canadienne
Canada's university

FACULTY OF GRADUATE AND POSDOCTORAL STUDIES

Pallavi Gupta
AUTEUR DE LA THÈSE / AUTHOR OF THESIS

M.Sc. (Biochemistry)
GRADE / DEGREE

Department of Biochemistry, Microbiology and Immunology
FACULTÉ, ÉCOLE, DÉPARTEMENT / FACULTY, SCHOOL, DEPARTMENT

Lamin A/C Mutations and Heart:
Nuclear Envelope Damage or Disruption of Transcription?

TITRE DE LA THÈSE / TITLE OF THESIS

Frederique Tesson
DIRECTEUR (DIRECTRICE) DE LA THÈSE / THESIS SUPERVISOR

CO-DIRECTEUR (CO-DIRECTRICE) DE LA THÈSE / THESIS CO-SUPERVISOR

Kristi Adamo

Marie-Andrée Akimenko

Nicholas Griffin (McMaster University)

Paul Rusnock

Gary W. Slater
Le Doyen de la Faculté des études supérieures et postdoctorales / Dean of the Faculty of Graduate and Postdoctoral Studies

LAMIN A/C MUTATIONS AND HEART: NUCLEAR ENVELOPE DAMAGE OR DISRUPTION OF TRANSCRIPTION?

Pallavi Gupta

Thesis submitted to the Faculty of Graduate and Postdoctoral Studies in partial fulfillment of the requirements for the MSc degree in Biochemistry.

Department of Biochemistry, Microbiology and Immunology
Faculty of Medicine
University of Ottawa

© Pallavi Gupta, Ottawa, Canada, 2010

Library and Archives Canada

Published Heritage Branch

395 Wellington Street
Ottawa ON K1A 0N4
Canada

Bibliothèque et Archives Canada

Direction du Patrimoine de l'édition

395, rue Wellington
Ottawa ON K1A 0N4
Canada

Your file Votre référence
ISBN: 978-0-494-66243-4
Our file Notre référence
ISBN: 978-0-494-66243-4

NOTICE:

The author has granted a non-exclusive license allowing Library and Archives Canada to reproduce, publish, archive, preserve, conserve, communicate to the public by telecommunication or on the Internet, loan, distribute and sell theses worldwide, for commercial or non-commercial purposes, in microform, paper, electronic and/or any other formats.

The author retains copyright ownership and moral rights in this thesis. Neither the thesis nor substantial extracts from it may be printed or otherwise reproduced without the author's permission.

AVIS:

L'auteur a accordé une licence non exclusive permettant à la Bibliothèque et Archives Canada de reproduire, publier, archiver, sauvegarder, conserver, transmettre au public par télécommunication ou par l'Internet, prêter, distribuer et vendre des thèses partout dans le monde, à des fins commerciales ou autres, sur support microforme, papier, électronique et/ou autres formats.

L'auteur conserve la propriété du droit d'auteur et des droits moraux qui protège cette thèse. Ni la thèse ni des extraits substantiels de celle-ci ne doivent être imprimés ou autrement reproduits sans son autorisation.

In compliance with the Canadian Privacy Act some supporting forms may have been removed from this thesis.

While these forms may be included in the document page count, their removal does not represent any loss of content from the thesis.

Conformément à la loi canadienne sur la protection de la vie privée, quelques formulaires secondaires ont été enlevés de cette thèse.

Bien que ces formulaires aient inclus dans la pagination, il n'y aura aucun contenu manquant.

Canada

ABSTRACT

Mutations in the *LMNA* gene, which encodes the nuclear lamin A/C protein, are implicated in the pathogenesis of over ten phenotypically diverse diseases, including dilated cardiomyopathy (DCM). Two hypotheses have been proposed to explain the tissue specificity of *LMNA* mutations: 1) Nuclear fragility which may affect to a greater extent mechanically stressed tissues such as cardiac muscle (structural hypothesis); and 2) dysregulation of gene transcription. The objective of this study was to determine which hypothesis explains how *LMNA* mutations cause DCM. In our cohort of 25 DCM patients, 34% displayed cardiomyocytes with nuclear abnormalities, however, point mutations or large deletions of the lamin A/C gene were found in both patients with or without nuclear envelope damage. Moreover, some DCM patients with nuclear damage were free of lamin A/C gene somatic mutation. These results provide support for the structural hypothesis, but do not exclude the hypothesis of dysregulation of gene transcription. To test the latter hypothesis, we used cellular models expressing lamin A/C mutant proteins. We showed that, although the distributions of some proteins known to be involved in transcription regulation, such as SUMO1 or Ubc9 are disturbed, lamin A/C mutants have no significant effect on transcriptional activity of GATA-4 and MEF2C, two sumoylated transcription factors involved in cardiac gene transcription. In conclusion, we confirmed that structural hypothesis plays a role in DCM pathogenesis, however at this point, the gene-regulation hypothesis can not be excluded. We showed for the first time that a large deletion encompassing several exons of the *LMNA* gene and leading to a marked reduction of lamin A/C proteins in cardiac tissue, and thus to haploinsufficiency, is a new molecular mechanism associated with dilated cardiomyopathy.

ACKNOWLEDGEMENTS

I would like to thank my thesis supervisor Dr. Frédérique Tesson for her support and encouragement at each and every step of my Master's training, and completion of this manuscript. Her constructive input and inspiring talks have helped me to put in my best during the tenure of my work. I am also grateful to other members of my thesis supervising committee, Dr. Frans Leenen, and Dr. Denis Bulman, for their valuable guidance.

I would also like to express my gratitude towards our research assistant Pierrette Bolongo for her constant help, cooperation and encouragement. I would also like to thank Akil Hamza for helping me with my experiments. The support rendered by all the other lab members Nicolas Sylvius, Tracy Jackson, Siham Yasari, Emilie Boudreau, and Sarah Labib is also acknowledged. Their guidance and support during all the hardships that I faced will always be cherished.

Last, but not least, I would like to thank my husband for his unconditional support and faith in me and boosting my morale at each and every step. I would also like to thank him for his novel insights when I faced obstacles in my work.

This project has been an enriching experience for me. It has helped me to recognize the effort that is put behind any scientific endeavour.

CONTRIBUTION OF COLLABORATORS

All experiments were done under the supervision of Dr. Frédérique Tesson at the University of Ottawa Heart Institute. All experimental work presented in Chapter 2 and Chapter 3 was done by Pallavi Gupta with the exception of recruitment of patients, electron microscopy pictures of cardiac tissues, immunostaining for lamin A/C in the cardiac tissue and screening of thymopoetin gene mutations. Recruitment of patients (Chapter 2) was done in collaboration with the members of the University of Ottawa Heart Institute and National Institute of Cardiology in Warsaw, Poland. Electron microscopy pictures of Cardiac tissue samples were obtained from John P. Veinot (Ottawa Heart institute) and Zofia T. Bilinska (Institute of cardiology, Poland). The light microscopy images of cardiac samples immunotained for lamin A/C were obtained from Zofia T. Bilinska (Institute of cardiology, Poland). The sequencing of thymopoetin gene in Chapter 2 was done by Emilie Boudreau.

TABLE OF CONTENTS

LIST OF ABBREVIATIONS

α-MHC	Alpha-myosin heavy chain
ANP	Atrial Natriuretic Peptide
BAF	Barrier Auto-integration factor
BHK-21	Syrian golden hamster kidney cells
BNP	Brain Natriuretic Peptide
CARP	Cardiac ankyrin repeat protein
CFP	Cyan Fluorescent Protein
CMT2	Charcot-Marie-Tooth disorder type 2
CT	Crossing point/threshold
DCM	Dilated cardiomyopathy
Dhand	Deciduum, heart, autonomic nervous system and neural crest derivatives-expressed protein 2
DMSO	Di-methyl Sulfoxide
EDMD	Emery-Dreifuss muscular dystrophy
FACS	Fluorescence activated cell sorting
FBS	Fetal Bovine Serum
FPLD	Familial partial lipodystrophy
FRAP	Fluorescent recovery after photobleaching
GAPDH	Glyceraldehyde-3-phosphate dehydrogenase
GATA-4	GATA binding factor 4
GFP	Green fluorescent protein
GFP	Green Fluorescent protein
HeLa	Cell line derived from cervical cancer cells from Henrietta Lacks
HGPS	Hutchinson-Gilford progeria syndrome
HPRT	Hypoxanthine-guanine phosphoribosyltransferase
IF	Intermediate Filaments
IPTG	Isopropyl-beta-D-thiogalactopyranoside
LAP2	Lamina-associated polypeptide 2 isoform alpha
LB	Luria Broth
Lef	Lymphoid enhancer-binding factor 1
LEM	BAF binding domain present in LAP2, Emerin and MAN1 (Inner nuclear membrane protein Man1)
LIM protein MLP	Muscle LIM protein (LIM: domain first discovered in proteins Lin11, Isl-1 & Mec-3)
LMNA	Lamin A/C
LVEDD	Left ventricular end diastolic diameter
LVEF	Left ventricular ejection fraction
MAD	Mandibuloacral dysplasia
MEF	Murine Embryonic Fibroblasts
MEF2C	Myocyte enhancing factor
MyoD	Myoblast determination protein 1
NFkB	Nuclear Factor- kappa B
NKX2-5	NK2 transcription factor related, locus 5
PBGD	Porphobilinogen deaminase

PBS	Phosphate buffered saline
PCNA	Proliferating Cell Nuclear Antigen
PCR	Polymerase Chain Reaction
PFA	Paraformaldehyde
PGK1	Phosphoglycerate kinase 1
PML	Promyelocytic leukemia
PPARγ	Peroxisome proliferator-activated receptor gamma
RanGAP1	Ran GTpase activating protein
Rb	Retinoblastoma protein
RD	Restrictive dermopathy
SP3	Specificity protein 3
SREBP	Serum Response Element Binding Protein
SrPK3	Serine/arginine-rich protein specific kinase 3
SUMO-1	Small Ubiquitin like modifier
SUN1	Sad1/unc-84 protein-like 1
Ubc9	Ubiquitin-conjugating enzyme
WS	Werner's syndrome
YFP	Yellow Fluorescent protein
ZMPSTE24	Zinc Metallopeptidase STE24 (homologue of STE24 from S. Cerevisae

LIST OF FIGURES

LIST OF TABLES

LIST OF APPENDICES

CHAPTER 1

GENERAL INTRODUCTION

1.1. Review of the Literature

1.1.1. Dilated Cardiomyopathy

Dilated cardiomyopathy (DCM) is characterized by dilatation of cardiac chambers and reduced systolic function, leading to heart failure and sudden death. It is the most common indication for heart transplantation. Some of the known causes of DCM are viral myocarditis, coronary artery disease, systemic disease, and myocardial toxins. However, about one-half of DCM cases are idiopathic. In the United States, idiopathic DCM has a prevalence of approximately 36.6 cases per 100,000 adults, with a death rate of about 10,000 per year and the mortality is estimated to be 30-50% at 5 years (Codd et al., 1989, Dec and Fuster et al., 1994). The incidence of DCM in U.S. children below the age of 18 has been estimated at 0.57 cases per 100,000 per year, which is about ten-fold lower than in adults (5.5 cases per 100,000 population per year) (Towbin et al., 2006). Age of onset and severity of symptoms differ among DCM patients.

DCM is diagnosed using echocardiography, through which the degree of dilatation and ejection fraction can be measured. Conduction abnormalities are detected through electrocardiography. More invasive techniques such as cardiac catheterization can also be sometimes employed to more precisely measure cardiac function. Pharmacological treatment of DCM consists of angiotensin-converting enzyme inhibitors, beta blockers, anticoagulants, digoxin, and diuretics (Dec and Fuster, 1994,). Progressive heart failure in DCM patients often necessitates heart transplantation (Hermida-Prieto et al. 2004, Sylvius et al. 2005).

1.1.2. Familial DCM: The genes involved

Familial DCM remained poorly characterized until the early 1990's. Grunig et al. reported that familial DCM may account for 35% of all idiopathic DCM cases (Grunig et al., 1998). Familial DCM can be autosomal dominant, autosomal recessive, X-linked, and mitochondrial, with autosomal dominant being the most common mode of inheritance (Ku et. al 2003, Mestroni et al., 1999). To date, mutations in 33 genes have been associated with dilated cardiomyoapthy. The genetic causes of DCM can be classified into different groups based on the function of the proteins encoded by these genes: 1) mutations in the genes encoding sarcomeric proteins such as cardiac beta-myosin heavy chain, troponin T, and cardiac actin; 2) mutations in genes encoding sarcomeric or extra-sarcomeric cytoskeleton proteins such as desmin, dystrophin, titin, and telethonin; 3) mutations affecting nuclear envelope proteins such as lamin A/C (encoded by *LMNA* gene) and thymopoetin; 4) mutations in proteins involved in ion homeostasis such as phospholamban. Mutations have also been found in proteins not belonging to these categories such as the transcription factors EYA5 and CARP, and the heat shock protein αB-crystallin (Olson et al., 2001, Fatkin et al., 2002, Olson et al., 2002, Mohapatra et al., 2003, Vatta et al. 2003, Schonberger et al., 2005, Inagaki et al., 2006, Karkkainen et al., 2007, Duboscq-Bidot et al., 2009, MIM#115200) (Table 1.1, Appendix 1). Certain chromosomal locations have also been linked to the disease without subsequent positional identification of the disease gene (Karkkainen et al., 2007). Of all the genes identified, the *LMNA* gene is the most frequently reported gene involved in the disease. This gene encodes for alternatively spliced A-type lamins (A and C), both of which are major components of nuclear lamina. Sylvius and Tesson (2006) reported that mutations in *LMNA* are responsible for 5% of DCM cases genotyped worldwide from 1999-2006

(Tesson et al., 2006). Age of DCM onset and disease severity in patients with *LMNA* mutations vary both within and across families (Taylor et al., 2003, Hermida-Prieto et al., 2004, Sylvius et al., 2006). Furthermore, 25% of the patients carrying *LMNA* mutations do not develop DCM, and remain asymptomatic for their entire life (Sylvius et al., 2006). Several groups have reported that symptomatic carriers of *LMNA* mutations are faced with a worse prognosis for DCM than carriers of mutation in another DCM gene (Taylor et al., 2003, Hermida-Preito et al., Sylvius et al., 2006, 2004, Karkkainen et al., 2007). A meta-analysis of 21 studies enrolling a total of 299 *LMNA* mutation carriers with DCM suggested that DCM patients with *LMNA* mutations have a high risk of dysrhythmia (92% of cases), heart failure (64% of the patients after the age of 50), and sudden death due to tachyarrhythmia (the most common cause of death in 46% of cases) (Van Berlo et al., 2005). In the same study, sudden death occurred in 43% of patients who had a pacemaker implanted, indicating that pacemaker implantation may not prevent this outcome. However, prophylactic therapy with implantable cardioverter defibrillator has been shown to be effective in preventing sudden death in DCM patients with *LMNA* mutations (Meune et al. 2006).

Because *LMNA* mutations are the most frequently reported cause of genetic DCM, a thorough understanding of the structure and function of nuclear lamins, as well as the consequences of *LMNA* mutations, is required to understand the pathogenesis of DCM caused by *LMNA* mutations.

1.1.3. Nuclear Envelope, Lamina and Lamins

The nucleus is surrounded by the nuclear envelope that separates nuclear contents from the cytoplasm. The nuclear envelope consists of inner and outer membranes separated by a perinuclear space, and connected at nuclear pores. Nuclear pores play a key role in regulating the transport of materials such as RNA and protein between the nucleus and cytoplasm. The nuclear lamina is a meshwork of proteins located beneath the nuclear membrane (Stuurman et al., 1998). Nuclear lamins are a type of intermediate filament (IF) proteins that comprise an integral part of the nuclear lamina (Fuchs et al., 1994, Fisher et al., 1986). The IF super-family consists of 60 members, belonging to 5 different groups (I-V). Most IF super-family proteins are cytoplasmic (from group I-IV), while lamins, which belong to group V, are nuclear (Hutchinson 2002). Lamins are not only found in the nuclear lamina, but also in the nucleoplasm (Stuurman et al., 1998).

1.1.4. Lamins: Assembly and Structure

There are two main types of lamins in vertebrate cells: A-type lamins and B-type lamins (Fuchs et al., 1994). The A-type lamins are encoded by a single gene, *LMNA,* whereas the B-type lamins: B1 and B2 are encoded by two separate genes, *LMNB1* and *LMNB2* (Broers et al., 2006). The B-type lamins are expressed at constant levels in all multi-cellular eukaryotic cells, the expression of A-type lamins is however more developmentally regulated. The expression of A-type lamins increases during differentiation and is highest in terminally differentiated cells (Stuurman et al., 1998).

The two major isoforms of A-type lamins are lamin A (70 kDA) and lamin C (60 kDA). Lamin A and lamin C are generated by alternative splicing of exon 10 of the *LMNA*

gene (Lin et al., 2003) (Figure 1.1). Lamin C is identical to lamin A for the first 566 amino acids, but lacks amino acids encoded by exon 11, and exon 12. Instead it carries 5 lamin C-specific amino acids before an early termination. Lamin A, on the other hand, also carries lamin A specific region from amino acid 566-664 (Zastrow et al., 2004) (Figure 1.1). Lamin C2 and Lamin AΔ10 are two other isoforms of A-type lamins (Furukawa et al., 1995, Machiels et al., 1996). Lamin C2 (52 kDA) is expressed exclusively in germ-cells. It is structurally similar to lamin C, however its N-terminal head is encoded by an alternative exon 1C2 located in the first intron of the *LMNA* gene (Furukawa et al., 1995). Lamin AΔ10 (65 kDA) is expressed in a variety of tissues, in relatively small amounts as compared to lamin A and lamin C. Structurally, it is very similar to lamin A, except that it lacks amino acids encoded by exon 10 (Machiels et al., 1996).

The carboxyl terminus of pre-lamin A and lamin B contains a CAAX box (cysteine-aliphatic-aliphatic-any residue), which is absent in lamin C (Lin et al., 2003, Zastrow et al., 2004). For conversion to lamin A, pre-lamin A is modified by isoprenylation (farsenylation) of the cysteine residue, followed by removal of the AAX sequence by ZMPSTE24 protease (Zastrow et al., 2004, Broers et al., 2006). Subsequently, the COOH-terminal cysteine residue undergoes carboxymethylation. Both these processes are important for localization of lamins to the inner nuclear membrane. Once at the nuclear membrane, lamin A is proteolytically cleaved by ZMPSTE24 zinc metalloproteinase to remove the modified cysteine and an additional 14 residues (Zastrow et al., 2004, Broers et al., 2006). Lamin B, however, remains isoprenylated. The process by which pre-laminA is converted to lamin A is essential for incorporation of lamin A into the nuclear lamina (Broers et al., 2006) (Figure 1.2).

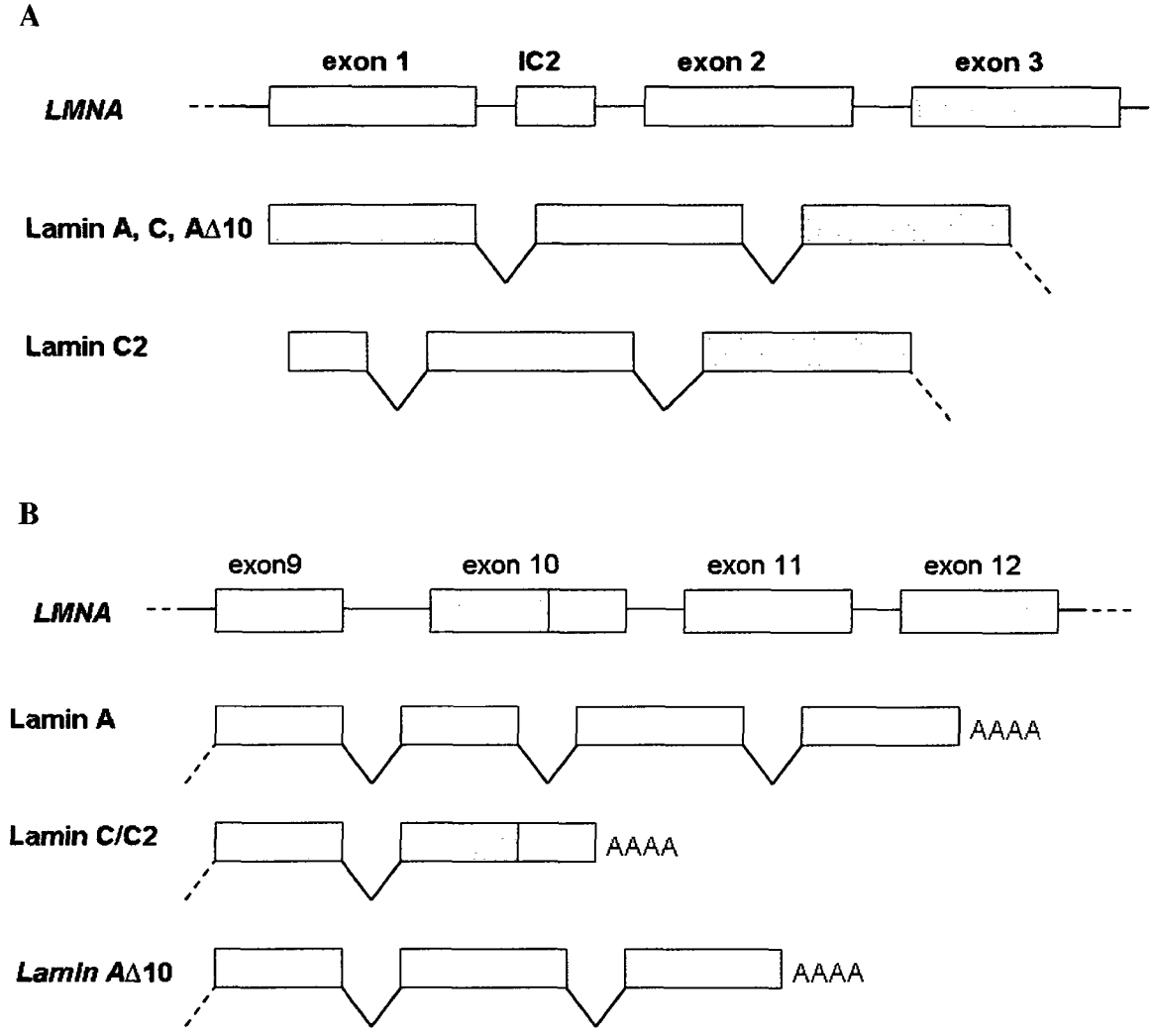

Figure 1.1: *LMNA* gene alternative splicing isoforms. Alternative splicing of the LMNA gene produces lamin A, lamin C, lamin AΔ10 and lamin C2. (A) Lamin C2 is produced by 5' alternative splicing, with its N-terminal head encoded by an alternative exon 1C2 located in the first intron of the *LMNA* gene. (B) *LMNA* gene also undergoes splicing at the 3' end to generate lamin C, lamin C2, lamin A and lamin AΔ10. Lamin C and lamin C2 lack exon 11, and exon 12. Lamin AΔ10 lacks exon 10.

Figure 1.2: Schematic representation of pre-lamin A processing to produce mature lamin A/C. Reproduced with permission of American Physiological society, from Nuclear Lamins: Laminopathies and their role in pre-mature ageing, J.L.V. Broers 86, 2006 (Copyright 2008); permission conveyed through Copyright Clearance Center, Inc.

Like all intermediate filament (IF) proteins, lamins consist of an N-terminal head domain, a central helical rod domain, and a C-terminal globular tail domain containing an immunoglobulin (Ig) fold and a nuclear localization signal (Zastrow et al., 2004, Fisher et al., 2006) (See Figure 1.3). The strongest homology among lamins is found in the two end rod segments which are about 30 amino acids long. These are also highly conserved among other IF proteins, and play an important role in forming higher order oligomers. The helical rod domain of nuclear lamins consists of helical segments 1A, 1B, 2A and 2B, separated by linker segments L1, L12, and L2 (Stuurman et al., 1998). The rod domain of the nuclear lamins have an extended Coil 1B, which makes then 42 amino acids longer than cytoplasmic IF proteins. This α-helical rod domain is responsible for the dimerization of two lamin monomers into a parallel coiled-coil homodimer, the basic structural unit of lamin assembly. These homodimers first interact in a head-to-tail fashion, and then laterally to create anti-parallel proto-filaments. Eight of these protofilamens combine to form the 10 nm intermediate filament structure (Burke et al 2001) (Figure 1.3).

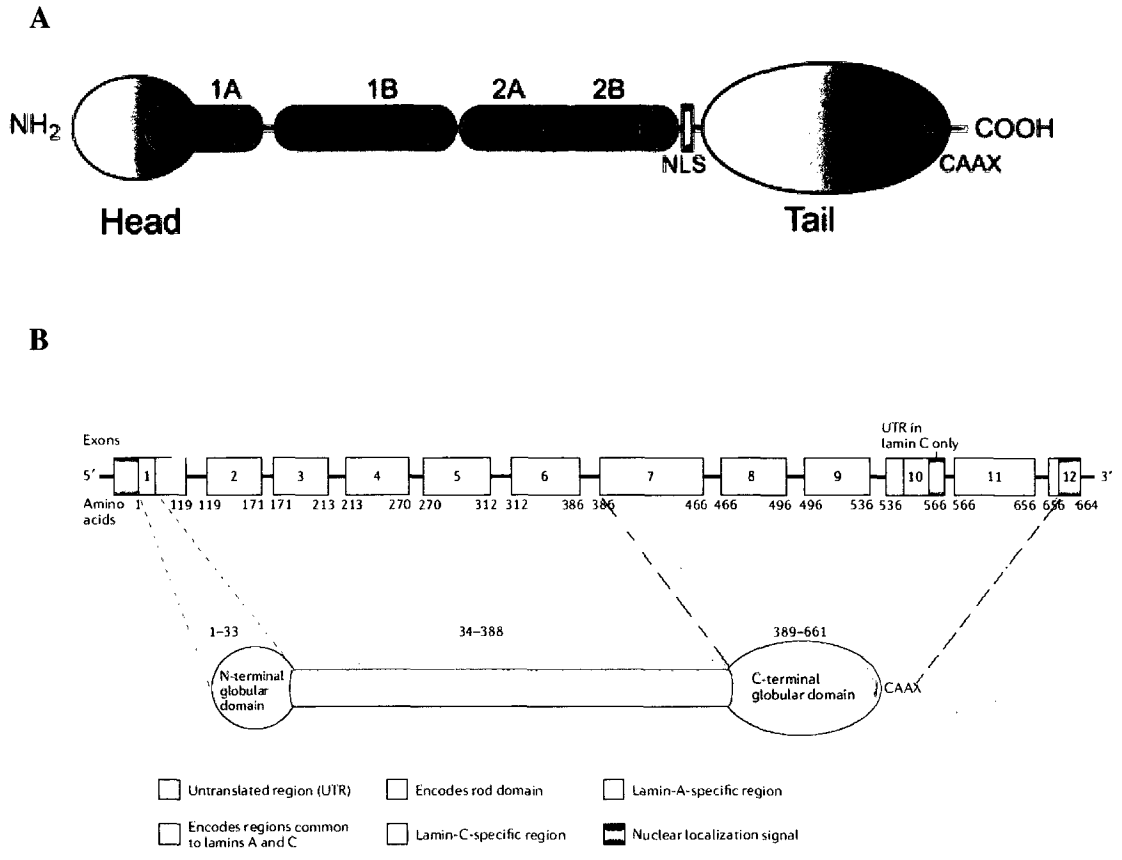

Figure 1.3: Schematic representation of the structure of lamin proteins. **A**: They consist of an N-terminal globular head domain and a C-terminal globular tail domain that flank the central rod domain, comprising four coiled-coil domains 1A, 1B, 2A and 2B. The globular tail domain consists of the nuclear localization signal (NLS) and CAAX motif (found in lamin A and lamin B, but not in lamin C) (Broers et al., 2006). Reproduced with permission with permission of American Physiological society, from Nuclear Lamins: Laminopathies and their role in pre-mature ageing, J.L.V. Broers 86, 2006 (Copyright 2008); permission conveyed through Copyright Clearance Center, Inc. **B**: Exons 1-12 encoding different domains of lamin A. Exon 1 encodes the N-terminal globular head domain. Exons 1-6 encode the rod domain and exons 7-10 encode the C-terminal tail domain of lamin C. Exons 7-12 encode the C-terminal tail domain of lamin A. Exons 8 and 9 form the Ig fold domain. Alternative splicing in exon 10 generates lamin C which carries extra lamin C-specific amino acids (56-572) (Capell et al., 2006). Reprinted by permission from Macmillan Publishers Ltd.

1.1.5. Lamin dynamics during Interphase and Mitosis

Lamin dynamics vary according to the stage of the cell cycle. Through the use of fluorescence bleaching techniques in cells expressing GFP-lamins, it has been demonstrated that lamins form stable structures in interphase cells; hence, their turnover during interphase is minimal (Broers et al., 2004b, Broers et al., 2006).

Cell division is associated with important changes in the organization of the lamina. During mitosis, lamins undergo depolymerization, a process believed to be caused by increased phosphorylation of lamin proteins by cyclin-dependent kinase 1 (Cdk1) (Peter et al., 1990). Following depolymerization, lamins A and C become completely solublized, whereas B-type lamins maintain their association with membrane vesicles (Gerace 1980, Burke et al., 1986, Nigg et al., 1992).

Following mitosis, both A and B–type lamins undergo dephosphorylation and reassemble to form the lamina (Burke et al., 1986) at about the same time as formation of the nuclear envelope (Goldman et al., 2002). Reassembly of all three A-type lamins does not begin until the later stages of cytokinesis, after the decondensation process of the chromosomes has been initiated, and nuclear pores have been formed (Broers et al., 1999, Moir et al., 2000). A-type lamins first accumulate in the nucleoplasm, and then are gradually incorporated into the lamina (Moir et al., 2000).

Data regarding the dynamics of lamin B re-assembly are conflicting. Some studies have demonstrated that lamin B1 associates with chromosomes during anaphase/telophase as they reach the spindle poles, suggesting that lamin B1 polymerization plays an integral role in both chromosomal decondensation and in the early stages of nuclear envelope assembly (Moir et al., 2000). However, others have shown that lamin B1 accumulation around chromatin

occurs during late telophase or early cytokinesis, once nuclear envelope has already been initiated and nuclear pores have been assembled (Chaudhary et al., 1993, Diagle et al., 2001). Taken together, these studies indicate that both A and B-type lamins are involved in nuclear envelope assembly, although their exact roles remain unclear.

1.1.6. Functions of Lamins

1.1.6.1. Role of A-type Lamins in Nuclear architecture

Many studies have shown that lamins play an important role in maintaining the shape and size of the nucleus (Hutchinson et al., 2002). Through interactions with the nuclear pore protein NUP153, lamins also play an important role in anchoring nuclear pore complexes to the inner nuclear membrane (Hutchinson et al., 2002). Liu et al. (2000) showed that depletion of a single lamin gene (*lmn-1*) in C. elegans resulted in the formation of smaller sized nuclei with abnormal nuclear morphology and clustering of nuclear pore complexes. Lmn-1, the only lamin found in C. elegans, is localized to the nuclear periphery, and is thought to perform the roles played by both A and B-type lamins in other species (Liu et al., 2000). Alterations in nuclear morphology such as elongation and irregular nuclear shape have been found in cells derived from *LMNA -/-* mice, suggesting a role for lamins in maintaining the shape of nuclei. Furthermore, aberrations in nuclear morphology such as membrane disruption, nuclear pore clustering, and dysmorphic nuclei have also been found in patients carrying *LMNA* mutations, indicating that lamins play an important role in maintaining nuclear envelope integrity and proper positioning of nuclear pores in the inner nuclear membrane (Vigouroux et al., 2001, Verga et al., 2003).

Lamins have been shown to be essential for the reassembly of the nuclear membrane following mitosis (Ultizur et al., 1992, Burke et al., 1996). To ensure assembly and maintenance of nuclear envelope integrity, lamins interact with a number of nuclear membrane proteins. Various interacting partners of lamin A/C are depicted in the figure 1.5 (For a complete list of interacting partners, see Table 2, Appendix 2).

One of these proteins LAP2α, also called thymopoetin, is the only known lamin A/C interacting protein that has been shown to carry a p.R690C mutation in 2 severely affected DCM siblings (Taylor et al., 2005). The identified mutation occurred in the C-terminal domain of the thymopoietin alpha, a region known to interact with lamin A/C (residues 319-566). LAP2α is a non-membrane isoform of the LAP2 family that binds to the C-terminal tail domain of lamins during interphase (G1 phase), and is thought to tether the A-type lamins to intranuclear sites (Dechat et al., 2000, Zastrow et al., 2004) .

A-type lamins also interact with nesprin 1 and nesprin 2 isoforms (Mislow et al., 2002, Zhang et al., 2004). These two proteins are of particular interest because nesprin 1 and 2 gene mutations have been found in Emery-Dreifuss muscular dystrophy (EDMD) patients, a disease also caused by mutations in the *LMNA* gene (Zhang et al., 2007). Moreover, nesprin 2 has been recently shown to have a general role in rendering the nuclear envelope less susceptible to mutant *LMNA*-induced nuclear deformations (Kandert et al., 2007). Nesprin-1α is a spectrin repeat containing transmembrane protein found in the inner nuclear membrane. It consists of a large nucleoplasmic domain containing 7 spectrin repeat domains, and a carboxy terminal membrane spanning domain, and an interrupted LEM domain. Nesprin-1α binds to the C-terminal domain of lamin A/C and the N-terminal domain of emerin (Mislow et al., 2002). Nesprin-2 isoforms (smaller isoforms of nesprin) are found in

the inner nuclear membrane where they bind to emerin and lamin. Furthermore, the giant isoforms of both nesprin 1 and nesprin 2 are found at the outer nuclear membrane. These isoforms consists of an N-terminal calponin homology domain, which is responsible for its interaction with actin. It also consists of a C-terminal KLS domain, which contains a transmembrane domain, and is necessary for nuclear envelope localization (Zhang et al., 2004). The two domains are separated by a variable repeat rod domain. The C-terminal KLS domain of nesprins has been shown to interact with SUN1 proteins. The SUN1 proteins are tethered to the inner nuclear membrane through the interaction of their N-terminal domain with lamin A. The C-terminal domain of SUN1 interacts with the KLS domain of nesprins in the nuclear envelope lumen. These observations suggest that nesprins and SUN1 proteins may play a role in connecting the nuclear matrix to cytoplasmic architecture by interacting with lamins and emerin in the inner nuclear membrane, and interacting with actin on the cytoplasmic side (Haque et al., 2006, Stewart et al., 2007) (Figure 1.4). From the perspective of DCM, in which most of the causative genes encode cytoplasmic or sarcomeric proteins, the connection between the cytoskeleton and the nuclear lamina provides a putative common mechanism by which mutations in the diverse proteins implicated in DCM cause the disease.

Emerin, another important architectural lamin A/C interacting protein, has been shown mutated in EDMD patients (Ostlund et al., 1999). Emerin is present in the inner-nuclear membrane and interacts with the tail domain of lamin A/C (Zastrow et al., 2004). Emerin is thought to play an important role in the nuclear architecture through its binding with lamins and other proteins.

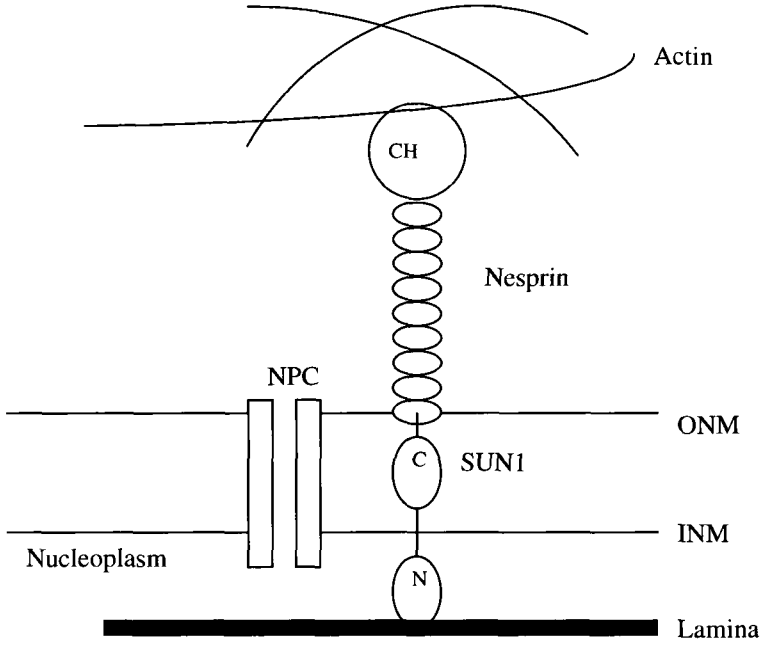

Figure 1.4: SUN1 localization and interaction with lamin A/C and nesprin at nuclear envelope. The nucleoplasmic domain of SUN1 lies in the nucleoplasm where it interacts with lamin A/C. Its C-terminal domain lies in the nuclear envelope lumen, where it interacts with KLS/KASH domain of nesprin. The N-terminal calponin homology domain of nesprin interacts with actin. In this manner, SUN1 helps in connecting the nucleus to the actin cytoskeleton (Adapted from Molecular and Cellular Biology, Haque et al. 2006).

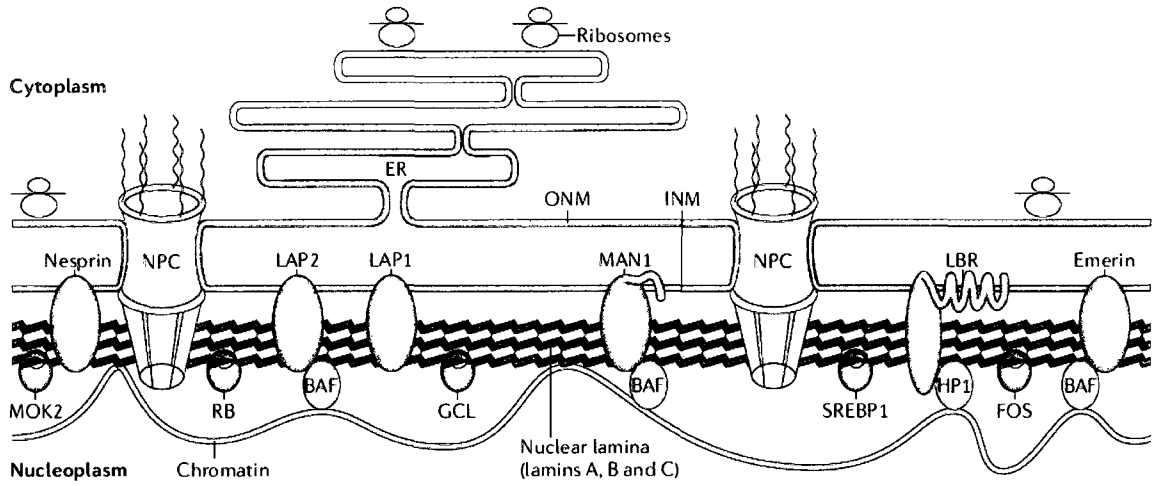

Figure 1.5: Schematic representation of lamins with some of its interacting partners. The nuclear lamina consisisting of lamin A, lamin C and lamin B lies on the inner side of the nuclear membrane. Nuclear lamins interact with nuclear pore complexes and chromatin. They also interact with several nuclear envelope proteins such as Nesprin, LAP2 (lamin associated protein), LAP1, MAN1 (Inner nuclear membrane protein Man1), LBR (Lamin B receptor) and Emerin. They also interact with transcription factors such as RB1 (Retinoblastoma protein), and SREBP1 (Serum response element binding protein (Capell et al., 2006). Reprinted by permission from Macmillan Publishers Ltd.

1.1.6.2. Role of A-type lamins in DNA Replication

Lamin-depleted *Xenopus* extracts assembled *in vitro* failed to initiate DNA replication (Meier et al., 1990, and Newport et al., 1990). Furthermore, addition of a dominant negative lamin A mutant (lacking the amino-terminal) to mammalian cells disrupted lamin organization and inhibited DNA synthesis (Spann et al., 1997). Similar results were obtained by over-expression of the lamin A/C C-terminal domain in mammalian cells (Shumaker et al., 2008). These studies suggest that normal lamin organization is required for DNA replication, yet the precise role of lamins remains unclear. It has been suggested that lamins may affect DNA replication in two possible ways. First, through the maintenance of nuclear envelope integrity, thus allowing for the selective import of replication factors, and creating the necessary nuclear environment for replication (Walter et al., 1998). Second, lamins may affect DNA replication by forming a scaffold for multi-protein complexes that play a role in DNA replication. Indeed, A-type lamins have been shown to bind with chromatin through their C-terminal tail domains, an interaction mediated through core histones (Taniuara et al., 1995). They have also been shown to bind directly to the minor groove of DNA (Luderous et al., 1994). A-type lamins also bind with Barrier-auto-integration factor (BAF), a DNA-binding protein (Zastow et al., 2004). Interestingly, the lamin A/C interacting protein emerin also binds to BAF through its LEM domain (Lee et al., 2001). Similarly, LAP2α (another LEM domain-containing protein) has separate binding sites for BAF, lamin A/C and chromatin (Zastrow et al., 2004). These studies indicate that BAF may function in linking lamin A/C and its binding partners to chromatin.

The scaffolding model is further supported by the existence of nucleoplasmic lamins. The nucleoplasmic lamins have been shown to exist as foci in the G1 and S-phase of the cell

cycle (Bridger et al., 1993, Kennedy et al., 2000). In primary mammalian cells in S-phase, these lamin A/C foci co-localized with the replication foci and replication factors such as Proliferating Cell Nuclear Antigen (PCNA), suggesting that lamins may play a role in organizing replication sites. Furthermore, the IgG fold domain in the C-terminal domain of lamin A and lamin C has been shown to interact with PCNA (Shumaker et al., 2008). It has also been demonstrated that the nucleoplasmic lamins are a component of the diffuse nucleoskeleton, which is present throughout the nuclear interior and is associated with chromatin and sites of DNA replication (Hozak et al., 1995, Neri et al., 1999). Taken together, these studies indicate that lamins may form a nuclear scaffold upon which chromatin organizes and associates with essential DNA replication factors or other proteins.

1.1.6.3. Role of A-type lamins in transcription

There is a growing body of evidence that A-type lamins play an important role in transcription, although their specific functions in regulating this process remain largely unknown. Similar to their role in DNA replication, it is suggested that A-type lamins could play a role in transcription by providing a scaffold for the organization of chromatin and protein complexes that play a role in regulating transcription (Zastrow et al., 2004). A-type lamins have been shown to interact with many transcription factors such as retinoblastoma protein 1 (pRb1), which is involved in transcriptional repression, via E2F (Zastrow et al., 2004). Retinoblastoma and E2F-1 have been found to co-localize with intranuclear sites of lamin A/C (Kennedy et al., 2000). Interestingly, the lamin A/C interacting protein LAP2α (thymopoietin) also interacts with pRb1, suggesting that *in vivo*, a complex containing lamin A/C, thymopoietin and pRb1 is involved in regulating gene transcription (Zastrow et al.,

2004). It has been shown that in cells lacking lamin A/C, the amount of retinoblastoma protein is also drastically reduced (Johnson et al., 2004). A-type lamins also interact with transcription factors Sterol Response Element Binding Proteins 1 and 2 (SREBP) and MOK2 (Dreuillet et al., 2002, Lloyd et al., 2002). SREBP proteins bind to the Ig fold domain of the lamin A/C tail and play an important role in regulating cholesterol biosynthesis and lipogenesis (Lloyd et al., 2002). It has been shown that lipodystrophy-causing *LMNA* mutations reduce the interaction of lamin A/C with SREBP by 25-50%. A-type lamins also interact with actin, which has been shown to play a role in mRNA processing and nuclear transport (Shumaker et al., 2003). The role of lamins A/C in transcription was particularly evident in a study showing that introduction of a dominant-negative lamin mutant (lacking the N-terminal domain) in BHK 21 cells (Baby Hamster Kidney cells) resulted in the disruption of lamin organization via the formation of abnormal nucleoplasmic aggregates in both the intranuclear lamin speckles and peripheral lamins. This disruption in lamin organization correlated with inhibition of polymerase-II (POLII)-mediated transcription, suggesting that normal organization of lamins is essential for nuclear transcription (Spann et al., 2002). Furthermore, it has been demonstrated that inhibition of RNA POLII mediated transcription in HeLa cells is followed by the synchronous and reversible enlargement of intranuclear lamin A/C speckles, together with enlargement of splicing factor compartments (SFC) speckles, which co-localize (Kumaran et al., 2002). Conversely, disruption of the intranuclear lamin foci led to the depletion of splicing factors and the down-regulation of transcription. The authors suggested that lamin speckles may help organize RNA POLII-mediated transcription and mRNA splicing in response to specific signals.

1.1.7. Laminopathies: *LMNA* mutations and other diseases

In addition to DCM, mutations in the *LMNA* are responsible for a variety of diseases, collectively called laminopathies, affecting either specific tissues (such as striated muscle, the peripheral nerves and adipose tissue) or in a systemic way (such as premature ageing syndromes) (Broers et al., 2004, Somech et al., 2005) (figure 1.6). Mutations found in laminopathies are located throughout the gene, and no correlation exists between either the type or location of mutations and the disease they cause (figure 1.6). The first identified laminopathy was the autosomal dominant form of Emery-Dreifuss muscular dystrophy (EDMD) (Bonne et al. 1999). Interestingly, the X-linked form of EDMD had previously been linked to mutations in the gene emerin, encoding an inner nuclear membrane protein that interacts with lamin A/C (Bione et al., 1994). Missense mutations in *LMNA* are also responsible for limb girdle muscular dystrophy (LGMD), familial partial lipodystrophy (FPLD), Charcot-Marie-Tooth disorder type 2 (CMT2), mandibuloacral dysplasia (MAD), Hutchinson-Gilford progeria syndrome (HGPS), atypical Werner's syndrome (WS), and restrictive dermopathy (RD). Clinical phenotypes of these diseases are reviewed in Table 1.1. Most *LMNA* mutations cause tissue-specific lamimopathies, although overlap has been reported in some cases. For example, lipodystrophy patients carrying *LMNA* mutations have been shown to present with both muscular dystrophy and dilated cardiomyopathy of varying severities (van der Kooi A.J. et al., 2002, Vantyghem et al., 2004Broers et al., 2006, Sylvius et al., 2006). Furthermore, the dominant missense *LMNA* mutation p.E33D was found in a father and daughter who both had a combination of axonal neuropathy, muscular dystrophy, and dilated cardiomyopathy (Goizet et al., 2004). Similarly, another dominant missense

LMNA mutation (p.R541C) in the lamin C specific tail region was found to be associated with both CMT2 and muscular dystrophy (Bennedetti et al., 2005).

These observations suggest that, while most *LMNA* mutations cause disease in a tissue-specific manner (e.g., only the myocardium is affected in DCM), they can also have simultaneously deleterious effects on a number of different tissues (e.g., in the cases demonstrating lipodystrophy with DCM and muscular dystrophy). There is no correlation between the location of the mutation and the associated phenotype.

Table 1.1: Mutations in *LMNA* lead to a variety of human degenerative disorders, collectively termed laminopathies. The table presents various laminopathies with their modes of inheritance and clinical phenotypes. Adapted from Nature Genetics 2006; 7:940-952 and Journal of Pathology 2004; 204:478-488.

Disease	Abbreviation	Form of inheritance	Clinical Phenotype
Emery-Dreifuss muscular dystrophy	EDMD	Autosomal Dominant. One Recessive case with mutation p.H222Y.	Slow progressive contractures and muscle weakness involving elbows, Achilles tendons and postcervical muscles, wasting of skeletal muscle and cardiomyopathy
Limb-girdle muscular dystrophy	LGMD	Autosomal Dominant	Slowly progressive pelvic girdle and shoulder muscle weakness. Later development of cardiac disturbances
Dilated cardiomyopathy with conduction system disease	DCM	Autosomal Dominant	Ventricular Dilatation, impaired systolic function and conduction system disease.
Familial partial lipodystrophy	FPLD	Autosomal Dominant	Subcutaneous fat loss, adipose tissue accumulation in face and neck, insulin resistance and diabetes.
Charcot-Marie-Tooth disorder type2	CMT2	Autosomal Recessive	Motor and sensory neuropathies. Axonal degeneration. Muscle weakness and walking difficulties and Foot deformities
Mandibuloacral dysplasia	MAD	Autosomal Recessive	Postnatal growth retardation, delayed closure of cranial sutures, Skeletal muscle malformations, mottled cutaneous

Disease	Abbreviation	Form of inheritance	Clinical Phenotype
			pigmentation, short stature, lipodystrophy, alopecia, mandibular and clavicular hypoplasia, insulin resistance
Hutchinson-Gilford progeria syndrome	HGPS	De novo mutations. C-to-T change at codon 608 in exon 11of *LMNA*, which activates a cryptic splice site, and generates a permanently farsenylated protein with 50 amino acids deleted at the C-terminus.	Premature aging, dwarfism, alopecia, craniofacial disproportion, delayed tooth formation, aged-looking skin, osteoporesis and joint problems, early death in teens due to atherosclerosis and cardiovascular disease.
Atypical Werner's syndrome	WS	Autosomal dominant	Premature aging, cataracts, Scleroderma-like skin, subcutaneous calcification, premature arteriosclerosis, diabetes, hair greying.
Restrictive dermopathy	RD	Heterozygous de-novo splicing mutations in *LMNA* leading to complete or partial loss of exon 11. This results in accumulation of pre-lamin A.	Early neonatal lethal course, intrauterine growth retardation, tight and rigid skin, microstomia, pulmonary hypoplasia, multiple joint contractures.

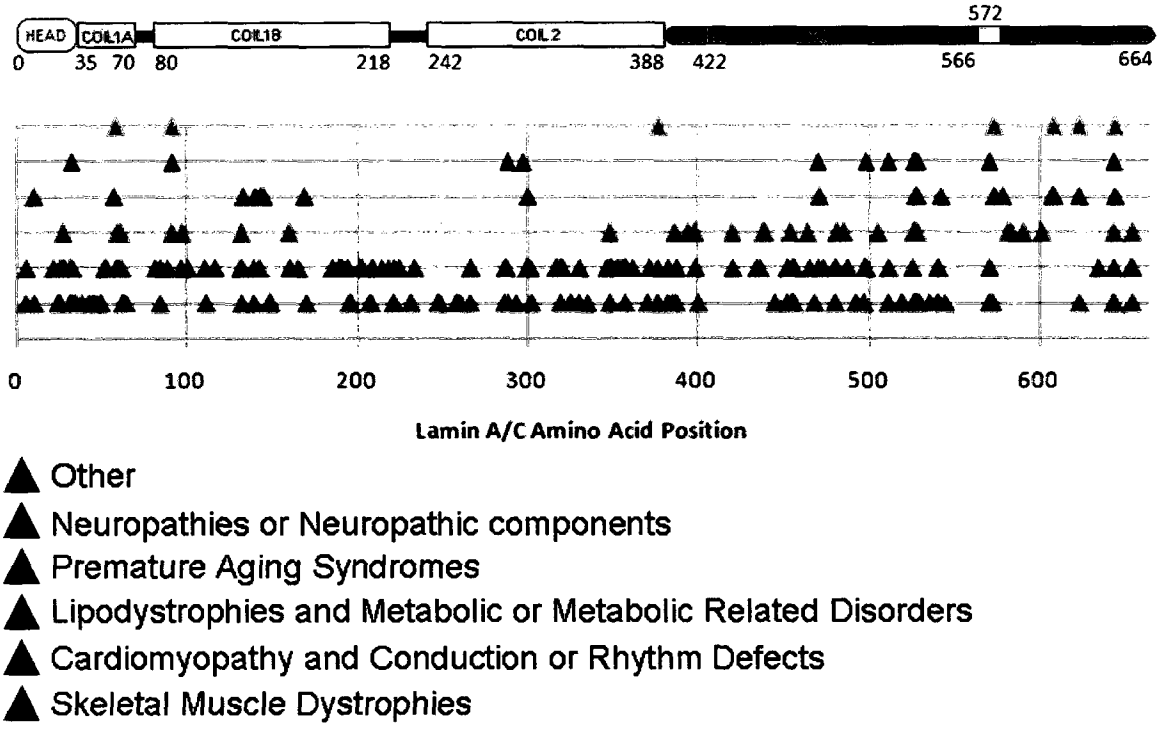

Figure 1.6: Schematic representation showing LMNA mutations found in laminopathies. The mutations are localized throughout the gene and there is no correlation between the location of mutation and the disease it causes.

1.1.8. Mouse Models of Laminopathies

Several knock-out and knock-in mouse models have been generated in order to gain insights into the functions of *LMNA* mutations. However, there have been significant challenges in using these models to predict the pathophysiological effects of heterozygous missense mutations commonly found in patients with laminopathies, including DCM. There are no in utero differences between $LMNA^{-/-}$ mice and their wild-type litter mates, however, $LMNA^{-/-}$ mice exhibited progressive growth retardation within 2-3 weeks after birth (Sulliman et al., 1999, Nikolova et al., 2004). By 4-6 weeks of age they manifested clinical and histological features of muscular dystrophy, followed by DCM with conduction abnormalities. All homozygous $LMNA^{-/-}$ mice died by 8 weeks (Sullivan et al., 1999, Nikolova et al., 2004). In most cases the age-matched heterozygous mice were, indistinguishable from wild-type (Sullivan et al., 1999, Nikolova et al., 2004). Only one study has reported $LMNA^{+/-}$ mice displaying cardiac abnormalities. These mice had normal cardiac structure and function until 4-6 weeks of age, but by 10 weeks of age they had developed conduction system defects such as defective AV node conduction and arrhythmias. DCM developed by 50-52 weeks of age (Wolf et al., 2008).

A number of researchers have attempted to develop genetically engineered mouse models harboring known laminopathy mutations with mixed results. Mounkes et al. (2003) aimed at producing an EDMD mouse model with the p.L530P point mutation. Surprisingly, the homozygous mouse developed clinical symptoms characteristic of human progeria syndrome, rather than the expected muscular dystrophy, while the heterozygote was symptomless.

Two groups have successfully generated one EDMD and one DCM mouse model. The *LMNA*$^{H222P/H222P}$ mouse model, harboring another EDMD mutation, developed muscular dystrophy and DCM with atrio-ventricular conduction defects in adulthood and died by 13 months of age (Arimura et al., 2005). Another knock-in-mouse model (*LMNA*$^{N195K/N195K}$), harboring the DCM-causing mutation p.N195K, was generated to study DCM with conduction system defects (Mounkes et al., 2005). These mice showed features characteristic of DCM, with conduction defects by 9 weeks of age, and death at 3 months of age due to arrhythmias. It was postulated by the authors that the observed conduction defects may have been due to reduced expression of gap junction proteins. Heart sections from the p,N195K mutant mice demonstrated reduced expression of connexin 40 (Mounkes et al., 2005), an important gap junction protein. Gap junction proteins are responsible for relaying electrical impulses through the myocardium. The authors suggested that the reduced expression of these proteins may have resulted from the downstream effects of mutant lamin protein on gene expression, however a link between lamins and connexin 40 expression has not been demonstrated experimentally (Mounkes et al., 2005).

In contrast to the corresponding human diseases, in which a single mutated gene copy is sufficient to cause disease, both heterozygous *LMNA* $^{H222P/+}$ and *LMNA* $^{N195K/+}$ mice had a similar phenotype and life expectancy as wild-type mice. This apparent difference between human and mouse manifestation of mutations indicates that downstream effects of the mutation differ between humans and mice (Arimura et al., 2003). It also suggests that additional genetic or environmental factors may play a role in the progression of the disease in humans (Mounkes et al., 2005).

1.1.9. Pathophysiological hypotheses for diseases caused by *LMNA* mutation

It is not surprising that *LMNA* mutations cause disease given the strong evidence suggesting that A-type lamins have many important roles in the nucleus such as maintaining nuclear architecture, DNA replication, and mRNA transcription. What is intriguing is how a ubiquitously expressed gene gives rise to a variety of tissue-specific disorders, alternatively affecting skeletal muscles and tendons, cardiac muscle, adipose tissue, bone, and even neurons.

Two hypotheses have been proposed to explain how mutations in *LMNA* can result in tissue-specific laminopathies. Since A-type lamins play an important role in maintaining the structural integrity of the nuclear envelope, a widely held hypothesis is the Mechanical Stress, or Structural hypothesis. According to this hypothesis, *LMNA* mutations lead to structural abnormalities within the nuclear lamina, thereby compromising the integrity of the nuclear envelope and resulting in nuclear fragility (Sullivan et al., 1999, Hutchison et al., 2001, Broers 2004b, Parnaik et al., 2006). While the Structural model may explain the development of disease in mechanically stressed tissues, it cannot explain the abnormal distribution of fat characteristic of FPLD, or the neurological defects observed in CMT2 patients. These diseases are better explained by the second model, the Gene Regulatory hypothesis, which suggests that *LMNA* mutations may deregulate gene expression in a tissue-specific manner. The defects in gene expression could occur due to loss of specific attachment sites on the nuclear lamina for either heterochromatin or transcription factors, which are needed to establish particular patterns of gene expression (Cohen et al., 2001, Wilson et al., 2001). It has been suggested that the two hypotheses may not be mutually exclusive (Sylvius et al., 2005).

1.1.9.1. Structural (Mechanical Stress) Hypothesis

Evidence in support of the Structural hypothesis, both *in vivo* and *in vitro*, has been generated more readily as compared to the Gene Regulatory hypothesis. The most important *in vivo* finding has been the observation of nuclear envelope abnormalities in carriers of *LMNA* mutations. For instance, muscle biopsies from an EDMD patient with *LMNA* mutation p.R377H showed reduced expression of A-type lamins as well as structural abnormalities (nuclear blebs and loss of peripheral heterochromatin) in approximately 10-20% of nuclei (Reichart et al., 2004). Myocardial sections from DCM patients with *LMNA* mutations showed ultra structural nuclear envelope defects such as irregular shape and loss of peripheral chromatin, along with presence of chromatin outside the nuclear membranes (Verga et al., 2003). Furthermore, heart tissue sections of a DCM patient with *LMNA* mutation p.D192G presented with complete loss of nuclear envelope (Sylvius et al., 2005). Nuclear envelope alterations such as nuclear blebs, honeycomb appearance of lamin A/C at the nuclear poles, and lamin A/C intranuclear aggregates have also been shown in skin fibroblasts from EDMD and DCM patients carrying *LMNA* mutations (Muchir et al., 2004).

LMNA$^{-/-}$ mouse models and embryonic fibroblasts from *LMNA*$^{-/-}$ mice (MEF$^{-/-}$) have also provided support in favour of the structural hypothesis. *LMNA*$^{-/-}$ mice develop muscular dystrophy and dilated cardiomyopathy and died at 8 weeks of age (Sullivan et al., 1999). Cardiomyocytes from such mice demonstrated nuclear envelope abnormalities such as aberrant nuclear morphology (elongation and bizarre shape of nuclei), heterochromatin clumping, disorganization of cytoskeletal desmin proteins (which play an important role in linking the nuclear surface to the cytoskeleton), and detachment of the nucleus from the cytoskeleton in certain regions (Nikolova et al., 2004).

In another study, fibroblasts from the *LMNA*$^{-/-}$ mouse model showed nuclear envelope defects such as abnormal shape, loss of lamin B from one nuclear pole, and herniations in the nuclear envelope. When mechanical strain was applied to these cells, they showed increased nuclear deformation, nuclear fragility, and attenuated expression of strain-induced NF-κb regulated genes (Lammerding et al., 2004). NF-κb is a transcription factor that regulates the expression of genes that inhibit apoptosis in response to mechanical stress.

Broers et al. (2004a), used a novel cell compression device to measure resistance to mechanical strain in *LMNA*$^{-/-}$ murine embryonic fibroblasts (MEF$^{-/-}$). This device allowed simultaneous quantification of resistance to compression, together with visualization of cell deformation and damage using confocal microscopy. They demonstrated that MEF$^{-/-}$ cells had decreased resistance to compression, and lower bursting force as compared to MEF$^{+/+}$ cells. MEF$^{-/-}$ cells also showed disorganization of cytoskeletal proteins such as actin (microfilament proteins), microtubules, and vimentin (intermediate filament protein).

The results of these three studies suggest that A-type lamins are important for linking the nucleus to the cytoskeleton. It has been suggested that the interaction between the nucleoskeleton (including the lamina) and cytoskeleton is important for maintaining cellular resistance to mechanical stress (Broers et al., 2004a). Furthermore, such cells also have impaired expression of stress response genes. Together, these deficits may lead to premature cell death in contractile tissues (Broers et al., 2004b).

Various *in vitro* studies in cell systems expressing *LMNA* mutations have provided further proof of the structural effects of such mutations. Raharjo et al. (2001) showed that expression of mutant lamin A constructs (both EDMD and DCM mutations) in HeLa cells and *LMNA*$^{-/-}$ fibroblasts resulted in the formation of abnormal intranuclear lamin A

aggregates, mislocalization of emerin, and improper assembly of lamins in the nuclear lamina (Raharjo et al. 2001). Similarly, C2C12 (mouse myoblast cell line) myoblasts transfected with FLAG-tagged lamin A containing DCM- and EDMD-associated point mutations demonstrated aberrant localization of mutant lamins into large intranuclear aggregates and decreased nuclear rim staining (Ostlund et al., 2001). Furthermore, COS7 cells expressing the DCM-causing lamin A/C mutation p.D192G presented with the formation of abnormal aggregates in the nuclear lamina (Sylvius et al. 2005). These studies show that *LMNA* mutations can lead to abnormal lamin assembly, disruption of emerin, and may lead to aberrant nuclear morphology.

Given that not all DCM and EDMD patients carrying *LMNA* mutations have nuclear envelope abnormalities, the structural hypothesis alone cannot explain the pathogenesis of DCM and EDMD despite the evidence in its favour. For example, Sylvius et al. (2005) found a DCM patient with *LMNA* mutation p.R514S but no nuclear envelope abnormalities in cardiac tissue sections. Similarly Muchir et al. (2004) also reported EDMD patients with *LMNA* mutations p.R249Q, p.I63S but no nuclear envelope defects in the skin fibroblasts of affected individuals. Furthermore, it is unclear how mutations within the same domain of lamin A/C that are postulated to have similarly detrimental effects on the nuclear envelope can give rise to phenotypically distinct diseases. For example, p.R453W causes EDMD and p.R482W causes lipodystrophy. Both mutations are present in the C-terminal IgG domain of lamin A/C, and both are thought to disrupt interactions with the same lamin partners, and have similar effects on the lamina and nuclear envelope integrity (Vigouroux et al., 2001, Favreau et al., 2003). It is therefore evident that mechanisms other than structural aberrations are involved in the pathogenesis of DCM and EDMD.

Nuclear envelope abnormalities have not only been found in DCM and EDMD patients carrying *LMNA* mutations, but also in patients with other laminopathies. However, the role of structural abnormalities in causing disease has been difficult to establish in affected tissues that are not subjected to a substantial degree of mechanical stress, for example, adipose tissues in FPLD and Hutchinson-Gilford progeria syndrome (HGPS).

The majority of HGPS cases are caused by a *de novo* heterozygous mutation C-to-T at position 1824 in exon 11 of *LMNA*. This mutation does not cause an amino acid change (G608G), but activates a cryptic splice site, resulting in abnormal splicing, and consequent deletion of 150 nucleotides from the lamin A/C mRNA. This results in the production of lamin A/C protein missing 50 amino acids in the C-terminal domain. The deleted portion includes the cleavage site for prelamin A, resulting in the accumulation of mutant pre-lamin A (Scaffidi et al., 2005). Many nuclear architectural defects such as changes in nuclear shape, lobulation of nuclear envelope, thickening of the lamina, loss of peripheral chromatin, and clustering of nuclear pores have been found in cultured fibroblasts of HGPS patients with *LMNA* mutations (Goldman et al., 2004). It was observed that these defects in the nuclear envelope were more frequent with increasing number of cell passages, due to increased accumulation of mutant protein in the late passage cells. It has been proposed that accumulated mutant pre-lamin A in HGPS fibroblasts may become irreversibly attached to the nuclear membrane and act in a dominant-negative manner to disrupt nuclear lamina functions, culminating in the nuclear envelope defects seen in HGPS fibroblasts (Capell et al., 2006). This is supported by studies demonstrating that nuclear morphology can be greatly improved in HGPS fibroblasts by inhibition of abnormal splicing, blocking of farnesyl transferase activity (an enzyme responsible for targeting pre-lamin to the nuclear

membrane), or reducing the levels of mutant pre-lamin A (i.e., progerin) by RNA interference (Scaffidi et al., 2005, Pranaik et al., 2006). Unlike diseases such as DCM or EDMD in which structurally stressed tissues are affected, it is less evident how nuclear envelope defects in HGPS patients can lead to pre-mature aging. One possibility is that gene expression is detrimentally affected by either nuclear pore defects that lead to deregulation of RNA and protein trafficking across the nuclear envelope, or by loss of peripheral chromatin (Goldman et al., 2004).

Similarly, nuclear envelope defects have been found in skin fibroblasts from FPLD patients carrying *LMNA* mutations. These include dysmorphic nuclei with occasional budding, honeycomb expression of A-type lamins, loss of lamin B from nuclear buds or nuclear poles, and loss of DNA staining from the buds. The fibroblasts from FPLD patients were also found to be more sensitive to heat shock, i.e. presented with more extensive nuclear deformations, as compared to treated control cells, or untreated FPLD fibroblasts (Vigouroux et al., 2001). However, the mechanical stress hypothesis is inadequate to explain how *LMNA* lamin mutations cause lipodystrophy, since adipose tissue is unlikely to experience the same degree of mechanical stress as cardiac or skeletal muscle cells. Instead, it is possible that expression of adipocyte-specific genes is adversely affected. Indeed, lamins have been shown to interact with Serum Response Element Binding Protein (SREBP), a transcription factor that regulates the expression of genes involved in adipogenesis (REF). Furthermore, some FPLD-causing mutations have been shown to abrogate the interaction of lamins with SREBP (Llyod et al., 2004). Alternatively, Raharjo et al. (2001) suggested that nuclear envelope defects caused by *LMNA* mutations may make the cells more prone to apoptosis due to loss of attachment sites at the nuclear periphery for

proteins that protect against apoptosis. Meaburn et al. (2007) provided support for this hypothesis by demonstrating that FPLD-causing mutations lead to increased apoptosis.

1.1.9.2. Gene Regulatory Hypothesis

Despite the evidence in support of the Structural hypothesis, recently, a number of studies have been published supporting the Gene Regulatory hypothesis. Zastrow et al. (2005) reported that the C-terminal Ig-fold domain of lamin A/C interacts with nuclear titin, a protein involved in chromosome organization, and that the *LMNA* mutations p.R527P and p.R482Q (which cause EDMD and FPLD, respectively) attenuate the interaction of lamin A with titin by 50%. Furthermore, Stierle et. al. (2003) demonstrated that lamin A/C dimers (411-533) interact with DNA, and that this interaction is disrupted by mutations in this site (i.e., the FPLD-causing mutations p.R482Q and p.R482W).

Insights into the role of DCM-causing *LMNA* mutations on cardiac gene expression have been provided by the $LMNA^{N195K/N195K}$ mouse model. These mice demonstrated reduced expression of Hf1b/SP4, a transcription factor that plays an important role in the development of the cardiac conduction system. Furthermore, expression of GATA-4 regulated genes such as atrial natriuretic peptide (ANP) and B-type natriuretic peptide (BNP) was upregulated. Further support in favour of the Gene Regulatory hypothesis was provided by the observation that the p.D192G mutant lamin A/C aggregate affected the intranuclear distribution of SUMO-1 such that SUMO-1 was mislocalized within lamin A/C aggregates (Sylvius et al., 2005). SUMO-1 is involved in post-translational modification of several proteins, many of which are transcription factors (Muller et al., 2001, Seeler et al., 2003).

LMNA mutations may also cause disease by disrupting the regulated expression of genes involved in tissue-specific differentiation pathways. These effects will be discussed in the following sections.

1.1.9.2.1. Effect of *LMNA* mutations on skeletal muscle differentiation

Studies have shown that *LMNA* mutations may lead to the decreased or delayed expression of genes necessary for the initiation and maintenance of differentiation, thus explaining how mutations may lead to skeletal muscle diseases (Pranaik et al., 2006). Indeed, some groups have studied the effect of *LMNA* mutations on skeletal muscle differentiation. Favreau et al. (2004) analyzed the effect of the EDMD-causing mutation p.R453W on C2C12 muscle differentiation. They found that C2C12 cells expressing mutant lamin A had reduced capacity for differentiation and formation of multinucleate fibers. These cells also demonstrated reduced expression of myogenic markers such as myogenin and cathepsin, improper exit from the cell-cycle, an increased pool of hyperphosphorylated retinoblastoma protein (pRB) (which is normally hypophosphorylated during myogenesis), and an increased propensity for apoptosis (Favreau et al., 2004). Other EDMD-causing mutations such as G232E, Q294P, and R386K have also been shown to impair the C2C12 cell differentiation (Pranaik et al., 2006).

Favreau et al. (2004) suggested two possible mechanisms by which *LMNA* mutations may impair the differentiation of C2C12 myoblasts. First, lamin A/C may interact with pRB protein (Johnson et al., 2004), which is required for proper differentiation of many cells, such as skeletal muscle cells and adipocytes. During differentiation, the cyclin-dependant kinase inhibitor p21 prevents phosphorylation of pRB. The hypophosphorylated form of

pRB binds to transcription factor E2F and represses its transcriptional activity (Flemington et al., 1993, Favreau et al., 2004). This in turn represses the synthesis of proteins required for entry into S phase, ultimately leading to cell cycle arrest. Following cell-cycle arrest, cells undergo differentiation to form multinucleated myotubes. Lamin A/C has been shown to control the stability, nuclear localization and activity of pRB (Johnson et al., 2004), therefore *LMNA* mutations may inhibit differentiation by deregulating pRB function (Favreau et al., 2004, Johnson et al., 2004).

The second possible mechanism invokes the importance of the nuclear lamina in organizing the chromatin remodeling events necessary for proper gene regulation during myogenesis, i.e., anchoring of chromatin and migration of proteins involved in gene silencing or activation (e.g., histone acetyl transfereases, histone deacetylases or methyl transferases). *LMNA* mutations may therefore inhibit myogenesis by affecting the structure of the nuclear lamina, thereby impairing normal chromatin remodeling. Disruption of these processes can inhibit the expression of genes required for differentiation. This hypothesis is supported by the observation that expression of myogenin is reduced in C2C12 cells expressing EDMD causing *LMNA* mutation p.R453W (Favreau et al., 2004, Hakelien et al., 2008). Hakelien et al. (2008) provided further evidence for this hypothesis by demonstrating that the chromatin remodeling processes required for activation of the myogenin promoter are disrupted in C2C12 cells differentiated in the presence of mutated lamin. They showed that the promoter of myogenin was maintained in a repressive state by persistent H3K9 dimethylation, which is associated with reduced gene expression. Furthermore, trimethylation of H3K4, which is associated with active gene expression, failed to occur in cells carrying mutant lamin.

These results suggest that EDMD-causing *LMNA* mutations may cause disease by: impairing 1) the ability of muscle cells to express muscle-specific genes such as myogenin; 2) the function of genes such as pRB that are involved in regulating differentiation. Either or both of these mechanisms will inhibit the ability of myoblasts to differentiate normally into myotubes. Furthermore, the repair and maintenance of myotubes will also be detrimentally affected because these processes also require cell differentiation. Together, these aberrations may lead to the muscle degeneration evident in EDMD.

1.1.9.2.2. Effect on adipocyte differentiation

The effect of *LMNA* mutations on adipogenesis has been studied by three different groups. Lloyd et al. (2004) demonstrated that the C-terminal domain of lamin A/C interacts with Sterol Regulatory Element Binding Protein 1 (SREBP1), a transcription factor that regulates the expression of genes involved in adipogenesis. It consists of an N-terminal transcription factor domain which is separated from the C-terminal regulatory domain by two transmembrane domains. It resides in the endoplasmic reticulum, and in response to low cholesterol, undergoes proteolytic cleavage by SREBP cleavage activating protein (SCAP). The cleaved N-terminal transcription factor enters the nucleus, and regulates the expression of genes involved in adipogenesis. Furthermore, these authors also demonstrated that *LMNA* mutations responsible for FPLD reduced interactions of lamin A/C with the transcription factor SREBP1 (Lloyd et al., 2004). This suggested that lamin A/C may be involved in stabilizing SREBP1, and that *LMNA* mutations may affect adipogenises by disrupting SREBP function.

However, this interpretation has recently been challenged by Cappani et al. (2005), who used an *in vivo* co-precipitation assay with lamin A/C antibody to show that lamin A/C does not interact with SREBP1. Instead, they reported evidence indicating that SREBP1 binds specifically to pre-lamin A, and not mature lamin A/C. It was also demonstrated that there was an increased amount of pre-lamin A in fibroblasts from FPLD patients as compared to control individuals. Furthermore, SREBP1 was found to be sequestered by pre-lamin A at the nuclear periphery in fibroblasts from these patients, as compared to being more uniformly distributed in the nucleus of control cells. Such sequestration reduced the size of the active SREBP pool in the nucleus, leading to reduced expression of peroxisome proliferator activated receptor gamma 2 (PPARγ) (involved in adipocyte differentiation). Consequently, adipocyte differentiation was inhibited (Cappani et al., 2005, Capell et al., 2006).

A third viewpoint was offered by Boguslavasky et al. (2006). They observed that overexpression of *LMNA* inhibits differentiation of 3T3-L1 cells into fat-containing adipocytes *in vitro*. This observation suggested that lamin A is an inhibitor of adipocyte differentiation. This was further supported by the observation that $LMNA^{-/-}$ fibroblasts had an increased ability to form adipocytes as compared to wild-type $LMNA^{+/+}$ cells. FPLD-causing *LMNA* mutations may therefore act as "gain-of-function" mutations, with a higher affinity for binding to an unidentified pro-adipogenic factor. This interaction may sequester the factor at the nuclear periphery, thereby inhibiting expression of genes involved in adipogenesis (Boguslavsky et al. 2006). It has been speculated in a recent review that the pro-adipogenic factor may in fact be SREBP1 (Parnaik et al., 2006).

Despite the differing results from the three studies, it is clear that *LMNA* mutations affect adipocyte differentiation, most likely through effects on SREBP1. It remains unclear whether it is pre-lamin or mature lamin that is responsible for the aberrant activity of SREBP1. Furthermore, it has yet to be confirmed whether SREBP1 is affected by lamin A/C through sequestration at the nuclear periphery, or through direct interaction and stabilization of the protein.

1.2. Rationale and Research Questions

1. The mechanisms by which *LMNA* mutations cause DCM are not well characterized, although there are considerably more data available in support of the structural hypothesis. To date, a number of case studies have indicated the presence of nuclear ultrastructural abnormalities in DCM patients with *LMNA* mutations (Verga et al., 2003, Sylvius et al., 2005). However, a comprehensive study of the relationship between *LMNA* mutations in DCM patients and nuclear structural abnormalities has not yet been conducted. Such an investigation is important to assess the relative importance of structural defects in DCM pathogenesis in patients with *LMNA* mutations. This is a prerequisite for further studies of the mechanisms by which *LMNA* mutations cause DCM.

2. There exists evidence that the structural hypothesis cannot explain the presence of DCM in all patients with *LMNA* mutations. Even prior to the results of our genotype-phenotype study, at least one report described a DCM patient with *LMNA* mutation p.R514S and no evidence of nuclear structural defects (Sylvius et al., 2005). This suggests an alternative mechanism by which *LMNA* mutations cause DCM in at least some patients. There is

preliminary evidence that this mechanism may involve changes in cardiac gene expression. For example, A *LMNA* mutant mouse model of DCM demonstrated misregulation of some cardiac genes (Mounkes et al., 2005). As well, our group showed that the distribution of SUMO-1, a moiety attached to a number of cardiac transcription factors, is disturbed by DCM-causing *LMNA* mutation p.D192G. Finally, *LMNA* mutations causing other laminopathies have been shown to disrupt gene regulation. Taken together, these findings suggest, but are not conclusive, in implicating disrupted cardiac gene expression as a possible pathogenic mechanism of *LMNA* mutations in DCM. Studies designed to measure cardiac gene expression in the presence of *LMNA* mutations are therefore important to further our understanding of how *LMNA* mutations cause DCM.

1.3. Research Objective

The overall objective of this research was to show that *LMNA* mutations can cause DCM by both the proposed mechanisms outlined earlier, i.e., by causing structural abnormalities within the nuclear lamina, and also by affecting tissue specific transcription factors.

CHAPTER 2

A LARGE DELETION IN LAMIN A/C GENE ASSOCIATED WITH CARDIOMYOCYTE NUCLEAR ENVELOPE DYSRUPTION IN PATIENTS WITH DILATED CARDIOMYOPATHY

Pallavi Gupta[a], Zofia T. Bilinska[b], Nicolas Sylvius[a,c], Emilie Boudreau[a], John P. Veinot[d], Sarah Labib [a], Pierrette M. Bolongo[a], Akil Hamza[a], Tracy Jackson[a], Rafal Ploski[e], Michal Walski[f], Jacek Grzybowski[b], Ewa Walczak[g], Grzegorz Religa[h], Anna Fidzianska[i] and Frédérique Tesson[a]

Article in press for the journal *Basic Research in Cardiology*

[a] Faculty of Health Sciences University of Ottawa, 451 Smyth, Ottawa ON K1H 8M5, Canada

[b] 1st Department of Coronary Artery Disease, Institute of Cardiology, Alpejska 42, 04-6 28 Warsaw, Poland

[c] Present address: Department of Biochemistry University of Leicester, Leicester LE1 9HN, UK

[d] Department of Pathology and Laboratory Medicine, University of Ottawa, Anatomical Pathology, Ottawa Hospital, Ottawa ON K1Y 4E9, Canada

[e] Department of Medical Genetics, Warsaw Medical University, Pawinskiego Street 3c, 02-106 Warsaw, Poland

[f] Department of Cell Ultrastructure, M Mossakowski Medical Research Centre, Polish Academy of Science, Pawinskiego Street 5, 02-106 Warsaw, Poland

[g] Department of Pathology, Institute of Rheumatology, Spartanska 1, 02-637 Warsaw, Poland

[h] 2nd Department of Cardiac Surgery, Institute of Cardiology, Alpejska 42, 04-628 Warsaw, Poland

[i] Neuromuscular Unit, Medical Research Center, Polish Academy of Science, ul.Pawińskiego 5, 02-097 Warsaw, Poland

Running Title: Cardiomyocyte Nucleus in DCM patients and Mutations in *LMNA* and *TMPO*

Correspondance to: Frédérique Tesson, PhD, Faculty of Health Sciences University of Ottawa, 451 Smyth, Ottawa ON K1H 8M5, Canada, tel: 613 562 5800 x 7370, fax: 613 562 5632, email: ftesson@uottawa.ca

2.1. Abstract

Major nuclear envelope abnormalities, such as disruption of nuclear envelope and/or presence of cytoplasmic organelles within the nucleus, have rarely been described in cardiomyocytes from DCM patients. In this study, we screened a series of 25 unrelated DCM patient biopsies for cardiomyocyte nuclear abnormalities. *LMNA* and *TMPO,* two genes encoding respectively lamin A/C and thymopoietin that are involved in maintaining nuclear envelope architecture, were found mutated in DCM patients. We therefore, screened *LMNA* and *TMPO* for mutations in an attempt to perform genotype-phenotype correlation.

Among the 25 heart biopsies investigated, we identified major cardiomyocyte nuclear abnormalities in 8 patients. Direct sequencing allowed the detection of 3 heterozygous *LMNA* mutations, one novel (p.Q353K,) and two that have been previously reported (p.D192G and p.R541S). By Multiplex Ligation-dependent Probe Amplification (MLPA)/quantitative real-time PCR, we found a heterozygous deletion encompassing exons 3-12 of the *LMNA* gene in one patient. Immunostaining demonstrated that this deletion led to a decrease in lamin A/C expression in cardiomyocytes from this patient. The patient with the *LMNA* deletion and the carrier of the p.D192G mutation displayed major cardiomyocyte nuclear envelope abnormalities, while the patients carrying p.Q353K and p.R541S mutations did not show any specific nuclear envelope abnormalities. None of the DCM patients included in the study carried a mutation in the *TMPO* gene.

Taken together, we found no evidence of a genotype-phenotype relationship between the onset or the severity of DCM, the presence of nuclear abnormalities, and the presence or position of *LMNA* mutations. We demonstrated that lamin A/C haplo-insufficiency caused by a large deletion in *LMNA*, and documented by reduced levels of the protein in the nuclear

envelope, can lead to cardiomyocyte nuclear envelope disruption, and thus underlie the pathogenesis of DCM.

Key words: lamin A/C, thymopoietin, mutation, dilated cardiomyopathy, cardiomyocyte, nucleus ultrastructure

2.2. Introduction

Dilated cardiomyopathy (DCM) is characterized by dilatation of cardiac chambers and impaired contraction. Severity of symptoms and age of onset are highly variable. To date, mutations in 28 genes have been associated with autosomal dominant DCM [3, 9, 10, 11, 18, 20, MIM#115200;]. *LMNA,* which encodes lamin A/C, is one of the most commonly implicated genes in DCM. Mutations in *LMNA* are associated with a high risk of dysrhythmia, sudden death and heart failure [4]. Furthermore, symptomatic DCM patients carrying *LMNA* mutations display a worse prognosis than other genetics forms of DCM [2, 17, 20, 27, 42, 44, and 46].

The A-type lamins A and C, alternatively spliced products from *LMNA*, are type V intermediate filament proteins expressed in terminally differentiated somatic cells. They are components of a thin filamentous meshwork - the nuclear lamina - underlying the nucleoplasmic side of the inner nuclear membrane, and are also present in the nucleoplasm [8, 21, 29, and 31]. Lamins have traditionally been considered key components in providing structural support to the nucleus and anchoring chromatin and nuclear pore complexes to the nuclear envelope [25, 39, 48, and 50]. Intranuclear lamins have proposed functions in DNA replication [21, 26, 29, and 31], transcription [40], and chromatin organization [37]. In order to carry out their functions, lamins interact with a number of nuclear envelope proteins, chromatin and transcription factors. Among the genes encoding the lamin A/C interacting proteins, *TMPO*, the gene encoding nucleoplasmic thymopoietin alpha (also called lamina-associated polypeptide 2 (LAP2) alpha) has been shown to harbour a mutation in DCM patients [45]. The identified mutation occurred in the C-terminal domain of thymopoietin alpha, a region known to interact with lamin A/C (residues 319-566) [9]. Three thymopoietin

isoforms, alpha, beta, and gamma are encoded by *TMPO* [6]. The three isoforms share an identical amino terminal sequence but have divergent carboxy terminal sequences [9]. Thymopoietin is thought to play an important role in maintaining nuclear architecture through its binding with lamins and other proteins.

Cardiomyocytes from some DCM patients with *LMNA* mutations exhibit the following characteristics: i) reduced lamin A/C expression in myocyte nuclei; ii) nuclear envelope damage, such as focal disruptions, blebs, and nuclear pore clustering; and/or iii) dramatic morphologic alterations, including a complete loss of the nuclear envelope and accumulation of mitochondria, glycogen and/or lipofuscin in the nucleoplasm (in a DCM patient carrying the p.D192G *LMNA* mutation) [2, 7, 13, 42, 49]. However, in non-genotyped DCM patients as well as in heart failure patients, minor nuclear defects such as irregular nuclear envelope, enlarged and bizarre shaped nuclei, giant and multiple nucleoli and irregularly distributed chromatin are commonly found [1, 4, 34, 36]. There is considerable heterogeneity in the abnormalities observed from one cardiac sample to the next as well as within one particular sample [1, 36].

The aim of the present study was to ascertain whether: 1) major nuclear envelope abnormalities are a common finding in patients with DCM; 2) presence of *LMNA* and/or *TMPO* mutations are associated with nuclear envelope defects in cardiomyocytes from a series of 25 unrelated DCM patients; and 3) there is a correlation between the presence of *LMNA* and/or *TMPO* gene mutations, presence of nuclear envelope defects and DCM severity

2.3. Materials and methods

2.3.1 Patient recruitment

Written informed consent was obtained for all patients in accordance with study protocols approved by the hospital ethics committees (Ottawa Heart Institute, Ottawa, Canada and Institute of Cardiology, Warsaw, Poland. Diagnosis of DCM was established based on WHO/ISFC criteria modified by Mestroni and colleagues [28] that included severe LV systolic dysfunction (LV dilatation exceeding 117% of normal value corrected for age and body surface area) and LV ejection fraction (LVEF) ≤ 45% measured in angiography, without significant coronary artery disease (> 50% lumen diameter reduction of one of the main coronary arteries), hypertension, or acquired or congenital heart disease. All patients underwent clinical examination, evaluation of functional status according to NYHA classification, ECG study, two-dimensional echocardiography with Doppler, and coronary angiography to exclude coronary artery disease. Left ventricular enlargement was calculated according to the method of Henry. A total of 25 index cases recruited in Canada and Poland were enrolled in the study.

2.3.2 Cardiac tissue collection, electron microscopy, and immunostaining

Cardiac tissue samples were collected from endomyocardial biopsies performed on clinical indication. Biopsies were immediately processed in 1.6-3% gluteraldehyde. Fixed heart tissues were processed into thick and thin sections and the tissue sections were examined with a Hitachi 7100 or JEM 1200EX electron microscope.

For indirect immunofluorescence examinations, 8 μm cryostat sections were stained with 3 monoclonal antisera against lamin A/C (NCL-LAM-A/C) (Novocastra Laboratories, Newcastle, UK); AC2 and A4, kindly provided by Dr. Hutchison (Department of Biological

Science, University of Dundee, UK)). A4 antibody detects only lamin A as its recognition site lies after amino acid 572. NCL-LAM-A/C and AC2 recognize both lamin A and lamin C. In brief, antibodies diluted 1:10 were applied to tissue sections for 60 minutes. Sections were rinsed with PBS and incubated for another 60 minutes with the appropriate Rhodamine Red X conjugated goat anti-rabbit IgG secondary antibody diluted 1:30 with PBS. After being washed with PBS, the sections were mounted in gelmount and viewed with an Opton Zeiss standard LAB16 microscope with epifluorescence optics.

2.3.3. Screening of *LMNA* and *TMPO* coding sequences

Genomic DNA was isolated from white blood cells (Qiagen Flexigene kit). To screen for somatic mutations, DNA was extracted from cardiac tissues using a Qiamp Mini DNA extraction kit (Qiagen).

Intronic oligonucleotide primers flanking each of the exons were designed based on published sequences (Genbank accession number: L123399, L12400, and L12401 for *LMNA*, and UCSC genome bioinformatics database for *TMPO*). All DNA samples were subjected to PCR and direct sequencing (ABI Prism Big Dye, ABI PRISM 3100 genetic analyzer). If there was any suspicion of genomic variation in a given patient, another sample of DNA collected independently was systematically double-strand sequenced. PCR conditions and primer sequences are available upon request. Sequences were compared to two control samples from individuals without known cardiovascular disease. Each sample's electropherogram was analyzed by two independent investigators.

Multiplex-ligation dependent probe amplification (MLPA) analysis was performed to screen for deletions and duplications in the *LMNA* gene coding sequence according to the

manufacturer's instructions (SALSA MLPA KIT Po48 LMNA, MRC Holland). The probe mix contained probes for 10 of the 12 coding exons of *LMNA*, but not for exons 5 and 9 because of the close proximity of exons 4 and 5, and exons 8 and 9. The probe mix also contained 13 probes for other human genes. Three of these probes recognize genes localized on chromosome 1. One of these probes was located 94 kb upstream of *LMNA* exon 1, and another 100 kb downstream of *LMNA* exon 12. MLPA amplification products were analyzed on an ABI model 3130XL Genetic Analyzer (Applied Biosystems) with the GeneMapper software V.3.7, using Genescan 500LIZ internal size standard (Applied Biosystems). Each peak in the electropherogram corresponded to the amplification product of a specific exon. Each patient's electropherogram was compared to three controls. We used the Coffalyzer MLPA DAT (MRC-Holland) software to analyze MLPA data. Resulting normalized ratios were ~ 1.0 for every wild-type peak, 0.5 for heterozygous deletions, and 1.5 for heterozygous duplications.

Quantitative real-time PCR was used to confirm the deletion found in *LMNA* (Roche LightCycler 2.0) [35]. Primers were designed for *LMNA* exon 9 (forward: 5'-*ggagcgctggggtaagtgtc*-3'; reverse: 5'-*ctcgtccagcaagcagcccag*-3'). PCR was set up in capillaries in a total volume of 20 μl; each PCR mixture contained 2.5 mM of $MgCl_2$ (2.5 mM), 2 μl of Sybr green mix, 0.6 μM of mixture of forward and reverse primers, and 20 ng of DNA. Standard curves for both the housekeeping gene (β2-microglobulin) and target gene were generated. Two different types of sample DNA (i.e., one sample from the DCM patient carrying the deletion and one sample from a DCM patient without the deletion) were utilized to ensure that the gene dosage ratio of the target to the housekeeping gene was disrupted only when a deletion was present. Using the slope and y-intercept of the standard curve, the

LightCycler system calculated the concentrations (M) of sample and control DNA for both the reference gene (Beta-2 microglobulin) and the target gene (Lamin A/C). These concentrations were then used to calculate the gene dosage ratio using the following equation:

$$R = \frac{M_{target}(patient)/M_{reference}(patient)}{M_{target}(control)/M_{reference}(control)}$$

where R = 0.5 (0.4-0.7) indicates deletion; R = 1 (0.8-1.2) indicates normal copy number and R= 1.5 (1.3-1.7) indicates duplication.

2.3.4. Statistical analysis

Left ventricular ejection fraction (LVEF) and Left ventricular end diastolic diameter LVEDD in % values (measure of severity of DCM) were compared between patients with major cardiomyocyte nuclear abnormality and patients with non-specific cardiomyocyte nuclear abnormality using a 2-tailed Student's *t* test (level of significance: 5%).

2.4. Results

2.4.1. Ultrastructural characteristics of endomyocardial biopsies

Ultrastructural analysis of endomyocardial samples enabled us to distinguish two groups of DCM patients. One group consisted of 8 individuals exhibiting major nuclear envelope abnormalities on electron micrographs (Figure 2.1), and the second consisted of 17 patients with minor and non-DCM specific abnormalities.

Among the patients with nuclear envelope defects, the proportion of defective cells ranged from a small percentage to as much as 30% (patient 2 and 6). The most obvious abnormality, occurring in 4 of 8 patients, was intrusion and accumulation of mitochondria and other cytoplasmic organelles into the nuclear matrix (patients 1, 2, 5, and 7) (Figure 2.1A, 1D). The membranes of these organelles appeared discontinuous from the nuclear envelope (Figure 2.1A and 2.1D). The nuclear envelope was usually irregular (Figure 2.1A, 2.1B, and 2.1C) and partially disrupted or totally missing in 6 of 8 patients (patients 1, 2, 4, 5, 6, and 7) (Figure 2.1A, 2.1C, 2.1D). Chromatin disorganization was also observed (patients 2 and 6). In contrast, samples from the 17 patients in the second group displayed modest and non-specific nuclear membrane alterations, such as nuclear irregularity, that are commonly found in DCM patients regardless of the presence of *LMNA* mutations (Figure 2.1E and 2.1F).

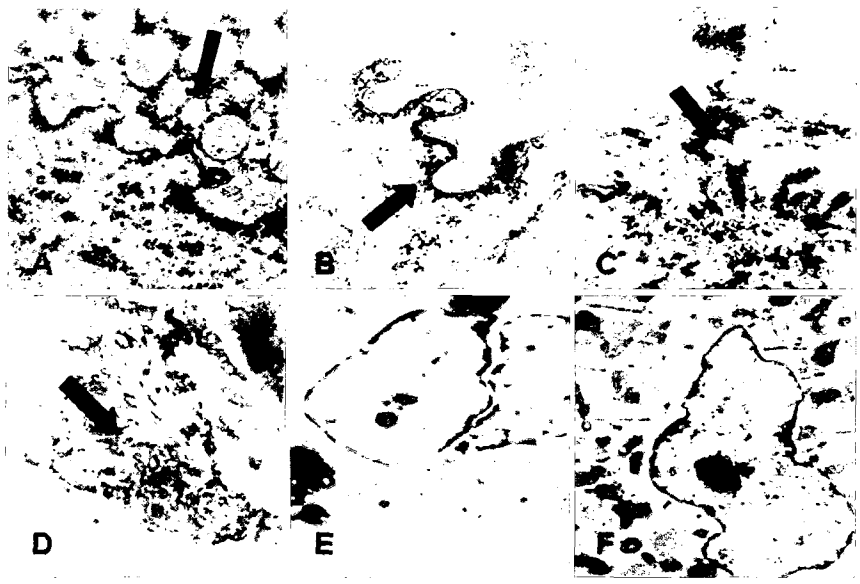

Figure 2.1: Electron micrographs of cardiomyocytes from dilated cardiomyopathy patients with or without *LMNA* mutation. A, B, C and D: Major nuclear abnormalities in respectively patient 1, 3, 4 and 5 (Table 2.1). Patient 1 carried the *LMNA* deletion exons 3-12, while patients 3, 4 and 5 had no *LMNA* nor *TMPO* mutation; A: accumulation of mitochondria around the nuclear envelope; B: blebbing of the nuclear envelope and separation of the inner and the outer nuclear membrane; C: extrusion of nucleoplasm from the cardiomyocyte nucleus into the cytoplasm; D: accumulation of cytoplasmic organelles in the nucleoplasm: E: non-specific nuclear alteration in patient 10 (Table 2.1) carrying the p.Q353K *LMNA* mutation; F: non-specific alterations in dilated cardiomyopathy patient 14 (Table 2.1) with wild-type *LMNA* and *TMPO*. (Original magnifications: A, 20,000X; B, 18,000X; C, 12,000X; D: 10,000X; E: 4,000X; and F: 4,000X)

2.4.2. Clinical characteristics of the patient cohort

Clinical characteristics of the 25 DCM patients (19 males and 6 females) included in our study are shown in Table 2.1. There was considerable heterogeneity in terms of the clinical characteristics and severity of DCM across the cohort of 25 patients.

In the group of 8 patients who exhibited nuclear envelope abnormalities, age at disease onset ranged from 14 to 63 years, 4 patients had a family history of DCM (Table 2.1, Figure 2.1, and 43), while none had a suspicion of muscular dystrophy. Disease severity ranged from mild DCM to progressive heart failure, and LVEF values ranged from < 10% to 50%. Various arrhythmias were present in all eight patients; 2 patients required ICD (patient 1 and 7) and 1 required pacemaker (patient 5). Three patients had received a heart transplant (patients 4, 5, and 6) and two patients had died of heart failure (patients 2 and 3). In addition, patient 5 presented with hypothyroidism and patient 7 with mild mental retardation. No other phenotypic abnormality was identified within this population.

A similar degree of heterogeneity was also observed among the 17 patients with no major nuclear envelope abnormalities: age at disease onset ranged from 12 to 61 years, 10 patients had a family history of DCM (Table 2.1, Figure 2.1, and [43]), 1 patient had documented skeletal myopathy (patient 10), and 1 had elevated CPK values (up to 600 U/I (patient 18)). LVEF values ranged from 10% to 38%; conduction defects were present in all but two patients (data were not available for 4 patients), four patients required ICD, and two had pacemakers. Twelve patients had received heart transplants and two patients had died of heart failure (patients 13 and 21).

We compared mean LVEF and LVEDD in % values between patients exhibiting major nuclear envelope abnormalities and patients with minor and non DCM-specific

abnormalities. No significant correlation between the severity of the phenotype and the presence of nuclear envelope defect was detected ($p>0.05$).

Table 2.1: Patients' clinical characteristics at the time of the biopsy, *LMNA* mutation status, and nuclear envelope defect

Patient	LMNA Mutation	Family History	Nuclear Envelope Defect	Sex / Age at onset (years)	NYHA Class	Echocardiography	Weight (kg)/Height (cm)/LVEDD in %	Dysrhythmias	Clinical Status
MAJOR NUCLEAR ENVELOPE DEFECTS AND LMNA MUTATION									
1	Deletion exons 3-12	Yes	Irregular and broken nuclear envelope; accumulation of mitochondria within and around the nuclei.	F/39	II	LVEDD 54mm, LVEF 50%	57/164/120.0	nsVT, couplets, frequent VE, ICD	Mild progressive HF No MD
2*	p.D192G (c.575A>G)	Yes	Complete loss of nuclear envelope, accumulation of mitochondria, glycogen and/or lipofuscin in the nucleoplasm, chromatin disorganization	M/26	IV	LVEDD 60mm, LVEF 20%	67/175/127.2	1 AVB, LAFB	Died at 27 while awaiting for a heart transplant No MD

MAJOR NUCLEAR ENVELOPE DEFECTS AND NO LMNA MUTATION									
3	No	Yes	Blebbing of nuclear envelope, separation of inner and outer nuclear membrane	M/63	III	LVEDD 64mm, LVEF 26%	71/180/136.5	SVT, VT	Died of progressive HF, 4 years after diagnosis No MD
4	No	Yes	Extrusion of nucleoplasm from the cardiomyocyte nucleus into the cytoplasm	M/21	III	LVEDD 75 mm, LVEF 25%	80/176/153.7	nsVT	HTx at 24 No MD
5	No	No	Irregular nucleus border; lack of nuclear membrane, presence of mitochondria within nuclear matrix	M/29	III	LVEDD 59 mm, LVEF 30%	84/176/120.5	RBBB, LPFB, nsVT, Pacemaker at 32	Progressive HF, HTx at 40 No MD
6	No	No	Local disruption of nuclear envelope, chromatin disorganization	F/14	IV	LVEDD 64 mm, LVEF<10%	55/152/144.7	recurrent VT/VF	HTx at 14 No MD
7	No	No	Misshapen nuclei, local disruption of nuclear	M/14	III	LVEDD 71 mm, LVEF 20%	57/168/155.6	nsVT, couplets, frequent VE, ICD at 20	Progressive HF No MD

			envelope, penetration of mitochondria into nucleus						
8	No	No	Irregular shape of nuclei	M/18	III	LVEDD 68mm, LVEF 20%	47/160/156.0	LBBB, nsVT	Progressive HF No MD
NON SPECIFIC NUCLEAR ENVELOPE DEFECTS AND LMNA MUTATION									
9*	p.R541S (c. 1621C>A)	Yes	No	M/12	IV	LVEDD 64mm, LVEF 25%	49/152/147.3	NA	HTx at 13 No MD
10	p.Q353K (c.1057C >A)	Yes	No	M/38	IV	LVEDD 62mm, LVEF 22%,	59/163/138.1	ICD	HTx at 38 Skeletal myopathy
NON SPECIFIC NUCLEAR ENVELOPE DEFECTS AND NO LMNA MUTATION									
11	No	Yes	No	M/27	II	LVEDD 60mm, LVEF 38%	100/186/117.2	permanent AF, single VE	Improved after AF ablation, LVEF 45% No MD
12	No	Yes	No	M/26	III	LVEDD 75mm, LVEF 20%	73/183/154.8	single VE	Stable HF No MD
13	No	Yes	No	M/40	NA	LVEDD 77mm, LVEF 19%	73/168/164.3	ICD, pacemaker	Died age 59, poor candidate denied for HTx No MD
14	No	Yes	No	F/14	IV	LVEDD 58mm,	37/155/139.4	No	HTx at 14

						LVEF14%			No MD
15	No	Yes	No	M/36	II	LVEDD 78mm, LVEF 25%	94/185/154.9	single Vex	Stable HF No MD
16	No	Yes	No	M/27	III	LVEDD 78mm, LVEF 10%	72/186/160.7	Sinus tachycardia	HTx within several months No MD
17	No	Yes	No	M/34	IV	LVEDD 78mm, LVEF 20%	73/178/163.1	I-degree AVB	Fulminant HF leading to HTx within several months No MD
18	No	Yes	No	M/35	III	LVEDD 58mm, LVEF 15%	80/170/121.1	Frequent sVT	Atrial septal aneurysm; HTx at 39 No MD CPK value up to 600 U/I
19	No	No	No	F/13	NA	LVEDD 69mm, LVEF10%	41/164/160.3	NA	HTx at 13 No MD
20	No	No	No	F/61	NA	LVEDD 69mm, LVEF 12%	88/165/145.3	ICD	Pericarditis, HTx at 62 No MD
21	No	No	No	M/54	III	LVEDD 88mm, LVEF 20%	109/175/175.1	Pacemaker	Died at 60,

									waiting for HTx No MD
22	No	No	No	M/40	III-IV	LVEDD 68mm, LVEF27%	71/160/147.8	No	HTx at 62 No MD
23	No	No	No	M/27	NA	LVEDD96mm, LVEF 13%	70/170/203.8	ICD	HTx at 57 No MD
24	No	No	No	F/12	NA	LVEF 13%	42/153/NA	NA	HTx at 12 No MD
25	No	No	No	M/20	NA	LVEF 13%	86.5/197/NA	NA	HTx at 22 No MD

Clinical characteristics and mutation carried were previously described for patients 2 and 9 [7, 42].

Note: AF, atrial fibrillation; AVB, atrioventricular block; HF, heart failure; HTx, heart transplantation; ICD, implantable cardioverter defibrillator; LAFB, left anterior fascicular block; LPFB, left posterior fascicular block; LVEDD, left ventricle end diastolic diameter; LVEF, left ventricle ejection fraction; MD, muscular disease; NA, not available; RBBB, right bundle branch block; VEX, ventricular extrasystole; VE, ventricular ectopy; VT, ventricular tachycardia; nsVT, nonsustained ventricular tachycardia; SVT: supraventricular tachycardia; VT/VF, ventricular tachycardia/ventricular fibrillation.

2.4.3. Screening of *LMNA* and *TMPO* coding sequences

We screened the complete coding sequence as well as the intron-exon boundaries of *LMNA* (12 exons) and *TMPO* (8 exons) for mutations using direct sequencing of DNA extracted from white blood cells of all 25 patients. We identified three patients with *LMNA* mutations, one in the group with major nuclear envelope defects (patient 2, p.D192G) and two in the group with non-specific nuclear envelope abnormalities (patient 9, p.R541S and patient 10, p.Q353K) (Figure 2.2). The *LMNA* mutations observed in patient 2 and 9 have been described previously [7, 42]. All these variations were absent in DNA from more than 100 controls. No mutation was found in *TMPO*. Previously reported polymorphisms in both *LMNA* (synonymous polymorphisms rs538089, rs505058, rs4641) and *TMPO* (non-synonymous polymorphism rs17459334) were detected. We also found a c.C1341A synonymous polymorphism in *LMNA* exon 6, which has not been previously reported, in two control individuals. Mutations in the corresponding codon have been previously reported in patients with limb-girdle muscular dystrophy 1B (p.R377H, [32]; p.R377L, [22]).

Sequencing analysis cannot detect large heterozygous deletions or duplications. In an attempt to ascertain whether the defects resulted from deletions or duplications in *LMNA,* we performed Multiplex Ligation-dependent Probe Amplification (MLPA) on the *LMNA* coding sequence in all 25 DCM patients. One DCM patient (Table 2.1, patient 1) with major nuclear abnormality displayed a MLPA normalized ratio peak area of ~0.5 for exons 3-12 (Figure 2.3A). This indicated the presence of a heterozygous deletion encompassing exons 3 to 12. The remaining probes, including those for exons 1 and 2, displayed a normalized ratio of ~1.0 indicating normal copy number (Figure 2.3A). We confirmed the presence of the

deletion using qPCR (R value of 0.5 for the patient with the deletion, and 1 for the patient without the deletion) (Figure 2.3B).

Lastly, to assess whether the nuclear envelope defects in the remaining patients could result from somatic mutations, we screened for *LMNA* and *TMPO* mutations in the heart from sporadic cases with nuclear envelope defect for which cardiac tissue was available (patients 5, 6). We conducted a similar analysis in patients without defective nuclear envelope (patients 19, 20, 21, 22, 23, 24, and 25). Somatic mutations were not identified in either set of patients.

In summary, a large degree of clinical heterogeneity was evident in the cohort of DCM patients studied regardless of the presence of nuclear envelope abnormalities, *LMNA* mutation, or family history of DCM.

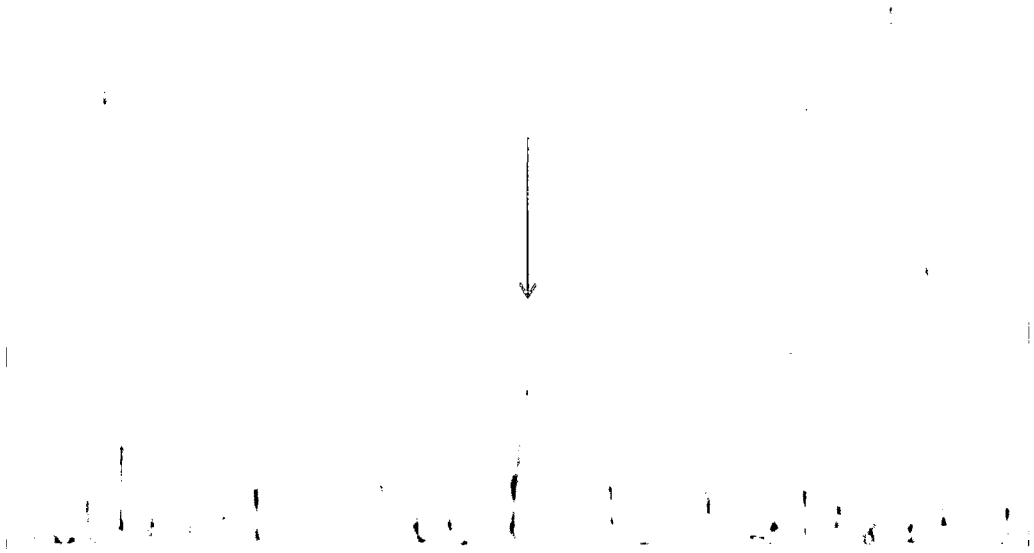

Figure 2.2: Results of sequence analysis for the heterozygous germline missense mutation p.Q353K in the patient 10.

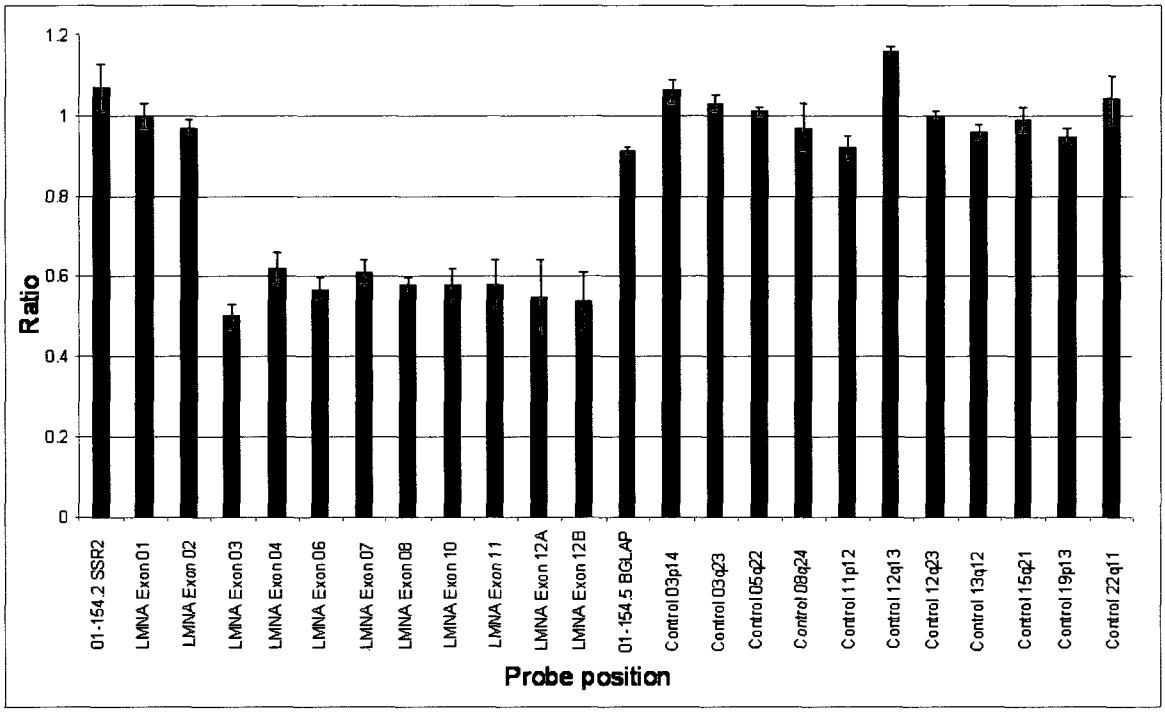

Figure 2.3A: MLPA analysis graph showing the heterozygous deletion of the exons 3-12 of the LMNA gene in patient 1. Exons 3-12 display a normalized ratio of ~0.5; indicating a loss. Exons 1, 2, and the remaining control probes display a normalized ration of ~1.0; indicating normal copy number. The control probes are targeted within the same chromosome and to different chromosomes as indicated by their locus.

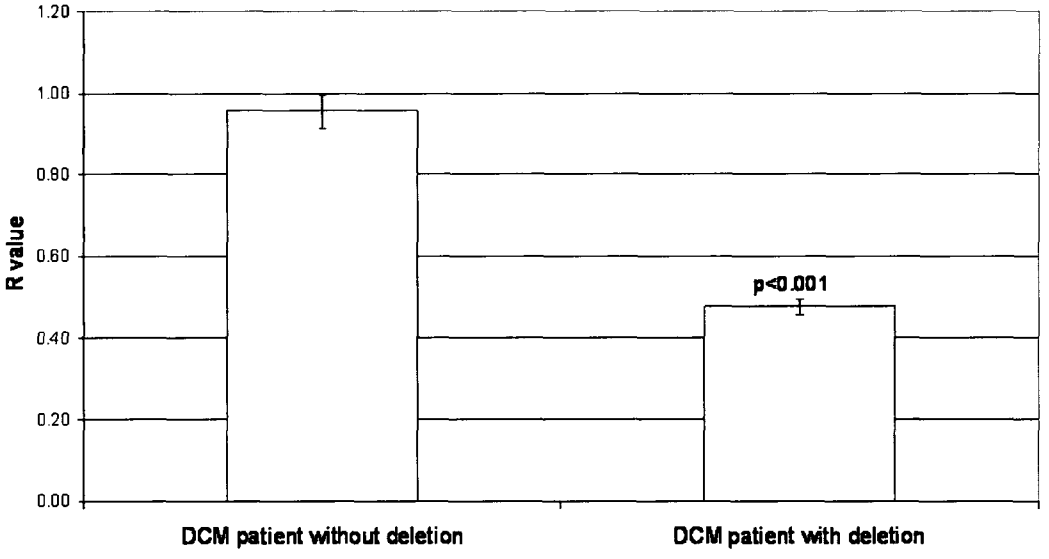

Figure 2.3B: Confirmation of the deletion of exons 3-12 in *LMNA* in the patient 1 using qPCR. R values were calculated as described in the Materials and methods section. Patient 15 without the deletion had a R value of 0.955, which indicates a normal copy number of the exon. The patient 1 had a R value of 0.476, which indicates deletion of one copy of the exon. (n=3).

2.4.4. Immunostaining results

To gain further insight into the functional significance of the heterozygous deletion of exons 3-12 of *LMNA* observed in patient 1, we performed indirect immunofluorescence analysis of endomyocardial biopsies from this patient as well as a control patient without *LMNA* mutation, using antibodies directed against both lamin A and C. All cardiomyocyte nuclei were immunostained with antibodies directed against lamin A and C epitopes (Figure 2.4). Immunostaining was markedly reduced in patient 1 as compared to the control patient indicating significant attenuation of lamin expression (Figure 2.4).

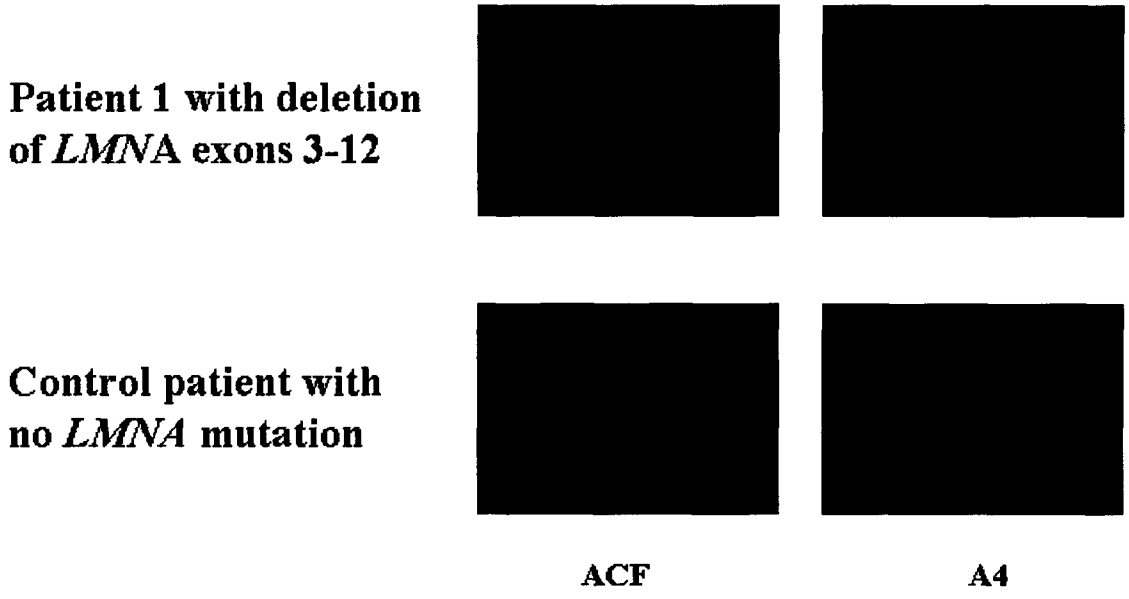

Figure 2.4: Indirect immunofluorescence analysis of endomyocardial biopsy from patient 1 carrying the *LMNA* heterozygous exon 3-12 deletion and from a control patient with no *LMNA* mutation. Endomyocardial biopsy were taken from the right ventricle. Immunostaining was performed using anti lamin A+C monoclonal antibodies ACF and antibody A4 which detects lamin A only (see Materials and Methods) and the goat anti-rabbit IgG secondary antibody. (Original magnifications 1,050X).

2.5. Discussion

Among heart biopsies from 25 unrelated DCM patients, we identified major cardiomyocyte nuclear abnormalities in 8 individuals, and non-specific nuclear abnormalities in the remaining patients. All patients displayed nuclear abnormalities and presented with conduction defects and/or severe heart failure leading to cardiac transplantation. This prompted us to analyze the sequence of *LMNA* and *TMPO*, two genes implicated in DCM that are involved in maintaining nuclear envelope architecture. Direct sequencing allowed the identification of 3 heterozygous *LMNA* genomic variations (p.D192G, p.R541S, and p.Q353K) in 3 patients. Since sequencing analysis cannot detect large heterozygous deletions or duplications, we performed Multiplex Ligation-dependent Probe Amplification (MLPA) on the *LMNA* coding sequence in all 25 DCM patients. We found a heterozygous deletion encompassing exons 3-12 of the *LMNA* gene. This deletion was confirmed using quantitative real-time PCR. All variations were absent in DNA from more than 100 controls. The occurrence of LMNA mutation in our population is high probably due to fact that the studied population presented with cardiac condition requiring undergoing endomyocardial biopsies or cardiac transplantation. Moreover, various arrhythmias were present in all but two patients. Since mutations in *LMNA* are usually associated with a worse prognosis than any other DCM-associated gene mutation [2, 17, 18, 26, 43, 45, 47] as well as with dysrhythmia [4], our population was probably biased toward LMNA mutations carriers. None of the patients carried a mutation in the *TMPO* gene. So far, only one *TMPO* mutation has been implicated as a cause of DCM in only one family [45].

The *LMNA* deletion of exons 3-12 was observed in a patient presenting with major nuclear envelope abnormalities - notably broken nuclear envelope and accumulation of

mitochondria within and around the nuclei. Immunostaining revealed reduced lamin A/C in the patient's cardiomyocyte nuclei suggesting that haplo-insufficiency was the mechanism underlying the observed nuclear abnormalities. Among their many functions, lamins play an integral role in maintaining the mechanical stability of the nucleus. Hence, reduced levels of lamin A/C protein have the potential to result in the nuclear envelope defects observed in cardiomyocytes from the patient carrying the *LMNA* deletion.

While rare findings of small deletions in the lamin A/C gene in patients with laminopathies have been reported previously, to our knowledge, this study is the first to document a large deletion encompassing most exons of the lamin A/C gene in a DCM patient.. Walter et al., [51] found a 15 nucleotide deletion (-3 to 12 nucleotides) in the 5' end of the *LMNA* gene in a patient with Emery-Dreifuss muscular dystrophy (EDMD) that resulted in loss of the translation initiator codon. Van Tintelen et al. (2007) [47] reported a 674 base pair deletion encompassing exon 1 and the adjacent non-coding exon in a patient with myocardial fibrosis. The presence of the exon 1 p.Q6Stop *LMNA* mutation resulting in reduced levels of lamin A/C proteins has also been reported in a family with EDMD [5].

Most *LMNA* mutations that cause DCM are heterozygous point mutations, only some of which have been associated with cardiomyocyte nuclear envelope defects [2, 7, 13, 42, and 49]. It has been suggested that mutations causing such abnormalities have a dominant-negative effect on the functions of normal lamin protein. For example, impaired lamin integration into the nuclear lamina due to the dominant-negative effects of a mutation may cause disruption of the lamina and ultimately compromise nuclear envelope integrity. Our results demonstrate that, apart from the dominant-negative effects of mutant lamin A/C protein, lamin haploinsufficiency can also cause nuclear envelope defects and underlie the

pathogenesis of DCM. That lamin haploinsufficiency can cause such defects is further corroborated by the fact that a heterozygous *LMNA*$^{+/-}$ mouse model in which cardiac lamin A/C levels were diminished by 50% compared to wild-type, demonstrated early-onset conduction system disease and late-onset DCM. Furthermore, misshapen cardiomyocyte nuclei and heterochromatin clumping were also observed [52].

Apart from the observed deletion, one of our patients with nuclear envelope defects carried a p.D192G point mutation in the *LMNA* gene. When expressed in COS-7 cells, this mutation resulted in a discontinuous nuclear lamina due to formation of multiple lamin aggregates [42, 43]. These results therefore corroborated the pathological findings from the patient with the mutation.

In our study, not all *LMNA* mutations were found to cause nuclear envelope abnormalities in patients' cardiomyocytes. Indeed, two patients with *LMNA* point mutations demonstrated no specific nuclear envelope abnormalities: One patient carried a p.Q353K mutation (reported here for the first time), while the second carried a p.R541S mutation. It is possible that the number of abnormal nuclei was so low in these two patients that it resulted in a false-negative finding. Patient age at time of tissue collection and the protein domain affected by the mutation were considered as possible explanations for the observed discrepancy in nuclear envelope phenotype between the patient with the deletion and the patient with the p.D192G point mutation. Age at time of tissue collection was 38 and 12 years for the patients carrying mutations p.Q353K and p.R541S, respectively, both of which were associated with normal nuclear envelope ultrastructure. The patients with *LMNA* deletion and p.D192G mutation, both of whom demonstrated nuclear envelope abnormalities, were 39 and 26 years of age, respectively. Hence, there was no apparent

relationship between age and observed nuclear envelope phenotype. It was also considered possible that the presence of nuclear envelope abnormalities may depend upon the protein domain affected by each mutation [12, 33]. The p.D192G mutation, which was associated with major nuclear envelope abnormalities, is located in the central α-helical rod domain at the distal end of coil 1B. This highly conserved region of the lamin A/C protein is critical for the formation of the α-helical coiled-coil dimer, the basic building block for the construction of lamin filaments. In contrast, the p.Q353K mutation in exon 6 affected a highly conserved residue localized in the central rod domain coil 2B fragment. Based on the coil 2B fragment crystal structure, mutations in this domain are unlikely to alter the dimer structure but may interfere with essential molecular interactions occurring in later stages of filament assembly, lamina formation, and/or chromatin interaction [41]. Similarly, the p.R541S mutation is located in a highly conserved residues in a region of gene shared by lamin A and C isoforms within the carboxyl-terminal end. The buried side chain of R541 participates in the stabilization of the carboxy-terminal β-sandwich through hydrophobic contacts with the core of the domain [23]. Mutations in this domain could therefore destabilize the three-dimensional structure of the C-terminal domain of lamin A/C. This domain also carries sites for many lamin A/C interacting proteins. Therefore, both p.Q353K and p.R541S mutations could theoretically disrupt multiple functions of lamin A and C, including the maintenance of nuclear architecture. Unexpectedly, the ultrastructural phenotype associated with these mutations was indistinguishable from controls. Hence, our results do not support the presence of a relationship between the position of the mutation and the resulting ultrastructural phenotype.

The seven patients demonstrating nuclear ultrastructural defects without *LMNA* or *TMPO* mutations showed that germ-line mutations in these genes are not a prerequisite for nuclear envelope defects. However, we could not discount the possibility that at least some of these individuals possessed somatic *LMNA* or *TMPO* mutations restricted to diseased cardiac tissue. The fact that only a percentage of observed cardiomyocytes from these patients displayed an abnormal nucleus lends support to this hypothesis. Indeed, somatic mutation occurring in a selective subpopulation of a progenitor cell-lineage is one of the molecular mechanisms leading to such tissue mosaicism. Furthermore, in other cardiovascular diseases such as idiopathic ventricular tachycardia or idiopathic atrial fibrillation, both germ-line and somatic missense mutations have been linked to disease [14, 24]. We therefore screened for the presence of lamin A/C mutations in DNA extracted from heart tissues of patients who did not have familial DCM, but were unable to identify any somatic mutations. Another possibility is that mutations in genes encoding lamin A/C-binding proteins are responsible for the major cardiomyocyte nuclear abnormalities observed in these patients [15, 16, 38, 53, 54, and 55].

We demonstrated that there is no clear correlation between the presence or position of *LMNA* mutation and either clinical phenotype with respect to DCM onset or severity, or nuclear envelope defects. That is, nuclear envelope defects were present in both patients with and without *LMNA* mutations. Furthermore, the severity of the nuclear envelope defect or the proportion of observed cells displaying abnormal nuclei did not correlate with the presence or position of the *LMNA* mutation. There was also no significant correlation between disease severity and the presence of ultra-structural nuclear envelope defects. Although a quantitative analysis was not possible due to the small sample size, overall, we

found no evidence of a relationship between onset and severity of DCM, nuclear abnormalities, and presence or position of *LMNA* mutations.

Taken together, our results are the first to show that lamin A/C haplo-insufficiency, documented by reduced protein level in the nuclear envelope caused by a large deletion in the *LMNA* gene, can lead to cardiomyocyte nuclear envelope disruption, and underlie the pathogenesis of DCM. However, the finding that two patients without major cardiomyocyte nuclear abnormalities had *LMNA* mutations indicates that *LMNA* mutations may not necessarily lead to major cardiomyocyte nuclear envelope defects. Furthermore, patients with major nuclear envelope abnormalities may not have *LMNA* or *TMPO* mutation. This demonstrates that patients with a clinical suspicion of laminopathy and marked abnormality of cardiomyocyte nuclei can be free of both *LMNA* and *TMPO* mutations and may carry a mutation in another gene encoding a protein involved in the maintenance of the nuclear architecture.

2.6. Acknowledgments

The work was supported by Canadian Institutes for Health Research operating grants 38054, 65152, and 77685, and by Heart and Stroke Foundation Grants NA 5101 and 6628 awarded to F. Tesson and by an internal grant from the Institute of Cardiology (Warsaw, Poland) no:2.57/VII/03. At the time the study was conducted, N. Sylvius was the recipient of the fellowships awarded by the Heart and Stroke Foundation of Ontario Program Grant 5275 and Astra Zeneca / Canadian Society of Hypertension / CIHR, and Pallavi Gupta was the recipient of Ontario Graduate Scholarship in Science and Technology (OGSST). We acknowledge the important contribution of the Canadian Cardiovascular Genetics Centre (Ottawa, Canada).

2.7. References

[1] Arbustini E, Gavazzi A, Pozzi R, Grasso M, Pucci A, Campana C, Graziano G, Martinetti M, Cuccia M, Salvaneschi L, Martinelli L, Montemartini C, Vigano M (1989). The morphologic spectrum of dilated cardiomyopathy and its relation to immune-response genes. Am J Cardiol 64: 991-995.

[2] Arbustini E, Pilotto A, Repetto A, Grasso M, Negri A, Diegoli M, Campana C, Scelsi L, Baldini E, Gavazzi A, Tavazzi L (2002). Autosomal dominant dilated cardiomyopathy with atrioventricular block: a lamin A/C defect-related disease. J Am Coll Cardiol 39: 981-990.

[3] Arimura T, Hayashi T, Matsumoto Y, Shibata H, Hiroi S, Nakamura T, Inagaki N, Hinohara K,Takahashi M, Manatsu S, Sasaoka T, Izumi T, Bonne G, Schwartz K, Kimura A (2007). Structural analysis of four and half LIM protein-2 in dilated cardiomyopathy. Biochem Biophys Res Com 357: 162-167.

[4] Baandrup U, Florio RA, Roters F, Olsen EG (1981). Electron microscopic investigation of endomyocardial biopsy samples in hypertrophy and cardiomyopathy. A semiquantitative study in 48 patients. Circulation 63: 1289-1298.

[5] Bécane HM, Bonne G, Varnous S, Muchir A, Ortega V, Hammouda EH, Urtizberea JA, Lavergne T, Fardeau M, Eymard B, Weber S, Schwartz K, and Duboc D (2000). High Incidence of Sudden Death with Conduction System and Myocardial Disease Due to Lamins A and C Gene Mutation. J of Pac Clin Electrophysiol 23: 1661-1666.

[6] Berger R, Theodor L, Shoham J, Gokkel E, Brok-Simoni F, Avraham KB, Copeland NG, Jenkins NA, Rechavi G, Simon AJ (1996). The characterization and localization of the

mouse thymopoietin/lamina-associated polypeptide 2 gene and its alternatively spliced products. Genome Res 6: 361-370.

[7] Bilinska ZT, Sylvius N, Grzybowski J, Fidzianska A, Michalak E, Walczak E, Walski M, Bieganowska K, Szymaniak E, Kusmierczyk-Droszcz B, Lubiszewska B, Wagner T, Tesson F, Ruzyllo W (2006) Dilated cardiomyopathy caused by *LMNA* mutations. Clinical and morphological studies. Polish Heart Journal 64: 812-818.

[8] Bridger JM, Kill IR, O'Farrell M, Hutchison CJ (1993). Internal lamin structures within G1 nuclei of human dermal fibroblasts. J Cell Sci 104: 297-306.

[9] Daehmlow S, Erdmann J, Knueppel T, Gille, C, Froemmel C, Hummel M, Hetzer R, Regitz-Zagrosek V (2002). Novel mutations in sarcomeric protein genes in dilated cardiomyopathy. Biochem Biophys Res Com 298: 116-120.

[10] Dechat T, Korbei B, Vaughan OA, Vlcek S, Hutchison CJ, Foisner R (2000) Lamina-associated polypeptide 2alpha binds intranuclear A-type lamins. J Cell Sci 113:3473-3484.

[11] Dubosc-Bidot L, Xu P, Charron P, Neyroud N, Dilanian G, Millaire A, Bors V, Komajda M, Villard E (2008). Mutations in the z-band protein myopalladin gene and idiopathic dilated cardiomyopathy. Cardiovas Res 77: 118-125.

[12] Favreau C, Dubosclard E, Ostlund C, Vigouroux C, Capeau J, Wehnert M, Higuet D, Worman HJ, Courvalin JC, Buendia B (2003). Expression of lamin A mutated in the carboxyl-terminal tail generates an aberrant nuclear phenotype similar to that observed in cells from patients with Dunnigan-type partial lipodystrophy and Emery-Dreifuss muscular dystrophy. Exp Cell Res 282: 14-23.

[13] Fidziańska A, Bilińska ZT, Tesson F, Wagner T, Walski M, Grzybowski J, Ruzyłło W, Hausmanowa-Petrusewicz I. (2008). Obliteration of cardiomyocyte nuclear architecture in a patient with LMNA gene mutation. J Neurol Sci. 271: 91-6.

[14] Gollob MH, Jones DL, Krahn AD, Danis L, Gong XQ, Shao Q, Liu X, Veinot JP, Tang AS, Stewart AF, Tesson F, Klein GJ, Yee R, Skanes AC, Guiraudon GM, Ebihara L, Bai D (2006). Somatic mutations in the connexin 40 gene (GJA5) in atrial fibrillation. N Engl J Med 354: 2677-2688.

[15] Gruenbaum Y, Margalit A, Goldman RD, Shumaker DK, Wilson KL (2005). The nuclear lamina comes of age. Nat Rev Mol Cell Biol 6: 21-31.

[16] Haque F, Lloyd DJ, Smallwood DT, Dent CL, Shanahan CM, Fry AM, Trembath RC, Shackleton S (2006). SUN1 interacts with nuclear lamin A and cytoplasmic nesprins to provide a physical connection between the nuclear lamina and the cytoskeleton. Mol Cell Biol 26: 3738-3751.

[17] Hermida-Prieto M, Monserrat L, Castro-Beiras A, Laredo R, Soler R, Peteiro J, Rodriguez E, Bouzas B, Alvarez N, Muniz J, Crespo-Leiro M (2004). Familial dilated cardiomyopathy and isolated left ventricular noncompaction associated with lamin A/C gene mutations. Am J Cardiol 94: 50-54.

[18] Inagaki N, Hayashi T, Arimura T, Koga Y, Takahashi M, Shibata H, Teraoka K, Chikamori T,Yamashina A, Kimura A (2006). α-B crystallin mutation in dilated cardiomyopathy. Biochem Biophys Res Com 342: 379-386.

[19] Ivorra C, Kubicek M, Gonzalez JM, Sanz-Gonzalez SM, Alvarez-Barrientos A, O'Connor JE, Burke B, Andres V (2006). A mechanism of AP-1 suppression through interaction of c-Fos with lamin A/C. Genes Dev 20: 307-320.

[20] Karkkainen S, and Peuhkurinen K (2007). Genetics of dilated cardiomyopathy. Annals of Medicine 39: 91-107.

[21] Kennedy BK, Barbie DA, Classon M, Dyson N, Harlow E (2000) Nuclear organization of DNA replication in primary mammalian cells. Genes Dev 14: 2855-2868.

[22] Ki CS, Hong JS, Jeong GY, Ahn KJ, Choi KM, Kim DK, Kim JW (2002). Identification of lamin A/C (*LMNA*) gene mutations in Korean patients with autosomal dominant Emery-Dreifuss muscular dystrophy and limb-girdle muscular dystrophy 1B. J Hum Genet 47: 225-228.

[23] Krimm I, Östlund C, Gilquin B, Couprie J, Hossenlopp P, Mornon JP, Bonne G , Courvalin J-C, Worman HJ, Zinn-Justin S (2002). The Ig-like structure of the C-terminal domain of lamin A/C, mutated in muscular dystrophies, cardiomyopathy and partial lypodystrophy. Structure 10: 811-823.

[24] Lerman BB, Dong B, Stein KM, Markowitz SM, Linden J, Catanzaro DF (1998). Right ventricular outflow tract tachycardia due to a somatic cell mutation in G protein subunit alpha i2. J Clin Inves 101: 2862-2868.

[25] Liu J, Ben-Shahar TR, Riemer D, Treinin M, Spann P, Weber K, Fire A, Gruenbaum Y (2000). Essential roles for Caenorhabditis elegans lamin gene in nuclear organization, cell cycle progression, and spatial organization of nuclear pore complexes. Mol Biol Cell 11: 3937-3947.

[26] Meier J, Campbell KH, Ford CC, Stick R, Hutchison CJ (1991). The role of lamin LIII in nuclear assembly and DNA replication, in cell-free extracts of Xenopus eggs. J Cell Sci 98: 271-279.

[27] Mercuri E, Brown SC, Nihoyannopoulos P, Poulton J, Kinali M, Richard P, Piercy RJ, Messina S, Sewry C, Burke MM, McKenna W, Bonne G, Muntoni F (2005). Extreme variability of skeletal and cardiac muscle involvement in patients with mutations in exon 11 of the lamin A/C gene. Muscle Nerve 31: 602-609.

[28] Mestroni L, Maisch B, McKenna WJ, Schwartz K, Charron P, Rocco C, Tesson F, Richter A, Wilke A, Komajda M (1999). Guidelines for the study of familial dilated cardiomyopathies. Collaborative Research Group of the European Human and Capital Mobility Project on Familial Dilated Cardiomyopathy. Eur Heart J 20: 93-102.

[29] Moir RD, Montag-Lowy M, Goldman RD (1994). Dynamic properties of nuclear lamins: lamin B is associated with sites of DNA replication. J Cell Biol 125: 1201-1212.

[30] Moir RD, Spann TP, Herrmann H, Goldman RD (2000a) Disruption of nuclear lamin organization blocks the elongation phase of DNA replication. J Cell Biol 149: 1179-1792.

[31] Moir RD, Yoon M, Khuon S, Goldman RD (2000b). Nuclear lamins A and B1: different pathways of assembly during nuclear envelope formation in living cells. J Cell Biol 15: 1155-1168.

[32] Muchir A, Bonne G, van der Kooi AJ, van Meegen M, Baas F, Bolhuis PA, de Visser M, Schwartz K (2000). Identification of mutations in the gene encoding lamins A/C in autosomal dominant limb girdle muscular dystrophy with atrioventricular conduction disturbances (LGMD1B). Hum Mol Genet 9: 1453-1459.

[33] Muchir A, Medioni J, Laluc M, Massart C, Arimura T, van der Kooi AJ, Desguerre I, Mayer M, Ferrer X, Briault S, Hirano M, Worman HJ, Mallet A, Wehnert M, Schwartz K, Bonne G (2004). Nuclear envelope alterations in fibroblasts from patients with muscular

dystrophy, cardiomyopathy, and partial lipodystrophy carrying lamin A/C gene mutations. Muscle Nerve 30: 444-450.

[34] Rowan RA, Masek MA, Billingham ME (1998). Ultrastructural morphometric analysis of endomyocardial biopsies. Idiopathic dilated cardiomyopathy, anthracycline cardiotoxicity, and normal myocardium. Am J Cardiovasc Pathol 2: 137-144.

[35] Schiender M, Franziska J, Sanz J, Kanel TV, and Gallati S (2006). Detection of exon deletions (CFTR) by relative quantification on the lightcycler. Clinical Chemistry 52: 2005-2012.

[36] Scholz D, Diener W, Schaper J (1994). Altered nucleus/cytoplasm relationship and degenerative structural changes in human dilated cardiomyopathy. Cardioscience 5: 127-138.

[37] Shimi T, Pfleghaar K, Kojima S, Pack CG, Solovei I, Goldman AE, Adam SA, Shumaker DK, Kinjo M, Cremer T, Goldman RD. (2008). The A- and B-type nuclear lamin networks: microdomains involved in chromatin organization and transcription. Genes Dev. 22: 3409-21.

[38] Shumaker DK, Kuczmarski ER, Goldman RD (2003) The nucleoskeleton: lamins and actin are major players in essential nuclear functions. Curr Opin Cell Biol 15: 358-366.

[39] Smythe C, Jenkins HE, Hutchison CJ (2000). Incorporation of the nuclear pore basket protein nup153 into nuclear pore structures is dependent upon lamina assembly: evidence from cell-free extracts of Xenopus eggs. Embo J 19: 3918-3931.

[40] Spann TP, Goldman AE, Wang C, Huang S, Goldman RD (2002). Alteration of nuclear lamin organization inhibits RNA polymerase II-dependent transcription. J Cell Biol 156: 603-308.

[41] Strelkov SV, Schumacher J, Burkhard P, Aebi U, Herrmann H (2004). Crystal structure of the human lamin A coil 2B dimer: implications for the head-to-tail association of nuclear lamins. J Mol Biol 343: 1067-1080.

[42] Sylvius N, Bilinska ZT, Veinot JP, Fidzianska A, Bolongo PM, Poon S, McKeown P, Davies RA, Chan KL, Tang AS, Dyack S, Grzybowski J, Ruzyllo W, McBride H, Tesson F (2005). In vivo and in vitro examination of the functional significances of novel lamin gene mutations in heart failure patients. J Med Genet 42: 639-647.

[43] Sylvius N, Hathaway A, Boudreau E, Gupta P, Labib S, Bolongo P, Rippstein P, Mcbride H, Bilinska ZT, and Tesson F (2008). Specific contributions of lamin A and lamin C in the development of laminopathies. Exp Cell Res 314: 2362-75.

[44] Taylor MR, Fain PR, Sinagra G, Robinson ML, Robertson AD, Carniel E, Di Lenarda A, Bohlmeyer TJ, Ferguson DA, Brodsky GL, Boucek MM, Lascor J, Moss AC, Li WL, Stetler GL, Muntoni F, Bristow MR, Mestroni L (2003). Natural history of dilated cardiomyopathy due to lamin A/C gene mutations. J Am Coll Cardiol 41: 771-780.

[45] Taylor MR, Slavov D, Gajewski A, Vlcek S, Ku L, Fain PR, Carniel E, Di Lenarda A, Sinagra G, Boucek MM, Cavanaugh J, Graw SL, Ruegg P, Feiger J, Zhu X, Ferguson DA, Bristow MR, Gotzmann J, Foisner R, Mestroni L (2005). Thymopoietin (lamina-associated polypeptide2) gene mutation associated with dilated cardiomyopathy. Hum Mutat 26: 566-574.

[46] van Berlo JH, de Voogt WG, van der Kooi AJ, van Tintelen JP, Bonne G, Yaou RB, Duboc D, Rossenbacker T, Heidbuchel H, de Visser M, Crijns HJ, Pinto YM (2005). Meta-analysis of clinical characteristics of 299 carriers of LMNA gene mutations: do lamin A/C mutations portend a high risk of sudden death? J Mol Med 83: 79-83.

[47] van Tintelen JP, Tio RA, Kerstjens-Frederikse WS, van Berlo JH, Boven LG, Suurmeijer AJH, White SJ, den Dunnen JTD, te Meerman GJ, Vos YJ, van der Hout AH, Osinga J, van den Berg MP, van Veldhuisen DJ, Buys CHC, Hofstra, RMW, Pinto YM (2007). Severe Myocardial Fibrosis Caused by a Deletion of the 5' End of the Lamin A/C Gene. JAm Coll Cardiol 49: 2430-2439.

[48] Vaughan OA, Whitefield WGF, Hutchinson CJ (2000). Functions of nuclear lamins. Protoplasma 211: 1-7.

[49] Verga L, Concardi M, Pilotto A, Bellini O, Pasotti M, Repetto A, Tavazzi L, Arbustini E (2003). Loss of lamin A/C expression revealed by immuno-electron microscopy in dilated cardiomyopathy with atrioventricular block caused by LMNA gene defects. Virchows Arch 443: 664-671.

[50] Vlcek S, DechatT, Foisner R (2001), Nuclear envelope and nuclear matrix: interactions and dynamics. Cell Mol Life Sci 58: 1758-1765.

[51] Walter MC, Witt TN, Weigel BS, Reilicha,P, Richard P, Pongratza D, Bonned G, Wehnert, MS, Lochmuller H (2005). Deletion of the LMNA initiator codon leading to a neurogenic variant of autosomal dominant Emery–Dreifuss muscular dystrophy. Neuromuscular Disorders 15: 40-44.

[52] Wolf CM, Wang L, Alcalai R (2008). Lamin A/C haploinsufficiency causes dilated cardiomyopathy and apoptosis-triggered cardiac conduction system disease. J Mol Cell cardiol 44: 293-303.

[53] Zastrow MS, Flaherty DB, Benian GM, Wilson KL (2006). Nuclear titin interacts with A- and B-type lamins in vitro and in vivo. J Cell Sci 119: 239-249.

[54] Zastrow MS, Vlcek S, Wilson KL (2004). Proteins that bind A-type lamins: integrating isolated clues. J Cell Sci 117: 979-987.

[55] Zhong N, Radu G, Ju W, Brown WT (2005). Novel progerin-interactive partner proteins hnRNP E1, EGF, Mel 18, and UBC9 interact with lamin A/C. Biochem Biophys Res Commun 338: 855-861.

CHAPTER 3

LMNA MUTATIONS IN DCM: INVESTIGATION OF THE GENE REGULATORY HYPOTHESIS IN A CARDIAC CELL MODEL

3.1. Introduction

3.1.1. A-type Lamins and their nuclear functions

A-type lamins (lamin A and lamin C) are a type of intermediate filament-type protein that comprise an integral part of the nuclear lamina, and are also found in the nucleoplasm (Fuchs et al., 1994, Stuurman et al., 1998). A-type lamins play an important role in the assembly and maintenance of the nuclear membrane, DNA replication, and transcription (Meier et al., 1990, and Newport et al., 1990, Bridger et al., 1993, Spann et al., 1997, Hutchinson et al., 2002, Kennedy et al., 2000, Liu et al., 2000, Dreuillet et al., 2002, Kumaran et al., 2002, Lloyd et al., 2002, Spann et al., 2002, Zastrow et al., 2004, Pranaik et al., 2008, Shumaker et al., 2008). Mutations in *LMNA* are implicated in the pathogenesis of tissue-specific laminopathies such as DCM, EDMD, and FPLD (Broers et al., 2006, Pranaik et al., 2008). Two hypotheses have been proposed to explain how *LMNA* mutations cause DCM, as well as the mechanism by which such mutations cause tissue-specific effects: 1) The Structural Hypothesis; and 2) The Gene Regulatory Hypothesis. According to the Structural Hypothesis, nuclear fragility caused by mutant lamin A/C may increase the likelihood of cell death in mechanically stressed tissues such as cardiac muscle to a greater extent than in other tissues. According to the Gene Regulatory Hypothesis, *LMNA* mutations may have deleterious tissue-specific effects on gene expression. It has been suggested that these two hypotheses may not be mutually exclusive. The Structural Hypothesis has been supported by both *in vitro* and *in vivo* studies, including ours. The key finding of these studies is the presence of nuclear structural abnormalities in both carriers of *LMNA* mutations, and in cells expressing exogenous lamin A/C mutant proteins (Ostlund et al., 2001, Raharjo et al., 2001, Verga et al., 2003, Muchir et al., 2004, Sylvius et al., 2005).

Evidence also exists to support the Gene Regulatory Hypothesis. The effect of *LMNA* mutations in gene regulation has been demonstrated for laminopathies such as EDMD and FPLD, although very preliminary data exist for their role in the pathogenesis of DCM. A mouse model carrying a DCM-causing *LMNA* mutation demonstrated reduced expression of Hf1B, a transcription factor involved in the development of the cardiac conduction system, in the hearts of mutant mice. This mouse model also demonstrated increased transcriptional activity of GATA-4, a cardiac-specific transcription factor that regulates the expression of genes important for myocardial differentiation and function. (Mounkes et al., 2005). Further support in favour of the Gene Regulatory Hypothesis was provided by the observation that aggregates formed by the lamin A/C mutant p.D192G (a DCM-causing mutation) affected the intranuclear distribution of SUMO-1, a post-translational-modifier of a number of transcription factors (Sylvius et al., 2005).

3.1.2. SUMO-1

3.1.2.1. The SUMO family of proteins

Four distinct small ubiquitin-like modifier (SUMO) proteins have been identified. SUMO-1 is an 11.5 kDA post translational-modifier that displays 18% sequence homology with ubiquitin (Melchoir, 2000). Expression of SUMO-1 has been demonstrated in the nucleus, nuclear pore complex, and cytoplasm of a wide range of tissues and cell types (Melchoir, 2000, Su et al., 2002). Despite the limited sequence homology between SUMO-1 and ubiquitin, the two molecules are similar in tertiary structure, i.e., they both contain the same ββαββαβ fold. Furthermore, the C-terminal di-glycine motif of SUMO-1 can be superimposed on the C-terminal glycine motif of ubiquitin (Zhao et al., 2007).

The three other SUMO proteins (SUMO-2, SUMO-3 and SUMO-4) expressed in mammalian cells are not as well-characterized as SUMO-1 (Melchoir et al., 2003, Zhao et al., 2007). SUMO-2 and SUMO-3 share 95% sequence identity, while SUMO-1 exhibits only 44% sequence identity with SUMO-2 and SUMO-3 (Su et al., 2002). Although little is known about SUMO-4, it has been characterized as a 95 amino-acid protein that has 87% sequence identity with SUMO-2, and is expressed mainly in kidney, lymph nodes and spleen (Bohren et al., 2004, Guo et al., 2004).

Most post-translational sumoylation in a normal, unstressed cell is performed by SUMO-1. In contrast, SUMO-2 and SUMO-3 exist primarily as free proteins under normal conditions, but become conjugated to other proteins during cellular stress (Manza et al., 2004). SUMO- 1, SUMO-2, and SUMO-3 also differ in their sub-cellular localization. Using FLAG-SUMO-1/SUMO-2/SUMO-3 in BHK-21 cells, Su et al. (2002) demonstrated that SUMO-1 is localized mainly in nuclear membrane, SUMO-2 in nuclear bodies, and SUMO-3 in cytoplasm.

We focused our study on SUMO-1 since this isoform is responsible for most of the sumoylation in a cell, and because SUMO-1 is localized in the nuclear membrane, where lamins are predominantly found. Furthermore, SUMO-1 is the best characterized SUMO protein in terms of the number of target proteins identified.

3.1.2.2. The Sumoylation Process

Like ubiquitination, sumoylation results in the formation of an isopeptide bond between the C-terminal glycine residue of SUMO and the ε -amino group of a lysine residue in the acceptor protein (Seeler et al., 2003). The process of sumoylation is also very similar to the process of ubiquitination. It is a reversible process that occurs in many steps (Muller et al.,

2001). The first step is the maturation of SUMO-1 precursors by SUMO-specific proteases, designated as the SENP family of proteases. These proteases possess C-terminal hydrolase activity that exposes the C-terminal di-glycine motif of SUMO-1. After maturation, SUMO-1 is further activated by the E-1 enzyme Aos1/Uba2 in an ATP-dependant manner. This involves the formation of a thioester bond between the C-terminal glycine in SUMO-1 and a cysteine residue in the E-1 activating enzyme. Unlike the ubiquitin E-1 enzyme, Uba1, SUMO E1 is a heterodimer of Aos1 (which is involved in adenylation), and Uba2 (which is involved in thoiesterification). Following activation, SUMO-1 is transferred to the E2 conjugating enzyme UBC-9, and subsequently ligated to the lysine residue of target proteins by one of three E3 ligases: protein inhibitor of activated STAT (PIAS) (Saitoh et al., 1998, Hochstrasser et al., 2001), RanBP2/NUP358 (Pichler et al., 2002), or polycomb protein Pc2 (Seeler et al., 2003). Unlike the process of ubiquitynation which relies on a number of E2 enzymes, UBC-9 is the sole E2 conjugating enzyme of the sumoylation pathway (Zhao et al., 2007). Due to the reversible nature of sumoylation, SUMO can be cleaved from target proteins with SUMO proteases (SENP family proteases) (Yeh et al 2000) (Figure 3.1).

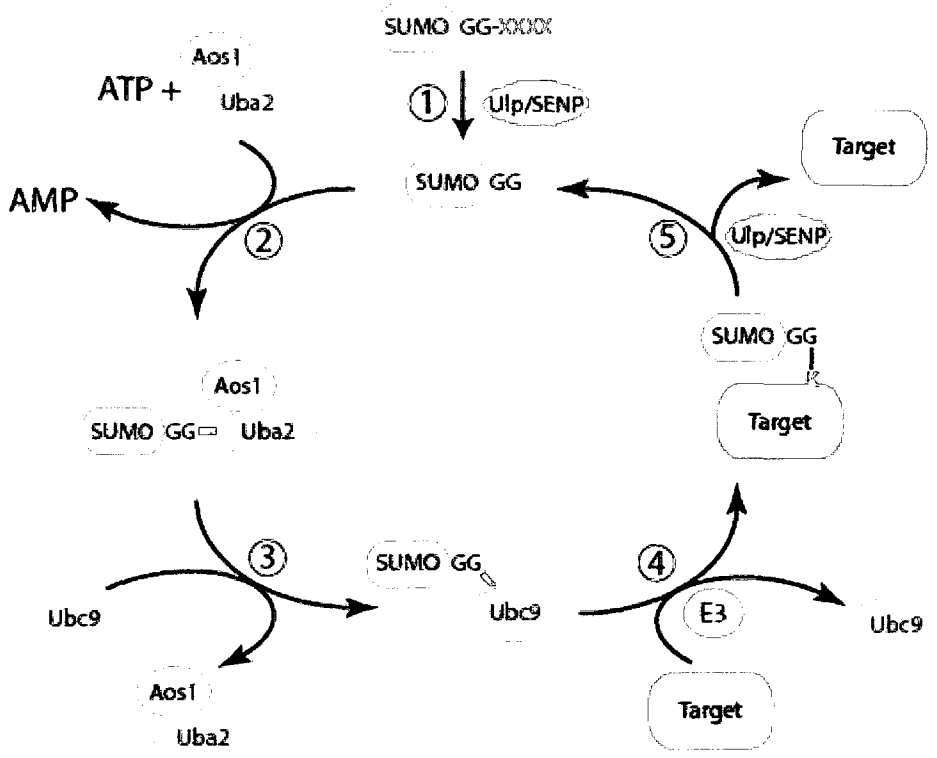

Figure 3.1: The sumoylation pathway: 1) Maturation of SUMO proteins by SENP family proteases); 2) Mature SUMO forms a thioester bond with the E1 enzyme Uba2/Aos1 through its C-terminal glycine; 3) Activated SUMO-1 is transferred to the E2 conjugating enzyme UBC-9; 4) SUMO forms an isopeptide bond with a lysine group on a target protein with the help of E3 ligases; 5) SUMO-1 can be cleaved off from the substrates with SENP proteases (Dassso et al., 2008).

3.1.2.3. Functions of SUMO-1

Unlike ubiquitynation, which primarily targets a protein for proteasome-mediated degradation, sumoylation regulates the function of substrates by altering subcellular localization, interaction with other proteins, or the pattern of other post-translational modifications (Zhao et al., 2007). These changes may in turn affect gene expression, chromosomal assembly and segregation, DNA repair and recombination, transport of RNA and other proteins in and out of the nucleus, or signal transduction. *LMNA* mutations have been shown to cause clustering of nuclear pore complexes, potentially affecting nucleo-cytoplasmic trafficking (Verga et al., 2003). *LMNA* mutations have also been shown to affect gene transcription (Lloyd et al. 2004, Mounkes et al., 2005). Since sumoylation plays a role in regulating these two functions, they are described in more detail below.

3.1.2.3.1. Role of SUMO-1 in Nuclear Trafficking

SUMO-1 was first identified in mammals as a post-translational modifier of RanGAP1, a protein involved in the activation of Ran GTPase and nucleocytoplasmic trafficking (Matunis et al., 1996, Mahajan et al., 1997). Unmodified RanGAP1 is located primarily in the cytoplasm, but when sumoylated, it translocates to the nuclear pores. At the nuclear pores, it interacts with the E3 ligase RanBP2/NUP358, a nuclear pore complex protein. Furthermore, other enzymes involved in the sumoylation process such as UBC-9 and SENP2 (a SUMO-cleaving protease) are also found in the nuclear pores (Zhang et al., 2002). SENP2 has also been shown to interact with NUP153, a protein involved in nuclear import and export (Zhang et al., 2002). The presence of various enzymes involved in reversible

SUMO-1 modification at the nuclear pores suggests that sumoylation may be involved in regulating nucleo-cytoplasmic trafficking (Marx et al., 2005).

3.1.2.3.2. Role of SUMO-1 in Regulation of Transcription Factors

Nearly one-third of sumoylated proteins are transcription factors (Vertegaal et al. 2006). One of the mechanisms by which sumoylation may regulate transcription factor activity is through targeting, either towards or away from their site of action. For example, sumoylation of heat shock proteins causes relocalization of these proteins to stress granules, as well as activation of their transcriptional activity (Seeler et al., 2002). In contrast, sumoylation of other transcription factors, such as Lef1 and SP3, leads to localization of these proteins to promyelocytic leukemia (PML) bodies, thereby reducing their transcriptional activity. Another mechanism by which sumoylation affects the activity of transcription factors is through changes in their binding affinity for DNA or other proteins (Marx et al., 2005).

3.1.2.4. GATA-4 and MEF2C: Sumoylated cardiac-specific transcription factors

GATA-4, a member of the GATA-binding family of structurally related transcription factors expressed in cardiac cells, regulates the expression of genes important for myocardial differentiation and function such as troponin C, troponin I, atrial natriuretic factor (ANF), cardiac α-myosin heavy chain (α-MHC), NKX2-5, and cardiac ankyrin repeat protein (CARP) (Pikkarainen et al., 2004). One of the characteristic features of GATA-4 transcription factors is a highly conserved C-terminal DNA binding domain. This domain consists of two adjacent zinc fingers (Cys-X2-Cys-X17-Cys-X2-Cys) and two adjacent

stretches of basic amino acids (Molkentin et al., 2004). The C-terminal zinc finger of GATA-4 is involved in binding to the minor groove of DNA. It also interacts with other transcription factors and co-factors such as MEF2C, NKX2-5, and P300. The N-terminal zinc finger binds to the major groove of DNA, and also with Friend of GATA (FOG2) transcription factors. The two separate transcription activation domains are present in the N-terminus of the protein. GATA-4 transcription factors are subjected to phosphorylation, acetylation, and many other post-translational modifications that influence their transcriptional activity (Molkenitin et al., 2004). Wang et. al. (2004) demonstrated that SUMO-1 modifies lysine 366 in the C-terminal domain of GATA-4, resulting in enhanced GATA-4 transcriptional activity, and possibly affecting GATA-4 nuclear localization.

Myocyte enhancing factor 2C (MEF2C) transcription factors, members of the MADS family of transcription factors, are involved in regulating cardiogenesis and myogenesis (Zhang et. al., 2004, Kang et al., 2006). Highly enriched in cardiac, skeletal, and neural tissues (Haberland et. al., 2007), these transcription factors consist of an N-terminal DNA binding domain, and a C-terminal transcription activation domain. They bind to the consensus sequence (T/C)TA(A/T)$_4$TA(G/A) and interact with other transcription factors, such as GATA-4 and dHAND, to regulate the expression of cardiac-specific genes such as ANF, BNP, and α- and β-myosin heavy chains (Pikkarainen et al., 2004, Zhang et. al., 2004). They also interact with myogenic basic-loop-helix proteins such as MyoD to regulate the expression of muscle-specific genes such as Serine/arginine-rich protein specific kinase 3(SrPK3), troponin C and myogenin (Haberland et al., 2007). The transcription factor activity of MEF2C is also affected by many post-translational modifications such as phosphorylation, acetylation and deacetylation (Angelelli et. al., 2007, Haberland et. al.,

2007). Kang et. al. (2006) showed that the activity of MEF2C can be downregulated by sumoylation of the K391 residue of the C-terminal domain.

The fact that GATA-4 and MEF2C are cardiac enriched sumoylated transcription factors makes them good candidates for studying the effect of DCM-causing *LMNA* mutations on the activity of sumoylated transcription factors.

3.2. Rationale and Hypothesis

An important function of A-type lamins is to anchor and space nuclear pore complexes (Smythe et al. 2000). Furthermore, several studies have shown that DCM patients with *LMNA* mutations demonstrate ultra-structural nuclear envelope abnormalities in their cardiomyocytes (Olson et. al., 1996, Verga et. al., 2003), including clustering of nuclear pore complexes. Certain SUMO-1 modification (e.g., UBC-9, RanBP2) and deconjugation (e.g., SENP2) enzymes are also located at nuclear pore complexes (Zhang et. al., 2002). Interestingly, SENP2 has been shown to interact with the FG repeat domain of NUP153, the nucleoporin that interacts with lamins. Furthermore, the sole E2 conjugating enzyme, UBC-9, has been shown to interact with lamin A/C (Zhong et. al., 2004). Our group previously demonstrated that the lamin A/C mutant p.D192G forms large intranuclear lamin C aggregates, and that SUMO-1 conjugates co-localized with these aggregates (Sylvius et al., 2005).

The available evidence therefore indicates that the presence of *LMNA* mutations can affect the distribution of the SUMO-1 conjugation/deconjugation system, and the localization of SUMO-1 and its conjugates. Since a number of cardiac transcription factors are sumoylated (e.g., MEF2C, GATA-4), we hypothesized that *LMNA* mutations affect the

transcriptional activity of these transcription factors through their effect on the sumoylation process.

3.3. Specific Objectives

1. Many groups, including ours, have studied the effect of DCM-causing *LMNA* mutations on the nuclear organization of lamin A/C in cell lines such as HeLa, fibroblasts, and C2C12 cells (Raharjo et al., 2001, Ostlund et al., 2001, Sylvius et al., 2005, Sylvius et al., 2008). However, these effects have not been assessed in a cardiac cell model, a model more relevant to the study of DCM. Therefore, as a first step we evaluated several cardiac cell models and found the H9C2 cell line to be the best suited model for our study. We therefore investigated the role of DCM-causing *LMNA* mutations on lamin distribution in the nuclear lamina of H9C2 (rat cardiomyoblasts cell line).

2. To study the effect of *LMNA* mutations on the intranuclear localization of SUMO-1 and UBC-9 in H9C2 cells.

3. To study the effect of *LMNA* mutations on the intranuclear localization of GATA-4, a cardiac-specific transcription factor regulated through sumoylation, in H9C2 cells

4. To study the effect of *LMNA* mutations on GATA-4 transcriptional activity by measuring the relative expression of GATA-4 regulated genes such as troponin C and ANF.

5. To study the effect of *LMNA* mutations on MEF2C (a cardiac and skeletal muscle-specific transcription factor regulated through sumoylation) transcriptional activity by measuring the relative expression of MEF2C regulated genes such as SrPK3.

3.4. Methodology

3.4.1. Construction of lamin A and lamin C- fluorescent expression plasmids

Our laboratory had previously cloned full-length, human, wild-type lamin A and lamin C cDNA's as C-terminal fusion proteins to the cyan fluorescent protein (pECFP) sequence of the pECFP-C1 fluorescent expression vector. Lamin C cDNA had also been cloned into pEYFP-C1 and pDsRed2-C1 expression vectors. The mutant lamin A/C constructs had been previously generated in the laboratory through site-directed mutagenesis of these wild-type constructs (Quick change II XL Site Directed Mutagenesis Kit, Stratagene). The various mutations used in the study are shown in Figure 3.2. As shown in Figure 3.2B, the mutations selected for this study exist in different domains of the lamin A/C protein. The p.L85R, p.D192G, and p.Q353K mutations are DCM-causing mutations, the latter two of which were found in DCM patients enrolled for genotyping by our laboratory. The mutations p.R386K and p.R482W, which cause EDMD and FPLD respectively, were also nstudied to verify the tissue-specificity of the selected *LMNA* mutations.

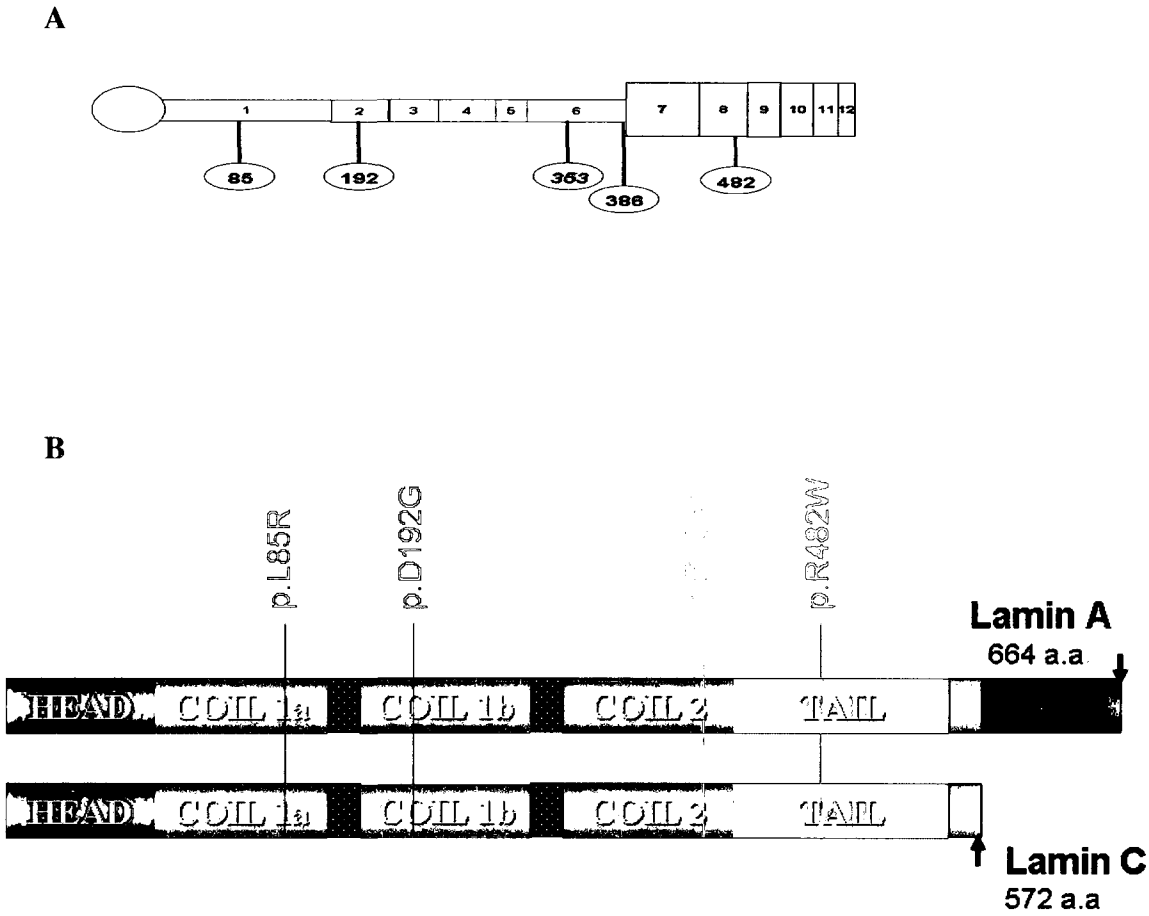

Figure 3.2: Schematic representation of missense mutations selected for *in vitro* characterization. Mutations pL85R, pD192G, pQ353K (shown in red) are associated with DCM. Mutation pR386K (shown in yellow) causes EDMD. Mutation pR482W (shown in green) causes FPLD. (A). Positions of selected mutations within *LMNA* exons. (B) Positions of selected mutations within domains of lamin A and lamin C proteins. Note that all selected mutations are present in the regions common to both lamin A and lamin C.

3.4.2. Cloning of UBC-9 into pEYFP and pECFP fluorescent vectors

Full-length, human, UBC9 cDNA was cloned as a C-terminal fusion to the enhanced cyan and green fluorescent sequence of the fluorescent expression vectors pECFP and pEGFP respectively. UBC9 cDNA was obtained by performing one-step RTPCR (One step RT PCR Kit, Qiagen) on human RNA extracted from heart biopsy of a DCM patient. Primers for the RTPCR were designed using the Primer 3 program, such that they contained the EcoRI and BamHI restriction sites at their 5' ends. The PCR product was directly cloned into TOPO TA vector using the TOPO TA cloning kit (Qiagen). The TOPO-TA clones thus obtained were digested with EcoRI and BamHI. The pECFP and pEYFP expression vectors were also digested with the same restriction enzymes. Digestion products from both the TOPO TA clones and expression vectors were electrophoresed on 1% agarose gel and the required bands (a 500 bp band for UBC-9 and a linearized 4 kb band for the expression vectors) were subsequently excised (Qiaquick gel extraction kit, Qiagen). The excised UBC-9 cDNA was ligated into the linearized pECFP and pEGFP expression vectors using the enzyme T4 ligase (Invitrogen). The ligation product was transformed into competent bacteria and grown on LB agar plates, from which colonies were picked and grown overnight in kanamycin-containing LB broth. Plasmid DNA was extracted from these cultures (Mini Prep Kit, Qiagen) and the presence of UBC-9 was confirmed by sequencing the clones.

3.4.3. Cell culture, transfection, and preparation for subsequent use

H9C2 and C2C12 cells (American Type Culture Collection) were grown in DMEM medium supplemented with 10% and 20% FBS, respectively and glutamine in an incubator at 37° C with 5% CO_2. For microscopy, H9C2 cells were plated at a density of 1 x 10^5 in a

24-well plate. Various combinations of single, double, and triple transfections with wild-type and mutant lamin A, lamin C and SUMO/UBC-9/GATA-4 (all three cloned into different expression vectors) were performed using lipofectamine LTX-plus. Eighteen to 22 hours following transfection, the medium was removed from the plates, and cells were washed twice with PBS. Cells were then fixed on microscopic slides using 400 ul/well of ice-cold methanol at -20° C, and washed thrice with PBS. Coverslips were mounted on the slides using fluorescent mounting medium (Dakocytomation #S3023). The slides were stored in darkness at 4 °C. For real-time PCR experiments, 4 x 10^5 H9C2 cells and 1x10^5 C2C12 cells were plated on six 60 mm tissue culture plates. Double-transfection with mutant or wild-type lamin A and C was performed on the following day using lipofectamine LTX. The cells in the 60 mm plates were collected using Trizol (Invitrogen) and cell scraper. They were frozen overnight at -80°C or subjected to RNA isolation the same day.

3.4.4. Immunocytochemistry

Immunocytochemistry was performed on cells grown on coverslips in 24 well plates. Cells grown on coverslips were fixed with 400 ul/well of 3% para-formaldehyde (PFA) in PBS for approximately 20 minutes. For immunostaining experiments on GATA-4, cultured cells were first transfected with lamin C (wild-type or mutant) and GATA-4 constructs, and fixed with PFA 18 to 22 hours after transfection. Following fixation, cells were washed three times with PBS, and PFA was quenched with 1 ml/well of 50 mM ammonium chloride (in PBS) for 30 minutes. Cells were then permeabilized using 0.1% TritonX100 in 5% FBS (in PBS) for 20 minutes at room temperature, washed thrice with PBS, and incubated for 20 minutes at room temperature with 200 ul/well of blocking solution (10% FBS in PBS). The

blocking solution was removed and cells were incubated for one hour at 37 ^{o} C with a solution consisting of primary antibodies (anti-rat GATA-4 goat polyclonal antibody [C-20] or anti-rat lamin A/C goat polyclonal antibody [Sc-6215]) diluted in 5% FBS (in PBS). Following three more washes with PBS, cells were hybridized with secondary antibody (Alexa Fluor-647-labeled rabbit anti-goat IgG [A-21446]), diluted in 5% FBS/PBS for one-half hour at 37 ^{o} C. Cells were then washed thrice with PBS. Glass coverslips were mounted on microscopic slides using fluorescent mounting medium (Dakocytomation #S3023).

3.4.5. Fluorescence microscopy

Cells were visualized through a Carl Zeiss Axio Imager .Z1 fluorescent microscope using the 63X oil immersion objective. Some images were also taken using Olympus Fluor View FV-1000 laser scanning confocal fluorescent microscope. Excitation wavelengths used for ECFP, EYFP, EGFP and pDsRed2 fluorescent vectors were 434 nm, 514 nm, 488 nm and 588 nm, respectively. All images were processed using Axio-vision, or Olympus FV-100 acquisition software, depending upon the microscope used.

3.4.6. Cloning of cDNA's into TOPO TA cloning vector for subsequent RT-PCR

The list of target and housekeeping genes cloned for use in real-time PCR experiments is shown in Table 3.1. The cDNA's of different genes were cloned to generate the required standard curves. Various primers were designed to amplify a fragment of approximately 100 bp to 150 bp using the Primer3 program. To clone the cDNA's into TOPO TA vector, one-step RT-PCR (Qiagen) was performed on RNA isolated from rat for H9C2 cells, and from mouse for C2C12 cells, using the above primers. The RT-PCR product

was directly cloned into the TA vector using the TA cloning kit (Invitrogen). Competent bacterial cells were transformed with the cloned TA vector using the standard transformation protocol. Transformed bacterial cells were plated on kanamycin/Xgal/IPTG plates and grown overnight at 37°C. Colonies containing the cloned cDNA's were selected on the basis of blue-white screening. Four or five white colonies were picked and grown individually overnight at 37°C with constant shaking in 4 to 5 ml of kanamycin-containing LB broth media. Mini-prep plasmid isolation was performed on these cultures using the kit from Qiagen. Isolated plasmid was electrophoresed on 5% agarose gel, and also subjected to a sequencing reaction using 3100 ABI prism sequencer to confirm the sequences of the TA clones. Maxi-prep plasmid isolation was performed on the clone having the correct cDNA sequence using the kit from Qiagen. Maxi-prep plasmids were quantified by absorbance at 280 nm.

Table 3.1: List of cloned target and housekeeping genes.

Gene	Purpose for cloning	Cell line
ANF	Target gene	H9C2
Troponin C	Target gene	H9C2
PGK1	Housekeeping gene	H9C2
SrPK3	Target gene	C2C12
PBGD	Housekeeping gene	C2C12
Beta-actin	Housekeeping gene	C2C12
PGK1	Housekeeping gene	C2C12

3.4.7. Generation of standard curves

To generate standard curves of the different TA clones, eight serial dilutions (ranging from 10 ng -0.001 pg) of maxi prep plasmids were made. These were subjected to real-time PCR using the SYBR green "taq-start" polymerase and light cycler adaptors according to the

manufacturer's instructions (Roche Diagnostics). PCR was conducted in capillaries in a total volume of 10 ul, consisting of 1 ul of SYBR Green, 5 ul (10 ng-.001 pg) of cloned cDNA, 1.2 uM of a mixture of forward and reverse primers, and 2.5mM ul of $MgCl_2$. Standard curves were generated by plotting CT values (crossing threshold) of various standard dilutions against the logarithm of the amount of input standard. Standard curves were generated for both target and housekeeping genes.

3.4.8. RNA isolation and DNase treatment

RNA was isolated from transfected H9C2 and C2C12 cells frozen at -80°C. Briefly, cells were thawed and resuspended in 100 µl of chloroform, and centrifuged at 12,000g at 4°C for 15 minutes to collect the clear aqueous phase. 250 µl of isopropanol was added, and the samples were incubated at room temperature for 10 min, followed by centrifugation at 12,000g at 4°C for 10 minutes to obtain a RNA pellet. The pellet was washed with 75% ethanol by centrifugation at 7,500g at 4°C for 5 minutes, and dissolved in 20 µl of RNase free water. DNase treatment was performed using the RNase-free DNase kit from Ambion according to the manufacturer's instructions. RNA was further purified using 1/10 volume of sodium acetate (pH 5.4) and 2.5 volume of 100% ethanol. This was frozen overnight. On the following day, the mixture was centrifuged at 12,000g at 4°C for 15 minutes. The pellet obtained was washed with 70% ethanol at 7,500g at 4°C for 5 minutes, and dissolved in 20 ul of nuclease free water. The RNA concentration was measured by taking the optical density at 260 nm. The purity of RNA was assessed by taking the optical density at 280 nm, and calculating the 260/280 ratio.

3.4.9. mRNA quantification using real-time PCR

Extracted RNA was subjected to first-strand cDNA synthesis using oligo $(dT)_{12-18}$ primers (Omniscript RT kit, Qiagen). Briefly, 2 ug of extracted RNA was added to RT mix prepared according to the manufacturer's instructions. This was then incubated at 37°C for one hour, and at 42°C for one hour. Under the same conditions previously standardized for the respective standard curves, 1ug of cDNA from each sample was subjected to real time PCR using gene-specific primers and SYBR green "taq-start" polymerase, according to the manufacturer's instructions. C_T values of the samples of interest were determined. The concentrations of target and reference genes in the sample were calculated by the LightCycler Software using C_T values and the appropriate standard curves. The normalized concentration of target gene was calculated by dividing the amount of target gene by the amount of reference gene.

3.5. Results

3.5.1. *In vitro* examination of *LMNA* mutations in a cardiac cell model (Objective 1)

3.5.1.1. Search for an appropriate cardiac cell model

The following cardiac cell models were tested: HL-1 cells (in collaboration with Dr. Patrick Burgon), P19 cells (in collaboration with Dr. Iona Skerianc), primary cardiomyocytes (in collaboration with Dr. Alex Stewart), and H9C2 cells (ATCC). HL-1 is a mouse cardiomyocyte cell line that has been shown to beat in cultures (Claycomb et al., 1998). We stained these cells for endogenous lamins with several antibodies, but could not find the proper lamin phenotype (Figure 3.3). P19 cells are embryonic mouse stem cells. In the presence of DMSO, P19 cells differentiate into cardiac cells (Jamali et al., 2001).

Differentiated P19 cells were shown to beat in culture after differentiation with DMSO (Van der hayden et al., 2003). However, we could not use P19 cells in our experiments because only 10% of treated cells were found to differentiate into cardiac cells. It would have been very difficult to determine if *LMNA* mutations cause perturbations in endogenous cardiac gene expression under these circumstances, since any effects would be diluted by the presence of non-differentiated cells in the culture. Use of primary cardiomyocytes has also been attempted in our laboratory, but they also demonstrated very poor transfection efficiency with commercially available transfection reagents. We stained H9C2 rat cardiomyoblasts, widely used as a cardiac cell model, for endogenous lamins (Kaneda et al., 2005, Sulliman et al., 2006, Tshori et al., 2006). We found that lamins were uniformly expressed in the nuclear lamina (Figure 3.3), indicating that these cells have a normal lamin A/C phenotype. We tested the transfection efficiency in this cell line with several transfection reagents such as SuperFect (Qiagen), TransFectin (Bio-Rad), Metafectene (Biontex), Lipofectamine 2000 (Invitrogen), and Lipofectamine LTX (Invitrogen). Except for Lipofectamine and Lipofectamine LTX, which produced transfection efficiencies of 10% to 15%, all reagents demonstrated exceedingly low rates of transfection. Given that the H9C2 cell line possessed the proper lamin phenotype and demonstrated higher transfection efficiency compared to the other cell lines tested, we decided to select H9C2 cells as a model to study the effects of *LMNA* mutations.

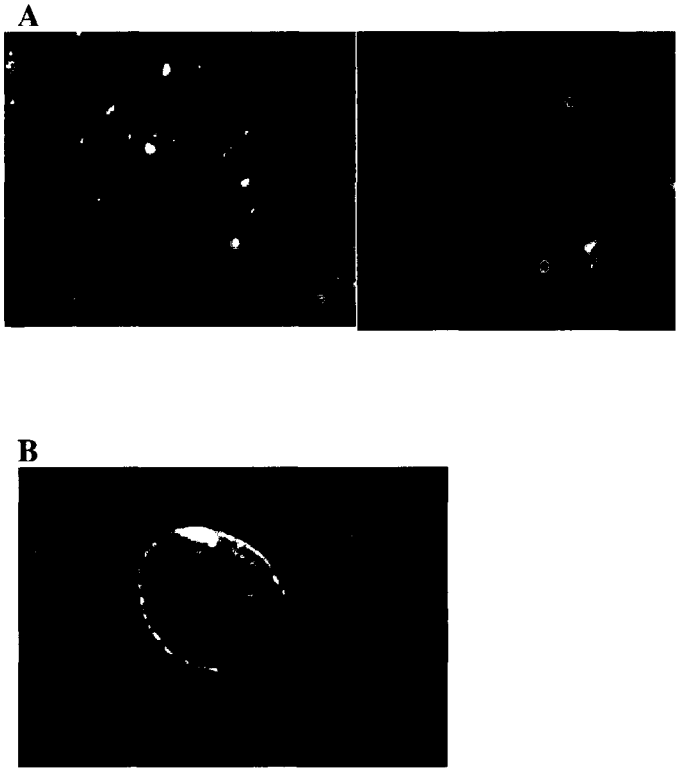

Figure 3.3: Cellular distribution of endogenous lamins in HL-1 (A) and H9C2 cells (B), stained with anti-rat goat polyclonal lamin A/C antibody (n=4). Alexa fluor-labeled rabbit anti-goat IgG (A-21446) was used as secondary antibody. Cells were visualized using wide-field fluorescent microscopy at the excitation wavelength for Alexa Fluor of 647 nm.

3.5.1.2. *In vitro* examination of *LMNA* mutations in H9C2 cells:

In vitro examination of *LMNA* mutations had previously been performed in COS-7 cells (Sylvius et al., 2008, Appendix 3). We wanted to confirm these results in H9C2 cells, a cell line more relevant to the study of DCM. Full-length lamin A and lamin C (wild type or mutant), fused to the C-terminus of variants of green-fluorescent protein (pEGFP) were expressed in H9C2 cells, and analyzed using the fluorescent microscope. In order to understand the roles of both lamin A and lamin C splice variants in the organization of nuclear lamina, we transfected H9C2 cells with wild-type or mutant lamin A or lamin C, separately or together. We studied DCM-causing *LMNA* mutations located in different domains of the protein as shown in Figure 3.3B. We also studied a mutation that causes EDMD (p.R386K), and another that causes FPLD (p.R482W), to test the tissue specificity of *LMNA* mutations.

3.5.1.2.1. Lamin A mutant aggregates

Wild-type lamin A cloned into pECFP-C1 (Cyan fluorescent protein) when expressed in H9C2 cells was homogenously expressed in the nuclear lamina, giving it a veil-like appearance that was similar to the phenotype of endogenous wild-type lamin A/C in H9C2 cells (Figure 3.3B, and Figure 3.4). We observed similar phenotypes upon expression of two distinct lamin A mutant constructs: p.L85R (DCM-causing mutation located in the central rod domain of lamin A/C) and p.R482W (FPLD-causing mutation located in the C-terminal tail region of lamin A/C).

In contrast, three other lamin A mutant constructs (DCM-causing mutations p.D192G and p.Q353K; EDMD-causing mutation p.R386K) formed small distinct aggregates in the

nuclear lamina, giving it a punctate appearance. These findings indicate that these lamin A mutants are able to localize at the nuclear envelope, although they form discontinuous lamina as compared to the veil-like structure of wild-type lamin (Figure 3.4). It is noteworthy that, although most of the aggregates seemed to be localized at the nuclear periphery, we cannot exclude the possibility that some aggregates may be present in the nucleoplasm as well.

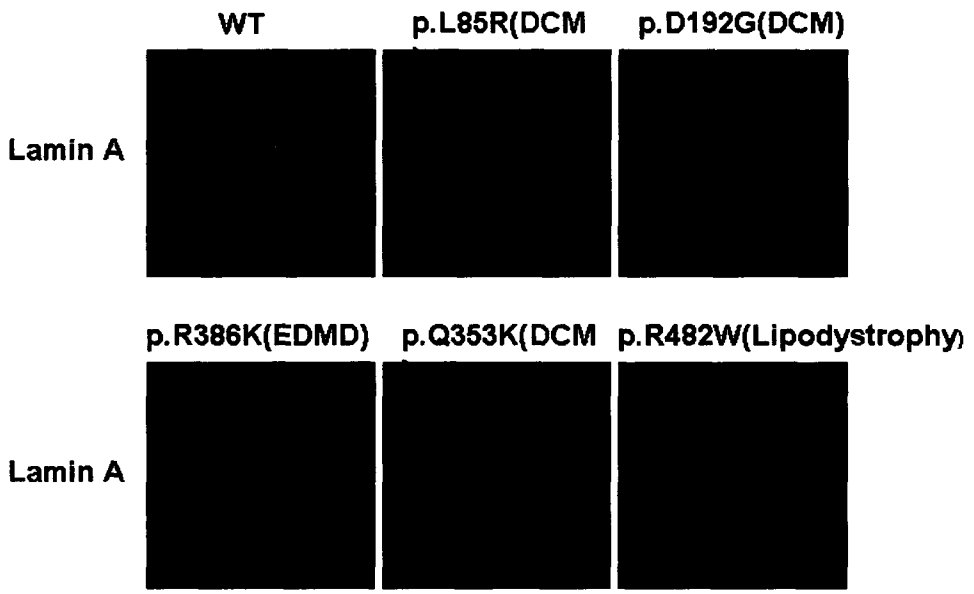

Figure 3.4: Fluorescence microscopy images of wild-type and mutant lamin A constructs (expressed as ECFP fusion protein) localized in the nuclei of H9C2 cells (n=4). Cells were visualized at an excitation wavelength of 433 nm for EFCP protein. The laminopathies associated with each mutation are shown in parenthesis. DCM: Dilated cardiomyopathy, EDMD Emery-Dreifuss Muscular dystrophy.

3.5.1.2.2. Lamin C mutant aggregates

In contrast to wild-type lamin A, wild-type lamin C formed multiple small, distinct, speckles in the nucleus, as has been described previously (Pugh et al., 1997, Motsch et al., 2005, Sylvius et al., 2005, Sylvius et al., 2008). Electron microscope images taken on COS-7 cells expressing wild-type lamin C indicated that lamin C speckles were localized in the nucleoplasm, but maintained close proximity with the nuclear envelope (Sylvius et al., 2008). A similar phenotype was observed for the lipodystrophy causing mutation p.R482W and for the DCM-causing mutation p.L85R. In contrast, the other three mutations (p.D192G, p.Q353K and p.R386K) resulted in the formation of large intranuclear lamin C aggregates in the majority of transfected cells (Figure 3.5). Furthermore, it was apparent from electron microscope images that the aggregates did not form a close connection with the nuclear envelope, suggesting that *LMNA* mutations abrogated the association of lamin C with the nuclear envelope (Sylvius et al., 2008)

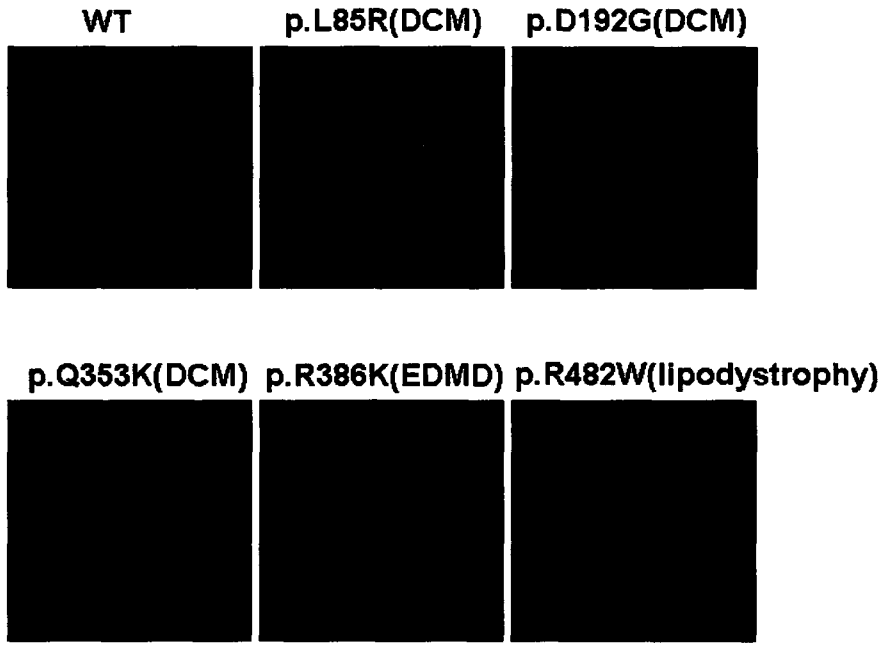

Figure 3.5: Fluorescence microscopy images of wild-type and mutant lamin C constructs (expressed as ECFP fusion protein) localized in the nuclei of H9C2 cells (n=4). Cells were visualized at an excitation wavelength of 433 nm for EFCP protein. The laminopathies associated with each mutation are shown in parenthesis. DCM: Dilated cardiomyopathy, EDMD: Emery-Dreifuss Muscular Dystrophy.

3.5.1.2.3. Co-transfection with wild-type or mutant lamin A and lamin C

In order to restore lamin A/C stoichiometry and thereby mimic a more physiologically relevant state, we performed double transfections of H9C2 cells with both lamin A and lamin C. To distinguish between the two isoforms, we cloned lamin A into pECFP-C1, whereas lamin C was cloned into pDSRed2-C1 (red fluorescent expression vector) or pEYFP-C1 (yellow fluorescent expression vector). Co-transfected wild-type lamin A and lamin C were uniformly expressed in the nucleus and formed a continuous lamina (Figure 3.6). Interestingly, a similar phenotype was observed upon transfection with the mutant lamin A/C constructs p.L85R and p.R482W. In these cases, expression of exogenous wild-type or mutant lamin A abrogated the formation of exogenous wild-type or mutant lamin C speckles, and gave rise to a uniform continuous lamina.

In contrast, upon expression of other lamin A/C mutant constructs (p.D192G, p.R386K, p.Q353K), lamin A and lamin C continued to form abnormal aggregates. This finding is consistent with previous studies in other cell models such as COS-7 cells, HeLa cells, MEF $^{+/+}$ cells (Sylvius et al., 2005, Raharjo et al., 2004). Both lamin A and lamin C co localized in aggregates and were localized in the nuclear lamina (figure 3.6). These results indicate that mutant lamin A retained its ability to drive mutated lamin C into the nuclear membrane, although the result was an abnormal distribution characterized by granular and discontinuous nuclear envelope.

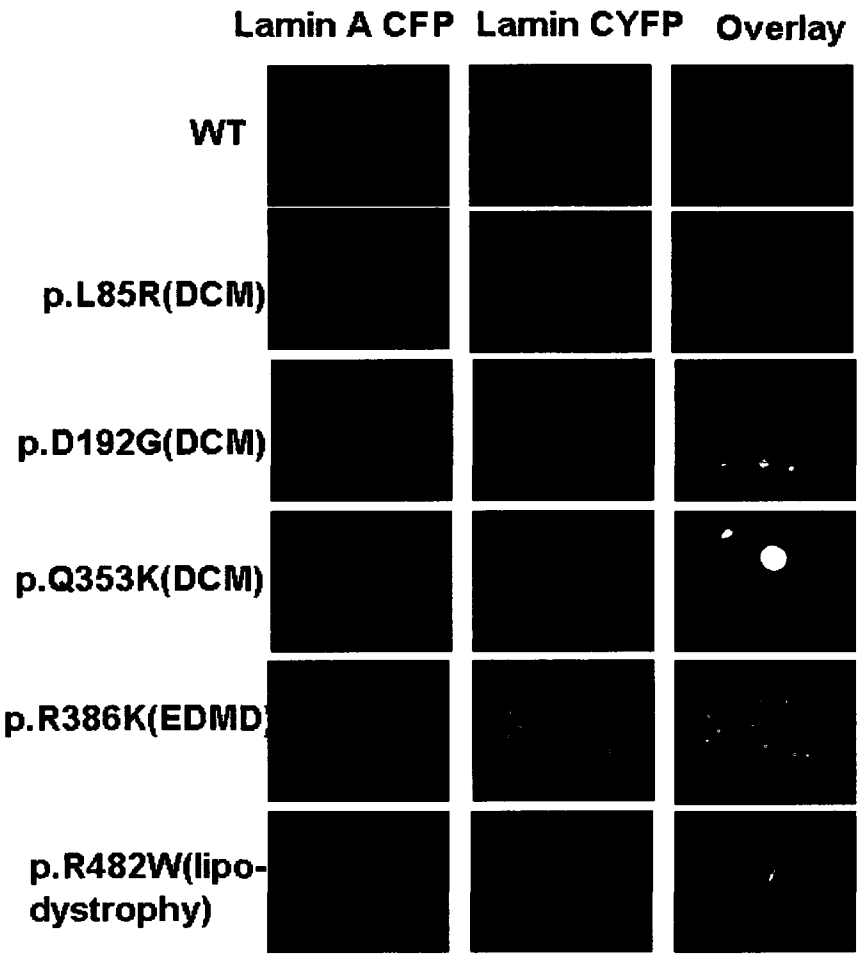

Figure 3.6: Confocal microscopy images of wild-type and mutant lamin A and lamin C constructs (expressed as ECFP fusion protein and DsRed2 fusion proteins respectively) localized in the nuclei of H9C2 cells (n=4). Lamin A is shown in red and lamin C in green. Cells were visualized at excitation wavelengths of 433 nm for lamin A-ECFP, and 558 nm for lamin C-DsRed2. DCM: Dilated cardiomyopathy, EDMD Emery-Dreifuss Muscular dystrophy.

3.5.2. Effect of *LMNA* mutations on the intranuclear localization of SUMO-1 and UBC-9 (Objective 2) (manuscript in preparation)

3.5.2.1. Effect on SUMO-1 and its conjugates

Apart from having a structural role in the nucleus, A-type lamins also play a role in mRNA transcription. Abnormal assembly of nuclear lamina along with formation of mutant lamin A/C aggregates may affect the distribution of important transcription factors or regulators, such as SUMO-1. Our group previously showed that the lamin A/C mutant p.D192G affected the intranuclear localization of SUMO-1 and its conjugates in COS-7 cells. In this study, we determined the effect of various DCM- and non-DCM causing lamin A/C mutations (i.e., p.L85R, p.D192G, and p.Q353K causing DCM, p.R482W causing lipodystrophy, and p.R386R causing EDMD) on the intranuclear localization of SUMO-1 and its conjugates in H9C2 cells. None of our lamin A constructs (wild-type or mutant) appeared to alter the distribution of SUMO-1 conjugates (Figure 3.7).

In the presence of wild-type lamin C, SUMO-1 was uniformly expressed in the nucleus. In contrast, all mutant lamin C constructs (p.L85R, p.D192G, p.Q353K, p.R386K, and p.R482W) affected the intranuclear distribution of SUMO-1 (Figure 3.8), such that the SUMO-1 conjugates either co-localized with the lamin C aggregates (p.Q353K, p.R386K, p.R482W) or were sequestered within the mutant lamin C aggregates (p.L85R, p.D192G).

All mutations were located within the lamin A and C common protein regions. Therefore, in order to determine if SUMO-1 is mislocalized in the physiologically relevant state when both mutated lamins are expressed, we performed triple transfections of H9C2 cells with wild-type or mutant lamin A (in ECFP expression vector), wild-type or mutant lamin C (in pDsRed2 expression vector), and SUMO-1 (in EYFP expression vector). As expected, SUMO-1 was uniformly distributed in the nucleus in the presence of wild-type

lamin A and lamin C. Not surprisingly, given the uniform distribution of lamin A and lamin C in the nuclear lamina of cells expressing mutations p.L85R, and p.R482W, co-expression of lamin A and lamin C led to the restoration of wild-type phenotype with respect to SUMO-1 distribution (i.e., a uniform distribution throughout the nucleus). In contrast, in the presence of mutations p.D192G, p.Q353K, and p.R386K, SUMO-1 conjugates were found to be sequestered within lamin A/C aggregates (Figure 3.9). It was also evident that sequestration of SUMO-1 conjugates within lamin A/C aggregates was driven by lamin C, because lamin A transfection alone did not appear to have a substantial effect on the intranuclear distribution of SUMO-1 conjugates.

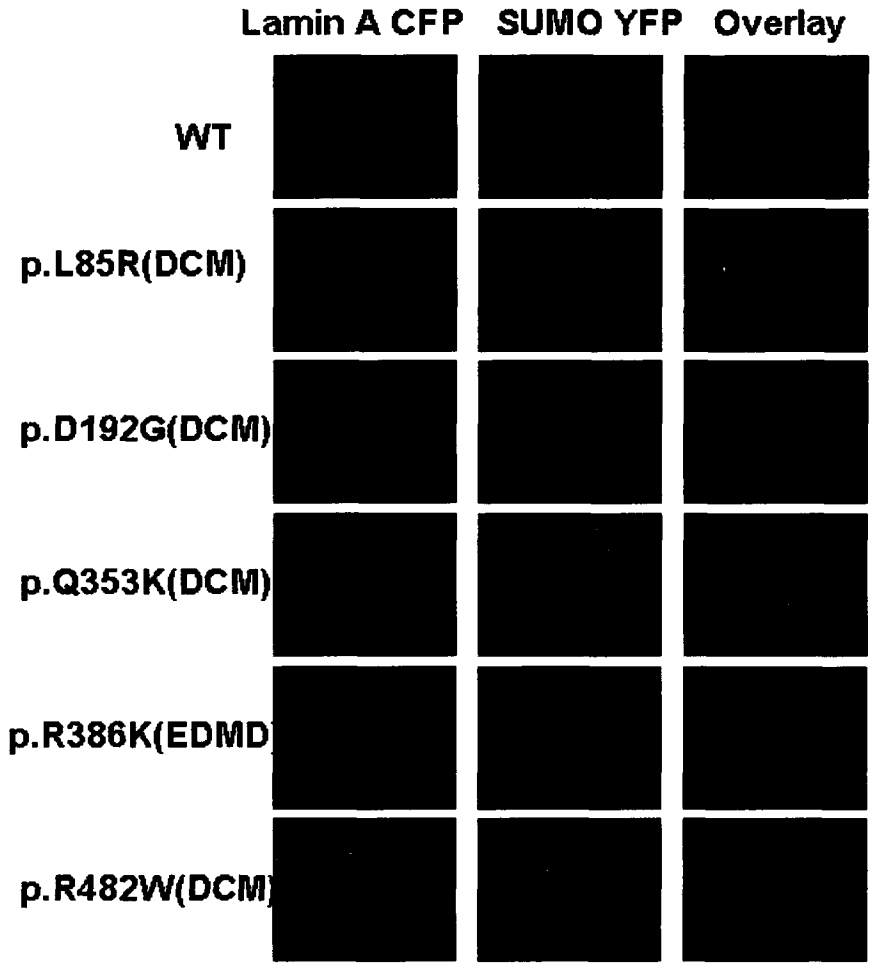

Figure 3.7: Fluorescence microscopy images showing nuclear localization of transfected SUMO-1 in the presence of either wild-type or mutant lamin A constructs in H9C2 cells (n=4). Lamin C is shown in red and SUMO-1 in green. Lamin A and SUMO-1 were cloned into pECFP-C1 and pEYFP-C1 fluorescent expression vectors, respectively. Cells were visualized at excitation wavelengths of 433 nm for lamin A-ECFP and 514 nm for SUMO-1-EYFP. DCM: Dilated cardiomyopathy, EDMD Emery-Dreifuss Muscular dystrophy.

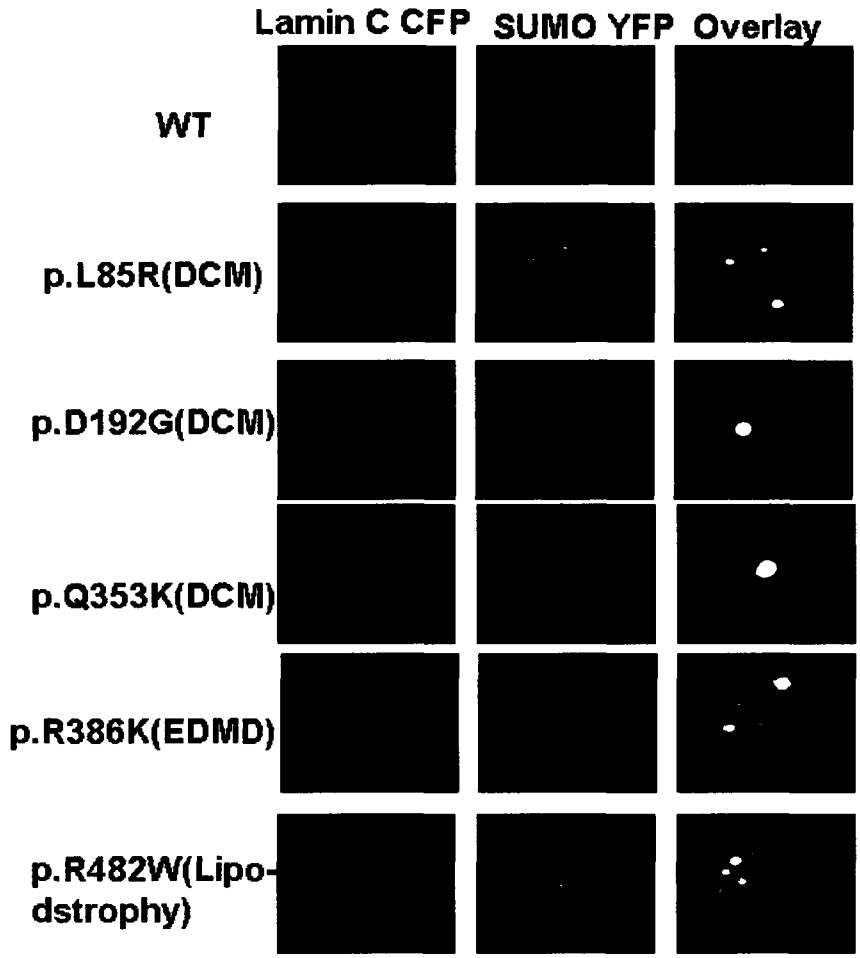

Figure 3.8: Fluorescence microscopy images showing nuclear localization of transfected SUMO-1 in the presence of either wild-type or mutant lamin C constructs in H9C2 cells (n=4). Lamin C is shown in red and SUMO-1 is shown in green. Lamin C and SUMO-1 were cloned into pECFP-C1 and pEYFP-C1 fluorescent expression vectors, respectively. Cells were visualized at excitation wavelengths of 433 nm for lamin C-ECFP and 514 nm for SUMO-1-EYFP. DCM: Dilated cardiomyopathy, EDMD Emery-Dreifuss Muscular dystrophy.

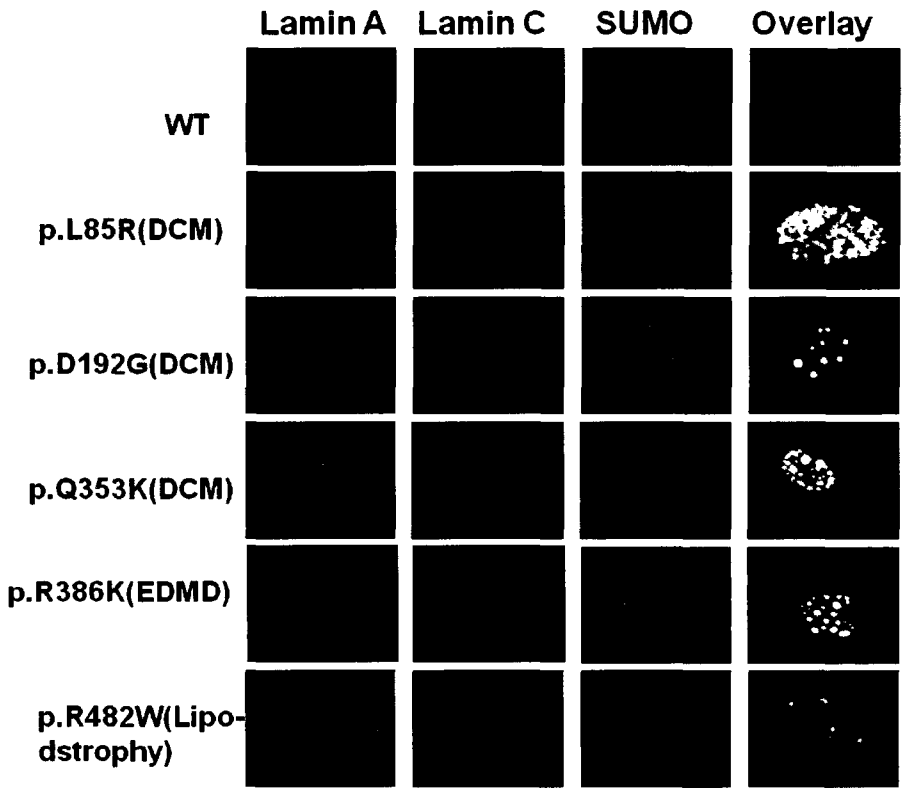

Figure 3.9: Confocal microscopy images showing nuclear localization of transfected SUMO-1 in the presence of wild-type or mutant lamin A and lamin C (n=4). Lamin A is shown in blue, lamin C in red, and SUMO-1 in green. Lamin A, lamin C and SUMO-1 were cloned into pECFP-C1, pDSRed2 and pEYFP-C1 fluorescent expression vectors, respectively. Cells were visualized at excitation wavelengths of 433 nm for lamin A-ECFP, 558 nm for lamin C-dsRed2 and 514 nm for SUMO-1-EYFP. DCM: Dilated cardiomyopathy, EDMD Emery-Dreifuss Muscular dystrophy.

3.5.2.2. Effect of *LMNA* mutations on UBC-9

UBC-9 is the sole E2 conjugating enzyme for covalent attachment of SUMO-1 to its substrates. Furthermore, UBC-9 has been shown to interact with A-type lamins (Zhong et al., 2004). We therefore sought to assess the effect of *LMNA* mutations on the localization of UBC-9 to the nuclear envelope (Zhang et al., 2002). In order to study the effect of *LMNA* mutations on the intranuclear distribution of endogenous UBC-9, we co-transfected H9C2 cells with wild-type or mutant lamin A or lamin C. We also performed triple transfections with lamin A, lamin C and UBC-9.

UBC-9 was found to co-localize at the nuclear periphery along with wild-type lamin A. DCM-causing mutation p.L85R and FPLD-causing mutation p.R482W demonstrated phenotypes that were similar to wild-type. In contrast, the DCM-causing mutation pD192G and p.Q353K, and the EDMD-causing mutation p.R386K, disrupted the uniform peripheral distribution of UBC-9, such that UBC-9 was found to co-localize with mutant lamin A aggregates (Figure 3.10).

As described previously, over-expression of wild-type lamin C led to the formation of multiple, small lamin C speckles that were uniformly distributed in the nucleus. UBC-9 was found to co-localize with these speckles. The lamin C mutants p.R482W and p.L85R demonstrated phenotypes similar to wild-type. On the other hand, the lamin C mutants, p.D192G, p.Q353K, and p.R386K formed large intranuclear aggregates with which UBC-9 was also co-localized (Figure 3.11).

Upon co-expression of UBC-9 with both wid-type lamin A and lamin C, all three proteins were found to be uniformly expressed at the nuclear periphery. Similar to the results obtained with lamin A mutants, co-expression of mutants p.L85R or p.R482W with UBC-9

did not affect nuclear localization of UBC-9. In the presence of lamin A/C mutations p.D192G, p.Q353K, and p.R386K, UBC-9 was found to co-localize with the mutant lamin A and lamin C aggregates (Figure 3.12).

The observed mislocalization of both SUMO-1 and UBC-9 by lamin A/C mutant aggregates demonstrated that *LMNA* mutations may exert their effects, at least in part, by interfering with the sumoylation pathway.

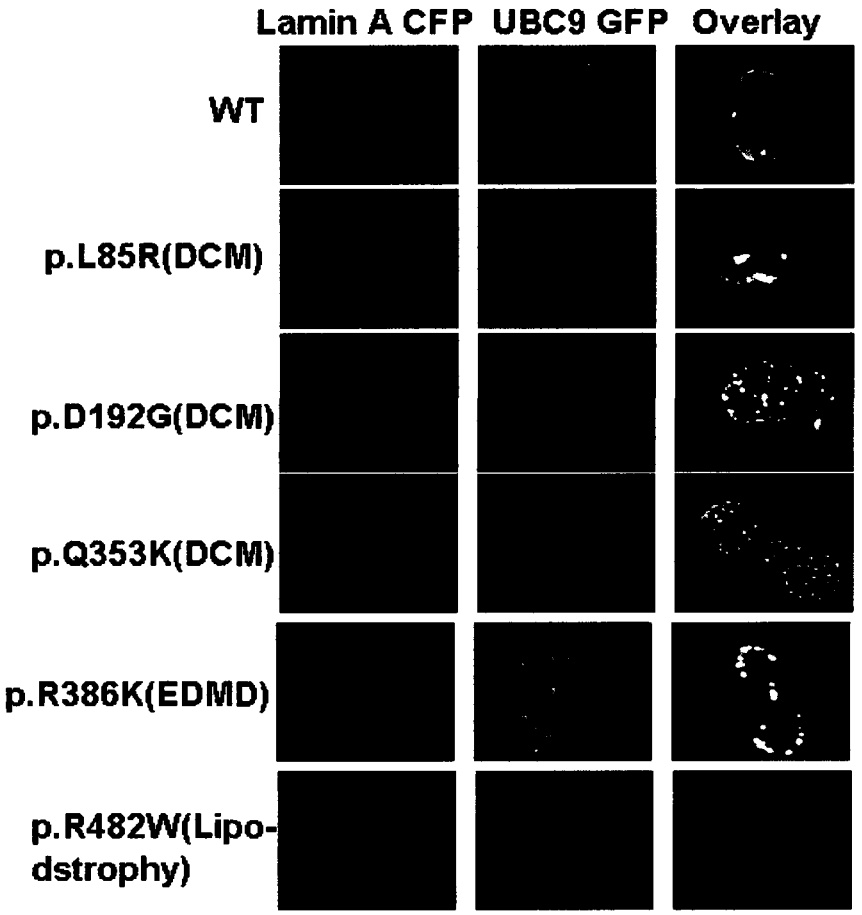

Figure 3.10: Fluorescence microscopy images showing nuclear localization of transfected UBC-9 in the presence of either wild-type or mutant lamin A constructs in H9C2 cells (n=4). Lamin A is shown in red and UBC-9 is shown in green. Lamin A and UBC9 were cloned into pECFP-C1 and pEGFP-C1 fluorescent expression vectors, respectively. Cells were visualized at excitation wavelengths of 433 nm for lamin C-ECFP and 488 nm for UBC9-EGFP. DCM: Dilated cardiomyopathy, EDMD: Emery-Dreifuss Muscular dystrophy.

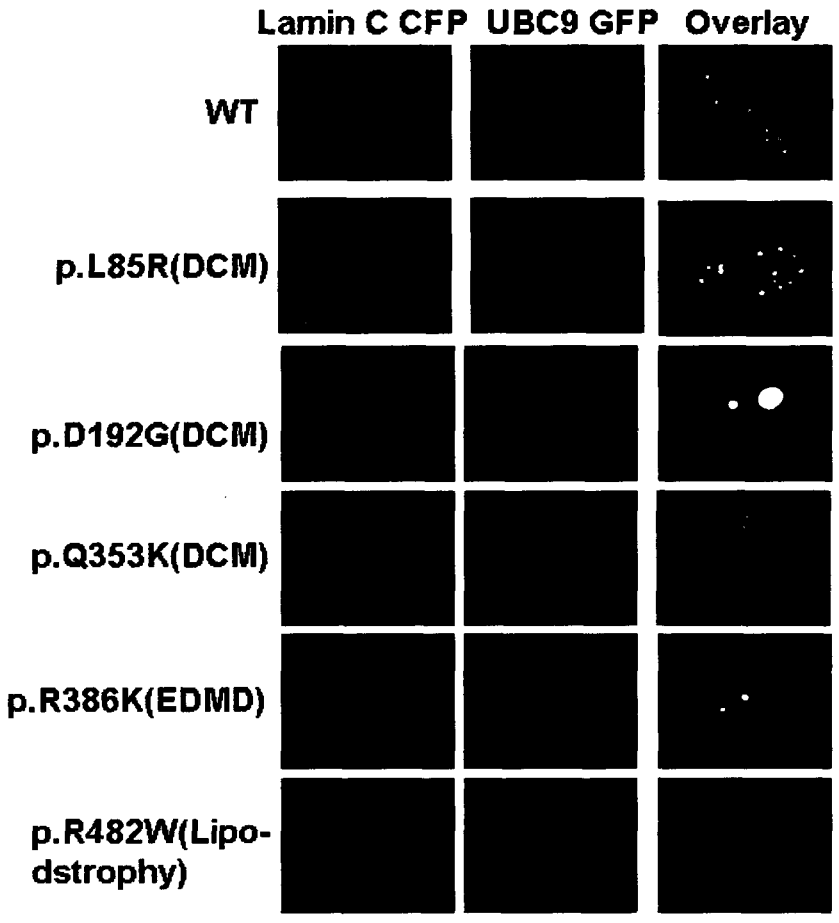

Figure 3.11: Fluorescence microscopy images showing nuclear localization of transfected UBC9 in the presence of either wild-type or mutant lamin C constructs in H9C2 cells (n=4). Lamin C is shown in red and UBC9 is shown in green. Lamin C and UBC9 were cloned into pECFP-C1 and pEGFP-C1 fluorescent expression vectors, respectively. Cells were visualized at excitation wavelengths of 433 nm for lamin C-ECFP and 488 nm for UBC9-EYFP. DCM: Dilated cardiomyopathy, EDMD: Emery-Dreifuss Muscular dystrophy.

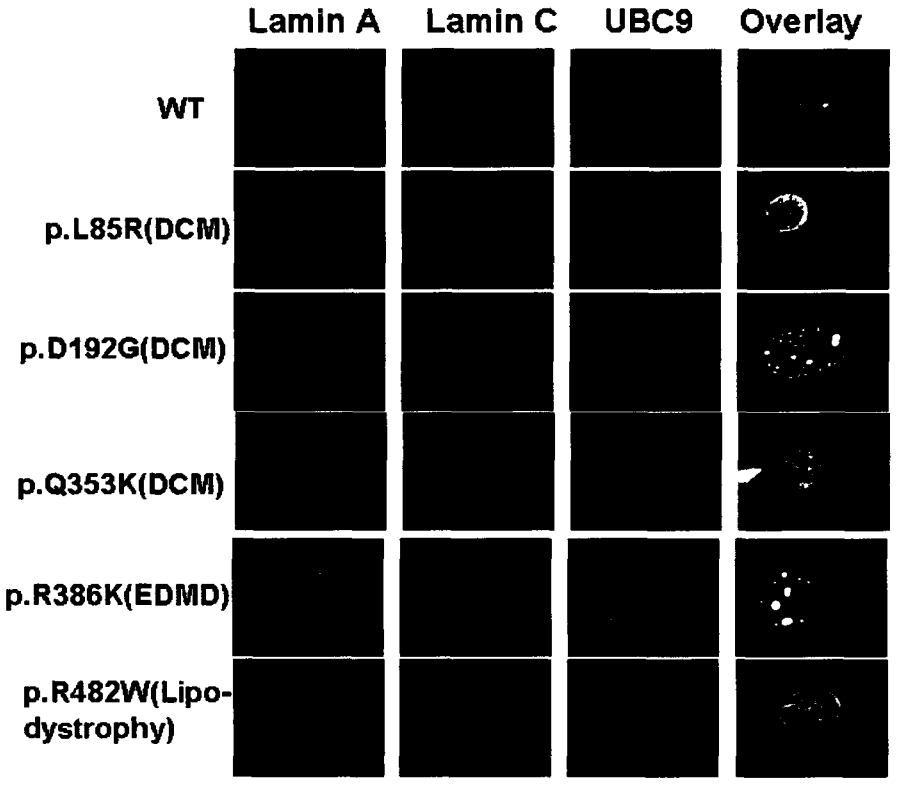

Figure 3.12: Confocal microscopy images showing nuclear localization of transfected UBC9 in the presence of either wild-type or mutant lamin A and C constructs in H9C2 cells (n=4). Lamin A is shown in blue, lamin C in red, and UBC9 in green. Lamin A, lamin C and UBC9 were cloned into pECFP-C1, pDsRed2 and pEGFP-C1 fluorescent expression vectors, respectively. Cells were visualized at excitation wavelengths of 433 nm for lamin A-ECFP, 558 nm for lamin C-DsRed2, and 488 nm for UBC9-EGFP. DCM: Dilated cardiomyopathy, EDMD: Emery-Dreifuss Muscular dystrophy.

3.5.3. Effect of *LMNA* mutations on intranuclear localization of GATA-4 (Objective 3)

Although *LMNA* mutations may affect a number of transcription factors directly, we chose to focus on sumoylated transcription factors based on our observations that some *LMNA* mutations caused marked disruption of SUMO-1 distribution. One such sumoylated transcription factor is GATA-4, a cardiac-enriched dual zinc-finger transcription factor that plays a critical role in regulating cardiac-specific genes such as ANF and troponin C. Sumoylation has been shown to enhance the transcriptional activity of GATA-4 (Wang et al., 2004). In order to determine the effect of *LMNA* mutations on the intranuclear localization of sumoylated GATA-4, we double-transfected H9C2 cells with wild-type or mutant lamin C and GATA-4 (rat-GATA-4 cloned into PCGNA vector, obtained from Dr. Mona Nemer). Intranuclear distribution of SUMO-1 appeared to be disrupted when cells were transfected with mutant lamin C, but not when transfected with mutant lamin A. SUMO-1 was also found to be mislocalized when cells were co-transfected with mutant lamin A and lamin C, suggesting that mislocalization of SUMO-1 is driven by lamin C. Since the most pronounced effect on SUMO-1 distribution was observed upon transfection with lamin C alone, we used wild-type or mutant lamin C to study the intranuclear distribution of GATA-4 (Figure 3.13). None of the mutations used in the study affected the intranuclear distribution of transfected GATA-4. The results for endogenous GATA-4 were similar (data not shown). One possible reason for the lack of an apparent effect of *LMNA* mutations on GATA-4 distribution is that at any given time, only 5% of proteins (including GATA-4) are sumoylated. Since only sumoylated GATA-4 is expected to be trapped in mutant lamin A/C aggregates, our methods may not be sufficiently sensitive to measure this effect.

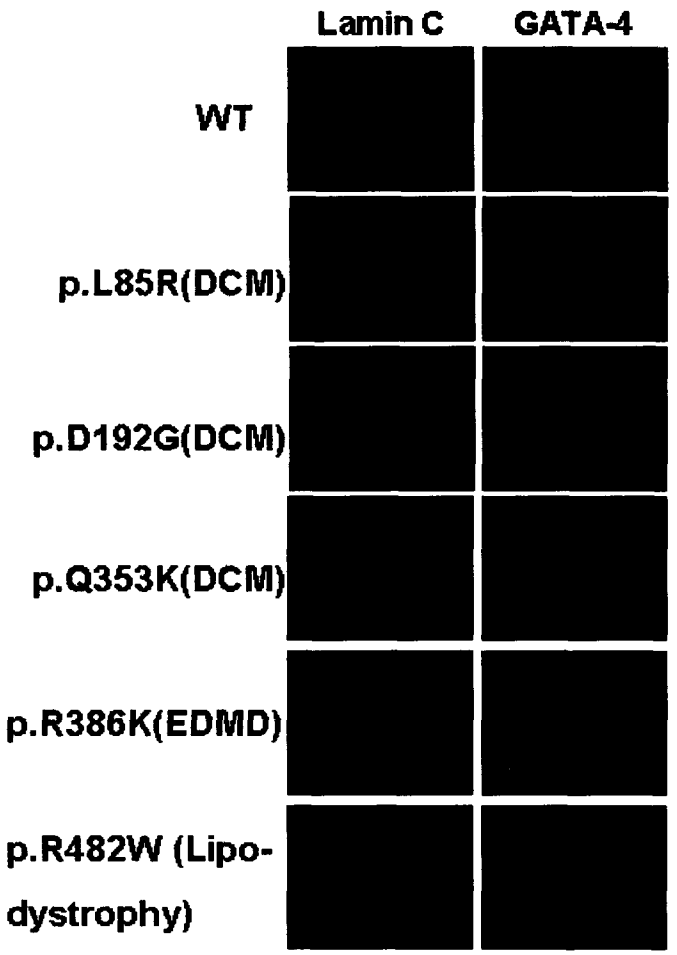

Figure 3.13: Confocal microscopy images showing nuclear distribution of transfected GATA-4 in the presence of wild-type or mutant lamin C constructs in H9C2 cells (n=4). Lamin C is shown in red and GATA-4 is shown in blue. Lamin C and GATA-4 were cloned into pECFP-C1, and PCGNA vectors (obtained from Dr. Mona Nemer), respectively. GATA-4 was stained using an anti-rat GATA-4 goat polyclonal antibody (C20). Rabbit anti-goat IgG (A-21446) Alexa-fluor labeled antibody was used as secondary antibody. Cells were visualized at excitation wavelengths of 433 nm for lamin C-ECFP-C1 and 647 nm for Alexa fluor (for GATA4). DCM: Dilated cardiomyopathy, EDMD: Emery-Dreifuss Muscular dystrophy.

3.5.4. Effect of *LMNA* mutations on GATA-4 transcriptional activity (Objective 4)

Since the results regarding GATA-4 co-localization in the presence of lamin C aggregates were inconclusive, we investigated the effect of *LMNA* mutations on GATA-4 transcriptional activity by assessing their effects on expression of GATA-4 regulated genes through real-time PCR.

3.5.4.1. Search for GATA-4 regulated target genes

GATA-4 regulates the expression of many cardiac-specific genes such as ANF, troponin C, troponin I, α-MHC, and NKX2-5. For real-time PCR, it is recommended that expression of the target gene be similar to that of the chosen housekeeping gene, in order to ensure maximal sensitivity in detection of small differences in expression (Silver et al. 2006, Roche Applied Science, technical Note No. LC 13/2002-selection of house-keeping gene, Psiotra et al., 2008). This consideration was especially important in our study since transfection efficiency in H9C2 cells was relatively low. We assessed the expression of several GATA-4 regulated genes such as ANF, troponin C, troponin I, and NKX2-5 through real-time PCR. Except for troponin C, most genes demonstrated low expression (i.e., a high CT value) in H9C2 cells (Figure 3.14). We measured the expression level of several candidate housekeeping genes such as phosphoglycerate kinase 1 (PGK1), beta-actin, glyceraldehyde 3-phosphate dehydrogenase (GAPDH), and Hypoxanthine-guanine phosphoribosyltransferase (HPRT) in order to identify one with a similar expression level to candidate target genes (figure 3.14). All of these demonstrated higher expression as compared to the target genes α-myosin, ANF, NKX2-5, and troponin I (low CT value). We

ultimately selected troponin C as our target gene because it had a higher expression level than the other candidates that was similar to that of the housekeeping gene PGK1.

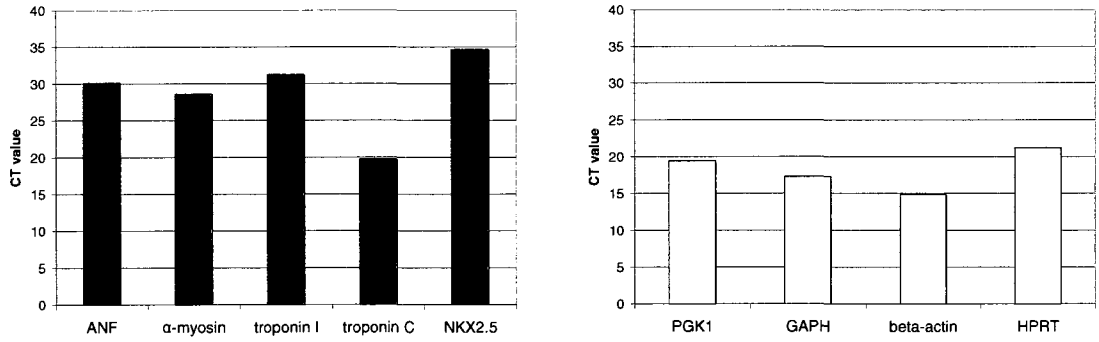

Figure 3.14: CT (Crossing threshold) values of candidate target and housekeeping genes. Troponin C was ultimately selected as target gene along with the housekeeping gene PGK1 due to their similar CT values.

3.5.4.2. Real-time PCR on troponin-C

Real time PCR on troponin C was performed using RNA obtained from H9C2 cells (transfected with wild type or mutant lamin A and lamin C) using the housekeeping gene PGK1 as a standard. Although there was a trend toward decreased expression of troponin C, a statistically significant difference in expression between wild-type and mutant was not observed (Figure 3.15). There are two possible reasons for this. First, it is possible that the low transfection efficiency (10%) reduced the sensitivity to detect differences in expression. As described previously, the maximum transfection efficiency achieved after a trial of several transfection agents was 10-15% with Lipofectamine LTX. It is therefore possible that endogenous wild-type lamin A/C expression may have attenuated the effect of transfected mutant lamin A/C on expression of troponin C. Second, since cardiomyocytes do not undergo replacement, it is conceivable that expression of a structural protein such as troponin C may not be as tightly regulated as other proteins such as transcription factors. Therefore, the expression of troponin C may not be affected by *LMNA* mutations. Since Since other GATA-4 regulated genes had a lower exression in H9C2 cells, we focused out study on another sumoylated cardiac enriched transcription factor: myocyte enhancing factor-2C.

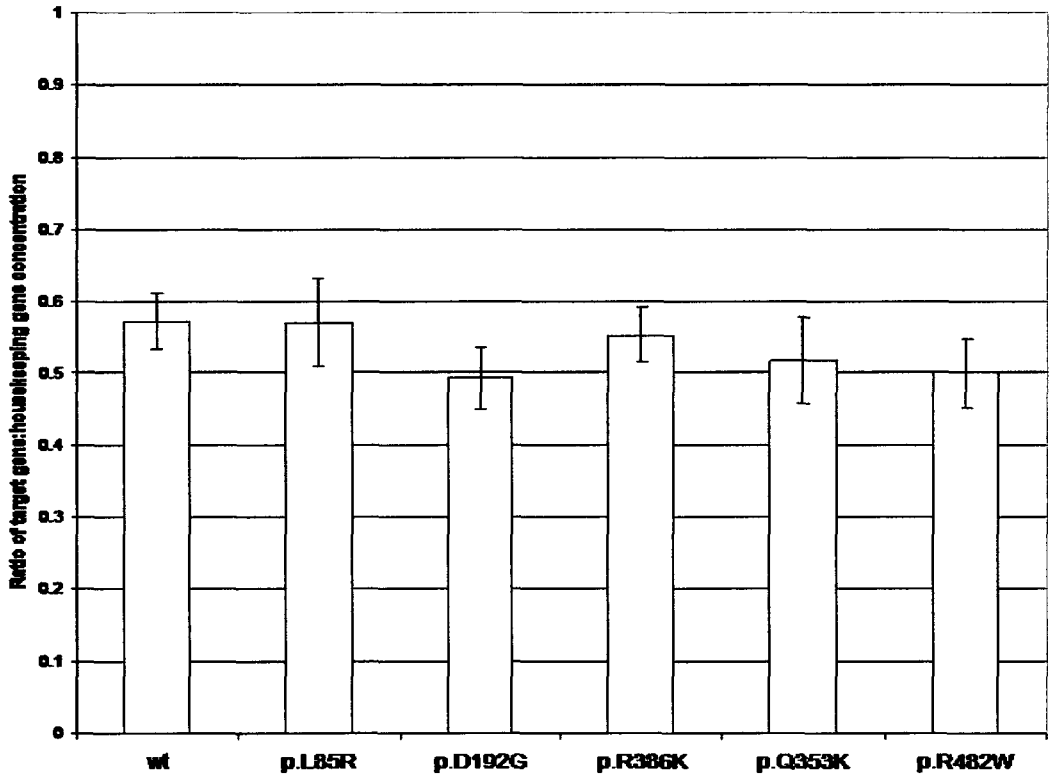

Figure 3.15: Real-time PCR on the GATA-4 regulated gene troponin C (normalized to the house-keeping gene PGK1) in H9C2 cells transfected with wild-type and mutant lamin A and lamin C (cloned into pECFP-C1 and pEYFP-C1 expression vectors, respectively). No statistically significant difference was observed between wild-type and the mutants. wt (n=12); 85 (n=9); 192 (n=12);, 386(n=10); 482 (n=10).

3.5.5. Effect of *LMNA* mutations on MEF2C transcriptional activity (Objective 5)

3.5.5.1. C2C12 cells

Skeletal and cardiac muscle share similar properties and express many of the same genes. Furthermore, some laminopathies are known to affect both cardiac and skeletal muscles (e.g., the EDMD-causing mutation p.R386K). Therefore, the C2C12 skeletal myoblast cell line was thought to be the most appropriate alternative to a cardiac cell line to test our hypothesis. Moreover, upon transfecting C2C12 cells with lamin A and lamin C with lipofectamine LTX, we found a transfection efficiency of 40-50%, higher than that observed in H9C2 cells. When cultured in the presence of low serum-containing growth medium, C2C12 cells exit the cell cycle and differentiate into skeletal myotubes. In this cell model, we wanted to investigate the effect of *LMNA* mutations on the transcriptional activity of myocyte-enhancing factor 2C (MEF2C), a transcription factor specific to cardiac, skeletal and brain tissue. This transcription factor regulates the expression of skeletal muscle genes such as SrPK3 and troponin C (Nagakawa et al. 2006) and is involved in regulating and maintaining differentiation of skeletal muscles. It has been shown that sumoylation represses the transcriptional activity of MEF2C (Kang et al., 2006). Because MEF2C plays a role in differentiation of C2C12 cells and is elevated in differentiated cells, we initially decided to use differentiated C2C12 cells as our model to study the effect of *LMNA* mutations on expression of SrPK3. We transfected C2C12 myoblasts with wild-type or mutant lamin A and lamin C. Following transfection, we induced differentiation by culturing in the presence of low serum-containing growth medium for approximately 72 hours. Interestingly, in contrast to untransfected cells and cells transfected with wild-type lamins, we found that some lamin A/C mutations (p.D192G, p.R386K, p.Q353K, p.L85R) affected the

differentiation of myoblasts into myotubes. (The mutation p.R482W did not appear to have a substantial effect on differentiation as compared to the wild-type.) This observation confirmed a previous report by Favreau et al. (2004) that *LMNA* mutations affect C2C12 differentiation. This model was therefore not suitable for our study since the degree of differentiation would vary across different lamin mutants, thereby confounding any differences in gene expression. We therefore proceeded to study the effect of *LMNA* mutations on MEF2C transcriptional activity in undifferentiated C2C12 myoblasts. We implemented specific measures in the protocol to maintain cells in an undifferentiated state in the culture medium. First, we plated the cells such that they were not more than 50% confluent at the time of transfection. Second, cells were grown in 20% FBS to prevent them from differentiating. Third, the potential presence of differentiated myotubes in C2C12 myoblast cultures was monitored by performing western blots of C2C12 protein lysate with anti-myogenin antibody, since myogenin protein is present only in differentiated myotubes (Favreau et al., 2004). No myogenin was observed, demonstrating that C2C12 myoblast cultures did not contain differentiated cells. (This experiment was done by Sarah Labib, a member of our laboratory.)

3.5.5.2. Real-time PCR on SrPK3 in undifferentiated C2C12 myoblasts

To study the effect of *LMNA* mutations on MEF2C regulated genes, SrPK3 was considered a relevant target gene because its over-expression was shown to cause DCM in mice (Nagakawa et al., 2005).

Real-time PCR on SrPK3 was performed using RNA obtained from undifferentiated C2C12 cells (transfected with wild type or mutant lamin A and lamin C). The housekeeping gene PBGD was used as a standard since its expression was similar to that of SrPK3.

There was no statistically significant difference between wild-type and mutants in the expression of SrPK3. However, from the mean ratios of target gene to housekeeping gene concentration, most mutations (p.D192G, p.Q353K, p.R386K, p.R482W) appeared to result in higher expression of SrPK3 as compared to wild-type (Figure 3.16). The lack of a significant difference cannot be considered conclusive due to the substantial variability observed between different replicates (n=3). Possible causes of the observed variability were considered, such as the presence of myogenin and cell confluence, as described previously. As well, DNA and protein (Rnase) contamination was ruled out since DNase treatment was performed and the 260/280 ratio (which determines protein contamination) was greater than two in all cases. Since a high degree of variability was also demonstrated by untransfected cells, it is possible that variability may be due to the intrinsic expression characteristics of SrPK3 in C2C12 cells.

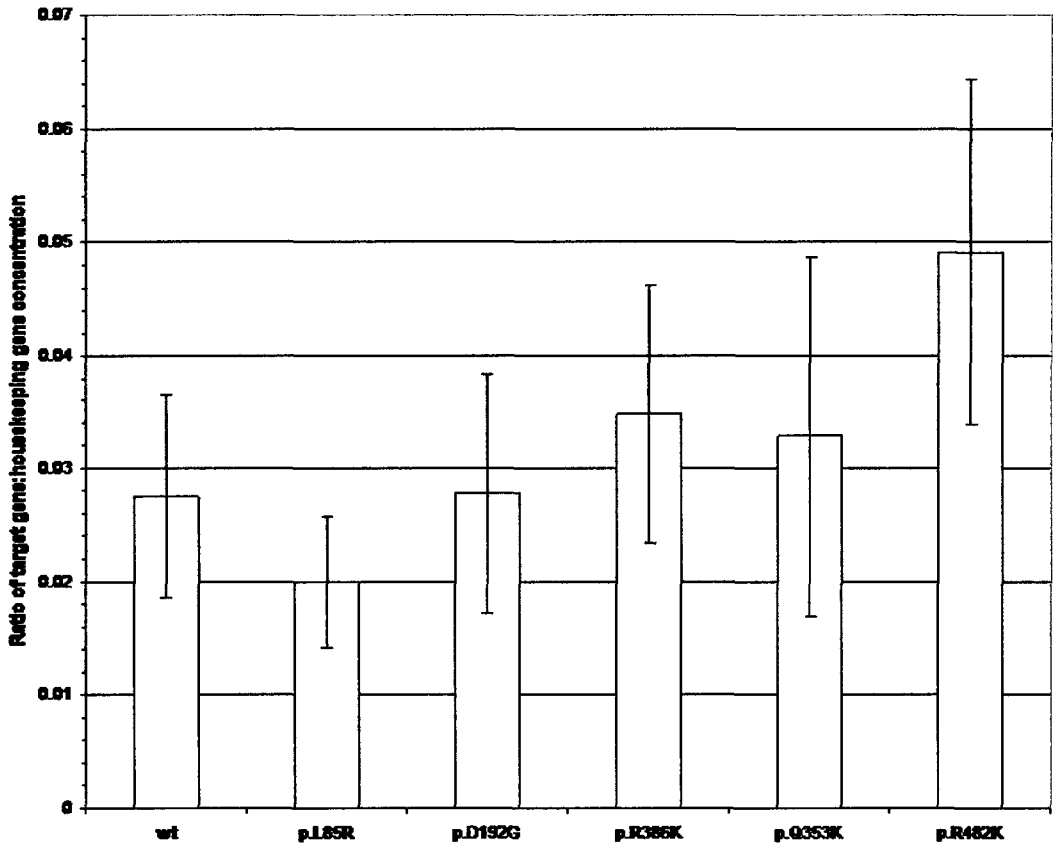

Figure 3.16: Real-time PCR on the MEF2C-regulated gene SrpK3 (normalized to the house-keeping gene PBGD) in C2C12 cells transfected with wild-type and mutant lamin A and lamin C (cloned into pECFP-C1 and pEYFP-C1 expression vectors, respectively). No statistically significant difference was observed between wild-type and the mutants.

3.6. Discussion

Our results indicate that some DCM-causing *LMNA* mutations lead to the formation of abnormal lamin A and lamin C aggregates in the nuclei of H9C2 cardiac cells. We also found that SUMO-1 and UBC-9, proteins involved in sumoylation and regulation of cardiac-specific transcription factors such as MEF2C and GATA-4, were sequestered within these aggregates. However, attempts to measure the effect of *LMNA* mutations on the expression of genes regulated by these transcription factors produced inconclusive results.

3.6.1. *LMNA* mutations caused abnormal nuclear distribution of lamin A and lamin C

We investigated the effect of *LMNA* mutations on the individual and conjoint functions of lamin A and lamin C in the organization of the nuclear lamina. Our results demonstrated that some mutant lamin A proteins (p.D192G, p.R386K, p.Q353K) form abnormal aggregates in the nuclear periphery. This suggests that, although these lamin A mutants were unable to form a continuous lamina, they maintained their association with the nuclear envelope. In contrast, two other lamin A mutants (p.L85R, p.R482W) had a phenotype similar to wild-type.

Unlike lamin A, wild-type lamin C formed multiple, small intranuclear aggregates, called speckles, that were distributed throughout the nucleus and were closely associated with the nuclear envelope. Two lamin C mutants (p.L85R, p.R482W) had a similar phenotype. However, three other lamin C mutants (p.D192G, p.R386K, p.Q353K) formed large intranuclear aggregates that did not exhibit close association with the nuclear envelope. Upon expression of both lamin A and lamin C in H9C2 cells, we observed that lamin A inhibited the formation of aggregates by wild-type, p.R482W, and p.L85R lamin C, and

restored the veil-like distribution of both lamins in the nuclear lamina. In contrast, upon expression of other lamin A/C mutants (p.D192G, p.R386K, p.Q353K), lamin A and lamin C continued to form abnormal aggregates, leading to the formation of discontinuous lamina. These results were similar to those obtained in COS-7 cells transfected with p.D192G, p.R386K, p.L85R, and p.R482W (Sylvius et al., 2005, Sylvius et al., 2008). We also extended these findings to the new mutation p.Q353K identified in our lab. Similar to our results, formation of nuclear lamin A/C aggregates have also been reported in previous studies of other DCM-causing mutations (Ostlund et al., 2001, Raharjo et al., 2001, Broers et al., 2005, Sylvius et al., 2005, Hubner et al., 2006, Hubner et al., 2006).

Formation of discontinuous lamina by EDMD- and DCM-causing mutations may render the nuclear envelope more fragile, especially in mechanically-stressed tissues such as cardiac and skeletal muscle (Ostlund et al., 2001, Raharjo et al., 2001, Broers et al., 2005, Sylvius et al., 2005, Hubner et al., 2006, Hubner et al., 2006). These observations support the role of the structural mechanism in the pathophysiology of DCM and EDMD. However, one DCM mutation (pL85R) demonstrated a normal lamina structure, similar to wild-type. Other groups have also reported DCM- and EDMD-causing mutations that have no effect on lamina integrity (Ostlund et. al., 2004, Sylvius et al., 2005). The fact that not all DCM- and EDMD-causing mutations affect the lamina therefore indicates that the structural mechanism alone cannot account for all DCM or EDMD cases.

The lipodystrophy-causing mutation p.R482W, which affects adipose tissue, did not appear to affect the integrity of the nuclear lamina. This suggests that the structural hypothesis may, at least in part, explain why this mutation specifically affects adipose tissue while sparing cardiac and skeletal muscles.

Our results also suggest that, although mutant lamin A and lamin C are both dysfunctional, they are differentially affected by the mutation. Mutations p.D912G, p.Q353K, and p.R386K resulted in nucleoplasmic aggregation of lamin C, and aggregation of the lamin A counterpart at the nuclear periphery. This shows that mutant lamin A retained its association with the nuclear envelope, while the lamin C counterpart did not. Such differential effects of the same mutation indicate that lamin A and lamin C may play different roles in the nucleus. Further support for this is provided by previous findings that lamin A and C have different binding affinities for emerin, despite possessing a common binding region (Vaughan et al., 2001), and that some *LMNA* mutations only affect the interaction of lamin A with emerin, and not lamin C (Motsch et al., 2005). It is therefore evident that investigations into the pathophysiology of DCM and EDMD due to *LMNA* mutations must assess effects on both lamin A and lamin C, separately and in combination, in order to dissect the role of each mutated protein.

Another significant finding is that wild-type lamin C when expressed alone in H9C2 cells is present in the form of intranuclear speckles that are in close proximity to the nuclear envelope. Consistent with our findings, previous *in vitro* studies have also demonstrated the nucleoplasmic distribution of lamin C in the form of small speckles in cells such as COS-7 cells (green monkey kidney fibroblasts), C2C12 cells (mouse myoblasts), Swiss 3T3 cells (mouse fibroblasts) (Pugh et al., 1997, Motsch et al., 2005, Sylvius et al., 2005,). It has been reported that proper localization of lamin C to the nuclear envelope may require the presence of lamin A (Pugh et al., 1997, Vaughan et al., 2001, Motsch et al., 2005, Sylvius et al., 2005). Therefore, the presence of lamin C in the form of speckles rather than a uniform veil in the nuclear lamina may be due to disruption of lamin A/C stochiometry caused by over-

expression of exogenous lamin C. This is further supported by the observation that the uniform veil-like distribution of lamin C is restored when wild-type lamin C is co-expressed with wild-type lamin A. However, the role of lamin A in the proper distribution of lamin C has been contradicted by a recent study involving a mouse model expressing lamin C alone (Fong et al., 2006). In embryonic fibroblast cells derived from these mice, lamin C was localized normally to the nuclear envelope despite the absence of lamin A. Furthermore, these mice were as healthy as wild-type mice, and demonstrated minimal alterations to the nuclear envelope. These results suggest that, at least in mice, lamin C expressed alone may substitute for lamin A in the nuclear envelope. The reason for the discrepant results between *in vivo* and *in vitro* experiments is unclear, however, it is possible that compensatory mechanisms in mice abrogate the effects of lamin A deficiency.

Some of the mutations described in our study have also been investigated by other groups. Consistent with our results, Ostlund et al. (2001) demonstrated that the p.L85R lamin A mutant is correctly localized to the nuclear envelope, and has a phenotype similar to wild-type. In contrast, Raharjo et al. (2001) demonstrated that p.L85R lamin A was slightly distinct from wild-type lamin A, and exhibited a punctate distribution in the nuclear lamina. Results regarding the mutation pR482W have also been inconsistent in *in vitro* studies. Consistent with our results, most *in vitro* experiments involving expression of this mutation in various cell lines have demonstrated that lamin A is correctly localized to the nuclear lamina, with a phenotype indistinguishable from wild-type lamin A (Ostlund et al., 2000, Lloyd et al., 2002, Raharjo et al., 2001). In contrast, other *in vitro* experiments have demonstrated the presence of nuclear envelope defects such as the presence of mutant lamin

A aggregates, dysmorphic nuclei, and loss of lamin A staining from nuclear poles or buds (Vigouroux et al., 2001, Broers 2005).

Unlike our results indicating the presence of lamin aggregates in the periphery, previous studies have suggested that mutant lamin A aggregates are found in the nucleoplasm (Ostlund et al., 2001, Raharjo et. al., 2001, Broers et al., 2005, Hubner et al., 2006, Hubner et al., 2006). Although lamins are generally localized at the nuclear lamina, some studies have reported the presence of endogenous intranuclear lamin A and lamin C (Goldman et al., 1992, Bridger et al., 1993, Hozak et al., 1999, Neri et al., 1999,). Intranuclear lamins have been suggested to play roles in DNA replication, transcription, and RNA processing (Jagatheesan et al., 1999, Hozak et al., 1995, Kennedy et al., 2001). Therefore, although lamin aggregates in our experiments appeared to be localized at the periphery, the possibility that some aggregates may be intranuclear cannot be entirely discounted.

The discrepancy between our *in vitro* results and previous studies may have been due to differences in: 1) the promoters within the expression vector used for transfection, which may dictate the level of expression of exogenous protein; 2) the expression vector tag attached to the lamin A/C gene, which may require direct or indirect immunofluorescence for detection of expressed protein; 3) the cell lines used, since each cell line varies in its expression of A-type lamins and hence in its handling of exogenous lamin A over-expression.

3.6.2. *LMNA* mutations affect the intranuclear distribution of SUMO-1 and UBC-9

Besides providing evidence in favour of the structural hypothesis, the finding that mutant lamins form nuclear aggregates also supports the hypothesis that *LMNA* mutations alter gene expression, since nuclear aggregates could affect the distribution of other nuclear proteins. Apart from the two mutations that did not cause formation of aggregates (i.e., p.R482W, p.L85R), our results indicated that the lamin A and lamin C mutants pD192G, p.Q353K, and p.R386K can affect the intranuclear distribution of SUMO-1 and its conjugates. An interesting observation was that the intranuclear distribution of SUMO-1 conjugates was affected when either lamin C mutants were expressed with SUMO-1, or when both lamin A and lamin C mutants were co-expressed with SUMO-1. This effect was not apparent when lamin A mutants were co-expressed with SUMO-1. These observations indicate that *LMNA* mutation had a differential effect on the two lamin isoforms. There are two possible factors that may explain this finding. First, mutant lamin A aggregation may occur in the nuclear periphery, while mutant lamin C aggregates in the nucleoplasm. The fact that most SUMO-conjugates are present in the nucleoplasm may explain why only mutant lamin C affected SUMO-1 distribution. Second, it is possible that there are differences in the interaction of lamin A and lamin C with SUMO-1. It was recently demonstrated that lamin A interacts with SUMO-2, but not SUMO-1 (Zhang and Kevin, 2008). This may explain why mutant lamin A do not appear to alter the localization of SUMO-1. The interaction of lamin C with SUMO-1 has not yet been tested. However, the consensus sequence (ψ K X D/E motifs) for sumoylation is present in the region common to both lamin isoforms, therefore it remains unclear why lamin C affects SUMO-1 distribution whereas lamin A does not. There is evidence in the literature that despite interacting with a region common to lamin A and

lamin C, the binding affinities of the two proteins for interacting partners can differ. Furthermore, the binding affinities of lamin A and lamin C may be differentially affected by *LMNA* mutations. For example, emerin has a stronger affinity for lamin C as compared to lamin A, and some *LMNA* mutations only affect interaction of emerin with lamin A, and not lamin C (Motsch et al., 2005). It is therefore possible that lamin C undergoes unique, as yet uncharacterized, interactions with SUMO-1. This distinguishing feature between lamin A and lamin C warrants further investigation.

The aggregates formed by the lamin A/C mutants p.D192G, p.Q353K, and p.R386K not only affected the nuclear localization of SUMO-1, but also UBC-9, the sole-E2 conjugating enzyme of the sumoylation pathway. In contrast with SUMO-1, UBC-9 mislocalization was seen in the presence of both lamin A and lamin C mutants, suggesting that both isoforms affect the distribution of this protein.

Our results demonstrated that *LMNA* mutations may interfere with cellular post-translational modifications such as sumoylation. The function of SUMO depends on a tightly regulated balance between sumoylation and SUMO-deconjugation. Thus, by decreasing the availability in the nucleus of both sumoylated proteins and the E2 conjugation enzyme UBC-9, *LMNA* mutations may disturb functions that depend on sumoylation.

Although our group was the first to study the effect of *LMNA* mutations on the intranuclear distribution of SUMO-1 and its conjugates, other studies have demonstrated that the presence of abnormal lamin A/C aggregates can affect the intranuclear distribution of other nuclear proteins (Sylvius et al., 2005). Hubner et al. (2006) reported that over-expression of mutant lamin A constructs (DCM causing mutation p.N195K and EDMD causing mutation p.R386K) led to the formation of mutant lamin A aggregates. They also

observed that the transcription factors SREBP1 and pRB were sequestered within these aggregates. Similarly, Dreuillet et al. (2008) demonstrated that aggregates formed by mutant lamin A affected the intranuclear distribution of the transcription factor MOK2. Interestingly, sumoylation of SREBP1 has been shown to decrease its transcriptional activity. This finding, along with our results showing mislocalization of SUMO-1 within lamin A/C aggregates, indicates that abnormal distribution of sumoylated transcription factors in mutant lamin aggregates may play a role in the pathophysiology of laminopathies. The sumoylation status of MOK2 and pRB is not currently known, therefore further experiments will be needed to corroborate this hypothesis.

3.6.3. Effect of *LMNA* mutations on the activity of sumoylated cardiac transcription factors

Sumoylation plays many important functions in the cell such as nucleo-cytoplasmic trafficking, chromosome segregation, and DNA repair, all of which could potentially be affected by the mislocalization of SUMO-1. One third of all sumoylated proteins are transcription factors (Vertegaal et al. 2006), therefore regulation of transcription factor activity is likely affected by SUMO-1 mislocalization. In order to understand the contribution of misregulated gene expression in the pathogenesis of DCM, we investigated the effect of *LMNA* mutations on the intranuclear distribution of the sumoylated transcription factor GATA-4. None of the mutations tested affected the intranuclear distribution of this transcription factor. One possible reason for the negative finding is that our methods may not have been sufficiently sensitive to detect the small percentage of GATA-4 that is sumoylated and trapped within lamin aggregates. We therefore studied the effect of *LMNA* mutations on

the expression of troponin C, a GATA-4 regulated gene, through real-time PCR. None of the mutations tested had a statistically significant effect on the expression of troponin C, relative to wild-type. While this may indicate that *LMNA* mutation has no effect on the expression of a structural gene such as troponin C, it is also possible that the low transfection efficiency (10%) in H9C2 cells caused any differences in expression to be attenuated. Despite the lack of statistically significant differences in expression between wild-type and mutants, we observed a trend that some mutations (p.D192G, p.R386K, p.Q353K) affecting the distribution of SUMO-1 appeared to decrease the expression of troponin C. In contrast, a previous study in a p.N195K mouse model found that GATA-4 regulated genes were upregulated (Mounkes et al., 2005). This discrepancy may indicate that GATA-4 is affected differently by various *LMNA* mutations. Sumoylation of GATA-4 has been shown to enhance its transcriptional activity (Wang et al., 2004). The observation that *LMNA* mutations decreased GATA-4 transcriptional activity may therefore indicate that these mutations decreased the availability of sumoylated GATA-4. Further studies with greater sensitivity to detect differences in gene expression are required to determine whether *LMNA* mutations indeed reduce GATA-4 mediated gene expression.

We also tested the effect of *LMNA* mutations on the transcriptional activity of MEF2C, another sumoylated cardiac transcription factor, by measuring effects on expression of SrPK3. None of the mutations were found to significantly affect the expression of SrPK3, as compared to wild-type. However, some mutations (p.D192G, p.R386K) that affected SUMO-1 distribution demonstrated a trend towards increased expression of SrPK3 relative to wild-type. The lack of statistical significance may be due to the high degree of variability observed between different replicates. Sumoylation has been shown to repress the

transcriptional activity of MEF2C (Kang et al., 2006). The trend towards increased SrPK3 expression may therefore indicate that *LMNA* mutation decreased the availability of sumoylated MEF2C. However, future studies with higher sensitivity to detect differences in MEF2C-mediated gene expression are required. An important requirement in future will be identification of a cell line with higher expression of MEF2C regulated genes.

In both the GATA-4 and MEF2C studies, mutations such as p.R482W that do not affect SUMO-1 distribution nevertheless appeared to affect the expression of troponin C and SrPK3. Furthermore, the mutation p.L85R does not affect SUMO-1, but still increased the expression of SrPK3. On the other hand, the mutation p.D192G, which affects SUMO-1, did not increase the expression of SrPK3. However, the lack of statistically significant differences between wild-type and mutant *LMNA* preclude any firm conclusions regarding the effect of these mutations on gene expression.

CHAPTER 4

DISCUSSION

Mutations in *LMNA*, a gene encoding a nuclear protein, are implicated in the pathogenesis of phenotypically diverse diseases such as DCM, EDMD, and FPLD. There are two putative mechanisms by which *LMNA* mutations may cause the tissue-specific effects in cardiac muscle underlying the pathogenesis of DCM: 1) Nuclear fragility caused by *LMNA* mutations may affect mechanically stressed tissues such as cardiac muscle to a greater extent than other tissues; and 2) *LMNA* mutations may cause dysregulation of cardiac-specific gene transcription. In order to understand the contribution of each of these mechanisms to the pathophysiology of DCM, we first carried out a genotype-phenotype analysis correlating the presence of *LMNA* mutations with the presence of nuclear envelope defects in cardiomyocytes from patients with DCM. We then investigated the effect of DCM-causing *LMNA* mutations on the assembly of nuclear lamina in our *in vitro* cardiac cell model, and on the interaction of lamins with SUMO-1 and UBC-9, two proteins involved in regulating the cardiac-specific transcription factors GATA-4 and MEF2C. Finally, we measured the effect of these mutations on expression of genes regulated by GATA-4 and MEF2C. In order to differentiate the effect of mutations on functions of lamin A and lamin C, we expressed these mutated lamins in the cell model both individually and together. The results of these studies have helped us further understand the contributions of the structural and gene-regulatory mechanisms to the pathogenesis of DCM caused by *LMNA* mutations.

4.1. Role of Structural and Gene regulatory mechanisms in the pathogenesis of DCM

The first phase of this study consisted of a genotype-phenotype correlation analysis, in which we found that about 34% of screened DCM patients displayed cardiomyocyte

nuclear envelope abnormalities. Only two patients with nuclear envelope defects carried *LMNA* mutations: 1) a novel large deletion encompassing exons 3-12 resulted in decreased expression of the lamin protein in one patient's heart tissue.and 2) a heterozygous p.D192G mutation which has been previously reported by our group (Sylvius et al., 2005). Other groups have also reported DCM patients with *LMNA* mutations demonstrating nuclear envelope defects in either cardiac tissue or skin fibroblasts (Arbustini et al. 2002, Verga et. al., 2003, Muchir et al., 2004).

The results of our *in vitro* experiments, in which we used a cardiac cell model to express mutations in the lamin A/C gene, provided further support for the structural hypothesis. We found evidence that the DCM-causing lamin A/C mutants p.D192G and p.Q353K formed abnormal lamin A/C aggregates in the nuclear lamina, leading to the formation of discontinuous lamina *in vitro*. Other studies in the literature have also reported the presence of lamin A/C aggregates in cells expressing *LMNA* mutations (Ostlund et al., 2001, Raharjo et al., 2001, Broers et al., 2005, Sylvius et al., 2005, Hubner et al., 2006, Hubner et al., 2006). Since the lamina plays an integral role in maintaining the structural integrity of the nuclear envelope, it is possible that lamin aggregation increases nuclear envelope fragility.

In summary, results from the genotype-phenotype correlation analysis and *in vitro* experiments indicate that *LMNA* mutations may cause damage to the nuclear envelope. They lend support to the structural hypothesis of DCM pathogenesis since nuclear envelope abnormalities and resulting fragility may be most likely to cause cell death in mechanically-stressed tissues such as cardiac muscle.

There is also evidence from this study, as well as past work from our laboratory, that not all DCM patients with lamin A/C mutations (e.g., p.Q353K, p.R541S) demonstrate nuclear envelope defects (Sylvius et al., 2005). Similarly, not all mutant lamin A/C constructs led to the formation of lamin A/C aggregates *in vitro*. In fact, mutations p.L85R (from the present study) and pR514S (from previous work in our laboratory) behaved in a manner similar to wild-type lamin A/C. These observations indicate that the presence of mutant lamin aggregation and the resulting nuclear envelope defects are not a prerequisite for the pathogenesis of DCM. Hence, the structural hypothesis does not fully explain the mechanism by which *LMNA* mutations cause DCM. Furthermore, the possibility that *LMNA* mutations cause misregulation of cardiac gene expression cannot be discounted based on the data pertaining to nuclear envelope defects and the abnormal distribution of mutant lamins *in vitro*.

For most mutations, *in vitro* results were correlated with *in vivo* observations. For example, results from *in vitro* and *in vivo* experiments provided similar results for the mutations p.D192G, and p.R541S (Sylvius et al., 2005). However, this was not the case for mutation p.Q353K. While a patient with this mutation did not have ultra-structural nuclear envelope defects, expression of this mutation in H9C2 cells resulted in the formation of abnormal lamin aggregates. One possible explanation for this discrepancy is that nuclear envelope defects may have affected only a small proportion of cells, therefore these abnormalities may simply have been missed in the electron microscope images. Nuclear envelope defects were only observed in about 30% of all cells in cardiac tissue from the patient with p.D192G mutation (Sylvius et al., 2005). Furthermore, in skin fibroblasts from patients carrying *LMNA* mutations, the percentage of cells with nuclear envelope defects is

only 10-15% (Muchir et al., 2004). It is not yet clear how a germ-line mutation can lead to nuclear envelope defects in only a small percentage of cells. Nevertheless, it is possible that the proportion of affected cells in the patient with the p.Q353K mutation may have been exceedingly small, a factor that raises the possibility of false negative classification.

In order to understand the contribution of the gene regulatory hypothesis in the pathogenesis of DCM, we focused our attention on SUMO-1 and UBC-9. We observed that both proteins were sequestered within mutant lamin aggregates. Given the importance of these molecules in post-translational modification (i.e., sumoylation), and activation of several cardiac transcription factors (such as MEF2C and GATA-4), this finding may have implications for the effect of *LMNA* mutations on gene expression in cardiac muscle.

Although we were not able to identify a satisfactory system to test the hypothesis that *LMNA* mutations affect gene expression, we did observe that some mutations that affected SUMO distribution also appeared to affect the expression of genes regulated by sumoylated transcription factors. However, none of the differences in gene expression between cells transfected with wild-type or mutated lamin were statistically significant. Therefore, further work is needed to confirm the role of *LMNA* mutations in the misregulation of cardiac genes.

Despite the inconclusive results regarding the effects of *LMNA* mutations on cardiac gene expression, the finding that *LMNA* mutations can alter the organization of lamin A/C in the nuclear lamina, as well as disrupt the normal distribution of SUMO-1 and UBC-9, suggests that the structural and gene regulatory mechanisms may not be mutually exclusive. However, some mutations, such as p.L85R, neither resulted in the formation of lamin aggregates nor affected the distribution of SUMO-1 and UBC-9. The structural mechanism does not appear to play a role in DCM pathogenesis in such patients, although the possibility

that cardiac gene expression is altered via mechanisms not involving SUMO-1 or UBC-9 cannot be ruled out. Taken together, our investigations into the effects of *LMNA* mutations on lamin aggregation, SUMO-1 and UBC-9 distribution, and gene expression demonstrated that the relative contributions of structural defects and aberrant gene expression to DCM pathogenesis may vary between mutations.

LMNA mutations not only cause DCM, but also several other tissue-specific disorders such as FPLD (which affects adipose tissue) and EDMD (which affects skeletal and cardiac muscle). In addition to the DCM-causing mutations, we also investigated the effects of two non-DCM mutations in our *in vitro* experiments: p.R386K which causes EDMD, and p.R482W which causes FLPD. This was done to compare the effects of DCM-causing and non DCM-causing mutations on cardiac cells, since any differences could shed light on the mechanisms by which *LMNA* mutations produce tissue-specific effects. The p.R386K mutation formed aggregates and also affected SUMO-1 and UBC-9, similar to the DCM-causing mutations. This indicates that the mechanism by which this mutation causes EDMD (with manifestations in both cardiac and skeletal muscle) may be similar to DCM, in that both the structural and gene regulatory mechanisms may play a role. Both cardiac and skeletal tissue are mechanically stressed, therefore both may be similarly affected by the loss of structural integrity of the nuclear envelope. Of course, the fact that this mutation affects skeletal muscle whereas DCM-causing mutations do not likely indicates that p.R386K affects the expression of genes specific to skeletal muscle.

In contrast to p.R386K, the p.R482W mutation did not result in formation of nuclear aggregates. Consequently, this mutation is unlikely to compromise nuclear envelope integrity. FPLD primarily affects adipose tissue, therefore this finding provides support to

the notion that *LMNA* mutations causing defects in the nuclear envelope preferentially affect mechanically stressed tissues such as cardiac muscle. This may explain why p.R482W does not affect cardiac tissue. It is noteworthy, however, that both *in vitro* and *in vivo* studies have reported contradictory results as to whether this mutation is associated with nuclear envelope abnormalities (Ostlund et al., 2000, Raharjo et al., 2001, Vigouroux et al., 2001, Lloyd et al., 2002, Broers 2005). For example, some studies have reported nuclear envelope defects in skin fibroblasts from FPLD patients with the p.R482W mutation, whereas others have not (Vigouroux et al., 2001, Lloyd et al., 2002). Therefore, the possibility that this mutation causes nuclear envelope defects cannot be entirely discounted at present. If p.R482W is eventually proven to cause nuclear envelope defects (especially in cardiac tissue), it will indicate that *LMNA* mutations cause tissue-specific effects by mechanisms other than differential sensitivity of mechanically stressed tissues to nuclear envelope abnormalities.

We also attempted to measure differences between p.R482W and wild-type lamin in cardiac gene expression (i.e. troponin C and SrPK3). However, no statistically significant differences in gene-expression were observed. Since this study was inconclusive with respect to the effect of both DCM-causing and other *LMNA* mutations due to the high variability of results, further study is required in this area.

4.2. Lamin haploinsufficiency: a novel mechanism for nuclear envelope abnormalities and DCM

In our mutation screening analysis, using MLPA, of a patient displaying major cardiomyoctye nuclear envelope damage, we identified a large deletion encompassing exons 3 to 12 in the lamin A/C gene. This deletion was absent in DNA from more than 100

controls. Since the deletion encompasses *LMNA* exon 3 to 12, it is likely that the observed nuclear abnormalities are not due to the expression of a putative truncated protein composed of exons 1-2 only. It was shown that the potential truncated protein resulting from the Y259X nonsense mutation (exon 4) was not detectable in patient fibroblasts (Muchir et al., 2003). Similarly, in the mouse model with the *LMNA* exon 8–11 deletion, the 54-kDa truncated protein resulting from this deletion was not detected (Sullivan et al., 1999) Furthermore, immunostaining revealed reduced lamin A/C in the patient's cardiomyocyte nuclei, thus indicating lamin A/C haploinsufficiency. Since lamins are implicated in the mechanical stability of the nucleus, and are reported to have numerous binding partners and functions, lamin A/C haploinsufficiency has the potential to have severely detrimental effects on cellular structure and function. One obvious consequence could be disturbance of the nuclear architecture, which was evidenced by the nuclear envelope defects observed.

Most mutations in *LMNA* are heterozygous point mutations, only some of which have been associated with cardiomyocyte nuclear envelope defects in DCM patients (Arbustini et al., 2002, Verga et al., 2004). These mutations have been suggested to have a dominant-negative effect on functions of normal lamin protein. For example, impaired lamin integration into the nuclear lamina due to the dominant-negative effects of a mutation ultimately disrupts the lamina and compromises nuclear envelope integrity. A few studies have previously reported the presence of small deletions in the lamin A/C gene. Walter et al., (2005) reported the presence of a 15 amino acid deletion (-3 to 12 nucleotides) in the 5' end of the *LMNA* gene, resulting in the loss of the translation initiator codon. van Tintelen et al. (2007) also reported the presence of a 674 base pair deletion encompassing exon 1 and the adjacent non-coding exon in a patient with myocardial fibrosis. Recently, this patient was

shown to have nuclear envelope defects such as extensively convoluted nuclear envelope along with large blebs in the nuclear membrane in the cardiomyocytes (Diercks et al., 2009). Although this has not yet been demonstrated, it is conceivable that loss of the translation initiator codon resulting from both of these mutations may cause lamin A/C haploinsufficiency. A third study demonstrated the presence of a null *LMNA* mutation (p.Q6STOP) in the exon 1 leading to lamin A/C haploinsufficiency in a family with EDMD (Becane et al., 2000). To the best of our knowledge, our results provide the first evidence of a large deletion encompassing most exons of the lamin A/C gene in a DCM patient. Apart from demonstrating that lamin haploinsufficiency may be involved in the pathophysiology of DCM, this is the first report of nuclear envelope structural defects in cardiomyocytes associated with lamin A/C haploinsufficiency. That lamin haploinsufficiency can cause nuclear envelope defects is corroborated by a heterozygous $LMNA^{+/-}$ mouse model that had 50% of normal cardiac lamin A/C levels and displayed abnormal nuclear architecture (Wolf et al., 2008).

4.3. Mutated lamin A and lamin C may have specific roles in disease pathogenesis

Our results demonstrated that lamin A and lamin C are not affected in a similar manner by *LMNA* mutations. Mutant lamin A aggregates were found in the nuclear lamina, whereas mutant lamin C aggregates were located in the nucleoplasm. Furthermore, SUMO-1 mislocalization inside mutant lamin aggregates was seen either when lamin C was expressed alone, or co-expressed with lamin A, but not when lamin A was expressed alone. These observations indicate that lamin A and lamin C are differentially affected by a given mutation, and that the two isoforms may have distinct functions within the cell. It is

therefore important that future studies investigate the effects of lamin A and lamin C separately as well as in combination, so that their specific functions and roles in disease pathogenesis can be dissected. Such studies may also aid in understanding the mechanisms by which *LMNA* mutations lead to the various tissue-specific laminopathies.

4.4. No genotype-phenotype correlation between *LMNA* mutations, presence of nuclear envelope defects, and DCM symptoms

A summary of the *LMNA* mutations, clinical characteristics, and nuclear envelope phenotypes (*in vivo* and *in vitro*) for each DCM patient enrolled in our study is presented in Table 4.1. A large degree of clinical heterogeneity was evident regardless of the presence of nuclear envelope abnormalities, or presence of *LMNA* mutation. No correlation was evident with respect to DCM severity (as determined by LVEF), age of onset, and either the presence of nuclear envelope abnormalities or presence and position of *LMNA* mutations. Nuclear envelope defects were present in both patients with *LMNA* mutations and without *LMNA* mutations, indicating the lack of a correlation between genotype and phenotype. The severity of the nuclear envelope defect or the proportion of observed cells displaying abnormal nuclei did not correlate with the presence of position of the *LMNA* mutation. These observations indicate that patients with a clinical suspicion of laminopathy and with marked abnormalities in cardiomyocyte nuclei can be free of *LMNA* mutations. Such patients may therefore carry a mutation in another gene encoding a protein involved in the maintenance of nuclear architecture. In contrast, some patients with *LMNA* mutations did not have nuclear envelope defects, and the mutant proteins did not result in discontinuous lamina *in vitro*.

This suggests that occurrence of a mutation in *LMNA* does not necessarily lead to cardiomyocyte nuclear envelope defects.

4.5. Future Directions

In our study, we showed that nuclear envelope defects caused by *LMNA* mutations may play a role in the pathogenesis of DCM. We also demonstrated that *LMNA* mutations may cause DCM by interfering with the sumoylation pathway, which regulates the activity of cardiac transcription factors. However, we could not conclusively demonstrate that *LMNA* mutations affect the expression of cardiac-specific genes.

One of the limitations of our experiments was the inability to identify an appropriate cardiac cell model to measure changes in cardiac gene expression. H9C2 cells had low transfection efficiency, while HL-1 cells did not have the proper lamin A/C phenotype. In future work, the inefficient transfection of H9C2 cells could be overcome by selecting successfully transfected cells using fluorescence activated cell sorting (FACS), thereby reducing the dilutive effects of non-transfected cells on gene expression (Kovala et al., 2000). Gene expression in transfected cells could then be measured using microarray analysis, allowing for simultaneous testing of the effect of *LMNA* mutations on the expression of multiple genes. This would permit rapid identification of up- or down-regulated genes that could be investigated further for their utility as target genes. These genes would be further subjected to real-time PCR to confirm changes in gene expression. In the present study, we attempted to measure the effect of *LMNA* mutations on expression of cardiac genes in the presence of both lamin A and lamin C, since such a system was physiologically relevant. However, since we found that *LMNA* mutations have differential

effects on the functions of the individual lamins, future experiments should test the effect not only of both mutated lamins, but also each one separately.

H9C2 cells have been widely used as a cardiac cell model (Kaneda et al., 2005, Sulliman et al., 2006, Tshori et al., 2006). However, these cells do not beat in cultures. They also demonstrate low expression of several GATA-4 regulated genes such as ANF. A long-term goal of our laboratory is to conduct these experiments in primary cardiomyocytes. Unfortunately, these cell lines are difficult to transfect with commercially available reagents. Therefore, we anticipate the need to standardize procedures for using electroporation for transfection. As an alternative, we may also create viral vectors carrying wild-type or mutant lamins to infect these cell lines (Tamamori et al., 1998, Aruda et. al., 2007).

In our study we also used two non-DCM mutations (EDMD-causing p.R386K, and FPLD-causing p.R482W) to check the tissue specificity of *LMNA* mutations. In the future, the cardiac cell line should also be transfected with these mutations in order to determine whether they have an effect on cardiac gene transcription. Similar experiments could also be performed in non-cardiac cell lines such as C2C12 cells (a skeletal muscle cell line) and 3T3-L1 (an adipose tissue cell line), to gain insights into the tissue-specific effects of *LMNA* mutations.

In order to obtain results *in vivo*, microarray analysis could be performed on RNA extracted from cardiac biopsies of DCM patients with *LMNA* mutations. This approach has been previously employed to identify the genes up- or down-regulated in DCM (Barrans et al., 2002, Hwang et al., 2002, Grzeskowiak et al., 2003). However, these studies did not genotype the DCM patients included, therefore it is unknown whether they carried *LMNA* mutations. Performing microarray analysis on biopsies from DCM patients carrying *LMNA*

mutations will provide further insights into the cardiac genes that may be affected by DCM-causing *LMNA* mutations. As an alternative, pre-existing mouse models carrying *LMNA* mutations (Arimura et al., 2005, Mounkes et al., 2005) could also be used in microarray analysis. In contrast to studies in DCM patients which would necessarily be restricted to cardiac tissue, micro-array analysis could be performed on RNA extracted from the cardiac, skeletal, and adipose tissues of mouse models to gain insights into possible mechanisms underlying tissue specificity. However, a disadvantage to the use of mouse models is the possibility that the genes affected by *LMNA* mutations may not be the same as in humans.

By using microarray analysis to measure differences in gene expression in the presence of *LMNA* mutations both *in vitro* and *in vivo*, we should also be able to determine the proportion of affected genes that are regulated by sumoylated transcription factors. Such findings will help elucidate whether the effect of *LMNA* mutations on gene expression is mediated primarily through SUMO-1.

In summary, our results provided important insights into the mechanisms by which *LMNA* mutations may cause DCM, especially with respect to the structural hypothesis. Further work is required to verify whether *LMNA* mutations cause changes in the expression of cardiac genes, and to unravel the mechanisms by which *LMNA* mutations lead to tissue-specific diseases.

Table 4.1: Genotype-phenotype correlation between *LMNA* mutations, presence of nuclear envelope defects, and DCM symptoms

Patient	LMNA Mutation	Family History	Nuclear Envelope Defect	In vitro Phenotype	Sex / Age at onset (years)	NYHA Class	Echo-cardiography	Weight (kg)/Height (cm)/LVEDD in %	Dys-rhythmias	Clinical Status
MAJOR NUCLEAR ENVELOPE DEFECTS AND LMNA MUTATION										
1	Deletion exons 3-12	Yes	Irregular and broken nuclear envelope; accumulation of mitochondria within and around the nuclei.		F/39	II	LVEDD 54mm, LVEF 50%	57/164/120.0	nsVT, couplets, frequent VE, ICD	Mild progressive HF No MD
2*	p.D192G (c.575A>G)	Yes	Complete loss of nuclear envelope, accumulation of mitochondria, glycogen and/or lipofuscin in the nucleoplasm, chromatin disorganization	Aberrant aggregation of mutant lamin A/C protein in the nuclear envelope	M/26	IV	LVEDD 60mm, LVEF 20%	67/175/127.2	1 AVB, LAFB	Died at 27 while awaiting for a heart transplant No MD
MAJOR NUCLEAR ENVELOPE DEFECTS AND NO LMNA MUTATION										
3	No	Yes	Blebbing of nuclear envelope, separation of inner and outer nuclear membrane		M/63	III	LVEDD 64mm, LVEF 26%	71/180/136.5	SVT, VT	Died of progressive HF, 4 years after diagnosis No MD
4	No	Yes	Extrusion of nucleoplasm from the cardiomyocyte		M/21	III	LVEDD 75 mm, LVEF 25%	80/176/153.7	nsVT	HTx at 24 No MD

			nucleus into the cytoplasm							
5	No	No	Irregular nucleus border; lack of nuclear membrane, presence of mitochondria within nuclear matrix		M/29	III	LVEDD 59 mm, LVEF 30%	84/176/120.5	RBBB, LPFB, nsVT, Pacemaker at 32	Progressive HF, HTx at 40 No MD
6	No	No	Local disruption of nuclear envelope, chromatin disorganization		F/14	IV	LVEDD 64 mm, LVEF<10%	55/152/144.7	recurrent VT/VF	HTx at 14 No MD
7	No	No	Misshapen nuclei, local disruption of nuclear envelope, penetration of mitochondria into nucleus		M/14	III	LVEDD 71 mm, LVEF 20%	57/168/155.6	nsVT, couplets, frequent VE, ICD at 20	Progressive HF No MD
8	No	No	Irregular shape of nuclei		M/18	III	LVEDD 68mm, LVEF 20%	47/160/156.0	LBBB, nsVT	Progressive HF No MD
NON SPECIFIC NUCLEAR ENVELOPE DEFECTS AND LMNA MUTATION										
9*	p.R541S (c. 1621C>A)	Yes	No	Uniform distribution of the mutant lamin A/C protein, similar to wild-type	M/12	IV	LVEDD 64mm, LVEF 25%	49/152/147.3	NA	HTx at 13 No MD
10	p.Q353K (c.1057C>A)	Yes	No	Aberrant aggregation of mutant	M/38	IV	LVEDD 62mm, LVEF 22%,	59/163/138.1	ICD	HTx at 38 Skeletal myopathy

				lamin A/C protein in the nuclear envelope						
NON-SPECIFIC NUCLEAR ENVELOPE DEFECTS AND NO LMNA MUTATION										
11	No	Yes	No		M/27	II	LVEDD 60mm, LVEF 38%	100/186/117.2	permanent AF, single VE	Improved after AF ablation, LVEF 45% No MD
12	No	Yes	No		M/26	III	LVEDD 75mm, LVEF 20%	73/183/154.8	single VE	Stable HF No MD
13	No	Yes	No		M/40	NA	LVEDD 77mm, LVEF 19%	73/168/164.3	ICD, pacemaker	Died age 59, poor candidate denied for HTx No MD
14	No	Yes	No		F/14	IV	LVEDD 58mm, LVEF14%	37/155/139.4	No	HTx at 14 No MD
15	No	Yes	No		M/36	II	LVEDD 78mm, LVEF 25%	94/185/154.9	single Vex	Stable HF No MD
16	No	Yes	No		M/27	III	LVEDD 78mm, LVEF 10%	72/186/160.7	Sinus tachycardia	HTx within several months No MD
17	No	Yes	No		M/34	IV	LVEDD 78mm, LVEF 20%	73/178/163.1	I-degree AVB	Fulminant HF leading to HTx within several months No MD
18	No	Yes	No		M/35	III	LVEDD 58mm, LVEF	80/170/121.1	Frequent sVT	Atrial septal aneurysm;

							15%			HTx at 39 No MD CPK value up to 600 U/I
19	No	No	No		F/13	NA	LVEDD 69mm, LVEF10%	41/164/160.3	NA	HTx at 13 No MD
20	No	No	No		F/61	NA	LVEDD 69mm, LVEF 12%	88/165/145.3	ICD	Pericarditis, HTx at 62 No MD
21	No	No	No		M/54	III	LVEDD 88mm, LVEF 20%	109/175/175.1	Pacemaker	Died at 60, waiting for HTx No MD
22	No	No	No		M/40	III-IV	LVEDD 68mm, LVEF27%	71/160/147.8	No	HTx at 62 No MD
23	No	No	No		M/27	NA	LVEDD96mm, LVEF 13%	70/170/203.8	ICD	HTx at 57 No MD
24	No	No	No		F/12	NA	LVEF 13%	42/153/NA	NA	HTx at 12 No MD
25	No	No	No		M/20	NA	LVEF 13%	86.5/197/NA	NA	HTx at 22 No MD
26	p.L85R	NA	NA	Uniform distribution of the mutant lamin A/C protein, similar to wild-type	30-40 years of age	NA	NA	NA	Permanent AF, pacemaker	NA

* Clinical characteristics and mutation carried where previously described for patients 2, 9, 26 (Bilinska et al., 2006, Sylvius et al., 2005, Fatkin et al., 1999).
Note: AF, atrial fibrillation; AVB, atrioventricular block; HF, heart failure; HTx, heart transplantation; ICD, implantable cardiac defibrillator; LAFB, left anterior fascicular block; LPFB, left posterior fascicular block; LVEDD, left ventricle end diastolic diameter; LVEF, left ventricle ejection fraction;NA, Not available; RBBB, right bundle branch block; VEX, ventricular extrasystole; SR, Sinus rhythm; VE, ventricular ectopy; VT, ventricular tachycardia; nsVT, nonsustained ventricular tachycardia; SVT: supraventricular tachycardia; VT/VF, ventricular tachycardia/ventricular fibrillation; VVIR pacemaker, ventricular inhibited rate adaptive pacing.

REFERENCES

Arbustini, E., Pilotto, A., Repetto, A., Grasso, M., Negri, A., Diegoli, M., Campana, C., Scelsi, L., Baldini, E, Gavazzi, A., Tavazzi, L. (2002) Autosomal dominant dilated cardiomyopathy with atrioventricular block: a lamin A/C defect-related disease. J Am Coll Cardiol 39, 981-990.

Arimura, T., Helbling-Leclerc A., Massart, C. Varnous, S., Niel, F., Lacène, E., Fromes,Y., Toussaint, M., Mura, A.M., Keller, D.I., Amthor, H., Isnard, R., Malissen, M., Schwartz, K., Bonne, G. (2005). Mouse model carrying H222P-Lmna mutation develops muscular dystrophy and dilated cardiomyopathy similar to human striated muscle laminopathies. Hum. Mol. Genet. 14, 155-169.

Arruda, L.H., Cestari, I.A., Leirner, A.A. and Cestari, I.N. (2007). Adenoviral Expression of Calmodulin Antisense Reduces Hypertrophy in Cultured Cardiomyocytes. Artificial organs 31, 274–277.

Barrans, J.D., Allen, P.D., Stamatiou, D. Dzau, V.J. and Liew, C. (2002). Global gene expression profiling of End-stage dilated cardiomyopathy using a human cardiovascular-based cDNA microarray. Am. J. Pathol. 160, 2035-2043.

Bécane, H.M., Bonne, G., Varnous, S., Muchir, A., Ortega, V., Hammouda, E.H., Urtizberea, J.A., Lavergne, T., Fardeau, M., Eymard, B., Weber, S., Schwartz, K., and Duboc, D. (2000). High Incidence of Sudden Death with Conduction System and Myocardial Disease Due to Lamins A and C Gene Mutation. J of Pac. Clin. Electrophysiol. 23, 1661-1666.

Benedetti, S., Bertini, E., Lannaccone, S., Angelini, C., Trisciani, M., Toniolo, D., Sferrazza, B., Carrera, P., Comi, G., Ferrari, M., Quattrini, A., and Previtali, S. C. (2005). Dominant LMNA mutations can cause combined muscular dystrophy and peripheral neuropathy. J Neurol Neurosurg Psych. 76, 1019-1021.

Bilinska, Z.T., Sylvius, N., Grzybowski, J., Fidzianska, A., Michalak, E., Walczak, E., Walski, M., Bieganowska, K., Szymaniak, E., Kusmierczyk-Droszcz, B., Lubiszewska, B., Wagner, T., Tesson, F., and Ruzyllo, W. (2006) Dilated cardiomyopathy caused by LMNA mutations. Clinical and morphological studies. Polish Heart Journal 64, 812-818.

Bione S., Maestrini E., Rivella S., Mancini, M., Regis, S., Romeo, G., and Toniolo, D. (1994). Identification of novel X-linked gene responsible for Emery-Dreifuss muscular dystrophy. Nat Genet 8: 323-327.

Bohren, K.M., Nadkarni, V., Song, J.H., and Gabbay, K.H., Owerbach, D. (2004). A M55V polymorphism in a novel SUMO-gene (SUMO-4) differentially activates heat shock transcription factors and is associated with susceptibility to type I diabetes mellitus. J. Biol. Chem. 279, 27233-27238.

Bonne G., Di Barletta M. R., Varnous S., Bécane, H.M., Hammouda, E.H., Merlini, L., Muntoni, F., Greenberg, C.R., Gary, F., Urtizberea, J.A., Duboc, D., Fardeau, M., Toniolo, D., Schwartz, K. (1999). Mutations in gene encoding lamin A/C cause autosomal dominant Emery-Dreifuss muscular dystrophy. Nat Genet 21: 285-288.

Boguslavsky R., Stewart, C.L. and Worman, H. (2006). Nuclear lamin A inhibits adipocyte differentiation: implications for Dunnigan-type familial partial dystrophy. Hum. Mol. Genet. 15, 653-663.

Bridger, J.M., Kill, I.R., O'Farrell, M., and Hutchison, C.J. (1993). Internal lamin structures with G1 nuclei of human dermal fibroblasts. J. Cell Sci. 104, 297-306.

Broers, J.L.V., Machiels, B.M., J.J.M., van Eys1, G., Kuijpers, H. J. H., Manders, E. M. M., van Driel, R. and Ramaekers, F. C. S. (1999). Dynamics of the nuclear lamina as monitored by GFP-tagged A-type lamins. J Cell Sci 112, 3463-3475.

Broers, J.L.V., Machiels, B.M., J.J.M., van Eys1, G., Kuijpers, H. J. H., Manders, E. M. M., van Driel, R. and Ramaekers, F. C. S. (1999). Dynamics of the nuclear lamina as monitored by GFP-tagged A-type lamins. J Cell Sci 112, 3463-3475.

Broers, J.L., Peters, E.A., Kuijpers, H.J., Endert, J., Bouten, C.V., Oomens, C.W., Baaijens, F.P., Ramaekers, F.C. (2004a). Decreased mechanical stiffness in LMNA -/- cells is caused by defective nucleo-cytoskeletal integrity: implications for the development of laminopathies. Hum Mol Genet. 13, 2567–80.

Broers, J.L.V., Hutchison, C.J., and Ramaekers, F.C.S (2004b). Laminopathies. J pathol. 204, 478-488.

Broers, J.L., Kuijpers, C., Ostlund, H.J., Endert, J., and Racemakers, F.C.S. (2005). Both lamin A and lamin C mutations cause lamina instability as well as loss of internal nuclear rim organization. Exp. Cell Res. 304, 582-592.

Broers J.L.V., Racemakers F.C.S., Bonne G., Yaou R.B., and Hutchinson C.J. (2006). Nuclear lamins: Laminopthies and their role in pre-mature ageing. Physiol Rev 86: 967-1008.

Burke, B., Mounkes L.C., and Stewart, C.L. (2001). The nuclear envelope in muscular dystrophy and cardiovascular diseases. Traffic 2, 675-83.

Burke, B. and Gerace, L. (1986). A cell free system to study reassembly of the nuclear envelope at the end of mitosis. Cell 44, 639-652.
Chaudhary, N., and Courvalin, J. (1993). Stepwise reassembly of the nuclear envelope at the end of mitosis. J Cell Biol. 122, 295-306.

Capell, B. and Collins, F.S. (2006). Human Laminopathies: Nuclei gone genetically awry. Nature 7, 940-942.

Cappani, C., Mattoli, E., Cloumbaro, M., Lucarelli, E., Parnaik, V.K., Novelli, G., Wehnert, M., Cenni, V., Maraldi, N.A., Squarzoni, S., and Lattanzi, G. (2005). Altered pre-lamin A processing is a common mechanism leading to lipodystrophy. Hum. Mol. Genet. 14, 1489-1502.

Cecillia, A., Magli, A., Ferrari, D. Ganassi, M., Matafora, V., Parise, F., Razzini, G., Bachi, A., Ferrari, S., and Molinari, S. (2007). Differentiation-dependant lysine 4 acetylation enhances MEF2C binding to DNA in skeletal muscle cells. Nuc. Acid Res. 36, 915-928.

Chen, J., Valle, G., and Towbin JA (2003). Mutations in Cypher/ZASP in patients with dilated cardiomyopathy and left ventricular non-compaction. J Am. Coll. Cardiol. 42, 2014-2027.

Claycomb, W.C., Lanson, N.A., Stallworth, B.W., Egeland, D.B., Delcarpio, J.B., Bahinski, A., and Izzo, N.J. (1998). HL-1 cells: A cardiac cell muscle cell line that contracts and retains phenotype characteristics of the adult cardiomyocytes. PNAS 1998; 95, 2979-2984.
Codd, M.B. Sugrue, D.D., Gersh, B.J., and Melton L.J. (1989). Epidemiology of idiopathic dilated and hypertrophic cardiomyopathy. A population-based study in Olmsted County, Minnesota, 1975-1984. Circulation 80, 564-72

Cohen, M., Lee, K.K., Wilson, K.L., and Gruenbaum, Y. (2001). Transcriptional repression, apoptosis, human disease and the functional evolution of the nuclear lamina. Trends Biochem. Sci. 26, 41-47.

Dasso, M. Emerging roles of the SUMO pathway in mitosis. Cell Div. 2008, 3-5.

Dechat, T., Korbel, B., Vaughan, O.A., Vicek, S., Hutchison, C.J., and Foisner, R. (2000). Lamina-associated polypeptide 2α binds intranuclear A-type lamins. J Cell Sci. 113, 3473-3484.

Dec, G.W., Fuster, V. (1994). Idiopathic dilated cardiomyopathy. N Engl J Med. 331, 1564-75.

Diagle, N., Beaudine, J., Hartnell, L., Imreh, G., Hallberg, E., Lippincott-Schwartz, J., and Ellenberg, J. (2001). Nuclear pore complexes form immobile networks and have a very low turnover in live mammalian cells. J Cell Biol. 154, 71-84.

Diane, F. and Graham, R.M. (2002). Molecular mechanisms of inherited cardiomyopathies. Physiol. Rev. 82, 945-980.

Diercks G.F., van Tintelen J.P., Tio R.A., Kerstjens-Frederikse R.S.,
Pinto Y.M., Suurmeijer A.J. (2009). Ultrastructural pathology of the nuclear envelope in familial lamin A/C cardiomyopathy. Cardiovascular Pathology

Dreuillet, C., Tillit, J., Kress, M., and Ernoult-Lange, M. (2002). In-vivo and In-vitro interaction between human transcription factor MOK2 and nuclear Lamin A/C. Nucleic Acids Res. 30, 4634-4642.

Dreuillet, C., Harper, M., Tillit J., Kress, M., and Ernoult-lange, M. (2008). Mislocalization of human transcription factor MOK2 in the presence of pathogenic mutations of lamin A/C. Biol. Cell 100, 51-61.

Duboscq-Bidot L, Charron P, Ruppert V,Fauchier L, Richter A, Tavazzi L, Arbustini E, Wichter T, Maisch B, Komajda M, Isnard R, and Villard E (2009). Mutations in the ANKRD1 gene encoding CARP are responsible for human dilated cardiomyopathy. Euro Heart J 30, 2128–2136.

Fatkin, D., Macrae, C., Sasaki, T., Wolff, M.R., Porcu, M., Frennaux, M., Atherton, J., Vidaillet, J. H., Spudich, S., Girolami, U.D., Seidman, J.G., Seidman, C.E. (1999). Missense mutations in the rod domain of the lamin A/C gene as causes of dilated cardiomyopathy and conduction-system disease. New Eng. J. Med. 341, 1715-1724.

Favreau C., Dubosclard E., Ostlund C., Vigouroux C., Capeau J., Wehnert M., Higuet D., Worman HJ, Courvalin JC, Buendia B. (2003) Expression of lamin A mutated in the carboxyl-terminal tail generates an aberrant nuclear phenotype similar to that observed in cells from patients with Dunnigan-type partial lipodystrophy and Emery-Dreifuss muscular dystrophy. Exp. Cell Res. 282, 14-23.

Favreau, C., Higuet, D., Courvalin, J., and Buenda, B. (2004). Expression of a mutant lamin A that causes Emery-Dreifuss Muscular Dystrophy inhibits in-vivo differentiation of C2C12 myoblasts. Mol. Cell Biol. 24, 1481-1492.

Fisher, D.Z., Chaudhary, N., and Blobel, G. (2006). cDNA sequencing of nuclear lamins A and C reveals primary and secondary structural homology to Intermediate filament proteins. PNAS 83, 6450-6454.

Flemington, E., Speck, S.H. and Kabelin, W. (1993). E2F-1 mediated transactivation is inhibited by complex formation with retinoblastoma susceptibility gene product. Proc. Nat. Acad. Sci. USA. 90, 6914-6918.

Fuchs, E. (1994). Intermediate filaments: Structure, dynamics, function, and disease. Annual reviews 63, 345-382

Furukawa, K., Inagaki, H., and Hotta, Y. (1994). Identification and cloning of an mRNA coding for a germ cell specific A-type lamin in mice. Exp. cell Res. 212, 426-430.

Georgatos, S.D., Athina, P., and Theodoropoulos P.A. (1997). Nuclear envelope breakdown in mammalian cells involves stepwise lamina disassembly and micro-tubule driven deformation of the nuclear membrane. J Cell Sci 110, 2129-2140.

Gerace, L., and Blobel, G. (1980). The nuclear envelope lamina is reversibly depolymerised during mitosis. Cell 19, 27-287.

Goizet C., Yaou R.B., Richard D.P. , Richard, P ., Bouillot, S., Rouanet, M., Hermosilla, E., Le Masson, G., Lagueny, A., Bonne, G., and Ferrer, X. (2004). A new mutation of the lamin A/C gene leading to autosomal dominant axonal neuropathy, muscular dystrophy, cardiac diseases, and leuconychia. J. Med. Genet. 41, e29.

Goldman, A.D, Moir, R.D., Montag-Lowy, M., Stewart, M., and Goldman, R.D. (1992). Pathway of incorporation of microinjected Lamin A into the nuclear envelope. J Cell Biol. 119, 725-735.

Goldman, R.D., Gruenbaum, Y., Moir ,R.D. Shumaker, D.K. and Spann, T.P. (2002). Nuclear lamins: building blocks of nuclear architecture. Genes and Dev 16, 533-547.

Goldman R.D., Shumaker D.K., Erdos M.R., Eriksson, M., Goldman, A.E., Gordon, L.B., Gruenbaum, Y., Khuon, S., Mendez, M., Varga, R., and Collins, F.S. (2004) Accumulation of mutant lamin A causes progressive changes in nuclear architecture in Hutchinson-Gilford Progeria syndrome. Proc Nat. Acad Sci USA, 101, 8963-8968.

Gruing, E. Tasman, J.A., Kucherer, H., Franz, W., Kubler, W., Hubo, F., Katus, A. (1998). Al. Frequency and phenotypes of familial dilated cardiomyopathy. J. Am. Coll. Cardiol. 31, 186-194.

Grzeskowiak, R., Witt H., Drungowski, M., Thermann, R., Hennig, F., Perrot, P., Osterziel, K.J., Klingbiel, D., Scheid, S., Spang, R., Lehracha, H., Ruiza, P. (2003). Expression profiling of human idiopathic dilated cardiomyopathy. Cardiovas Res. 59, 400-411.

Guo, D., Li, M., Zhang., Y., Eckenrode, S., Hopkins, D., Zheng, W., Purohit S., Podolsky, R.H., Muir, A., Wang, J., Dong, J. (2004). A functional variant of SUMO-4, a new I-kappa-B-modifier, is associated with type 1 diabetes. Nature Genet. 36, 837-841.

Haberland, M., Arnold, M.A., McAnally, J., Phan, D., Kim, Y., and Olson, E.N. (2007). Regulation of HDAC9 gene expression by MEF2 establishes a negative-feedback loop in the transcriptional circuitry of muscle differentiation. Mol Cell Biol 27, 518-525.

Hakelien A., Delbarre, E., Gaustad, K.G., Buendia, B., and Collas, P. (2008). Expression of myodystrophic mutation of lamin A in C2C12 myoblasts causes promoter-specific and global epigenetic defects. Exp. Cell Res. 314, 1869-1880.

Haque, F., Lyold, D., Smallwood, D.T., Dent, C.L., Shanahan, C.M., Fry, A.M., Trembath, R.C. and Shackleton, S. (2006). SUN1 interacts with nuclear lamin A and cytoplasmic nesprins to provide a physical connection between nuclear lamina and cytoskeleton. Mol. Cell Biol. 26, 3738-3751.

Hermida-Preito, M., Monserrat, L., Castro-Beiras, A. Laredo, R., Soler, R., Peteiro, J., Rodríguez, E., Bouzas, B., Alvarez, N., Muñiz, J., and Crespo-Leiro, M. (2004). Familial dilated cardiomyopathy and isolated left ventricular non compaction associated with lamin A/C mutations. Am. J. Cardiol 94, 50-54.

Hochstrasser M. (2001). SP-RING for SUMO: new functions bloom for a ubiquitin-like protein. Cell 107, 5-8

Hozak, P., Sasseville, A.M., Raymond, R., and Cook, P.R. (1995). Lamin proteins form an internal nucleoskeleton as well as peripheral lamina in human cells. J Cell Sci. 108, 635-644.

Hubner, S., Eam, J.E., Wagstaff, D.A. and Jans, D.A. (2006a). Quantitative analysis of localization and nuclear aggregates formation induced by GFP-lamin A mutant proteins in living HeLa cells. J. Cell Biochem. 98, 810-826.

Hubner S., Eam J.E., Wagstaff D.A. and Jans D.A. (2006b). Laminopathy-inducing lamin A mutants can induce re-distribution of lamin binding poteins into nuclear aggregates. Exp. Cell. Res. 312, 171-183.

Hutchison, C.J. (2002). Lamins: Building blocks or regulators of gene expression? Nature 3, 848-858.

Hutchinson, C.J., Alvarez-Reyes, M., and Vaughan, O.A. (2001). Lamins in disease. Why do ubiquitously expressed nuclear envelope proteins give rise to tissue specific disease phenotypes? J Cell Sci. 114, 9-19.

Hwang, J., Allen, P.D., Tseng, G.C., Lam, C., Fananapazir, L., Dzau, V.J., and Liew, C. (2002). Microarray gene expression profiles in dilated and hypertrophic end-stage heart failure. Physiol. Genom. 10, 31-44.

Inagaki, N., Hayashi, T., Arimura, T., Koga, Y., Takahashi, M., Shibata, H., Teraoka K., Chikamori, T., Yamashina, A., and Kimura, A. (2006). Alpha B-crystallin mutation in dilated cardiomyopathy. Biochem Biophys Res Commun 342, 379-86.

Jagatheesan, G., Thanumalayan, S., Muralikrishna, B.H., Rangaraj, N., Karande, A.A and Parnaik, V. K. (1999). Colocalization of internal lamin foci with RNA splicing factors. J Cell Sci. 112, 4561-4661.

Jamali, M., Rogerson, P.J., Wilton, S., and Skerjanc, I.S (2001). Nkx2-5 activity is essential for cardiomyogenises. J Biol. Chem. 276, 42252-42258.

Johnson BR, Nitta RT, Frock RL, et al. (2004). A-type lamins regulate retinoblastoma protein function by promoting subnuclear localization and preventing proteasomal degradation. Proc Nat. Acad Sci U S A 101: 9677-82.

Kandert, S., Lüke, Y., Kleinhenz, T., Neumann, S., Lu, W., Jaeger, V.M., Munck, M., Wehnert, M., Müller, C.R, Zhou, Z., Noegel, A.A., Dabauvalle, M.C., Karakesisoglou, I. (2007). Nesprin-2 giant safeguards nuclear envelope architecture in LMNA S143F progeria cells. Hum. Mol. Genet. 16, 2944-59.

Kaneda, R., Ueno, S., Yamashita, Y., Choi, Y.L., Koinuma, K., Takada, S., Wada, T., Shimada, K., and Mano, H. (2005). Genome-Wide Screening for Target Regions of Histone Deacetylases in Cardiomyocytes. 97, 210-218

Kang, J., Christian, B.C. and Yu, H. (2006). Phosphorylation-facilitated sumoylation of MEF2C negatively regulates its transcriptional activity. BMC Biochem 7:5.

Karkkainen S., and Peuhkurinen, K. (2007). Genetics of dilated cardiomyopathy. Annals of Medicine 39, 91-107.

Kennedy, B.K, Barbie, D.A, Classon, M., Dyson, N., Harlow, E. (2000). Nuclear organization of DNA replication in primary mammalian cells. Genes Dev. 14, 2855-2868.

Kovala, A.T., Harvey, K.A., Mcglynn, P., Boguslawski, G., Garcia, J.G.N. and English, D. (2000). High-efficiency transient transfection of endothelial cells for functional analysis. FASEB J. 14, 2486–2494.

Ku, L., Feiger, J., Taylor, M. and Mestroni, L. (2003). Familial Dilated cardiomyopathy. Circulation 108, 118-121.

Kumaran, R.I., Muralikrishna, B., and Parnaik, V.K. (2002). Lamin A/C speckles mediate spatial organization of splicing factor compartments and RNA polymerase II transcription. J Cell Biol. 159, 783-93.

Lammerding, J., Schulze, P.C., Takahashi, T., Kozlov, S., Sullivan, T., Kamm, R.D., Stewart, C.L., Lee, R.T. (2004). Lamin A/C deficiency causes defective nuclear mechanics and mechanotransduction. J Clin Invest 113, 370–78.

Lee, K.K., Haraguchi, T., Lee, R.S., Koujin, T., Hiraoka, Y., and Wilson, K.L. (2001). Distinct functional domains in emerin bind Lamin A and DNA bridging protein BAF. J Cell Sci. 114, 4567-4573.

Lin, F., and Worman, H.J. (1993). Structural organization of the human gene encoding nuclear lamin A and lamin C. J Biol. chem. 268, 16321-16326.

Liu, J., Ben-Shahar, T.B., Riemer, D., Treinin, M., Spann, P., Weber, K., Fire, A., Gruenbaum, Y. (2000). Essential roles for *Caenorhabditis elegans* lamin gene in nuclear organization, cell cycle progression, and spatial organization of nuclear pore complexes. Mol. Biol. Cell 11, 3937-3947.

Lloyd, D.J., Trembath, R.C., and Shackleton, S. (2002) A novel interaction between lamin A and SREBP1: implications for partial lipodystrophy and other laminopathies. Hum. Mol. Gen. 11, 769-777.

Luderus, M.E., den Blaauwen, J.L., de Smit, O.J., Compton, D.A., and van Driel, R. (1994). Binding of matrix attachment regions to lamin polymers involves single-stranded regions and the minor groove. Mol. Cell Biol. 14, 6297-6305.

Machiels, B.M., Zorenc, A.H.G., Endert, J.M., and et al (1996).. An alternate splicing product of the Lamin A/C gene lacks exon 10. J Biol Chem 271: 9259-9253

Mahajan, R., Delphin, C., Guan, T., Gerace, L., Melchior, F. (1997). A small ubiquitin-related polypeptide involved in targeting RanGAP1 to nuclear pore complex protein RanBP2. Cell 88, 97-107.

Manza, L.L., Codreanu, S.S., Stammer, S.L. Smith, D.L., Roberts, R.L., and Liebler, D.C. (2004). Global shifts in protein sumoylation in response to electrophile and oxidative stress. Chem. Res. Toxixol. 17, 1706-1715.

Marx, J. (2005). SUMO wrestles its way to prominence in the cell. Science 307, 836-839.

Matunis, M.J., Coutavas, E, and Blobel, G. (1996). A novel ubiquitin-like modification modulates the partitioning of the Ran-GTPase-activating protein RanGAP1 between the cytosol and the nuclear pore complex. J Cell Biol. 135, 1457-70.

Meaburn, K.J., Cabury, E., Bonne, G., Levy N., Morris, G.E., Novell, G., Kill, I.R., and Bridge J.M. (2007). Primary laminopathy fibroblasts display altered genome organization and apoptosis. Aging Cell 6, 139-153.

Meier, J., Campbell, K.H., Ford, C.C., Stick, R., Hutchison, C.J. (1990). The role of lamin LIII in nuclear assembly and DNA replication, in cell-free extracts of Xenopus eggs. J Cell Sci. 98, 271-279.

Mestroni, L., Maisch, B., Mckenna, W.J., Schwartz, K, Charron, P., Rocco, C., Tesson, F., Richter, A., Wilke, A., Komajda, M. (1999). Guidelines for the study of familial dilated cardiomyopathies. European Heart Journal 20, 93-102.

Melchior, F. (2004). SUMO--nonclassical ubiquitin. Annual Rev. Cell Dev. Biol. 16, 591-626.

Mislow, J.M.K., Holaska, J.M., Kim, M.S., Lee, K.K., Segura-Totten, M., Wilson, K.L., McNally, E.M. (2002). Nesprin-1α self associates and binds directly to emerin and lamin A in-vitro. FEBS lett. 525, 135-140.

Mohapatra B., Jimenez S., Lin J.H., Bowles, K.R., Coveler K.J., Marx, J.G., Chrisco, M.A., Murphy, R.T., Lurie, P.R., Schwartz, R.J., Elliott, P.M., Vatta, M., McKenna, W., Towbin, J.A., and

Bowles, N.E. (2003). Mutations in the muscle Lim protein and alpha-actinin 2 genes in dilated cardiomyopathy and endocardial fibroelastosis. Mol Genet Metab 80, 207-215.

Moir, R.D., Yoon, M., Khuon, S and Goldman, R.D. (2000). Nuclear lamins A and B1: Different pathways of assembly during nuclear envelope formation in living cells. J Cell Biol 151, 1155-1168.

Molkentin, J.D. (2000). The Zinc Finger-containing transcription factors GATA-4, 5 and 6. J Biol. Chem. 275, 38949-38952.

Motsch, I., Kaluarachchi, M., Emerson, L.J., Brown, C.A., Brown, S.C., Dabauvalle, M., and Ellisa, J. (2005). Lamin A and C are differentially dysfunctional in autosomal dominant Emery-Dreifuss Muscular Dystrophy. Eur J Cell Biol. 84, 765-781.

Mounkes, L.C., Kozlov, S., Hernandez, L., Sullivan, T., Stewart, C.L. (2003). A progeroid syndrome in mice is caused by defects in A-type lamins. Nature 423, 298-301

Mounkes, L.C., Kozlov, S.V., Rottman, J.N., Stewart, C.L. (2005). Expression of an LMNA-N195K variant of A-type lamins results in cardiac conduction defects and death in mice. Hum. Mol. Genet. 14, 2167-2180.

Muchir, A., Medioni, J., Laluc, M., Massart, C., Arimura, T., van der Kooi, A.J., Desguerre, I., Mayer, M., Ferrer, X., Briault, S., Hirano, M., Worman, H.J., Mallet, A., Wehnert, M., Schwartz, K., Bonne, G. (2004). Nuclear envelope alterations in fibroblasts from patients with muscular dystrophy, cardiomyopathy, and partial lipodystrophy carrying lamin A/C gene mutations. Muscle Nerve 30, 444-450.

Muchir A, van Engelen BG, Lammens M, Mislow JM, McNally E, Schwartz K, Bonne G (2003). Nuclear envelope alterations in fibroblasts from LGMD1B patients carrying nonsense Y259X heterozygous or homozygous mutation in lamin A/C gene. Exp Cell Res. 291:352-62.

Muller, S., Hoege, C., Pyrowolakis, G., Jentsch, S. (2001). SUMO, ubiquitin's mysterious cousin. Nat. Rev. Mol. Cell Biol. 2, 202-210.

Nakagawa, O. and Arnold, M. (2005). Centronuclear myopathy in mice lacking a novel muscle specific protein kinase transcriptionally regulated by MEF2. Genes and development; 19, 2066-2077.

Neri L.M., Raymond Y., Giordano A., Capitani, S., and Martelli, A. M. (1999). Lamin A is a part of internal nucleoskeleton of human erythroleukemia cells. J Cell Physiol 178: 284-195.

Newport, J.W., Wilson, K.L., and Dunphy, W.G. (1990). A lamin independent A lamin independent pathway for nuclear envelope assembly. J Cell Biol. 111, 2247-2259.

Nikolova, V., Leimena, C., McMahon, A.C., Tan, J.C., Chandar, S., Jogia, D., Kesteven, S.H., Michalicek, J., Otway, R., Verheyen, F., Rainer, S., Stewart, C.L., Martin, D., Feneley,

M.P., Fatkin, D. (2004). Defects in nuclear structure and function promote dilated cardiomyopathy in lamin A/C-deficient mice. J Clin. Invest. 113, 357-69.

Nigg, E.A. (1992). Assembly and cell cycle dynamics of the nuclear lamina. Cell Biology 3, 245-253.

Olson, T.M., Kishimoto, N.Y., Whitby, F.G. and Michels, V.V. (2001). Mutations that alter the surface charge of alpha-tropomyosin are associated with dilated cardiomyopathy. J Mol Cell Cardiol 33, 723-732.

Olson T.M., Illenberger, S., Kishimoto N.Y. Huttelmaier, S., Keating, M.T., Jockusch, B.M. (2002). Metavinculin mutations alter actin interaction in dilated cardiomyopathy. Circulation 105, 431-437.

Ostlund, C., Ellenberg, J., Hallberg, E., Lippincott-Schwartz, J., Worman, H.J. (1999). Intracellular trafficking of emerin, the Emery-Dreifuss muscular dystrophy protein. J Cell Sci. 112, 1709-1719.

Ostlund, C., Bonne, G., Schwartz, K., and Worman, H.J. (2003) Properties of lamin A mutants found in Emery- Dreifuss muscular dystrophy, cardiomyopathy, and Dunningan-type partial lipodystrophy. J Cell Sci. 114, 4435-4445

Parnaik, V. and Manju, K. (2006). Laminopathies: Multiple disorders arising from defects in nuclear architecture. J. Biosci. 31, 405-421.

Peter, M., Nakagawa, J., M., Doree M., Labbe, J. C. and Nigg, E. A. (1990). In Vitro Disassembly of the Nuclear Lamina and M Phase-Specific Phosphorylation of Lamins by cdc2 Kinase. Cell 61, 591-602.

Pichler, A, Gast A, Seeler, J.S., Dejean, A., and Melchior, F. (2002). The nucleoporin RanBP2 has SUMO1 E3 ligase activity. Cell 108, 109-20.

Pikkarainen, S., Heiki, T., Kerkela, R., and Heiki, R. (2004). GATA transcription factors in the developing and adult heart. Cardiovascular Research 63, 196-207.

Tsiotra, P.C., Tsigos, C., Anastasiou, E., Yfanti, E., Boutati, E., Souvatzoglou, E., Kyrou, I., and Raptis S.A. (2008). Peripheral Mononuclear Cell Resistin mRNA Expression Is Increased in Type 2 Diabetic Women. Mediators Inflamm. 2008, 892864 (Epub 2008, Dec 21)

Pugh, G.E., Coates, P.J. Lane, E.B., Raymond, Y., and Quinlan, R.A. (1997). Distinct nuclear assembly pathways for lamin A and lamin C lead to their increase during quiescence in swiss 3T3 cells. J Cell Sci. 110, 2483-2493.

Raharjo,W.H., Enarson, P., Sullivan, T., Stewart, C.L., and Burke, B. (2001). Nuclear envelope defects associated with *LMNA* mutations cause dilated cardiomyopathy and Emery-Dreifuss muscular dystrophy. J Cell Sci. 114, 4447-57.

Reichart B., Klafke R., Dreger C., Krüger, E., Motsch,, I., Ewald, A., Schäfer, J., Reichmann, H., Müller, C.R., and Dabauvalle, M.C. (2004). Expression and localization of nuclear proteins in autosomal dominant Emery-Dreifuss muscular dystrophy with LMNA R377H mutation. BMC Cell Biol 5: 12.

Saitoh, H., Sparrow, D.B., Shiomi, T. Pu, R.T., Nishimoto, T., Mohun, T.J., Dasso, M. (1998). Ubc9p and the conjugation of SUMO-1 to RanGAP1 and RanBP2. Curr Biol. 8: 121-4.

Seeler, J.S., and Dejean, A., (2003) Nuclear and unclear functions of SUMO. Nat Rev Mol Cell Biol 4: 690-699.

Scaffidi, P., and Misteli, T. (2005). Reversal of the cellular phenotype in the pre-mature aging disease Hutchinson-Gilford progeria syndrome. Nature medicine 11, 440-445.

Schonberger J., Wang, L., Shin J.T., Kim S.D., Depreaux, F.F.S., Zhu H., Zon, L., Pizard, A., Kim, J.B., MacRae, C.A., Mungall, A.J., Seidman, J.G., and Seidman, C.E. (2005). Mutations in the transcriptional coactivator EYA4 causes dilated cardiomyopathy and sensorineural hearing loss. Nature Gen. 37, 418-422.

Shumaker, D.K, Kuczmarski, E.R., and Goldman, R.D. (2003). The nucleoskeleton: lamins and actin are major players in essential nuclear functions. Curr. Opin. Cell Biol. 15, 358-66.

Shumaker D.K., Solimando, L., Sengupta, K., Shimi, T., Adam, S.E., Grenwald, A., Strelkov, S.V., Aebi., U., Cardoso, C., and Goldman, R. (2008). The highly conserved nuclear lamin Ig-fold binds to PCNA: its role in DNA replication. J Cell Biol 181, 269-280.

Silver, N., Best, S., Jiang, J., and Thein, S.L. (2006). Selection of housekeeping genes for gene expression studies in human reticulocytes using Real-time PCR. BMC Molecular Biology 7, 33.

Smythe, C., Jenkins, H.E., and Hutchison, C.J. (2000). Incorporation of the nuclear pore basket protein nup153 into nuclear pore structures is dependent upon lamina assembly: evidence from cell-free extracts of Xenopus eggs. Embo J. 19: 3918-31.

Somech R., Shakalai S., Amariglio N., Rechavi, G., and Simon A.J. (2005). Nuclear envelopathies—raising the nuclear veil. Pediat. Res. 57: 8R-15R.

Spann, T.P., Goldman, A.E., Wang, C.E., Huang, S., Goldman, R.D. (2002). Alteration of nuclear lamin organization inhibits RNA polymerase II-dependent transcription. J Cell Biol. 156, 603-608

Stewart, C.L., Roux, K.J., Burke, B. (2007). Blurring the boundary: the nuclear envelope extends its reach. Science 318, 1408-12.

Stierle, V., Couprie, J., Ostlund, C., Krimm, I., Zinn-Justin, S., Hossenlopp, P., Worman, H.J., Courvalin, J.C., and Duband-Goulet, I. (2003). The carboxyl-terminal region common to lamins A and C contain a DNA binding domain. Biochemistry 42: 4819-4828.

Stuurman, N., Heins, S., and Aebi, U (1998). Nuclear lamins: Their structure, assembly, and interactions. J Struc Biol. 122, 42-66.

Su H.L. and Li S.S. (2002). Molecular features of human ubiquitin-like SUMO genes and their encoded proteins. Gene 296: 65-73

Suliman, H.B., Carraway, M.S., Tatro, L.G., and Piantadosi, C.A. (2006). A new activating role for CO in cardiac mitochondrial biogenesis. J Cell Sci. 120, 299-308.

Sullivan, T., Escalante-Alcade, D., Bhatt, H., Anver, M., Bhat, N., Nagashima, K., Stewart, C.L., and Burke, B. (1999). Loss of A-type lamin expression compromises nuclear envelope integrity leading to muscular dystrophy. J Cell Biol 147, 913-920.

Sylvius, N., Bilinska, Z.T., Veinot, J.P. Fidzianska, A., Bolongo, P.M., Poon, S., McKeown, P., Davies, R.A., Chan, K.L., Tang, A.S., Dyack, S., Grzybowski, J., Ruzyllo, W., McBride, H., Tesson, F. (2005). In vivo and In vitro examination of the functional significance of novel lamin gene mutations in heart failure patients. J Med. Genet. 42, 639-647.

Sylvius, N and Tesson, F. (2006). Lamin A/C and cardiac diseases. Curr. Opin. Cardiol. 21, 159-165.

Sylvius N., Hathaway A., Boudreau E., Gupta P., Labib S., Bolongo P., Rippstein P., Mcbride H., Bilinska Z.T., and Tesson F. Specific contributions of lamin A and lamin C in the development of laminopathies. Exp. Cell Res. 2008; 314: 2362-75

Taylor M., Fain P.R., Singara G., Robinson, M.L., Robertson, A.D., Carniel, E., Di Lenarda, A., Bohlmeyer, T.J., Ferguson, D.A., Brodsky, G.L., Boucek, M.M., Lascor, J., Moss, A.C., Li, W.L., Stetler, G.L., Muntoni, F., Bristow, M.R., Mestroni, L. (2003). Natural history of dilated cardiomyopathy due to lamin A/C gene mutations. J Am. Coll. Cardiol. 41, 2954-2956.

Taylor, M.R., Slavov, D., Gajewski, A., Vlcek, S., Ku, L., Fain, P.R., Carniel, E., Di Lenarda, A., Sinagra, G., Boucek, M.M., Cavanaugh, J., Graw, S.L., Ruegg, P., Feiger, J., Zhu, X., Ferguson, D.A., Bristow, M.R., Gotzmann, J., Foisner, R., Mestroni, L., (2005). Thymopoietin (lamina-associated polypeptide 2) gene mutation associated with dilated cardiomyopathy. Hum. Mutat. 26, 566-574.

Tamamori, M., Ito, H., Hiroe, M., Terada, Y., Marumo, F.,and Ikeda, M. (1998) Essential roles for G1 cyclin-dependent kinase activity in development of cardiomyocyte hypertrophy. Am J Physiol Heart Circ Physiol 275, 2036-2040.

Taniuara, H., Glass, C., and Gerace, L. (2006). A chromatin binding site in the tail domain of nuclear lamins that interacts with core histones. J Cell Biol 131: 33-44.

Towbin, J.A., Lowe A.M., Colan S.D., Sleeper, L.A., Oray, E.J., Cluine, S., Messere, J., Cox, J.F., Luri, P.R., Hsu, D., Canter, C., Wilkinson J.D., and Lipshulz, S.E. (2006). Incidence, causes, and outcomes of dilated cardiomyopathy in children. JAMA 296, 1867-1876.

Tshori, S., Gilon, D., Beeri, R., Nedhushtan, H., Dmitry, K., Pikarsky, E., and Razin, E. (2006). Transcription factor MITF regulates cardiac growth and hypertrophy. J. Clin. Invest. 116, 2673–2681.

Ulitzur, N., Harel, A., Feinstein, N. and Gruenbaum, Y. (1992). Lamin activity is essential for nuclear envelope assembly in a drososphilla embryo cell-free extracts. J Cell Biol. 119, 17-25.

Van Berlo, J.H., de Voogt, W.G., van der Koori, A.J. van Tintelen, J.P., Bonne, G., Yaou, R.B., Duboc, D., Rossenbacker, T., Heidbüchel, H., de Visser, M., Crijns, H.J., and Pinto, Y.M. (2005) .Meta-analysis of clinical characteristics of 299 carriers of *LMNA* gene mutations: do lamin A/C mutations portend a high risk of sudden death? J Mol. Med. 83, 79-83.

Van der hayden, M.A.G, Van Kempen, M.J.A., Tsuji, Y., Rook , M.B., Jongsma , H.J., and Opthof, T. (2003). P19 embryonal carcinoma cells; a suitable model system for cardiac electrophysiological differentiation at the molecular and functional level. Cardiovascular Res. 58, 410-422.

van der Kooi A.J., Bonne G., Eymard B., Duboc, D., Talim, B., Van der Valk, M., Reiss, P., Richard,P., Demay, L., Merlini,L., Schwartz, K., Busch, H.F.M., and de Visser, M. (2002). Lamin A/C mutations with lipodystrophy, cardiac abnormalities, and muscular dystrophy. Neurology 59, 620-623.

van Tintelen, J.P., Tio, R.A., Kerstjens-Frederikse, W.S., van Berlo, J.H., Boven, L.G., Suurmeijer, A.J.H., White, S.J., den Dunnen, J.T.D., te Meerman, G.J., Vos, Y.J., van der Hout, A.H., Osinga, J., van den Berg, M.P., van Veldhuisen, D.J., Buys, C. H. C. M., Hofstra, R.M. W., Pinto, Y.M. (2007). Severe Myocardial Fibrosis Caused by a Deletion of the 5' End of the Lamin A/C Gene. J Am. Coll. Cardiol. 49, 2430-2439.

Vantyghem, M.C., Pigny, P., Maurage, C.A., Rouaix-Emery, N., Stojkovic, T., Cuisset, J. M., Millaire, A., Lascols, O., Vermersch, P., Wemeau, J. L., Capeau, J., and Vigouroux, C. (2004). Patients with Familial Partial Lipodystrophy of the Dunnigan Type Due to a *LMNA* R482W Mutation Show Muscular and Cardiac Abnormalities. J. Clin. Endocrinol. Metab. 89, 5337-5346.

Vatta M., Mohapatra B., Jimenez S., Sanchez, X., Faulkner, G., Perles, Z., Sinagra, G., Lin, J.H., Vu, T.M., Zhou, Q., Bowles, K.R., Di Lenarda, A., Schimmenti, L., Fox, M., Chrisco, M.A., Murphy, R.T., McKenna, W., Elliott, P., Bowles, , K.R., Di Lenarda, A., Schimmenti, L., Fox, M., Chrisco, M.A., Murphy, R.T., McKenna, W., Elliott, P., Bowles, N.E., Chen, J., Valle, G., and Towbin JA(2003). Mutations in Cypher/ZASP in patients with dilated cardiomyopathy and left ventricular non-compaction. J Am. Coll. Cardiol. 42, 2014-2027.

Vaughan, O. A., Alvarez-Reyes, M., Bridger, J.M., Broers J.L., Ramaekers, F.C, Wehnert, M., Morris, G.E., Whitfield, W.G.F., and Hutchison C.J. (2001). Both emerin and lamin C depend on lamin A for localization at the nuclear envelope. J Cell Sci. 114, 2577-2590.

Verga, L., Concardi, M., Pilotto, A., Bellini, O., Pasotti, M., Repetto, A., Tavazzi, L., and Arbustini E. (2003). Loss of lamin A/C expression revealed by immuno-electron microscopy in dilated cardiomyopathy with atrioventricular block caused by LMNA gene defects. Virchow Arch. **443**, 664-71.

Vertegaal, A.C., Andersen, J.S., Ogg, S.C. Hay, R.T., Mann, M., and Lamond, A.I. (2006). Distinct and overlapping sets of SUMO-1 and SUMO-2 target proteins revealed by quantitative proteomics. Mol Cell Proteomics 5, 2298-310.

Vigouroux C., Auclair M., Dubosclard E., Pouchelet, M., Capeau, J., Courvalin, J., and Buendia, B. (2001). Nuclear envelope disorganization in fibroblasts from lipodystrophy patients with heterozygous R482Q/W mutations in the lamin A/C gene. J Cell Sci 114: 4459-4461.

Walter, J., Sun, L., and Newport, J. (1998). Regulated chromosomal DNA replication in the absence of nucleus. Mol. Cell 1, 519-529.

Walter, M.C., Witt T.N., Weigel, B.S., Reilicha, P., Richard, P., Pongratza, D., Bonned, G., Wehnert, M.S., Lochmuller, H. (2005). Deletion of the LMNA initiator codon leading to a neurogenic variant of autosomal dominant Emery–Dreifuss muscular dystrophy. Neuromuscular Disorders 15, 40-44.

Wang J., Feng X., and Scwartz J. (2004). SUMO-1 modification activated GATA-4-dependant cardiogenic activity. J Biol Chem 47: 49091-49098.

Wilson, K.L., Zastrow, M.S., and Lee, K.K. (2001). Lamins and disease: insights into nuclear infrastructure. Cell 104:647-650.

Wolf, C.M., Wang, L., Alcalai, R., Pizard, A., Burgon, P.G., Ahmad, F., Sherwood, M., Branco, D.M., Wakimoto, H., Fishman, G.I., See, V., Stewart, C.L., Conner, D.A., Berul, C.I., Seidman, C.E., and Seidman, J. (2008). Lamin A/C haploinsufficiency causes dilated cardiomyopathy and apoptosis-triggered cardiac conduction system disease. J Mol. Cell cardiol. 44, 293-303.

Yeh, E.T., Gong, L., and Kamitani, T. (2000). Ubiquitin-like proteins: new wines in new bottles. Gene 248, 1-14.

Zastrow, M.S., Vicek, S., and Wilson, K.L (2004). Proteins that bind A-type lamins: integrating isolated clues. J Cell Sci. 117, 979-987.

Zastrow, M.S., Flaherty, D.B., Benian, G.M., and Wilson, K.L. (2005) Nuclear Titin interacts with A- and B-type lamins in-vitro and in-vivo. J Cell Sci 119: 239-249.

Zhang, H., Saitoh, H., and Matunis, M.J. (2002). Enzymes of the SUMO modification pathway localize to filaments of the nuclear pore complex. Mol. Cell Biol. 22, 6498-508.

Zhang, Q., Ragnauth, C.D., Skepper, J.N., Worth, N.F., Warren, D.T., Roberts, R.G.,. Weissberg, P.L., Ellis, J.L., and Shanahan, C.M. (2004a). Nesprin-2 is a multi-isomeric protein that binds lamin and emerin at the nuclear envelope and forms a subcellular network in skeletal muscle. J Cell Sci. 118, 673-687.

Zhang, M., Li, Y., Wang H. Wang, J., and Jia, H. (2004b). Cooperative interaction between the basic helix-loop-helix transcription factor dHAND and myocyte enhancer factor MEF2C regulates myocardial gene expression. J Biol. Chem. 279, 54258-54263.

Zhang, Q, Bethmann, C, Worth, N.F. Davies, J.D., Wasner, C., Feuer, A., Ragnauth, C.D., Yi, Q., Mellad, J.A., Warren, D.T., Wheeler, M.A., Ellis, J.A., Skepper, J.N., Vorgerd, M., Schlotter-Weigel, B., Weissberg, P.L., Roberts, R.G., Wehnert, M., Shanahan C.M. (2007). Nesprin-1 and -2 are involved in the pathogenesis of Emery Dreifuss muscular dystrophy and are critical for nuclear envelope integrity. Hum. Mol. Genet. 16, 2816-33.

Zhang, Y., Sarge, K. (2008). Sumoylation regulates lamin A function and is lost in lamin A mutants associated with familial cardiomyopathies. J. Cell Biol. DOI: 10.1083/jcb.200712124. Epub ahead of print.

Zhao J. (2007). Sumoylation regulates diverse biological processes. Cell Mol. Life Sci 64, 3017-33.

Zhong, N., Radu, G., Ju, W., and Brown, W.T. (2005). Novel progerin-interactive partner proteins hnRNP E1, EGF, Mel 18, and UBC9 interact with lamin A/C. Biochem. Biophys. Res. Commun. 338, 855-61.

APPENDIX 1: List of genes implicated in DCM

Gene Symbol	Chromosome locus	Mode of inheritance	Protein encoded	Protein functions	Postulated Disease-causing Mechanism	References
Sarcomere Proteins						
ACTC	15q14	Autosomal dominant	α- cardiac actin	Major component of the thin filament of the sarcomere. It is an essential component of the contraction unit of heart muscle.	**Impaired force transmission** from sarcomere to extrasarcomeric cytoskeleton.	Olson et al. Science (1998), 280: 750-752.
MYH7B	14q12	Autosomal dominant	Cardiac β-myosin heavy chain	Forms a part of the think filament of the sarcomere. Consists of a heavy mersomysin domain (binds to actin and has ATpase activity). This is attached to light meromysin domain which binds to myosin binding protein C and titin.	Disrupts interaction between actin and myosin, affects ATP/ADP processing, reduces efficiency of contraction--- **Impaired force generation**	Kamisago et al. New Eng J Med (2000), 343:1688-1696. Daehmlow et al. Biochem Biophys Res. Comm. (2002), 298 : 116-120. Villard et al. Eur Heart J. (2005), 26 : 794-803. Karkkainen et al. Eur J. Heart Failure (2004), 6 :861-868.
TPM1	15q22	Autosomal dominant	α tropomyosin	Component of thin filament and interacts with troponin complex. Plays a role in stabilizing actin filaments and a regulatory role in excitation-contraction, by undergoing a conformation change upon Calcium binding to troponin complex.	Alters the interaction between actin and tropomyosin or affects the structural integrity of tropomyosin--- **Impaired force generation**	Olson et al. J Mol Cell Cardiol (2001), 33: 723-732.
TNNT2	1q32	Autosomal dominant	Cardiac troponin T	Forms the troponin complex along with troponin C and troponin I. Interacts with tropomyosin Helps in positioning of tropomyosin on	Inhibits the binding with troponin C and tropomyosin, and leads to diminished activation of	Kamisago et al. New Eng J Med (2000), 343:1688-1696. Robinson et al. J of Biol Chem. (2002), 277:

Gene Symbol	Chromosome locus	Mode of inheritance	Protein encoded	Protein functions	Postulated Disease-causing Mechanism	References
				actin, and interlocking troponin complex with tropomyosin. Troponin C-troponin T interaction plays a role in controlling sliding velocity between thick and thin filaments.	actomyosin Atpase. Reduces Ca2+ sensitivity---- **Impaired force generation.**	40710-40716. Villard et al. Eur Heart J. (2005), 26 : 794-803 Morgensen et al. J Am. Coll. Cardiol. (2004), 44: 2033-2040.
MYBPC3	11p11	Autosomal dominant	Cardiac-Myosin-binding protein C	Binds to myosin and titin. Phosphorylation of MyBP-C regulates attachment rates of myosin cross bridges and calcium sensitivity of force production.	Specific effect of the single mutation identified in this is gene is not known.	Daehmlow et al. Biochem Biophys Res. Comm. (2002), 298 : 116-120.
TNNI3	19q13	Autosomal Recessive	Troponin I	Forms the troponin complex along with troponin C and troponin T. At low $Ca2^{+}$ concentrations, it plays an inhibitory role in muscle contraction by binding to actin-tropomyosin, and inhibiting actomyosin ATPase. Binds to troponin C and troponin T	Inhibits the interaction between troponin I and troponin T: decreases force of contraction---- **Impaired force generation**.	Murphy et al. The Lancet (2004), 363: 371-372
TNNC1	3p21	Autosomal dominant	Troponin C	Forms the troponin complex along with troponin I and troponin T. Binding of troponin C to calcium induces a conformational change in troponin-tropomyosin complex, that initiates muscle contraction	Affects affinity of troponin C with calcium: Reduced myocardial contractility---- **Impaired force generation.**	Morgensen et al. J Am. Coll. Cardiol. (2004), 44: 2033-2040.
Sarcomeric cytoskeletal proteins						
TTN	2q31	Autosomal dominant	Titin	Main components of sarcomeric cytoskeleton	Decrease binding of titin to other Z disc	Gerull et al. Nat. Genet. (2002), 14: 14.

Gene Symbol	Chromosome locus	Mode of inheritance	Protein encoded	Protein functions	Postulated Disease-causing Mechanism	References
				(which provide scaffolding for the sarcomere). Control thin filament assembly, force transmission, maintenance of resting tension, and myofibrillar elasticity. Interact with myopalladin, actinin, telethonin, Myosin binding protein C, α-actin	proteins, result in truncated non function protein, affect interaction with FHL2 and αB crystalline. **Affects the stretch sensory mechanism or impair force transmission**	Satoh et al. Biochem. Biophys. Res. Commun. (2002), 291-385-393. Karrkainen et al. Annals of Med. (2007), 39: 91-107
TCAP	17q12	Autosomal dominant	Titin-cap(Telethonin)	Titin interacting protein. Also interact with cardiac muscle LIM protein (CLP) in the Z disc. Plays an important role in assembly of sarcomere and along with CLP is a key component of cardiomyocyte strech sensory machinery	Loss of interaction between telethonin with CLP or Titin. **Affect stretch sensory mechanism**	Hayashi et al. J Am. Coll. Cardiol. (2004), 44: 2192-2201. Knoll et al. Cell (2002), 111: 943-955.
CSRP3, CLP, MLP	11p15	Autosomal dominant	Cysteine-and-glycine-rich protein 3(Muscle-LIM protein)	Z-disc protein. Plays a role in sarcomere assembly and cytoskeleton integrity by interacting with Zyxin (involved in actin organization), α -actinin, telethonin. Forms a part of the cardiomyocyte sensory starch mechanism.	Disrupts interaction with Telethonin, and α –actinin. **Affects the stretch sensory mechanism**.	Knoll et al. Cell (2002), 111: 943-955. Mohapatra et al. Mol Genet Metab. (2003), 80: 207-215.
ACTN2	1q42	Autosomal dominant	α-actinin 2	Found in the z-disc. Involved in cross linking actin filaments in adjacent sarcomeres. Also binds to other Z disc proteins such as CLP.	Affects interaction with CLP. **Impaired force transmission**	Mohapatra et al. Mol Genet Metab. (2003), 80: 207-215.
ZASP, LDB3	10q22.2-23.2	Autosomal dominant	Cypher, LIM	Z-line protein. Plays a role in bridging sarcomere to the	Affects the stability of the actin	Vatta et al. J Am. Coll Cardiol. (2003), 42: 2014-

Gene Symbol	Chromosome locus	Mode of inheritance	Protein encoded	Protein functions	Postulated Disease-causing Mechanism	References
			domain-binding protein 3	cytoskeleton. It interacts with α-actinin and PKC (protein Kinase C). Interact with proteins involved in targeting or clustering of membrane proteins such as actin	cytoskeleton network. Also affects interaction with α-actinin (which interacts with actin filaments). **Impaired Force transmission**	2027.
MYPN, MYOP	10q21.1	Autosomal dominant	Myopalladin	Structural member of the Z disc of the sarcomeric apparatus. Interacts with actinin and Titin (other members of Z disc). Also interacts with nuclear factor CARP, which is activated in hypertrophy. Myoplladin/titin/CARP complex is involved in mechanical stretch response in cell.	Affects the ability of myopalladin to interact with the cardiac sarcomeric structure (reduced localization in the z disc region): **Affects stretch sensory mechanism.**	Duboscq-Bidot et al. Cardiovascular Res. (2008) 77: 118-125.
Extra-sarcomeric cytoskeleton proteins						
DES	2q35	Autosomal dominant	Desmin	Belongs to IF-family proteins. Encircles Z-disc and connects adjacent myofibrils. Interacts with actin and dystrophin, connecting myofibrils to plasma membrane. Also connects the sarcomere to nuclear envelope.	Specific effect of mutation not known, but may result in ineffective force transmission	Li et al. Circulation (1999), 100: 461-464.
DMD	Xp21	X-linked	Dystrophin	A large cytoskeleton protein, part of the dystrophin associated glycoprotein complex It interacts with actin cytoskeleton. Plays a role in force transmission, and	Reduced dystrophin expression in the heart, Affects protein structure, affects integrity of the plasma membrane	Towbin et al. Circulation (1993), 87: 1854-1865. Karrkainen et al. Annals of Med. (2007), 39: 91-107.

Gene Symbol	Chromosome locus	Mode of inheritance	Protein encoded	Protein functions	Postulated Disease-causing Mechanism	References
				membrane stability and organization of cytoskeleton.		
VLN	10q22-q23	Autosomal dominant	Metavinculin	Membrane-associated proteins found in intercalated discs and costameres. Binds to actin cytoskeleton, plays a role in force transmission, and stability of the cellular membrane	Disruption of the force transmission at the actin-intercalated disc interface **Impaired Force transmission**	Olson et al. Circulation (2002), 105: 431-437.
Nuclear proteins						
LMNA	1q21.2-21.3	Autosomal dominant	Lamin A/C	Structural integrity of the nucleus, replication, transcription. Interacts with many structural proteins such as LAP2, DNA and transcription factors.	Nuclear envelope damage may lead to cell death and tissue damage, May affect cardiac specific gene expression	Bonne et al. Nature (1999), 21: 285-288.
TMPO(LAP 2)	12q22	Autosomal dominant	α-Thymopoetin (Lamina-associated polypeptide 2 isoform (LAP2 α))	Structural integrity of the nucleus, transcription. Interacts with LaminA/C	Affects LAP2 and lamin A/C binding	Taylor et al. Human Mut. (2005), 26: 566-574.
Proteins involved in Ion Homeostasis						
ABBC9 SUR2	12p12	Autosomal dominant	ATP-binding cassette transporter (Sulfonylurea receptor 2)	Regulatory subunit of ATP-sensitive potassium channels. Forms K_{ATP} channels with KIR6.2. KIR6.2 forms the channel pore while SUR2 is required for activation and regulation of channel in response to intracellular energetic demands (through its nucleotide binding domain)	Malfunctioning of the ion channel. Defects in ATP-ADP hydrolysis dependant gating of the channel, leading to defective metabolic signal decoding : **Defective Ion channel function**	Bienengraeber et al. Nature genetics (2004), 36: 382-387.

Gene Symbol	Chromosome locus	Mode of inheritance	Protein encoded	Protein functions	Postulated Disease-causing Mechanism	References
PLN, PLB	6q22.1	Autosomal dominant	Phospholamban	Regulates the Ca^{+2} ATpase SERCA2a (involved in cardiac relaxation through calcium reuptake). When unphosphorylated, inhibits SERCA2a. Phosphorylation of phospholamban rescues this inhibition	Mutation has a dominant negative effect on the wild-type protein and inhibits its phosphorylation, leading to chronic inhibition of SERCA2a: **Ca^{+2} regulation**	Schmitt et al. Science (2003), 299:1410-1413.
SCN5A	3p22-p25	Autosomal dominant	Sodium Channel protein type 5 subunit alpha	Forms sodium channels which transport positively charged sodium ions into cardiac muscle cells, and play a role in electrical conduction in the heart, thereby maintaining a normal heart rhythm.	The mutation shifted the activation curve of the channel conductance by 3.8mV. This shift towards more positive voltage may result in reduced excitability of cardiac cells.	McNair et al. Circulation (2004), 110: 2163-2167.
Miscellaneous						
PSEN1	14q24.3	Autosomal dominant	Presenilin 1	Transmembrane protein, forms a part of γ-secretase complex, involved in processing of Notch, transcriptional regulator of heart growth and development	Specific effect not known.	Duanxiang et al. Am. J. Hum. Genet. (2006), 79: 1030-1039.
PSEN2	1q31-q42	Autosomal dominant	Presenilin 2	Transmembrane protein, forms a part of γ-secretase complex, involved in processing of Notch, transcriptional regulator of heart growth and development	Specific effect not known	Duanxiang et al. Am. J. Hum. Genet. (2006), 79: 1030-1039.
CRYAB,	11q21.2-q22.3	Autosomal	Alpha-	Heat-shock protein found in	Disrupts interaction	Natsuko et al. Biochem

Gene Symbol	Chromosome locus	Mode of inheritance	Protein encoded	Protein functions	Postulated Disease-causing Mechanism	References
CRYA2		dominant	crystallin B chain	the I band region of sarcomere. Interacts with desmin, titin. Protects the muscle fibers from the damaging effect of ischemia (apoptosis, reduced contractility).	with Titin. May affect the localization of the protein in I-band, thereby causing heart failure under stressed conditions.	Biophys Res. Comm. (2006), 342: 379-386.
tRNA^{Ile}	Mitochondrial DNA	Mitochondrial matrilineal inheritance	mt DNA tRNAIle (heteroplasmy	Protein synthesis	May affect the ability of tRNA to be aminoacylated. Deficiency of mitochondrial respiratory chain enzymes in the cardiac tissues of patients.	Mahjoub et al. Diag Mol Path (2007), 12: 238-242.
Cav3		Autosomal Recessive	Caveolin3	1) Principal components of Caveolae (vascular invaginations of plasma membrane) which play a role in endocytosis, signal transduction. 2) By recruiting phosphofructokinase to plasma membrane, regulates energy metabolism of muscle cells .	Specific effect of the mutation not known	Traverso et al. Lab Invest. (2007), 88:275-283.
EYA4	6q23	Autosomal dominant	Eyes absent homolog 4	Transcription co-activator. Interacts with transcription factors Six and Datch. Phosphatase activity in Eya4 releases transcription repression mediated by Datch and Six. Crucial for normal	Affects the interaction of EYA4 with transcription factors Six1 and Six2, but specific effect in the heart is not known.	Schonberger et al. Nature Genetics (2005), 37: 418-422.

Gene Symbol	Chromosome locus	Mode of inheritance	Protein encoded	Protein functions	Postulated Disease-causing Mechanism	References
				Heart morphology and Physiology		
Taffazin	*Xq28*	X-linked	Tafazzin	Involved in Biosynthesis of cardiolipin (found in mitochondrial membrane and plays an important role in stabilizing protein complexes important for electron transport chain).	Specific effect of the mutation not known	Adamo et al. Am. J. Hum. Genet. (1997), 61: 862-867.
FHL2	2q12–q13	Autosomal dominant	FHL2 - Four and half LIM protein 2	Adaptor protein coupling metabolic enzymes to the site of high energy consumption in the cardiac sarcomere through interaction with titin	Disrupts interaction of FHL2 with both N2B (I band part of Titin) and is2 (M band part of titin) domains of titin, thereby affecting the recruitment of metabolic enzymes to cardiac sarcomere.	Arimura et al. Biochem Biophys. Res. Comm (2007), 357 : 162-167.
SGCD	5q33	Autosomal dominant	δ-sarcoglycan	Sarcolemmal transmembrane glycoprotein. The δ-sarcoglycan interacts with α, β, and γ proteins to form a sarcoglycan complex, which is component of dystrophin-associated glycoprotein complex. Forms a link between cytoskeleton and extracellular matrix	Alters the three-dimensional structure of the protein: **Impaired force transmission.**	Tshubata et al. J Clin Invest (2000), 106: 655-662
FKTN,FCMD	9q13	Autosomal Dominant	Fukutin	Unknown. May be involved in the post-translational modification of alpha-dystroglycan. May interact with a large dystroglycan	Unknown.	Murakami et al. Ann Neurol (2006),60;597-602

Gene Symbol	Chromosome locus	Mode of inheritance	Protein encoded	Protein functions	Postulated Disease-causing Mechanism	References
				complex encompassing the outside and inside of muscle membranes		
ANKRD1	10q23.31	Autosomal Dominant	Cardiac Ankyrin Repeat Protein	Interacts with Myopalladin and titin at the I-band. It is displaced to the nucleus after mechanical stretch or pressure overload, where it acts as a co-repressor of genes regulated during cardiac remodelling.	CARP mutants may not be bale to translate physiological sarcomeric stretch signal into the nucleus. This may lead uncompensated transcriptional response and ultimately to dilation and heart failure.	Dubosq-bidot et al. Eur Heart J (2009), 30; 2128-2136
DSG2, CDH5	18q12.1-q12.2	Autosomal Dominant	Desmogelin-2	Component of intercellular desmosome junctions. Desmoglein-2 (DSG2) provide cellular adhesion and force transduction by cell-to-cell anchorage	Unkown.	Posh et al., Mol Genet Metab (2008), 95; 75-80

APPENDIX 2: List of known lamin A/C binding proteins

Proteins	Characteristics	References	Domain of Interaction
Proteins associated with the inner nuclear membrane			
Lamin B1 (LMNB1)	Intermediate filament protein. Component of the nuclear lamina.	C. Ostlund, et al., J Cell Sci 114, 4435-45 (Dec 2001).	
Emerin (EMD)	Member of the nuclear lamina-associated protein family	L. Clements et al., Biochem Biophys Res Commun 267, 709-14 (Feb 2000).	384-566
Lamina-associated polypeptides 1A and 1B (LAP1A, 1B)	Interact with both A and B-type lamins	C. Ostlund, et al., J Cell Sci 114, 4435-45 (Dec 2001), R. Foisner et al., Cell 73, 1267-79 (Jul 1993).	
Lamina-associated polypeptide 2A (TMPO)	Alfa isoform is distributed throughout the nucleus. Beta and gamma isoforms are localized to the nuclear membrane.	T. Dechat et al., J Cell Sci 113 Pt 19, 3473-84 (Oct 2000).	319-566
Lem domain-containing 3 (MAN1)	Integral membrane protein of the inner nuclear membrane	M. Mansharamani et al., J Biol Chem (Jan 2005)	
E1B 19K	Associated with intermediate filament proteins in the cytoplasm and the nuclear lamina. Protect against cell death.	L. Rao et al., Oncogene 15, 1587-97 (Sep1997).	252-390
Synaptic Nuclear Envelope Protein 1 SYNE1 (Nuclear Envelope Spectrin Repeat Protein 1, Nesprin-1, MYNE-1)	Transmembrane protein of the inner nuclear membrane. Connects the nucleus to the cytoskeleton by interacting with the nuclear envelope and with F-actin in the cytoplasm.	J.M.K. Mislow et al., J Cell Sci 115, 61-70 (Jan 2002), J.M.K. Mislow et al., FEBS Letters 525, 135-140 (July 2002).	476-916
Nesprin-2, SYNE2, NUANCE	A multi-isomeric protein that binds both lamin A and emerin. Localize at nuclear envelope in C2C12 cells. Highly abundant in skeletal and cardiac cells compared to Nesprin-1. Also interacts with F-actin at outer nuclear membrane.	Q. Zhang et al., J Cell Sci 118, 673-687 (Jan 2005).	
LUMA	Highly conserved integral inner nuclear membrane protein. Co-IP lead researchers to believe they interact with lamin a/c.	L. Bengtsson and H. Otto, J Cell Sci 121, 536-548 (Feb 2008).	

Proteins	Characteristics	References	Domain of Interaction
SUN1	Role in nuclear positioning by connecting nuclear envelope to cytoskeleton.	F. Haque et al., Molecular and Cellular Biology 26:10, 3738-3751 (May 2006).	
DNA-binding proteins			
Zinc Finger Protein 239 (ZNF239, Zinc Finger Protein MOK2)	DNA, RNA and nuclear ribonucleoproten-binding proteins. Transcription factor.	C. Dreuillet et al., Nucleic Acids Res 30, 4634-42 (Nov 2002).	243-387
Barrier-To-Autointegration Factor 1 (BAF)	May play a role in chromatin attachment to membranes and chromatin decondensation during nuclear assembly. Also interacts with emerin, LAP2 Beta and MAN1.	J.M. Holaska et al., J Biol Chem 278, 6969-75 (Nov 2002).	
Mel 18	Zinc finger protein. Localized in the nucleus. Sequence-specific DNA-binding protein and is a negative transcriptional regulator.	N. Zhong et al. Biochem and Biophys Res Commun 338, 855-861 (Oct 2005).	
Sterol regulatory element binding transcription factor 1 (SREBP1)	Regulates the transcription of genes for sterol biosynthesis and the LDL receptor gene.	D.J. Lloyd et al., Hum Mol Genet 11, 769-77 (Apr 2002).	379-664
Enzymes			
Protein Kinase C alpha (PKCA, PRKCA)	Calcium-activated and phospholipid-dependent kinase involved in signal transduction and cell communication.	A.M. Martelli et al., J Cell Biochem 86, 320-30 (2002).	499-702
12-lipoxygenase (ALOX12B)	Oxyreductase that converts arachidonic acid to 12R-hydroperoxyeicosatetraenoic acid.	K. Tang et al., Biochemistry 39, 3185-91 (Mar 2000).	463-664
Ubiquitin Conjugating Enzyme E21 (UBC9, UBE1)	Involved in 6-step ubiquitin-proteosome system. Functions in the transfer of ubiquitin to an active Cys residue of a ubiquitin carrier substrate protein. Also involved in tagging proteins with ubiquitin-like proteins (SUMO1, SUMO2, SUMO3...).	N. Zhong et al. Biochem and Biophys Res Commun 338, 855-861 (Oct 2005).	
Nuclear Prelamin A Recognition Factor (NARF)	Component of the endoprotease complex likely involved in the postranslational maturation of prelamin A to lamin A.	R.M. Barton et al., J Biol Chem 274, 30008-18 (Oct 1999).	Farnesylated prelamin A 389-664

Proteins	Characteristics	References	Domain of Interaction
Miscellaneous			
Actin	Cytoskeletal protein	A.M. Sasseville et al., FEBS Lett 425, 489-9 (Apr 1998).	
Retinoblastoma 1	Regulator of cell proliferation and differentiation. Tumor suppressor factor.	M.A. Mancini et al., Proc Natl Acad Sci USA 91, 418-22 (Jan 1994); T. Ozaki et al., Oncogene 9, 2649-53 (1994).	247-355
Lamin companion 1 (Lco1)	Intranuclear lamin-binding protein.	S. Vlcek et al., Exp Cell Res 298, 499-511 (Aug 2004).	
Nuclear Titin (TTN)	In non-muscular cells, nuclear isoforms of titin are essential for chromosome condensation and chromosome segragation during mitosis.	M.S. Zastrow et al., Journal of Cell Science 119, 239-49 (2006).	394-664
c-FOS	Involved in transcriptional and cell cycle control in mammalian cells. One component of the dimeric AP-1 transcription factor complex in the regulation of a variety of cellular processes (cell differentiation, cell proliferation, neoplasmic transformation	C. Ivorra et al., Genes and Development 2, 307-320 (2006).	
hnRNP	Involved in several RNA-related biological processes such as transcription, pre-mRNA processing, mature mRNA transport to the cytoplasm and translation. Regulates initiation of RNA replication and translation.	N. Zhong et al. Biochem and Biophys Res Commun 338, 855-861 (Oct 2005).	
Epidermal Growth Factor (EGF)	Promotes growth and differentiation.	N. Zhong et al. Biochem and Biophys Res Commun 338, 855-861 (Oct 2005).	
Cyclin D3	Forms insoluble complexes with cell-cycle regulatory factors in muscle cells.	I. Mariappan et al., Biochem and Biophys Res Commun 355, 981-85 (Feb 2007).	383-474

APPENDIX 3

Specific contribution of lamin A and lamin C in the development of laminopathies

Reprinted from Experimental Cell research 2008, 314: 2362-2375; Nicolas Sylvius, Andrea Hathaway, Emilie Boudreau, Pallavi Gupta,Sarah Labib, Pierrette M. Bolongo, Peter Rippstein, Heidi McBride, Zofia T. Bilinskac, Frédérique Tesson; Specific contribution of lamin A and lamin C in the development of laminopathies Copyright (2008), with permission from Elsevier

EXPERIMENTAL CELL RESEARCH 314 (2008) 2362–2375

available at www.sciencedirect.com

www.elsevier.com/locate/yexcr

Research Article

Specific contribution of lamin A and lamin C in the development of laminopathies

Nicolas Sylvius[a,*,1], *Andrea Hathaway*[a], *Emilie Boudreau*[a], *Pallavi Gupta*[a], *Sarah Labib*[a], *Pierrette M. Bolongo*[a], *Peter Rippstein*[b], *Heidi McBride*[b], *Zofia T. Bilinska*[c], *Frédérique Tesson*[a]

[a]*Laboratory of Genetics of Cardiac Diseases, University of Ottawa Heart Institute, 40 Ruskin Street, Ottawa, Canada K1Y 4W7*
[b]*University of Ottawa Heart Institute, 40 Ruskin Street, Ottawa, Canada K1Y 4W7*
[c]*First Department of Cardiac Disease, Institute of Cardiology, Alpejska 42, 04-628 Warsaw, Poland*

ARTICLE INFORMATION

Article Chronology:
Received 4 January 2008
Revised version received
28 April 2008
Accepted 28 April 2008
Available online 10 May 2008

Keywords:
Lamin A/C gene
Laminopathy
Nuclear envelope
FRAP
Electron microscopy

ABSTRACT

Mutations in the lamin A/C gene are involved in multiple human disorders for which the pathophysiological mechanisms are partially understood. Conflicting results prevail regarding the organization of lamin A and C mutants within the nuclear envelope (NE) and on the interactions of each lamin to its counterpart. We over-expressed various lamin A and C mutants both independently and together in COS7 cells. When expressed alone, lamin A with cardiac/muscular disorder mutations forms abnormal aggregates inside the NE and not inside the nucleoplasm. Conversely, the equivalent lamin C organizes as intranucleoplasmic aggregates that never connect to the NE as opposed to wild type lamin C. Interestingly, the lamin C molecules present within these aggregates exhibit an abnormal increased mobility. When co-expressed, the complex formed by lamin A/C aggregates in the NE. Lamin A and C mutants for lipodystrophy behave similarly to the wild type. These findings reveal that lamins A and C may be differentially affected depending on the mutation. This results in multiple possible physiological consequences which likely contribute in the phenotypic variability of laminopathies. The inability of lamin C mutants to join the nuclear rim in the absence of lamin A is a potential pathophysiological mechanism for laminopathies.

© 2008 Elsevier Inc. All rights reserved.

Introduction

The lamin A/C gene (*LMNA*) has been implicated in numerous diseases referred to as "laminopathies" that affect the heart, skeletal muscle, adipose tissue, bones, peripheral nerves, skin, or cause premature aging [1].

Lamins A and C are type V intermediate filament proteins expressed in terminally differentiated somatic cells, and synthesized by alternative splicing of *LMNA*. Both proteins share the same first 566 amino acids but differ in their carboxyl terminus. Lamins A and C have 646 and 572 amino acids respectively and are known for their structural role in supporting the nuclear architecture and anchoring chromatin and the nuclear pore complexes to the nuclear membrane. Indeed, along with B-type lamins, they are the main components of the lamina, a filamentous meshwork underlying the inner nuclear

* *Corresponding author.* CEA/Institut de Génomique, Centre National de Génotypage, 2 rue Gaston Crémieux, Bâtiment G2, CP 5721, 91057 Evry Cedex, France.
E-mail address: sylvius@cng.fr (N. Sylvius).
[1] Current address: Centre National de Génotypage, 2 rue Gaston Crémieux, CP 5721, 91 057 Evry Cedex, France.

0014-4827/$ – see front matter © 2008 Elsevier Inc. All rights reserved.
doi:10.1016/j.yexcr.2008.04.017

membrane. However, they are also present within the nucleus [2]. In addition to participating in nuclear architecture, there is a growing body of evidence showing that lamin A/C plays a key role in gene transcription regulation, DNA repair and replication [1,3], and cell differentiation regulation [1,4,5]. The list of lamins A and C partners is regularly growing [2,6–9], which confirms that these proteins are involved in multiple functions, some of which are still being unravelled. For instance, it has recently been shown that lamins A and C are tightly connected to the cytoskeleton, thus revealing a nuclear–cytoskeletal continuity [10]. Also, some *LMNA* mutations have been reported to affect the posttranslational machinery of the cell. It has been shown that the nuclear localization of SUMO1 (ubiquitin-related modifier1) is totally disrupted in the presence of the DCM-associated D192G lamin C mutant [11].

Whether or not lamin A is required for lamin C to be localized into the nuclear envelope remains debated. The early death of lmna knockout mice ($lmna^{-/-}$) [12] or the dramatic lamina defects observed when silencing lamin A/C in human endometrial stromal cells [13], clearly demonstrates that at least one of the two proteins is required for survival. However, a recent study in fibroblasts from mice expressing only lamin C have shown that lamin C is normally targeted to the nuclear envelope [14]. As well, nuclei shape from these fibroblasts is only mildly altered and the mice do not exhibit any symptoms of muscle diseases. Furthermore, lamin C has also been shown to be sufficient for proper localization of both emerin [14] and nesprin-2 [15] at the nuclear envelope. These studies therefore suggest that lamin C can substitute for lamin A on its own and provide functional support to the nuclear envelope. However, these results strikingly contradict several other studies which showed that lamin A targets both lamin C and emerin to the nuclear envelope [16–19].

Furthermore, nuclear envelope alterations associated with *LMNA* mutations have long been reported [11,20–23]. Mice expressing M371K lamin A exhibit cardiomyocytes with convoluted nuclear envelopes, intranuclear inclusions and chromatin clumps in nuclei [24]. Several *LMNA* mutations are known to result in the aggregation of lamin A *in vitro* [18,25–27]. In a previous report, we found DCM-causing *LMNA* mutations leading to the aggregation of nuclear lamin C as well [11]. However, the physiological consequences of these aggregates as well as the impact of these mutations on lamin C specifically or on the complex lamin A/lamin C have only been partially investigated. It is unclear whether or not these lamin A and lamin C aggregates retain the capability to incorporate themselves into the nuclear envelope either in combination or independently.

In humans, most reported *LMNA* mutations are found in Emery–Dreifuss muscular dystrophy and dilated cardiomyopathy (DCM) but the spectrum of phenotypes is constantly extending [28]. Nuclear fragility and/or abnormalities in the tissue/cell-specific gene expression are the main two hypotheses proposed to explain how mutations in this gene cause such a large spectrum of diseases [1]. However, the exact pathophysiological mechanisms remain puzzling. In this study, we propose to further examine wild type and mutated lamin A and C behaviour separately and then in combination. In an attempt to better clarify the lamin A and lamin C respective functions and shed light on the properties of lamin A/C affected in laminopathies, we compared various *LMNA* mutations previously reported in DCM (L85R, D192G, N195K) [29], autosomal dominant Emery–Dreifuss muscular dystrophy (R386K) [30] or lipodystrophy (R482W) [31].

Methods

Expression plasmid and mutagenesis

Our cloning procedures of wild type and mutated full-length human lamins A and C as C-terminal fusions to either the enhanced cyan, yellow or red fluorescent protein sequence of, respectively pECFP-C1, pEYFP-C1, and pDsRed2-C1 fluorescent expression vectors, have previously been described [11]. L85R, D192G, N195K, R386K and R482W point mutations were introduced in the lamin A and lamin C cDNAs by site directed mutagenesis using primers previously published [11,18,27]. All clones were systematically sequenced.

Fluorescent microscopy

Images were captured on an Olympus 1×70 inverted microscope and processed using TILLvisION software (version 4.0), or an Olympus Fluoview FV1000 confocal microscope with a 100× 1.4 NA oil immersion objective (UplanSApo) and using the Olympus FV-10 acquisition software, version 5.0, to acquire images.

Fluorescence recovery after photobleaching experiments (FRAP)

FRAP experiments were performed on living transfected COS7 cells at 37 °C. Only the transfected cells displaying a phenotype characteristic of the mutation investigated were considered for FRAP experiments. To minimize cell physiology disturbance, we chose to photobleach selected areas for 10 iterations at 16% power of the argon laser. After photobleaching, 42 images were captured every 5 s for 210 s at 1.5% power of the argon laser. FRAP was performed during such a short period of time to limit bias due to nuclear rotation and cell movement. Average fluorescence intensity in each region of interest was normalized to total cellular fluorescence loss during bleach and imaging phase as $I_{rel}=T_0I_t/T_tI_0$ as described by Phair et al. [32] (T_0, total cellular intensity during prebleach; T_t, total cellular intensity at time t; I_0, average intensity in the region of interest during prebleach, I_t, average intensity in the region of interest at time t). Fluorescence of surrounding cells was taken into account in cases of cells exhibiting a single speckle (mutation D192G and R386K). A non linear regression was used to create a best fit curve. Difference in the $t_{1/2}$ between L85R, D192G, R386K and wild type lamin C aggregates was assessed by a *T*-test.

Immunocytochemistry

Transfected cells were fixed on coverslips with 4% paraformaldehyde in phosphate buffered saline (PBS) and permeabilized with 10% Triton-100 for 5 min. Cells were incubated with the primary antibody (RanGap1 (N-19) polyclonal antibody (Santa Cruz)) in 10% fetal bovine serum (1:50) and with Alexa Fluor 594-labeled Rabbit Anti-Goat antibody (Molecular Probes) for 30 min. The coverslips were mounted on a glass slide with mowiol.

Immunoblotting

Western blot analyses were performed as previously described by Sylvius et al. [11]. The primary antibody used was goat anti-lamin A/C (N-18) polyclonal antibody and mouse anti beta actin (C4) monoclonal antibody (Santa Cruz) and the secondary antibodies were peroxidase-linked anti-goat and anti-rabbit antibodies (Santa Cruz).

Cell preparation for EM

Cells were fixed in 1.6% glutaraldehyde in 0.1 M sodium cacodylate buffer pH 7.2. They were then resuspended in 15% bovine serum albumin infiltrated for 30 min and pelleted by centrifugation. The supernatant was removed and the cell pellets were coagulated with 1.6% glutaraldehyde in 0.1 M sodium cacodylate buffer pH 7.2. The resulting firm pellets were cut into 1 mm pieces post-fixed in 1% osmium tetroxide dehydrated in ascending alcohols and embedded in Spurr epoxy resin. Thin sections were stained with uranyl acetate and lead citrate and examined with a Jeol 1230 TEM equipped with AMT software.

Results

We transiently expressed the full-length human wild type and the various mutant lamins A and C cDNAs fused to the C-terminus of variants of the *Aequorea victoria* green fluorescent protein (GFP) (lamin-FP) in fibroblast COS7 and rat cardiomyoblast H9C2 cells. To assess the consequences of mutations on

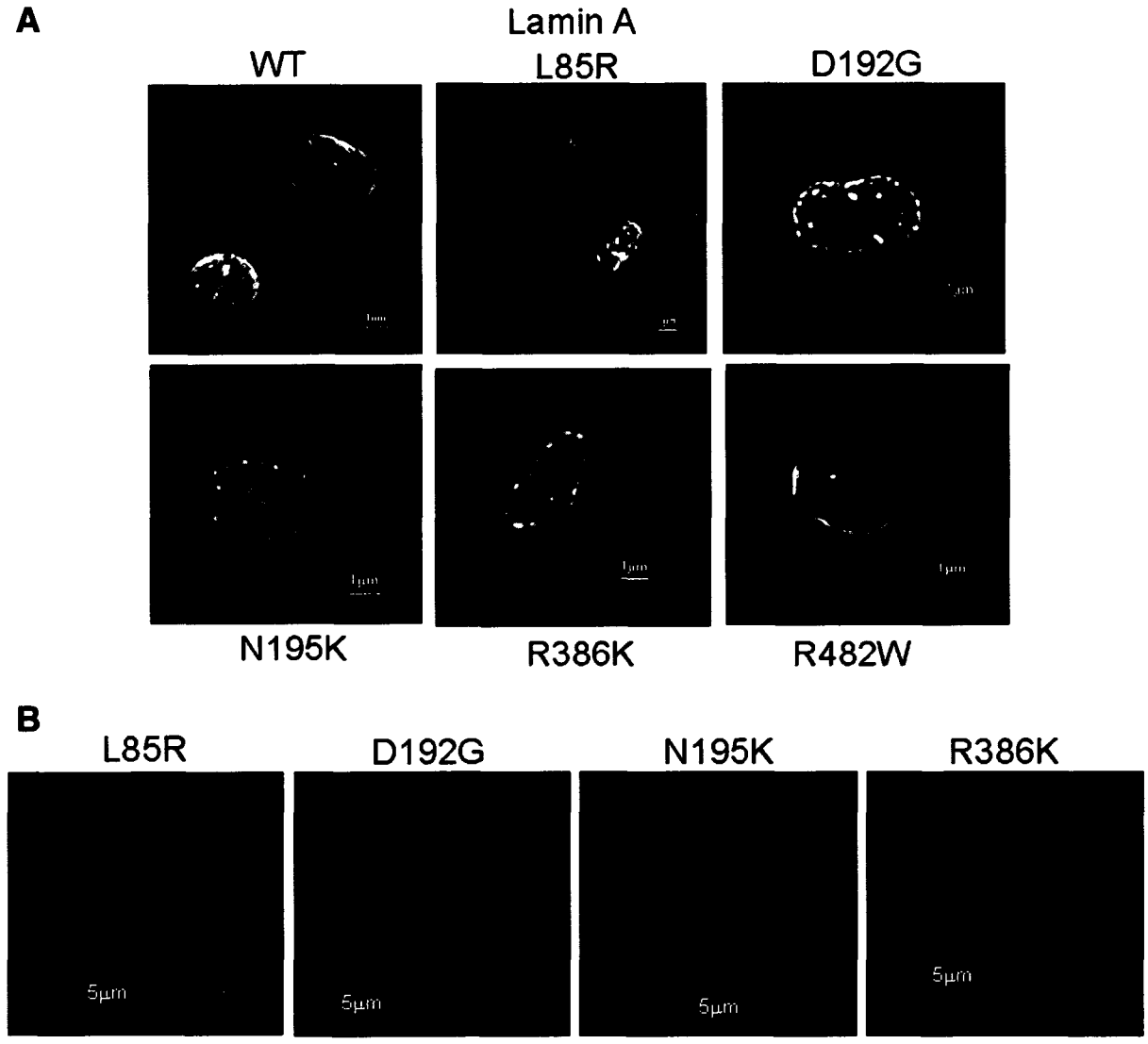

Fig. 1 – A. Nuclei expressing wild type or the various lamin A mutant constructs transiently expressed as ECFP fusion protein in COS7 cells. Cells were visualized by wide-field fluorescence microscopy with an excitation wavelength of 433 nm. Wild type lamin A, as well as L85R and R482W lamin A mutants homogeneously organize throughout the nucleus. In contrast, D192G, N195K and R386K lamin A mutants accumulate in abnormal aggregates. The nuclear membrane appears granular and discontinued. B. The abnormal lamin A aggregation previously found in COS7 cells expressing D192G, N195K and R386K lamin A, was confirmed in nuclei of rat cardiomyoblast H9C2 cells as opposed to cells expressing wild type or L85R lamin A (not shown).

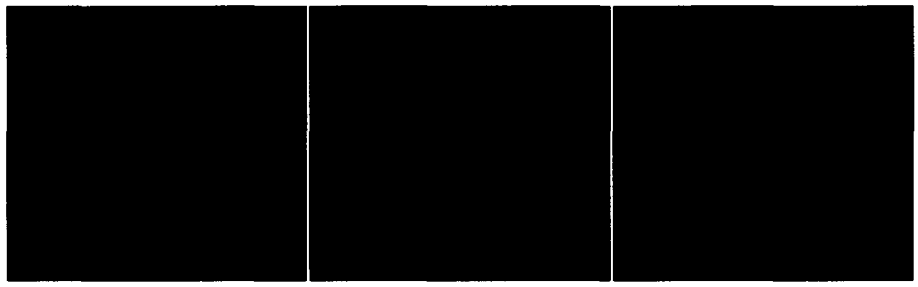

Fig. 2 – Confocal microscopy picture of H9C2 cell nuclei transiently expressing D192G lamin A as ECFP fusion protein. Mutated lamin A organizes as aberrant aggregates. However, the spherical organization of these aggregates reveal that they are likely embedded in the nuclear envelope.

lamin A and C properties specifically, we used confocal immunofluorescence microscopy to examine the cells expressing lamins A-FP and C-FP separately and then together.

Lamin A mutants aggregate

The wild type phenotype was characterized by a homogeneous distribution of the protein throughout the nucleus (Fig. 1A). L85R and R482W lamin A-FP did not exhibit any aberrant phenotype compared to the wild type (Figs. 1A and B). It is noted that the images of cells expressing L85R lamin A were carefully analyzed since this mutant was previously reported as slightly different from the wild type [18]. In contrast, D192G, N195K and R386K lamin A-FP accumulated in abnormal, giant aggregates (Figs. 1A and B), which is consistent with results already described in C2C12 or COS7 cells [11,26,27]. Several immunofluorescence microscopy studies performed on cells lines transfected with lamin A/C have reported the aggregation of lamin A as intranuclear foci or nuclear aggregates inside the nucleoplasm [18,25–27]. To confirm this statement in our analyses, we used confocal immunofluorescence microscopy and 3D reconstruction of the cell (Fig. 2). Although we could not exclude the presence of nucleoplasmic aggregates, it was obvious that the aggregates were massively present at the periphery of the nucleus and led to a punctate aspect of the nucleus, as shown on Fig. 2. This punctate aspect suggests that lamin A-FP mutants retain the ability to locate at the nuclear envelope, albeit not properly.

Abnormal lamin C aggregation is a common feature of several LMNA mutations

We then examined the effect of these mutations on lamin C only. As previously described, wild type lamin C-FP gave rise to multiple small intranuclear aggregates, known as speckles,

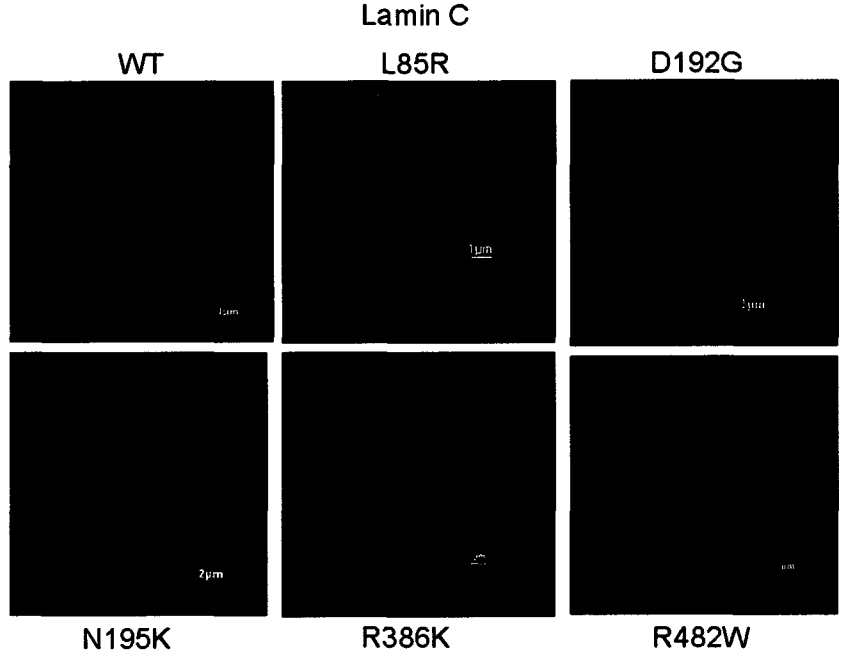

Fig. 3 – Nuclei expressing wild type or the various mutated lamin C constructs transiently expressed as ECFP fusion protein in COS7 cells. Prior to visualization by wide-field fluorescence microscopy, Hoechst 33258 dye was used to locate the nuclei (in blue). Excitation wavelengths were 433 nm for lamin C-ECFP and 365 nm for Hoechst 33258. Note that the aberrant aggregation of the lamin C (in red) within the nucleus visualized by Hoechst 33258 dye is common to several *LMNA* mutations. Only R482W lamin C mutants responsible for lipodystrophy gave rise to a phenotype similar to the wild type.

that are evenly distributed throughout the nucleus [11]. R482W lamin C-FP showed a phenotype similar to the wild type whereas D192G lamin C-FP accumulated in one or two intranuclear giant speckles (Fig. 3), which agrees with previously published studies performed on COS7 or HeLa cells [11,18]. Interestingly, L85R, D192G, N195K, and R386K lamin C-FP mutants also showed a dramatic aggregation in the vast majority of transfected cells (Fig. 3). In COS7 cells, the respective mean speckle diameters were 4.7+/−2 μm (n=9) for L85R lamin C-FP, 5.2+/−1 μm (n=11) for D192G lamin C-FP, 5.3+/−2.5 μm (n=3) for N195K lamin C-FP, 7.1+/−4 μm (n=10) for R386K lamin C-FP, and 2.9+/−1.5 μm (n=11) for wild type lamin C-FP. The mean nuclear diameter was 15 μm (+/−1.5 μm) for all transfected COS7 cells. Intriguingly, L85R lamin C-FP exhibited an aberrant phenotype compared to wild type lamin C-FP, as opposed to its counterpart lamin A-FP which behaved similarly

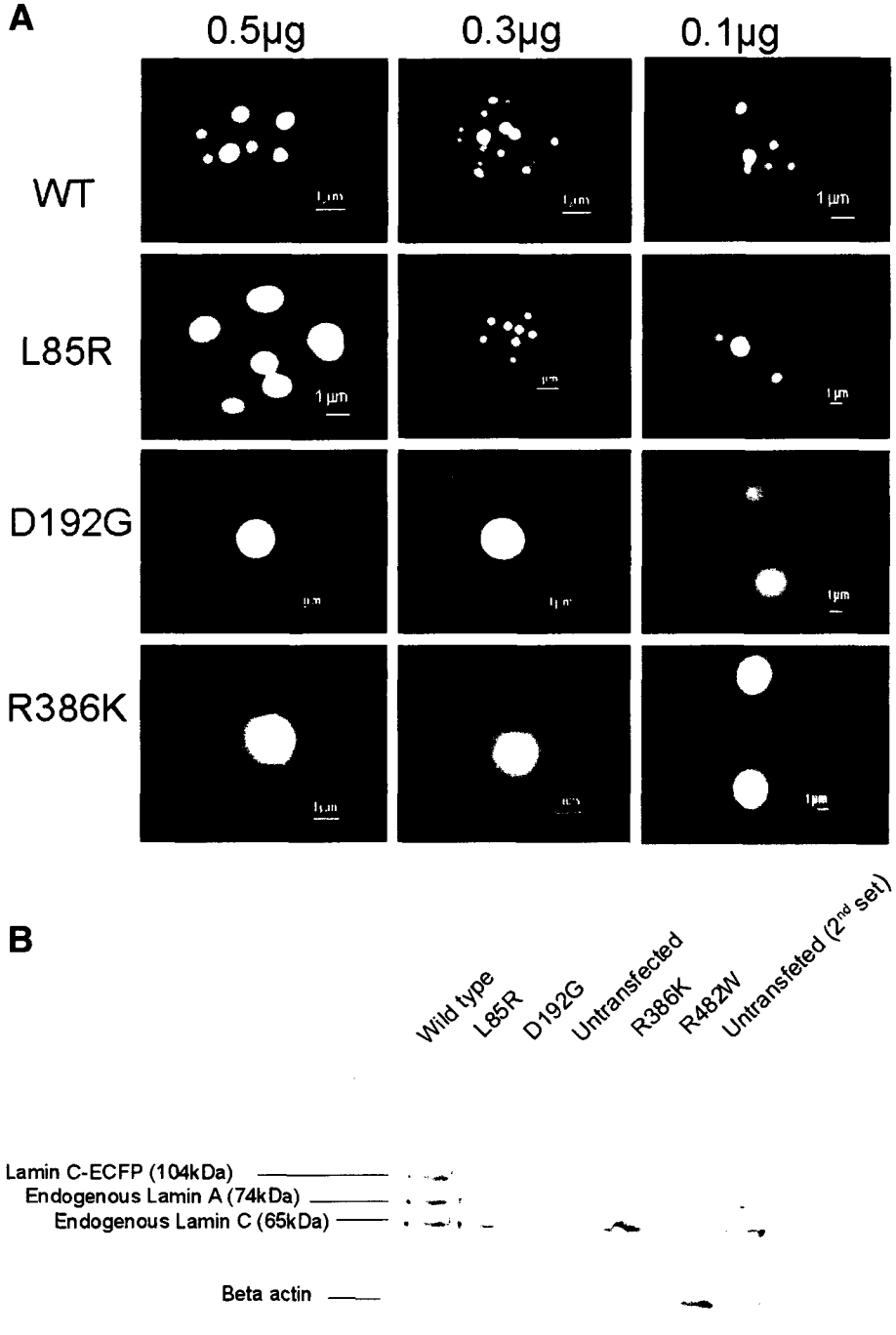

Fig. 4 – A. Transient transfections of COS7 cells with varying quantity of either wild type or mutated lamin C-FP constructs. Cells were visualized by wide-field fluorescence microscopy with an excitation wavelength of 433 nm. The phenotype observed with mutated lamin C-FP is not due to a too elevated quantity of vectors used to transfect the cells. B. Representative Western blot analysis of COS7 cells transfected with the different lamin C-FP variants and using anti lamin A/C antibody. Results show equal over-expression for all construct.

to the wild type lamin A-FP. This suggests that both proteins were differentially affected by the mutation. Aberrant aggregation of nuclear lamin C-FP was observed in less than 20% of COS7 cells expressing wild type lamin C-FP. This proportion was similar to that we previously reported [11].

To ensure that this abnormal lamin C aggregation was not an artifact due to the over-expression of the protein we transfected COS7 cells using lower concentrations of constructs (0.3 μg and 0.1 μg). Lamin C-FP mutants formed giant aggregates at each tested concentration indicating that the formation of large

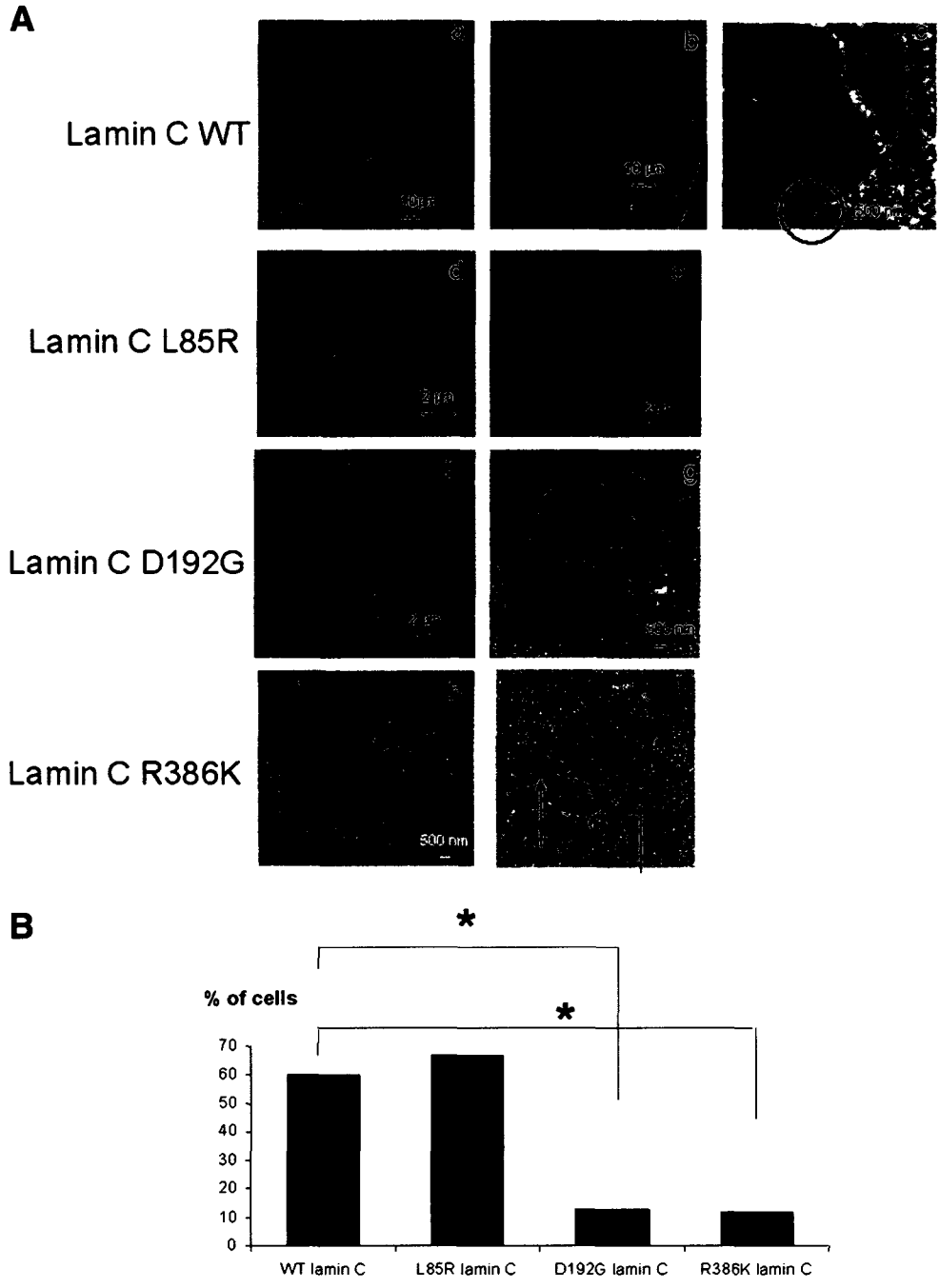

Fig. 5 – A. Electron micrographs of COS7 cells transiently transfected with lamin C-FP constructs. In 60% of cells, wild type lamin C nuclear aggregates were localized in close contact with the nuclear envelope (a–c). Notably, wild type aggregates were able to establish close contact with the nuclear envelope (circle) (c). Similarly, L85R lamin C aggregates organized in contact with the nuclear envelope (d–e). Conversely, in 88% and 87.5% of cells respectively, D192G and R386K lamin C aggregates were found within the nucleoplasm without any contact with the nuclear envelope (f–i). In 30% of cells expressing R386K lamin C, nuclei presented with lamin C aggregates localized outside the nuclear envelope (j–k). B. Percentage of transfected cells displaying lamin C nuclear aggregates in direct contact with the nuclear envelope. χ^2 test showed that the number of cells displaying lamin C aggregates in close contact with the nuclear envelope is significantly different in transfected cells expressing D192G or R386K lamin C mutants compared to the wild type ($p<0.01$).

aggregates was not an artifact due to an exaggerated dose of DNA (Fig. 4A). Furthermore, Western blotting quantification of lamin mutants did not reveal any difference in the transfection efficiency compared to the wild type, confirming that these giant aggregates did not result from transfection artifact (Fig. 4B).

Mutated lamin C loses its ability to incorporate into the nuclear envelope

We further assessed whether lamin C aggregates retain their ability to join the nuclear envelope. As a means to better see envelope shape and potential misshapen nuclei, we chose to

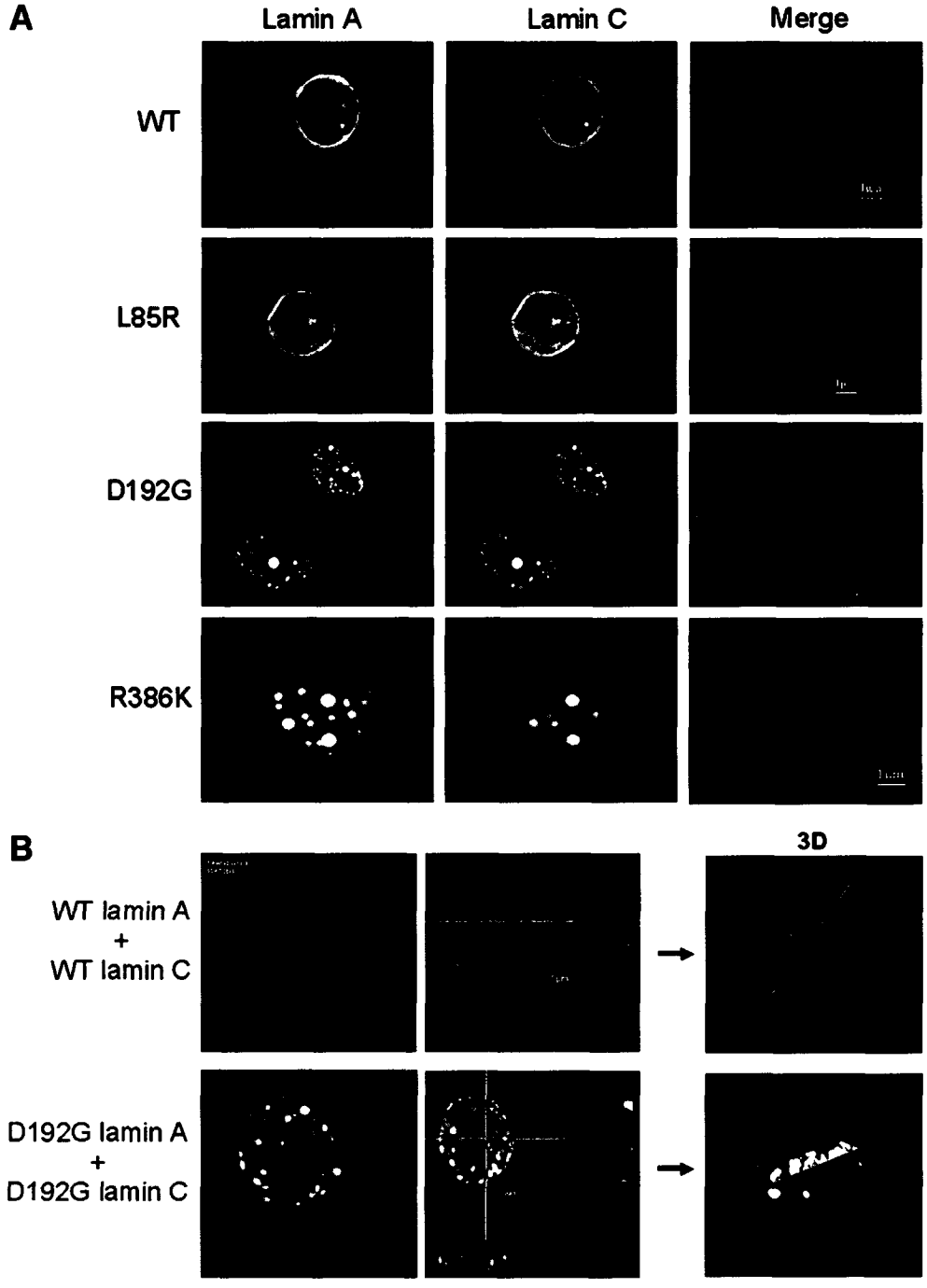

Fig. 6 – A. COS7 cell nuclei transiently co-expressing wild type or mutated lamin A and lamin C constructs. Lamins A and C were inserted into pECFP-C1 and pDsRed2-C1 fluorescent expression vectors respectively. Cells were visualized by wide-field fluorescence microscopy with excitation wavelengths of 433 nm for lamin A-FP and 558 nm for DsRed2-lamin C. Compared to the wild type, the complex lamin A/C forms aggregates and the membrane appears granular and discontinued.
B. Laser-scanning confocal microscopy of COS7 cells nuclei transiently co-transfected with either wild type or mutated lamin A and lamin C. Lamin A (in red) and lamin C (in green) were inserted into pECFP-C1 and pEYFP-C1 fluorescent expression vectors; respectively. Excitation wavelengths were 433 nm for lamin A-FP and 558 nm for DsRed2-lamin C.

perform electron microscopy on COS7 cells expressing the wild type or the various lamin C-FP mutants. We restricted the analysis to wild type lamin C and L85R, D192G and R386K lamin C mutants since each of these mutants are representative of a single phenotype. No nuclear deformation was observed in any of the transfected cells. However, in most cells expressing wild type lamin C-FP (60%), lamin C aggregates were in close contact with the nuclear envelope (Fig. 5Aa–b). Clearly, close connections between wild type lamin C aggregates and the nuclear envelope are possible (Fig. 5Ac). Conversely, the number of cells exhibiting such a proximity between aggregates and the nuclear envelope was dramatically reduced in the case of D192G and R386K lamin C-FP (12% and 12.5% respectively; wild type: $n=47$; D192G: $n=38$, $p<0.01$; R386K: $n=17$, $p<0.01$) (Figs. 5Af–i and B). In most of these cells, speckles were found within the nucleoplasma and did not exhibit any close connection with the nuclear envelope as opposed to cells expressing wild type lamin C-FP. In the case of L85R lamin C-FP, the percentage of cells exhibiting lamin C aggregates in contact with the nuclear envelope was similar to the wild type (L85R, $n=24$, $p<0.1$) (Fig. 5B). This finding implies that wild type lamin C is able to establish connections with the nuclear envelope in the absence of lamin A. This also implies that mutations D192G and R386K caused the inhibition of the lamin C/nuclear envelope connection. The L85R mutation had no effect on this contact. Again, this supports the hypothesis that each *LMNA* mutation has specific consequences in regards to lamin A/C properties. It is noteworthy to mention that a significant proportion of cells (30%, $n=17$, $p<0.05$) expressing R386K lamin C exhibited aggregates abnormally localized outside the nuclear membrane (Arrows in Fig. 5Ai). This is rarely observed in nuclei of cell expressing wild type (<8%, $n=47$), or the other lamin C mutants (<18% for D192G, $n=38$, $p>0.05$; <12% for L85R, $n=24$, $p>0.05$). However, electron microscopy analysis of the nuclear envelope of cells expressing R386K lamin C did not reveal any obvious abnormality.

Nuclear localization of lamin A/C mutant complexes in COS7 cells

To find out whether lamin A/C complexes localized in the nuclear envelope, we then co-expressed the wild type and each mutated lamin A-FP with its corresponding lamin C, except for N195K and R482W lamin A/C since these mutants are similar to D192G and wild type respectively. To circumvent bleedthrough issues due to confluent spectral profiles exhibited by C-FP and YFP fluorophores, the wild type and the various lamin A-FP mutants were expressed concomitantly with their counterpart lamin C cloned in pDsRed2-C1 expression vectors. When co-expressed, wild type lamin A-FP and wild type DsRed2-lamin C were homogeneously distributed throughout the nuclear envelope, conferring the nucleus with a veil-like appearance (Fig. 6A). In contrast, D192G and R386K mutants resulted in abnormal aggregations of the complex lamin A/C, which is

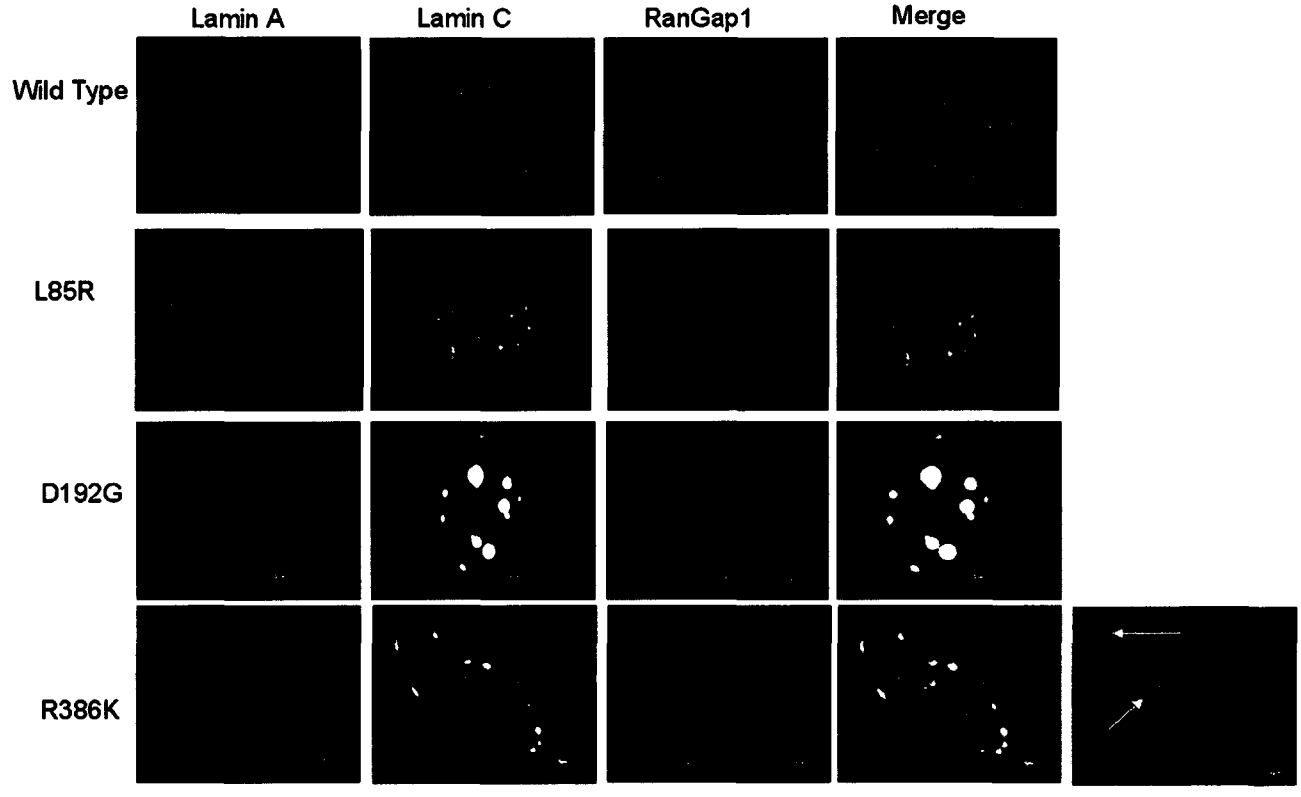

Fig. 7 – Confocal immunofluorescence microscopy pictures of COS7 cells nuclei transiently co-expressing wild type or mutated lamin A-FP and lamin C-FP and immunostained with the anti RanGaP1 polyclonal antibody (N-19). RanGap appears normally distributed in the nuclear envelope. Arrows indicate nuclei with R386K lamin C aggregates localized outside the nuclear envelope.

consistent with previous results [11,18]. Cells expressing L85R lamin A-FP and L85R DsRed2-lamin C exhibited a phenotype similar to the wild type, which suggests that co-expression of both lamins rescues the wild type phenotype. Although L85R DsRed2-lamin C formed speckles within the nucleus (Figs. 3 and 4), we showed that these speckles retained the capacity to make contact with the nuclear envelope (Fig. 5A). Most importantly, even when mutated, lamins A and lamin C always co-localized and were situated in close contact with the nuclear envelope as made evident by confocal microcopy (Fig. 6B). However, in some cells expressing R386K lamins A and C, we observed aberrant localizations of lamin A/C aggregates outside of the nuclear envelope visualized by anti RanGap1 (Arrows in Fig. 7), similarly to cells expressing R386K lamin C-FP only (Fig. 5Ai). Furthermore, the expression of lamin A mutants did not disturb the distribution of endogenous RanGap1 as revealed by immunostaining with an anti RanGap1 (N-19) polyclonal antibody (Fig. 7). Notably, Rangap1 was not enriched in lamin A/C aggregates (Fig. 7). Since RanGAP1 is a Ran GTPase-activating protein present on the cytoplasmic side of nuclear pore complex during interphase, this result suggests that the nuclear pore complexes were correctly localized in the nuclear rim of transfected cells.

Mutated lamin C molecules present in giant aggregates exhibit increased mobility

It has been shown that some LMNA mutations are associated with an increased mobility of lamin A within the nuclear envelope [33] which indicates that some LMNA mutations affect the mobility of lamin A/C molecules. We hypothesized that the inability of lamin C mutants to properly incorporate into the nuclear envelope would reflect a different rigidity of the molecular structure of lamin C aggregates compared to the wild type. This would lead to defective connection with the nuclear envelope. To assess the mobility of the lamin C molecules inside the aggregates, we performed Fluorescence Recovery After Photobleaching (FRAP) on living COS7 cells expressing L85R, D192G, R386K or wild type lamin C-FP. A defined area of selected aggregates was bleached by a series of high-powered spot laser pulses (Fig. 8A). The recovery of fluorescence in this area was then monitored as a mean to assess the mobility of lamin C

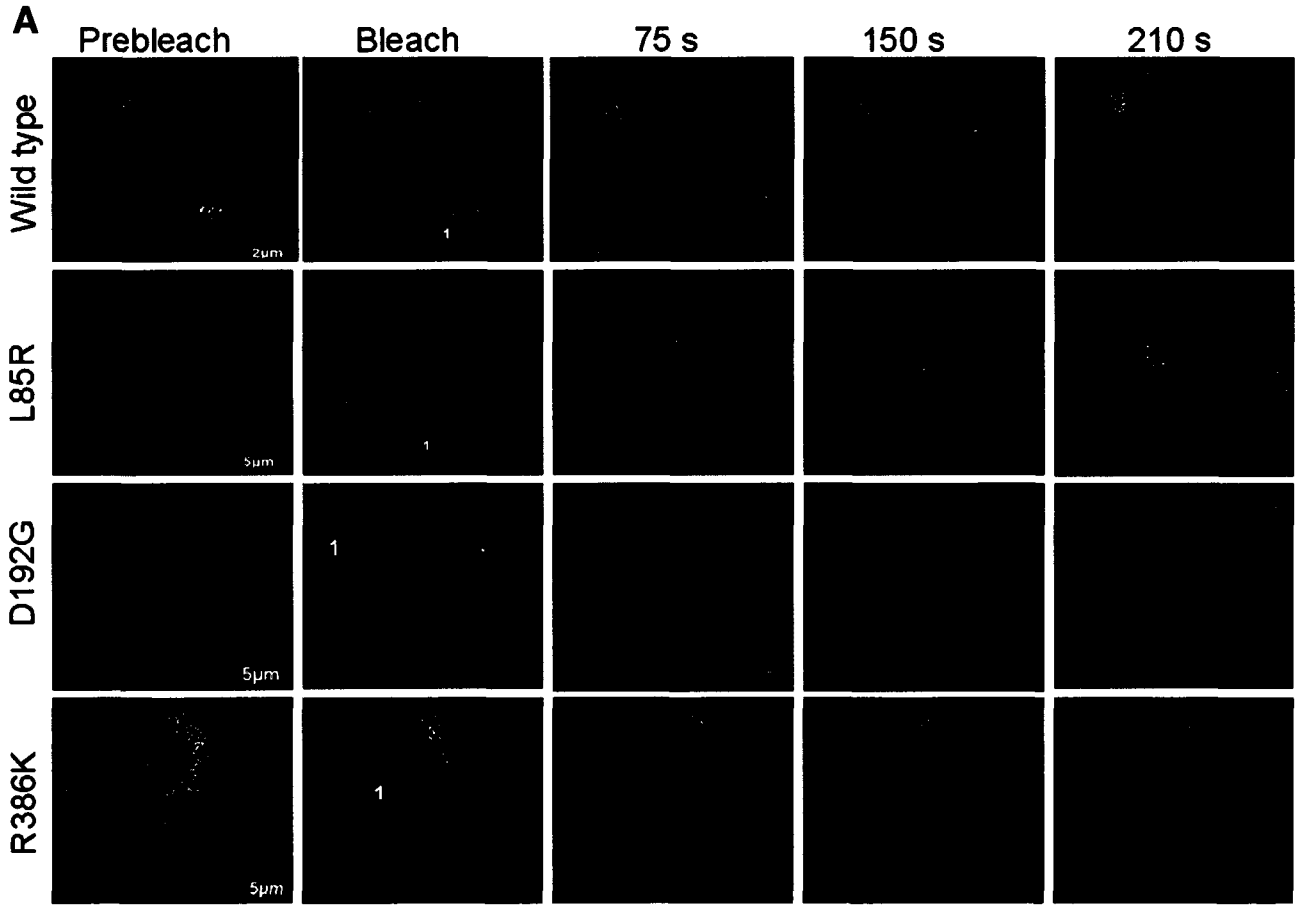

Fig. 8 – A. FRAP experiments on wild type and L85R, D192G and/ or R386K lamin C nuclear aggregates of COS7 cells. The boxed regions were bleached and the fluorescence recovery was monitored over a 210 s period. B. Quantitative experiments showing normalized fluorescence recovery after photobleaching of a targeted region of the lamin C nuclear aggregates in COS7 cells. (a) The fluorescence intensity in the bleached area is expressed as a relative recovery. Error bars indicates SEM, $n=7$. 1 is the level of fluorescence before bleaching. (b) We assessed the time after photobleaching required for fluorescence to recover the median value between the prebleach and just after the bleach ($t_{1/2}$) as a mean to reflect the dynamics of molecule.

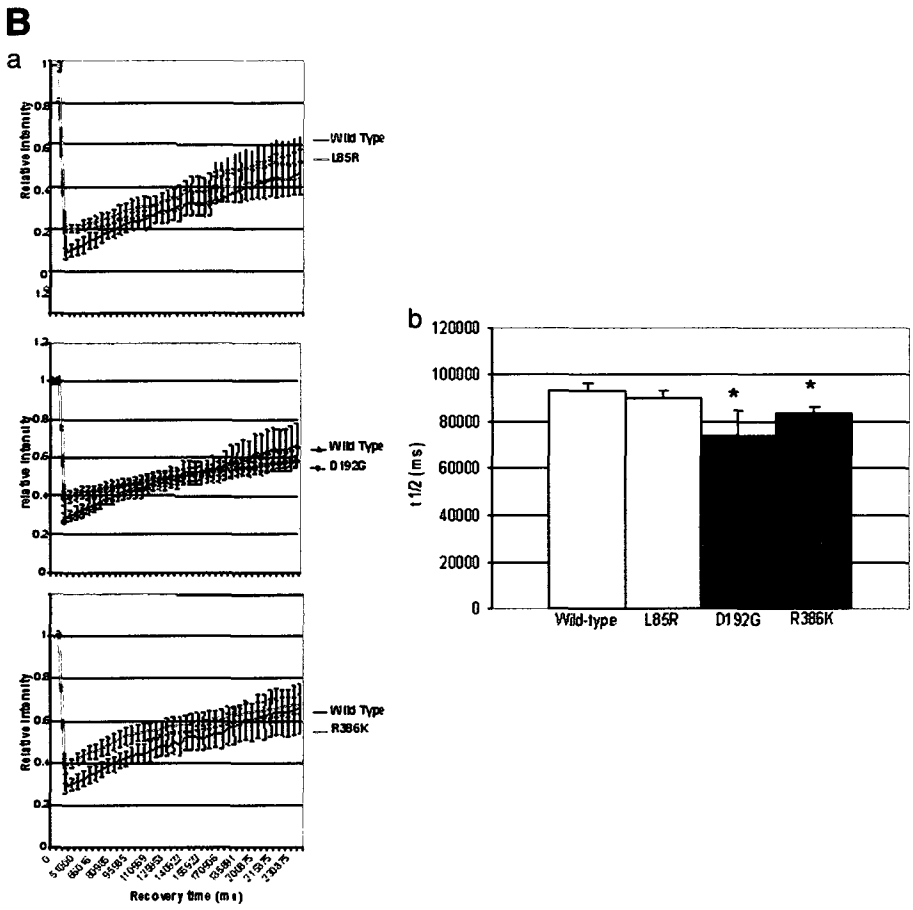

Fig. 8 (continued).

molecules within each aggregate. T-test confirmed that the time after bleaching required to recover 50% of the plateau ($t_{1/2}$, half time recovery) was significantly decreased in D192G ($p=0.02$) or R386K ($p=0.03$) lamin C-FP aberrant speckles compared to wild type lamin C-FP speckles (Fig. 8B), thus revealing that the dynamics of mutated lamin C molecules is significantly higher within D192G and R386K lamin C aggregates than within wild type aggregates. In contrast, in L85R lamin C aggregates, the difference is not significant. Therefore, in comparison to the wild type, the D192G and R386K lamin C intra-aggregates molecules appeared to be more mobile which is indicative of a less stable structure of the mutants. This finding was corroborated by three-minute films showing that R386K lamin C-FP speckles were more prone to move and fuse to each other (data not shown). No difference was observed with L85R (Figs. 8A and B) and R482W (data not shown) aggregates compared to the wild type.

Discussion

In order to better differentiate and define lamin A and lamin C functions, we used a cell model to express the lamins individually and then together. In view of the conflicting results in previous studies regarding the effect of *LMNA* mutations, we duplicated some of the experiments in COS7 cells and H9C2 rat cardiomyoblasts. Results are summarized in Table 1.

Mutated lamins A organize as nuclear envelope aggregates

Our results showed that some mutated lamin A (D192G, N195K, R386K) form abnormal aggregates when expressed alone, which is consistent with previous studies [11,26,27]. However, in contrast to previous studies reporting lamin aggregates described as intranuclear [18,25–27], we found that lamin A aggregates mainly localized at the nuclear periphery of the nucleus, suggesting that although unable to properly organize in the nuclear rim and form the lamina, lamin A mutants keep the capability of associating with the nuclear envelope. Alternatively, other mutants (L85R, R482W) behaved in a way that was indistinguishable from the wild type.

Lamin C mutants form aberrant intranucleoplasmic aggregates and lose their ability to join the nuclear envelope

We also expressed lamin C alone and showed that aberrant lamin C aggregation within the nucleoplasm is a defect common to several *LMNA* mutations (L85R, D192G, N195K, R386K). Interestingly, only the mutations responsible for skeletal and cardiac diseases were found to result in this atypical aggregation whereas mutation R482W involved in human lipodystrophy, did not result in noticeable abnormalities in the location or distribution of either lamin A or lamin C. This finding suggests that the pathophysiological mechanism of laminopathies with

Table 1 – Summary of the phenotypes observed for the LMNA mutations selected in the study

Variants	Diseases	Phenotypes		
		Lamin A alone	Lamin C alone	Lamin A+C
Wild type		Homogenous distribution throughout the nuclear envelope	Numerous small intranuclear aggregates mainly in close contact with the nuclear envelope	Homogenous distribution throughout the nuclear envelope
L85R	DCM	Homogenous distribution throughout the nuclear envelope similarly to the wild type	Rare intranuclear giant aggregates which may make contact with the nuclear envelope	Homogenous distribution similarly to the wild type
D192G	DCM	Aggregates located at the periphery of the nucleus	Rare intranuclear giant aggregation without contact with the nuclear envelope. Lamin C molecules display increased mobility.	Aberrant aggregation of lamin A/C complexes connected to the nuclear envelope
N195K	DCM	Aggregates located at the periphery of the nucleus	Rare intranuclear giant aggregates	
R386K	EDMD	Aggregates located at the periphery of the nucleus.	Rare intranuclear giant aggregates without contact with the nuclear envelope. Significant proportion of these aggregates localize outside the nuclear membrane. Lamin C molecules display increased mobility.	Aberrant aggregation of lamin A/C complexes connected to the nuclear envelope
R482W	FPLD	Homogenous distribution throughout the nucleus similarly to the wild type	Phenotype indistinguishable from the wild type	

AD-EDMD: Autosomal dominant muscular dystrophy, DCM: Dilated cardiomyopathy, and FPLD: Dunningan-type familial partial lipodystrophy.

cardiac involvement is distinct from lipodystrophy and engages lamin C but not lamin A as made evident by the absence of abnormal phenotype in cells expressing lamin A with the dilated cardiomyopathy mutation L85R. Other mutations responsible for cardiomyopathy or muscular dystrophy have also been reported to result in aberrant lamin A or C aggregation such as mutations E358K, M358K [27], or R453W [25]. However, all mutations should be tested to corroborate this conclusion and determine if this lamin C aggregation inside the nucleoplasm could be regarded as a potential hallmark of laminopathies with cardiac or muscular involvement. So far, more than two hundred mutations have been reported of which most are listed in the database http://www.dmd.nl/nmdb/index.php?select_db=LMNA.

Compared to some previous reports [16–19], we sometimes obtained divergent phenotypes of cells expressing the lamin mutants. For example, Raharjo et al. showed that L85R lamin A exhibits a punctate distribution across the nuclear surface slightly different from the wild type, which opposes our results and other studies [27]. Also, N195K and R386K lamin A mutants have been shown to re-localize to the nucleoplasm [18,27,34]. These discrepancies may be explained by protocol differences such as i) the antibody used which can be directed against lamin A, lamin C, or both lamins; ii) the expression vectors used for the transfection which requires either direct or indirect immunofluorescence analysis; iii) the cell lines used (C2C12, HeLa, COS7, SW13, H9C2) since each cell type expresses different levels of endogenous A-type lamin and differently handles the expression of exogenous lamin A/C.

It is interesting to note that aberrant lamin C aggregation may also be present in a small proportion of nuclei expressing wild type lamin C. This suggests that the presence of these aggregates corresponds to a transient stage of the cell cycle. We can hypothesize that cells expressing these mutants would be longer fixed in this stage. Recently, it has been shown that the mutant lamin A involved in Hutchinson–Gilford Progeria Syndrome and harboring a 50 amino acid deletion alters the cell cycle progression [35].

Furthermore, several studies have suggested that lamin A plays a key role in targeting lamin C and Emerin to the nuclear envelope [16–19]. However, recent work in embryonic fibroblasts from mice expressing lamin C only (lco) showed that lamin C and emerin are normally localized into the nuclear envelope even in the absence of lamin A [14]. Furthermore, $Lmna^{lco/lco}$ fibroblasts from these mice display nuclear envelope with only very minimal alterations. The extrapolation of these results to human is hazardous since mouse models often exhibit differences compared to human laminopathies [36,37]. For example, two mutated H222P alleles are necessary to develop muscular dystrophy in mice, whereas the patients are heterozygous [36]. Similarly, the clinical phenotype of LmnaL530P/L530P mice, harboring an Emery–Dreifuss mutation, is consistent with human progeria syndrome [38]. In this study, we used a cell model expressing lamin C only, and brought evidence that wild type lamin C has the capacity to establish close connections with the nuclear envelope on its own (Figs. 5Ac and B). This strongly suggests that lamin C can behave independently and that lamin A is not necessary for lamin C to be present in the nuclear envelope. This finding also argues in favor of a potential substitution of lamin A by lamin C in the nuclear envelope which is consistent with the study by Fong et al. However, it is important to note that our finding does not contradict the fact that lamin C is intranuclear when expressed alone and is re-incorporated into the nuclear lamina when expressed with lamin A, as previously reported [11,16–19]. This likely reflects that the presence of lamin C in the nuclear lamina requires a precise lamin C/lamin A stoichiometry to be respected. This may also explain why the incorporation of lamin C into the nuclear lamina proceeds via intranuclear foci [17].

Furthermore, our results showed that the lamin C mutants tested here were seldom part of the nuclear lamina (Fig. 5A). As a consequence, an altered ability of lamin C to establish connections with the nuclear envelope due to mutations in *LMNA* gene should also be considered to explain the major alterations of the nuclear membrane observed in cardiomyocytes from patients [11,20,22]. To further analyze the pathophysiology of laminopathies and propose a potential explanation as for why the mutant lamin C connections with the nuclear envelope is altered, we performed FRAP experiments on the nuclear aggregates formed by lamin C mutants. Our result revealed that lamin C molecules were significantly more mobile within D192G and R386K lamin C-FP intranuclear aggregates compared to the wild type, thereby indicating that these aberrant lamin C aggregates were significantly less stable. Interestingly, the increased lamin C velocity was observed only with the mutants that exhibited an altered ability to interact with nuclear envelope and that led to an abnormal aggregation in the nucleoplasm (D192G, R386K). In view of these results, we can postulate that the lamin C molecules involved in these aggregates preferably interact with each other to the detriment of the nuclear envelope. However, it would be interesting to investigate other mutants to corroborate a potential correlation between the size of intranuclear aggregates, the velocity of nuclear lamin C and its capacity to associate with the nuclear envelope. Altogether, these results provide novel insight into the pathophysiological mechanism of laminopathies.

LMNA mutations alter lamin A and C interactions with their partners but not RanGap 1 distribution

We showed that L85R lamin C aggregates exhibited neither altered stability nor altered capacity to be connected to the nuclear membrane, as opposed to D192G, N195K, and R386K mutants. These findings likely indicate that the maintenance of these properties is not correlated to the size of nuclear aggregates. However, we cannot exclude that the formation of such aberrant intranuclear accumulations did not affect other lamin A/C properties, such as the interactions with lamin A/C partners. Nuclear lamina is known to participate in the organization of nuclear pores within the nuclear membrane [39]. Since we did not find any mislocalization of RanGap1 with any of the mutants tested, we can hypothesize that the localization of nuclear pore complex within the nuclear envelope is not affected. Therefore, in our cell model, the nuclear-cytoplasm trafficking of macromolecules through the nuclear envelope is most likely unaffected by the presence of mutated lamin A/C (Fig. 7). However, further experiments have to be performed to confirm this hypothesis. Indeed, it has been shown that embryonic fibroblasts from mice lacking A-type lamin exhibited a loss of the nuclear pore protein Nup153 from one pole of the nuclei indicating exclusion of nuclear pore complex from this area [40]. Similarly, Muchir et al. found that Nup153 was absent in pole of fibroblasts from patients with type 1B limb-girdle muscular dystrophy and carrying the nonsense Y259X mutation [21]. Recently, the prelamin A Y646F mutant has been found to co-localize with nuclear pore complex in embryonic kidney (HEK-293) cells [41]. Our divergent results may be explained by the fact that the mutations we investigated are not responsible for either 1B limb-girdle muscular dystrophy or progeria and that the cell type used in our model has endogenous lamin A/C which is likely sufficient to anchor nuclear pore complexes in the nuclear envelope.

Lastly, in a previous report, we showed that lamin C nuclear aggregation results in the aberrant trapping of SUMO1, a post translational modifier of numerous proteins [11]. Among these proteins, there are several transcription factors including the cardiac specific transcription factor GATA4 [42]. Similarly, Hubner et al. demonstrated that the over-expression of lamin A mutant led to the sequestration of the lamin A/C interacting partners pRb (retinoblastoma protein) and SREBP1a (sterol responsive element binding protein 1a) into lamin A nuclear aggregates [34]. Such aberrant interactions with lamin A/C partners may also be considered as a potential pathophysiological mechanism for laminopathies.

LMNA gene mutations and the variety of human phenotypes

Defects in gene regulation and/or abnormalities in nuclear architecture causing cellular fragility are the main two hypotheses that have been proposed to explain the variability of phenotypes due to *LMNA* mutations [1]. Our previous study was in favor of nuclear fragility since we observed dramatic nuclear envelope discontinuity in cardiomyocytes from *LMNA* mutated patients [11]. Here, we better dissect the properties of each of lamins A and C specifically and show that they can be differentially affected by a given mutation. These results with others [16,18,27], clearly showed that the consequences of *LMNA* mutation on the cell physiology is different from one mutation to another. Therefore, we can conclude that i) the type of mutation and ii) its consequence on the unique properties of each lamin specifically, are two key factors that has to be considered in predicting the potential consequences on nuclear function. The combination of these two factors can result in multiple consequences on the cell physiology which likely contributes to explain the variability and complexity of phenotypes in human disease and may be regarded as an additional working hypothesis to explain how mutations in *LMNA* gene lead to so many phenotypes in humans.

Lamins A and C support conjoint and also separate functions

Lastly, we showed that connections between the nuclear envelope and some mutated lamin C-FP (D192G, R386K) are absent which is not the case with the equivalent mutated lamin A. Conversely, other mutants, such as L85R led to aberrant lamin C aggregation but did not alter lamin A organization within the nuclear envelope. The fact that a mutation has different effects on lamin A and lamin C, shows that lamins A and C have to be investigated not only together but also separately in order to better dissect their function and specific role in the occurrence of disease. Also, this likely suggests that each protein may support distinct functions. This is in agreement with a previous study showing that lamins A and C do not play the same role in the nuclear lamina assembly characteristics [16]. In particular, the emerin-lamin A and emerin-lamin C interactions appear to be functionally different and are differently affected by some Emery–Dreifuss *LMNA* mutations [16]. As a conclusion, a closer look at the functions of lamins A and C specifically may allow resolution of conflicting results and may also help define

genotype–phenotype correlation in laminopathies which has been difficult thus far.

Acknowledgments

The Laboratory of Genetics of Cardiac diseases is part of the John and Jennifer Ruddy Canadian Cardiovascular Genetics Centre. This research was supported by Canadian Institutes for Health Research operating grants 38054 and 65152, and by Heart and Stroke Foundation grant NA 5101 awarded to F Tesson. N Sylvius was the recipient of the fellowship awarded by the Heart and Stroke Foundation of Ontario Program grant 5275 and by the Astra Zeneca/Canadian Society of Hypertension/CIHR fellowship.

REFERENCES

[1] N. Sylvius, F. Tesson, Lamin A/C and cardiac diseases, Curr. Opin. Cardiol. 21 (2006) 159–165.
[2] D.K. Shumaker, E.R. Kuczmarski, R.D. Goldman, The nucleoskeleton: lamins and actin are major players in essential nuclear functions, Curr. Opin. Cell Biol. 15 (2003) 358–366.
[3] C.J. Hutchison, Lamins: building blocks or regulators of gene expression? Nat. Rev., Mol. Cell Biol. 3 (2002) 848–858.
[4] R.L. Boguslavsky, C.L. Stewart, H.J. Worman, Nuclear lamin A inhibits adipocyte differentiation: implications for Dunnigan-type familial partial lipodystrophy, Hum. Mol. Genet. 15 (2006) 653–663.
[5] D. Constantinescu, H.L. Gray, P.J. Sammak, G.P. Schatten, A.B. Csoka, Lamin A/C expression is a marker of mouse and human embryonic stem cell differentiation, Stem Cells 24 (2006) 177–185.
[6] Y. Gruenbaum, A. Margalit, R.D. Goldman, D.K. Shumaker, K.L. Wilson, The nuclear lamina comes of age, Nat. Rev., Mol. Cell Biol. 6 (2005) 21–31.
[7] M.S. Zastrow, D.B. Flaherty, G.M. Benian, K.L. Wilson, Nuclear titin interacts with A- and B-type lamins in vitro and in vivo, J. Cell Sci. 119 (2006) 239–249.
[8] M.S. Zastrow, S. Vlcek, K.L. Wilson, Proteins that bind A-type lamins: integrating isolated clues, J. Cell Sci. 117 (2004) 979–987.
[9] N. Zhong, G. Radu, W. Ju, W.T. Brown, Novel progerin-interactive partner proteins hnRNP E1, EGF, Mel 18, and UBC9 interact with lamin A/C, Biochem. Biophys. Res. Commun. 338 (2005) 855–861.
[10] F. Haque, D.J. Lloyd, D.T. Smallwood, C.L. Dent, C.M. Shanahan, A.M. Fry, R.C. Trembath, S. Shackleton, SUN1 interacts with nuclear lamin A and cytoplasmic nesprins to provide a physical connection between the nuclear lamina and the cytoskeleton, Mol. Cell. Biol. 26 (2006) 3738–3751.
[11] N. Sylvius, Z.T. Bilinska, J.P. Veinot, A. Fidzianska, P.M. Bolongo, S. Poon, P. McKeown, R.A. Davies, K.L. Chan, A.S. Tang, S. Dyack, J. Grzybowski, W. Ruzyllo, H. McBride, F. Tesson, In vivo and in vitro examination of the functional significances of novel lamin gene mutations in heart failure patients, J. Med. Genet. 42 (2005) 639–647.
[12] J. Lammerding, P.C. Schulze, T. Takahashi, S. Kozlov, T. Sullivan, R.D. Kamm, C.L. Stewart, R.T. Lee, Lamin A/C deficiency causes defective nuclear mechanics and mechanotransduction, J. Clin. Invest. 113 (2004) 370–378.
[13] S. Tulac, C. Dosiou, E. Suchanek, L.C. Giudice, Silencing lamin A/C in human endometrial stromal cells: a model to investigate endometrial gene function and regulation, Mol. Hum. Reprod. 10 (2004) 705–711.
[14] L.G. Fong, J.K. Ng, J. Lammerding, T.A. Vickers, M. Meta, N. Cote, B. Gavino, X. Qiao, S.Y. Chang, S.R. Young, S.H. Yang, C.L. Stewart, R.T. Lee, C.F. Bennett, M.O. Bergo, S.G. Young, Prelamin A and lamin A appear to be dispensable in the nuclear lamina, J. Clin. Invest. 116 (2006) 743–752.
[15] T. Libotte, H. Zaim, S. Abraham, V.C. Padmakumar, M. Schneider, W. Lu, M. Munck, C. Hutchison, M. Wehnert, B. Fahrenkrog, U. Sauder, U. Aebi, A.A. Noegel, I. Karakesisoglou, Lamin A/C-dependent localization of Nesprin-2, a giant scaffolder at the nuclear envelope, Mol. Biol. Cell 16 (2005) 3411–3424.
[16] I. Motsch, M. Kaluarachchi, L.J. Emerson, C.A. Brown, S.C. Brown, M.C. Dabauvalle, J.A. Ellis, Lamins A and C are differentially dysfunctional in autosomal dominant Emery–Dreifuss muscular dystrophy, Eur. J. Cell Biol. 84 (2005) 765–781.
[17] G.E. Pugh, P.J. Coates, E.B. Lane, Y. Raymond, R.A. Quinlan, Distinct nuclear assembly pathways for lamins A and C lead to their increase during quiescence in Swiss 3T3 cells, J. Cell Sci. 110 (Pt 19) (1997) 2483–2493.
[18] W.H. Raharjo, P. Enarson, T. Sullivan, C.L. Stewart, B. Burke, Nuclear envelope defects associated with LMNA mutations cause dilated cardiomyopathy and Emery–Dreifuss muscular dystrophy, J. Cell Sci. 114 (2001) 4447–4457.
[19] A. Vaughan, M. Alvarez-Reyes, J.M. Bridger, J.L. Broers, F.C. Ramaekers, M. Wehnert, G.E. Morris, W.G.F. Whitfield, C.J. Hutchison, Both emerin and lamin C depend on lamin A for localization at the nuclear envelope, J. Cell Sci. 114 (2001) 2577–2590.
[20] E. Arbustini, A. Pilotto, A. Repetto, M. Grasso, A. Negri, M. Diegoli, C. Campana, L. Scelsi, E. Baldini, A. Gavazzi, L. Tavazzi, Autosomal dominant dilated cardiomyopathy with atrioventricular block: a lamin A/C defect-related disease, J. Am. Coll. Cardiol. 39 (2002) 981–990.
[21] A. Muchir, B.G. van Engelen, M. Lammens, J.M. Mislow, E. McNally, K. Schwartz, G. Bonne, Nuclear envelope alterations in fibroblasts from LGMD1B patients carrying nonsense Y259X heterozygous or homozygous mutation in lamin A/C gene, Exp. Cell Res. 291 (2003) 352–362.
[22] L. Verga, M. Concardi, A. Pilotto, O. Bellini, M. Pasotti, A. Repetto, L. Tavazzi, E. Arbustini, Loss of lamin A/C expression revealed by immuno-electron microscopy in dilated cardiomyopathy with atrioventricular block caused by LMNA gene defects, Virchows Arch. 443 (2003) 664–671.
[23] C. Vigouroux, M. Auclair, E. Dubosclard, M. Pouchelet, J. Capeau, J.C. Courvalin, B. Buendia, Nuclear envelope disorganization in fibroblasts from lipodystrophic patients with heterozygous R482Q/W mutations in the lamin A/C gene, J. Cell Sci. 114 (2001) 4459–4468.
[24] Y. Wang, A.J. Herron, H.J. Worman, Pathology and nuclear abnormalities in hearts of transgenic mice expressing M371K lamin A encoded by an LMNA mutation causing Emery–Dreifuss muscular dystrophy, Hum. Mol. Genet. 15 (2006) 2479–2489.
[25] J.L. Broers, H.J. Kuijpers, C. Ostlund, H.J. Worman, J. Endert, F.C. Ramaekers, Both lamin A and lamin C mutations cause lamina instability as well as loss of internal nuclear lamin organization, Exp. Cell Res. 304 (2005) 582–592.
[26] S. Hubner, J.E. Eam, K.M. Wagstaff, D.A. Jans, Quantitative analysis of localization and nuclear aggregate formation induced by GFP-lamin A mutant proteins in living HeLa cells, J. Cell Biochem. 98 (2006) 810–826.
[27] C. Ostlund, G. Bonne, K. Schwartz, H.J. Worman, Properties of lamin A mutants found in Emery–Dreifuss muscular dystrophy, cardiomyopathy and Dunnigan-type partial lipodystrophy, J. Cell Sci. 114 (2001) 4435–4445.
[28] J. Rankin, S. Ellard, The laminopathies: a clinical review, Clin. Genet. 70 (2006) 261–274.
[29] D. Fatkin, C. MacRae, T. Sasaki, M.R. Wolff, M. Porcu, M. Frenneaux, J. Atherton, H.J. Vidaillet Jr., S. Spudich, U. De

Girolami, J.G. Seidman, C. Seidman, F. Muntoni, G. Muehle, W. Johnson, B. McDonough, Missense mutations in the rod domain of the lamin A/C gene as causes of dilated cardiomyopathy and conduction-system disease, N. Engl. J. Med. 341 (1999) 1715–1724.

[30] G. Bonne, M.R. Di Barletta, S. Varnous, H.M. Becane, E.H. Hammouda, L. Merlini, F. Muntoni, C.R. Greenberg, F. Gary, J.A. Urtizberea, D. Duboc, M. Fardeau, D. Toniolo, K. Schwartz, Mutations in the gene encoding lamin A/C cause autosomal dominant Emery–Dreifuss muscular dystrophy, Nat. Genet. 21 (1999) 285–288.

[31] H. Cao, R.A. Hegele, Nuclear lamin A/C R482Q mutation in canadian kindreds with Dunnigan-type familial partial lipodystrophy, Hum. Mol. Genet. 9 (2000) 109–112.

[32] R.D. Phair, T. Misteli, High mobility of proteins in the mammalian cell nucleus, Nature 404 (2000) 604–609.

[33] S. Gilchrist, N. Gilbert, P. Perry, C. Ostlund, H.J. Worman, W.A. Bickmore, Altered protein dynamics of disease-associated lamin A mutants, BMC Cell Biol. 5 (2004) 46.

[34] S. Hubner, J.E. Eam, A. Hubner, D.A. Jans, Laminopathy-inducing lamin A mutants can induce redistribution of lamin binding proteins into nuclear aggregates, Exp. Cell. Res. 312 (2006) 171–183.

[35] T. Dechat, T. Shimi, S.A. Adam, A.E. Rusinol, D.A. Andres, H.P. Spielmann, M.S. Sinensky, R.D. Goldman, Alterations in mitosis and cell cycle progression caused by a mutant lamin A known to accelerate human aging, Proc. Natl. Acad. Sci. U. S. A. 104 (2007) 4955–4960.

[36] T. Arimura, A. Helbling-Leclerc, C. Massart, S. Varnous, F. Niel, E. Lacene, Y. Fromes, M. Toussaint, A.M. Mura, D.I. Keller, H. Amthor, R. Isnard, M. Malissen, K. Schwartz, G. Bonne, Mouse model carrying H222P-Lmna mutation develops muscular dystrophy and dilated cardiomyopathy similar to human striated muscle laminopathies, Hum. Mol. Genet. 14 (2005) 155–169.

[37] L.C. Mounkes, S.V. Kozlov, J.N. Rottman, C.L. Stewart, Expression of an LMNA-N195K variant of A-type lamins results in cardiac conduction defects and death in mice, Hum. Mol. Genet. 14 (2005) 2167–2180.

[38] L.C. Mounkes, S. Kozlov, L. Hernandez, T. Sullivan, C.L. Stewart, A progeroid syndrome in mice is caused by defects in A-type lamins, Nature 423 (2003) 298–301.

[39] J.M. Holaska, K.L. Wilson, M. Mansharamani, The nuclear envelope, lamins and nuclear assembly, Curr. Opin. Cell Biol. 14 (2002) 357–364.

[40] T. Sullivan, D. Escalante-Alcalde, H. Bhatt, M. Anver, N. Bhat, K. Nagashima, C.L. Stewart, B. Burke, Loss of A-type lamin expression compromises nuclear envelope integrity leading to muscular dystrophy, J. Cell Biol. 147 (1999) 913–920.

[41] Y. Pan, A. Garg, A.K. Agarwal, Mislocalization of prelamin A Tyr646Phe mutant to the nuclear pore complex in human embryonic kidney 293 cells, Biochem. Biophys. Res. Commun. 355 (2007) 78–84.

[42] J. Wang, X.H. Feng, R.J. Schwartz, SUMO-1 modification activated GATA4 dependent cardiogenic gene activity, J. Biol. Chem. 279 (2004) 49091–49098.